UNIVERSITÀ
degli STUDI
di CATANIA

University of Catania

Ph.D. in Computer Science

Georgia Fargetta

Variational inequality and metaheuristic approaches to model and investigate the agents' strategies

Ph.D. Thesis

Supervisor: Prof. Mario F. Pavone

Co-Supervisor: Prof.ssa Laura R.M. Scrimali

Academic Year: 2021/2022 (XXXV Cycle)

Contents

List of Figures

List of Tables

Introduction

During my Ph.D. experience, research work led to the development of numerous scientific articles which revolve around the understanding of the human mentality and behavior. A model is an abstract representation of reality that includes aspects relevant to the purpose of its study. Modeling reality and its behavior represents one of the most investigated topics of scientific research in the field of operational research. The investigation moved through two main approaches: mathematical models of variational inequalities and metaheuristic algorithms and both of them are complex decision-making systems. The two approaches, the variational one and the metaheuristic one, can both be represented and modeled through networks. In the study of a phenomenon, after a careful analysis, a mathematical model is developed. It must represent the problem effectively and take into consideration all the agents involved and the relevant aspects. In the first approach, the model is analyzed from a strictly mathematical point of view: the constraints are formalized and through a variational game theory approach an equilibrium point is determined that maximizes profit or minimizes cost for all agents. Through the metaheuristic approach the problems are analyzed with probabilistic algorithms. This approach has the advantage of being able to simultaneously analyze a very high number of

agents and to progressively investigate the states of the problem and observe the behavior and reactions of the agents in the development of the situation. Nowadays, due to the development of new technologies, smartphones and internet connectivity devices are becoming cheaper and easier to access, thus expanding the possibilities to approach other people. As a consequence, a first line of my research is focused on a game theoretical approach to investigate the strategic behavior of content providers in relation to the viewers of their videos. The goal of content providers is to maximize their profit as a result of their reputation, the quality of the content uploaded and the income through the various advertisements or sponsors and the number of views obtained. I decided to improve the previous model by considering a dependence on time in order to better analyze how the profits of content providers change after different instants of time as a consequence of their strategies which in both models are characterized by the number of views and the quality of the content. In these two models the focus was concentrated on the analysis of the behavior of content providers who post videos on the YouTube platform. Then the eBay platform was studied. I decided to develop another model where the behavior of a production chain was investigated starting from manufacturers passing through retailers to consumers. Unlike the well-known production supply chain, a closed-loop network is studied. In this work the study of behavior is not limited to consumers. In fact some consumers decide to resell their used products through an e-commerce platform such as eBay, and these items will be bought back by others. Consumers thus make this chain a closed-loop network. The results show that customer loyalty is important for every level of decision makers. Also this model has been extended considering the time dependence even if these results will not be analyzed in the thesis. During my first and second year of Ph.D.,

the outbreak of the Covid-19 pandemic in early 2020, prompted me to study healthcare models. The first scientific paper in this area, that I analyze in this thesis, was developed in collaboration with the local speech therapy center, which required staff assignments to patients with different levels of priority, optimizing the working hours of the few employees specialized in some particular therapies and not, and finally optimizing their path to visit patients in their homes and in the various speech centers in the area. The analysis of the pandemic situation has led to the study of emergency models under uncertainty. In particular, at the beginning of 2020, I started the study of two-stage stochastic variational inequalities models considering the behavior of warehouses in relation to hospitals, which sell medical material to the latter. The goal is to minimize transportation time, transportation cost and unmet demand. This model was subsequently extended and published in *Journal of Optimization Theory and Applications*. At the same time, the behavior of agents during an evacuation situation was investigated. The issue of evacuation was analyzed following two different approaches: the first by analyzing the optimal strategies through a two-stage stochastic variational model, the second by observing and studying the strategies and in particular the behavior of agents in an emergency situation. The objective of the first model is to minimize the transportation cost, the transportation time, the penalty cost on the links with training to evacuate the greatest number of agents who have to escape from an area that is no longer safe to a shelter. The results showed that the values of the deterministic profit functions are greater than the respective values of the Lagrange relaxation approach, used in this model. This observation implies that the stochastic framework and the real-time updating of information allow one to evaluate more precisely the situation, and to lower evacuation costs. The other

approach, used to solve this second evacuation model, represents an agent based model in which two different types of agents, cooperative and non-cooperative, must reach the exit from a fixed income by minimizing the path, in a dynamic graph. The goal is minimizing the time of the path and costs and maximizing the number of agents who reach the exit. The algorithm created incorporates Ant Colony Optimization (ACO), a Methaeuristic Swarm Intelligence. I investigate the Ant Colony Optimization correlating with the study of agent-based model associated with game theory and optimization model. Game theory is the study of mathematical models of strategic interaction among rational decision-makers, on the other hand, ACO is a probabilistic technique for solving computational problems for multi-agent methods inspired by the behaviour of real ants. The main relationship between ACO and Game Theory is that both of them try to find a good solution in a situation where agents, with different ideas and strategies have to share a particular environment. As the crowd, a group of ants tries to achieve the exit, as safe as is possible. The Ant Colony Optimization's works are connected to the work on two stage stochastic variational model on evacuation. Furthermore, the study of immunological metaheuristics was carried out. Two algorithms have been developed respectively called Opt-IA and Hybrid-Ia. Both are immunological algorithms, for clustering problems, that in our specific case have been applied to social networks and then to biological networks. The purpose of these two algorithms is to analyze the interaction between agents or molecules, respectively for social networks and biological networks. I detect highly linked communities in a network with the aim to understand relationships between entities or interactions between biological genes.

Objectives and contents The work presented in this thesis represents an excursus of some approaches, such as game theory, variational inequality models and metaheuristic algorithms, used for the study and resolution of mathematical models with the aim to investigate human behavior and strategies. I have completed and published on proceedings or journals 12 works in different fields, such supply chain, healthcare, evacuation, agents based models and community detection. In details, the thesis is structured as follow:

In Chapter 1, a dynamic model of competition for the diffusion of online contents in a two-layer network consisting of content providers and viewers is presented. Each content provider seeks to maximize the profit by determining the optimal views and quality levels. I assume that there is a known and fixed limit to the number of times each viewer can access a content. This requirement generates shared constraints for all the providers. The problem is expressed as a Generalized Nash equilibrium with shared constraints that is then formulated via a variational inequality. I construct the locally projected dynamical system model, which provides a continuous-time evolution of views and quality levels, and whose set of stationary points coincides with the set of solutions to the variational inequality. I discuss some stability conditions using a monotonicity approach, and, finally, I present some numerical examples (see [89]).

In Chapter 2, I extend the model in Chapter 1 and I develop a dynamic network model of the competition of digital contents on social media platforms, assuming that there is a known and fixed upper bound on the total amount of views. In particular, I consider a two-layer network consisting of creators and viewers. Each creator seeks to maximize the profit by determining views and likes. The problem is formulated as a time-dependent generalized Nash equilibrium for which

I provide the associated evolutionary variational inequality, using the variational equilibrium concept. It is also discussed a possible differential game formulation. Finally, using a discrete-time approximation of the continuous time adjustment process, I present a numerical example (see [91]).

In Chapter 3, a closed-loop supply chain network equilibrium problem with online second-hand trading of high-uniqueness products is studied. The closed-loop supply chain network consists of manufacturers, retailers, demand markets, and one online second-hand platform engaging in both horizontal and vertical competition. The optimal behaviors of all the decision-makers are modeled as variational inequality problems, and the governing closed-loop supply chain network equilibrium conditions are given (see [88]).

In Chapter 4, I propose a multi-stage integer linear programming problem to solve the scheduling of speech-language pathologists involved in conventional treatments as well as in augmentative and alternative communication therapies. In order to reduce the complexity of this problem, I suggest a hierarchical approach that breaks the problem into three sub-problems: patient selection for augmentative and alternative communication therapies, therapists' shift assignment, and routing optimization of home-based rehabilitation services. The resulting models were tested on data collected in a physiotherapy centre in *Acireale* (*Catania, Italy*), using AMPL optimization package and Genetic Algorithm implemented in Matlab. From the results of the case study, the model ensures the maximization of the number of patients eligible for augmentative and alternative communication therapies, the assignment of sustainable therapist schedule, and the optimization of the home therapy routing (see [86]).

In Chapter 5 and 6, the competition of healthcare institutions for medical supplies

in emergencies caused by natural disasters is studied. In particular, in Chapter 5 I develop a two-stage stochastic programming model in a generalized Nash equilibrium framework. It provides the optimal amount of medical supplies from warehouses to hospitals, in order to minimize both the purchasing cost and the transportation costs. For effective disaster planning, I allow for real-time information spreading and up-to-date disaster evaluation. Thus, each institution deals with a two-stage stochastic programming model that considers the unmet demand at the first stage, and the consequent penalty. Then, the institutions simultaneously solve their own stochastic optimization problems and reach a stable state governed by the stochastic generalized Nash equilibrium concept. Moreover, I formulate the problem as a two-stage variational inequality. I also present an alternative two-stage variational inequality formulation using the Lagrangian relaxation approximation (see [87]). Also, in Chapter 6 I modelled a medical supply network that involves warehouses and hospitals with multiple medical items and multiple transportation modes during emergencies situations, in a random environment. I consider a pre-event policy, in which each healthcare institution seeks to minimize the purchasing cost of medical items and the transportation time from the first stage, and a recourse decision process to optimize the expected overall costs and the penalty for the prior plan, in response to each disaster scenario. Thus, each institution deals with a two-stage stochastic programming model that takes into account the unmet demand at the first stage, and the consequent penalty. Then, the institutions simultaneously solve their own stochastic optimization problems and reach a stable state governed by the stochastic Nash equilibrium concept, unlike the Chapter 5 in which a generalized Nash equilibrium problem has been studied. Moreover, I formulate the problem as a variational inequality; both the

discrete and the general probability distribution cases are described. In Chapter 6, I also present an alternative formulation using infinite dimensional duality tools, characterizing the second-stage equilibrium, in the case of general probability distribution, by means of infinite-dimensional Lagrange duality. Finally, we test the equilibrium model with two different numerical illustrations with realistic data, investigating the different strategies used by hospital in situation with high or low penalty on the unfulfilled demand, applying the Progressive Hedging Method (see [84]). The results reveal that hospitals are able to re-arrange timely their requests in order to satisfy the need for medical items. In emergencies, uncertainty plays a fundamental role in the success of disaster management.

In Chapter 7, I focus on evacuation planning which is a complex and challenging process able to predict or evaluate different disaster scenarios. In particular, I present an evacuation model where a population has to be evacuated from crisis areas to shelters, and propose an optimization formulation for minimizing a combination of the transportation cost and the transportation time. In addition, I admit uncertainty in the size of the population to be evacuated and provide a two-stage stochastic programming model. I propose an equivalent two-stage variational inequality formulation, using the Lagrangian relaxation approach. In order to illustrate the modeling framework, I present a numerical example, solving the deterministic and the stochastic model. From the results has been emerged that the values of the deterministic profit functions are greater than the respective values of the two-stage evacuation model without the Lagrange relaxation. This confirms the efficiency of the stochastic approach (see [90]).

In Chapter 8, I introduce some new methodologies in a general path problem. Finding a good path is always a desirable task and it can be also crucial in

emergency and panic situations, in which people tend to assume different and unpredictable behaviors. In this Chapter, I analyze an escape situation in which the environment is a labyrinth and people are agents that act as two different kinds of ant colonies. In particular, I assume that people act according to opposite behaviors: (i) cooperatively, helping each other and the group; (ii) non cooperatively, helping just themselves, and not caring about the rest of the group. So, I use in a path problem an Ant Colony Algorithm based on two breeds of colonies: a cooperative and a non-cooperative one. I imagine that their task is to find the exit of the labyrinth making decisions according to the ACO rules and according to their breed. Every breed has, in fact, two different strategies. Via a game theory approach, I investigate how these two strategies affect the final payoff of each breed. In particular, I notice that if a number of evacuees choose cooperative strategies, then the function's value is higher than the same number of evacuees can gain playing a competitive strategy (see [47]).

In Chapter 9, I present an agent-based model to evaluate the effects of different behaviors in a crowd simulation. Two different behaviours of agents were considered: collaborative, acting attentively and collaboratively, and defector who, on the other hand, acts individually and recklessly. Many experimental simulations on different complexity scenarios were performed and each outcome proves how the presence of a percentage of defector agents helps and motivates the collaborative ones to be better and more fruitful. This investigation was carried out considering the (i) number of agents evacuated, (ii) exit times and (iii) path costs as evaluation metrics. It has been emerged that a mixed crowd in which are presented both behaviors is more efficient not only in obtaining the best values of the metrics used but also in the transmission of the information from one group to another (see

[46]).

In Chapter 10, I present an experimental analysis of how different behavior performed by a group of ants affects the optimization efficiency of the entire colony. Two different interaction ways of the ants with each other and with the environment, that is a weighted network, have been considered: (*i*) *Low Performing Ants* (LPA), which destroy nodes and links of the network making it then dynamic; and (*ii*) *High Performing Ants* (HPA), which, instead, repair the destroyed nodes or links encountered on their way. The purpose of both ant types is simply to find the exit of the network, starting from a given entrance, whilst, due to the uncertainty and dynamism of the network, the main goal of the entire colony is maximize the number of ants that reach the exit, and minimize the path cost and the resolution time. From the analysis of the experimental outcomes, it is clear that the presence of the LPAs is advantageous for the entire colony in improving its performances, and then in carrying out a better and more careful optimization of the environment. An excess of information is self-defeating for the group because, since their actions are calibrated according to this quantity, it does not allow the ants to explore the rest of the network, letting them choose the same path over and over (see [45]).

In Chapter 11 and 12, I present a challenging problem i.e. community detection. Community detection is an interesting and valuable approach to discover the structure of the community in a complex network, revealing the internal organization of the nodes, and has been designed as a leading research topic in the analysis of complex networks. Being able to detect highly linked communities in a network can lead to many benefits, such as understanding relationships between entities or interactions between biological genes, for instance. In particular, in Chapter 11, two different immunological algorithms have been designed for this problem,

called OPT-IA and HYBRID-IA, respectively. The main difference between the two algorithms is the search strategy and related immunological operators developed: the first carries out a random search together with purely stochastic operators; the last one is instead based on a deterministic Local Search that tries to refine and improve the current solutions discovered. The robustness of OPT-IA and HYBRID-IA has been assessed on several real social networks. These same networks have also been considered for comparing both algorithms with other seven different metaheuristics and the well-known greedy optimization LOUVAIN algorithm. The experimental analysis conducted proves that OPT-IA and HYBRID-IA are reliable optimization methods for community detection, outperforming all compared algorithms. Finally, I give some conclusions (see [50]). Otherwise, in Chapter 12 is investigated the link between biological modules and network communities in a test-case biological networks that are commonly used as a reference point and which include *Protein-Protein Interactions Networks*, *Metabolic Networks* and *Transcriptional Regulation Networks*. In order to identify small and structurally well-defined communities in biological context, a hybrid immune metaheuristic algorithm HYBRID-IA is proposed. The proposed algorithm performs community detection based on the modularity maximization, and it is compared to several metaheuristics, hyper-heuristic, and the well-known greedy algorithm LOUVAIN. Considering the limitation of modularity optimization, which can fail to identify smaller communities, the efficiency and reliability of HYBRID-IA were also analyzed with respect to the *Normalized Mutual Information* (NMI), an evaluation metric that allows to assess how similar the detected communities are concerning to real ones. Finally, inspecting all outcomes and comparisons performed, if on one hand HYBRID-IA finds slightly lower modularity values than LOUVAIN, but

outperforming all other metaheuristics, on the other hand, it is able to detect more similar communities to the real ones compared to those detected by LOUVAIN (see [51]).

Finally, in Chapter 13, I present the final conclusion of my thesis.

To sum up the main objectives in this thesis, they are as follows:

1. Investigate and solve deterministic models as dynamics of popularity of online contents, a closed-loop supply chain network for second-hand trading of high-uniqueness products and scheduling problem of speech-language pathologists.

2. Develop two-stage procurement planning model in a random environment, during emergency situations as health emergency or natural disasters.

3. Study the behavior of agents that have to escape or have to group in communities.

Chapter 1

Generalized Nash equilibrium and dynamics of popularity of online contents

1.1 Introduction

Online contents represent the largest part of Internet traffic. Individuals can use Internet to access as well as to distribute contents. Most of such contents are multimedia products posted online by the contents' owners. The content distribution is provided by user-generated content (UGC) platforms, like commercial platforms or social network platforms. One of the world's biggest UGC platform is YouTube, with more than 1,8 billion people registered on the site to watch daily 5 billion videos.

An important feature for the contents' owners is the viewcount, namely the number of times a content has been accessed. In fact, content providers can profit from their potential viewers. Due to the finite size of the browser's window, only

contents with the highest number of views can be visible on a webpage without scrolling. Therefore, providers are willing to promote their contents and accelerate the views. Platforms like YouTube provide tools to boast the distribution of contents, introducing recommendation lists and other ranking mechanisms. In addition, the popularity of a content can be increased by paying a cost for hosting advertisement. As a result, the content gains some priority in the recommendation lists and will be accessed more frequently. The acceleration mechanisms generate competition among content providers to obtain popularity, visibility and influence.

Game theory represents an excellent methodological framework for the investigation of decision-makers who compete amongst themselves and need to determine the benefit of advertisement investments so as to accelerate the views. The literature on the competition of online contents is vast and mainly focuses on the evolution of popularity of online contents; see [34, 35]. The aim is to develop models for early-stage prediction of contents' popularity. In [5, 6, 62], the authors model the behavior of contents' owners as a dynamic game. In addition, some acceleration mechanisms of views are incorporated in the formulation. In [85], the authors develop a non cooperative model for the diffusion of online contents. The content providers, the players, compete amongst themselves and seek to maximize their profits while investing in acceleration mechanisms. The underlying equilibrium concept is that of Nash equilibrium. The problem is then formulated as a variational inequality (see [78, 72] for backgrounds on variational inequalities), and the role of Lagrange multipliers is also analyzed.

In this paper, I extend the model in [85] in two directions. First, I require a reasonable limit to the number of times each viewer can access a content. I consider this limit as known and fixed: this generates common constraints to all

the providers. Thus, each player's strategy implicitly depends on the rival players' strategies through the shared constraints, and the governing concept is that of generalized Nash equilibrium (GNE).

GNE (see [7, 77, 76, 112, 176, 194]) is a generalization of the well-known Nash equilibrium problem (see [165, 166]), where each player's strategy set may depend on the rivals' strategies. There is a large interest in GNE problems, as there are many notable applications, ranging from economics to engineering; see [43, 60, 172]. If a Nash equilibrium problem, when each player solves a convex programming problem, can be formulated as a variational inequality (see, [78, 72]), GNE can be formulated as a quasi-variational inequality (see [112]). However, a GNE with shared constraints can be also obtained via a variational inequality; see [77, 76, 153]. Thus, I formulate our model as a variational inequality for which the existence of solutions is guaranteed.

Our second improvement of the model in [85] is the study of the continuous-time evolution of views and quality levels. In particular, I construct a locally projected dynamical system model, whose set of stationary points coincides with the set of solutions to the variational inequality. I also prove the stability of the unique solution via the strict monotonicity of the operator of the variational inequality. I describe a dynamic adjustment process for the evolution of the equilibrium pattern, and derive some important characteristics of the model, discussing some combinations of active and non-active constraints. I then present some numerical examples to illustrate our results.

The paper is organized as follows. In Section 1.2, I present the model, and give the variational inequality formulation. In Section 1.3, I recall some theoretical preliminaries. In Section 1.4, I discuss the stability of solutions, and, in Section

1.5, I provide the dynamic adjustment process. In Section 1.6, I illustrate some examples, and, finally, in Section 1.7, I draw our conclusions.

1.2 The game theory model

In this section, I present an online content diffusion network with views and quality competition, that consists of m content providers and n viewers, see Figure 1.1 (see also [85]). Each content provider i, $i = 1, \ldots, m$, posts one content that

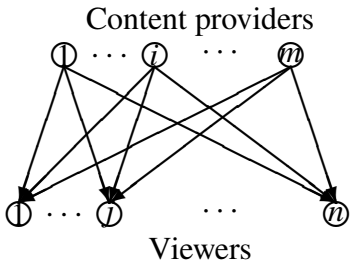

Figure 1.1: The two-layer online content diffusion network

can be accessed by each viewer j, $j = 1, \ldots, n$. The contents are assumed to be homogeneous, namely, of the same type (for instance, blogs, videos, podcasts, social media contents, ebooks, photos, etc.), and of a similar topic (for instance, music, travels, film reviews, recipes, etc.). The viewers can access each of the m contents at the first opportunity. Let $Q_{ij} \geq 0$ denote the accesses of content i selected by viewer j. I group the Q_{ij} elements for all j into the vector $Q_i \in \mathbb{R}^n_+$, and then I group all the vectors Q_i for all i into the vector $Q \in \mathbb{R}^{mn}_+$. In this model, I assume that Q_{ij} are continuous variables. This allows us to take into account whether a content is watched entirely or partially.

In addition, q_i denotes the quality level of content i and takes a value in the interval $I = [\underline{q}_i, \overline{q}_i] = [1, 5]$, from 1 = sufficient to 5 = excellent. I group the quality levels

of all providers into the vector $q \in \mathbb{R}^m_+$. All vectors here are assumed to be column vectors, except where noted.

I define the viewcount of content i, $i = 1, \ldots, m$, as the number of times content i has been fully accessed, and is given by $\left\lfloor \sum_{j=1}^{n} Q_{ij} \right\rfloor$. Usually, a content must reach a minimum amount of accesses to gain the interest of viewers and be in competition with the other homogeneous contents. I denote this threshold by $s > 0$. Thus, for each posted content i, the amount of views must satisfy the condition

$$\sum_{j=1}^{n} Q_{ij} \geq s, i = 1, \ldots, m. \tag{1.1}$$

Even if a content can be repeatedly accessed, it is reasonable to require a limit to the number of times a viewer can access a content. Hence, for each viewer j, I introduce an upper bound on the total amount of views, denoted by d_j. It suggests the satisfaction towards the contents posted by all the providers, and reflects the taste for the digital products. In addition, I assume d_j to be known and fixed, and the following condition must hold:

$$\sum_{i=1}^{m} Q_{ij} \leq d_j, \quad j = 1, \ldots, n. \tag{1.2}$$

Following network economic models as in [159, 160, 156], I now introduce specific functional forms which are then utilized in the numerical examples. I associate with each content provider i a production cost

$$f_i(Q, q_i), \quad i = 1, \ldots, m, \tag{1.3}$$

and assume that the production cost of provider i depends on the general attractiveness of the topic of the contents, namely, on the total amount of views, and on the quality of the content itself. I assume that the production cost is convex and continuously differentiable.

Due to the finite size of the browser's window, only contents with the highest number of views can appear in the recommendation lists, and be visible on a webpage without scrolling. Therefore, providers are willing to promote their contents and accelerate the views. Thus, I assume that providers pay a fee for the advertisement service in the UGC platform. Hence, for each provider i, I introduce the advertisement cost function

$$c_i \sum_{j=1}^{n} Q_{ij}, \quad i = 1, \dots, m, \tag{1.4}$$

with $c_i > 0$, $i = 1, \dots, m$. Similarly, the revenue of provider i (revenue for hosting advertisements, benefits from firms, etc.) is given by

$$p_i \sum_{j=1}^{n} Q_{ij}, \quad i = 1, \dots, m, \tag{1.5}$$

with $p_i > 0$, $i = 1, \dots, m$. Each viewer j reflects the preferences through the evaluation function that represents the feedback of the contents

$$E_j(Q, \bar{q}), \quad j = 1, \dots, n, \tag{1.6}$$

where $\bar{q} = \frac{1}{m} \sum_{i=1}^{m} q_i$ is the average quality level. Thus, I can write $E_j(Q, \bar{q}) = E_j(Q, q)$, for all j, and consider the case where the evaluation function may depend on the taste and the expertise of viewers, represented by the entire amount of accesses Q, and on the total quality level. Now, I can define the reputation or popularity function of provider i as the function

$$\sum_{j=1}^{n} E_j(Q, q) \cdot Q_{ij}, \quad i = 1, \dots, m. \tag{1.7}$$

I assume that the reputation function is concave and continuously differentiable. The content diffusion competition can be represented as a game where I define players, strategies and profits; see also [160]. Players are content providers,

who compete for the diffusion of their contents. Viewers are not strategic, and simply provide their preferences through their evaluation functions, that reflect the attractiveness of the topic of the contents, given by the entire amount of views, and on the average quality level. The scope of the game is to find the number of views and the quality target to maximize the profit and predict how much the advertisement strategies of content providers can be remunerative.

Strategic variables are content views Q and quality level q. Profit for player i is the difference between total revenues and total costs, namely,

$$U_i(Q,q) = \sum_{j=1}^{n} E_j(Q,q) \cdot Q_{ij} + p_i \sum_{j=1}^{n} Q_{ij} - f_i(Q,q_i) - c_i \sum_{j=1}^{n} Q_{ij},\ i = 1,\dots,m.$$

Let $\mathbb{K}_i$ denote the feasible set of content provider i, where

$$\mathbb{K}_i = \left\{(Q_i,q_i) \in \mathbb{R}^{n+1} :\ Q_{ij} \geq 0, \forall j; \sum_{j=1}^{n} Q_{ij} \geq s; \underline{q}_i \leq q_i \leq \overline{q}_i\right\}.$$

I also define $\mathbb{K} = \prod_{i=1}^{m} \mathbb{K}_i$.

In addition, players have to satisfy the shared constraints (1.2). Hence, I define the set $\mathcal{S}$ as follows:

$$\mathcal{S} = \left\{Q \in \mathbb{R}^{mn+m} : \sum_{i=1}^{m} Q_{ij} \leq d_j, \quad j = 1,\dots,n\right\}.$$

In my model, the m providers post their contents and behave in a non-cooperative fashion, each one trying to maximize his own profit. I note that the production cost functions capture competition for contents since the production cost of a particular provider depends not only on his views, but also on those of the other providers. Moreover, the evaluation functions show that viewers care about the quality level associated with their favorite contents, but also on that of the other contents, as well as the views. Since players have to satisfy the shared constraints (1.2), each

player's strategy vector (Q_i, q_i) belongs to the set $\mathbb{K}_i$, but implicitly depends on the rival players' strategies through the constraints $Q \in \mathcal{S}$. Therefore, the underlying equilibrium concept will be that of Generalized Nash equilibrium; see [77, 76, 112, 176].

Definition 1.2.1. (Generalized Nash equilibrium) *A view amount and quality level pattern* $(Q^*, q^*) \in \mathbb{K}, \forall Q \in \mathcal{S}$ *is said to be a Generalized Nash equilibrium if for each content provider* $i; i = 1, \ldots, m$,

$$U_i(Q_i^*, q_i^*, Q_{-i}^*, q_{-i}^*) \geq U_i(Q_i, q_i, Q_{-i}^*, q_{-i}^*), \quad \forall (Q_i, q_i) \in \mathbb{K}^i, \forall Q \in \mathcal{S}, \tag{1.8}$$

where Q_{-i} *denotes the amount of views of contents posted by all the providers except for* i. *Analogously,* q_{-i} *expresses the quality levels of all the providers' contents except for* i.

According to the above definition, a Generalized Nash equilibrium is established if no provider can unilaterally improve upon his profit by choosing an alternative vector of views and quality level, given the amount of views of the contents posted and quality level decisions of the other providers, and the shared constraints. The above GNE belongs to a special class of GNE problems, where the constraint functions that depend on rivals' strategies are identical for all players. A solution of such a GNE problem can be found solving a quasi-variational inequality as in [78, 112]. However, a GNE with shared constraints can be also obtained via a variational inequality; see [77, 76, 131, 142].

Definition 1.2.2. *Let us assume that for each content provider* i *the profit function* $U_i(Q, q)$ *is concave with respect to the variables* $(Q_{i1}, \ldots, Q_{in})$, *and* q_i, *and is continuous and continuously differentiable. A variational inequality approach to*

finding a GNE is to define the set $\mathcal{K} = \mathbb{K} \cap \mathcal{S}$*, and to solve the variational inequality*

$$-\sum_{i=1}^{m}\sum_{j=1}^{n}\frac{\partial U_i(Q^*,q^*)}{\partial Q_{ij}}\times\left(Q_{ij}-Q_{ij}^*\right)-\sum_{i=1}^{m}\frac{\partial U_i(Q^*,q^*)}{\partial q_i}\times\left(q_i-q_i^*\right)\geq 0, \quad (1.9)$$

$\forall (Q,q)\in\mathcal{K}$.

It is worth noting that, with the variational approach, the Lagrange multipliers for the shared constraints are identical for all players. Since players usually have different objective functions, the multipliers for the shared constraints are not necessarily equal. Thus, with the variational approach, only a part of the GNE can be found. In addition, as noted in [11] and references therein, it is not possible to obtain a full characterization of the solutions of a GNE problem as solutions of a variational inequality. For this reason, recently, the research of non variational equilibria has raised large interest; see [11, 80, 153]. However, in view of the study of the dynamics of this model, I adopt a variational approach to my GNE problem.

I can put the above variational inequality into the standard form. Thus, I define the $(mn+m)$-dimensional vector $X=(Q,q)$ and the $(mn+m)$-dimensional row vector $F(X)=(F^1(X),F^2(X))$, with the (i,j)-th component of $F^1(X)$, and the i-th component of $F^2(X)$, respectively, given by

$$F_{ij}^1(X)=-\frac{\partial U_i(Q,q)}{\partial Q_{ij}},\quad F_i^2(X)=-\frac{\partial U_i(Q,q)}{\partial q_i}.$$

Then, problem (1.9) can be written as

$$\langle F(X^*),X-X^*\rangle\geq 0,\forall X\in\mathcal{K}. \quad (1.10)$$

Problem (1.9) or (1.10) admits a solution since the classical existence theorem, which requires that the set $\mathcal{K}$ is closed, convex, and bounded, and the operator is continuous, is satisfied (see [78, 148]).

1.3 Theoretical preliminaries

I recall some typical concepts of convex analysis (see, for instance, [120, 193]), and confine my attention to the Euclidean space. Let $\Omega \subseteq \mathbb{R}^n$ be a non-empty, closed and convex set, the tangent cone to Ω at x, $T_\Omega(x)$, and the normal cone to Ω at x, $N_\Omega(x)$, are defined, respectively, by

$$T_\Omega(x) = \overline{\cup_{h>0}(\Omega - x)/h}, \quad N_\Omega(x) = \{v \in \mathbb{R}^n : \langle v, y - x\rangle \leq 0, \forall y \in \Omega\}.$$

If $\Omega \subseteq \mathbb{R}^n$ is a polyhedral set, namely,

$$\Omega = \{x : \langle a_i, x\rangle \leq \alpha_i, i = 1, \ldots, m\},$$

where $a_i \in \mathbb{R}^n$ and $\alpha_i \in \mathbb{R}$, $\forall i$, then it results

$$N_\Omega(x) = \{y_1 a_1 + \ldots, y_m a_m | y_i \geq 0, i \in I(x), y_i = 0, \forall i \notin I(x)\},$$
$$I(x) = \{i : \langle a_i, x\rangle = \alpha_i\}.$$

If $C = C_1 \times \cdots \times C_m$ for closed sets $C_i \in \mathbb{R}^{n_i}$, $n_i \in \mathbb{N}$ for all i, then at any $\bar{x} = (\bar{x}_1, \ldots, \bar{x}_m)$ with $\bar{x}_i \in C_i$, I have $N_C(\bar{x}) = N_{C_1}(\bar{x}_1) \times \cdots \times N_{C_m}(\bar{x}_m)$. Let us introduce the projection operator $P_\Omega : \mathbb{R}^n \to \Omega$, where $P_\Omega(z)$ is such that

$$\|P_\Omega(z) - z\| = \inf_{y \in \Omega} \|y - z\|.$$

I also consider the operator $\Pi_\Omega : \Omega \times \mathbb{R}^n \to \mathbb{R}^n$, defined by the directional derivative

$$\Pi_\Omega(x, v) = \lim_{t \to 0} \frac{P_\Omega(x + tv) - x}{t}.$$

Thus, $\Pi_\Omega(x, v) = P_{T_\Omega(x)}(v)$, namely, $\Pi_\Omega(x, v)$ is the metric projection of v onto the tangent cone to Ω at x. In addition, as in [40] and references therein, there exists $n \in N_\Omega(x)$ such that

$$v \in \Pi_\Omega(x, v) + n. \tag{1.11}$$

Following [72, 164], a locally projected dynamical system (PDS) is an ordinary differential equation of the form

$$\dot{x} = \Pi_{\Omega}(x, -\varphi(x)), \tag{1.12}$$

where $\varphi : \Omega \to \mathbb{R}^n$ is a given vector field. A solution to (1.12) is a function $x : [0, \infty) \to \Omega$ that is absolutely continuous and satisfies

$$\dot{x}(t) = \Pi_{\Omega}(x(t), -\varphi(x(t))),$$

except for a set of Lebesgue measure zero.

The problem is complemented by the initial condition $x(0) = x^0 \in \Omega$. Problem (1.12) is a non standard ordinary differential equation, where the right-hand side is related to the projection operator, and thus, is discontinuous on the boundary of Ω. I also note that a solution of the dynamical system belongs to the constraint set Ω. A vector x^* is a critical point or stationary point of the locally projected dynamical system if x^* satisfies

$$\Pi_{\Omega}(x^*, -\varphi(x^*)) = 0.$$

This means that once the locally projected dynamical system reaches x^* at some time $t \geq 0$, it will remain at x^* for all future times.

An important feature of locally projected dynamical systems is that the set of stationary points coincides with the set of solutions of the finite-dimensional and time-independent variational inequality (see [72])

$$\langle \varphi(x^*), x - x^* \rangle \geq 0, \quad \forall x \in \Omega.$$

Moreover, problem (1.3) is equivalent to $\dot{x} = P_{T_{\Omega}(x)}\Big(- \varphi(x)\Big)$. Due to (1.11), the initial value problem

$$\dot{x} = \Pi_{\Omega}(x, -\varphi(x)), \quad x(0) = x^0 \in \Omega \tag{1.13}$$

consists in finding the solution of minimal norm to the initial condition $x(0) = x^0 \in \Omega$ and the differential variational inequality

$$\dot{x}(t) = -\Big(N_\Omega(x(t)) + \varphi(x(t))\Big). \tag{1.14}$$

The above problem is, in turn, equivalent to finding the solution of minimal norm to the initial condition $x(0) = x^0 \in \Omega$ and the projected variational inequality

$$\dot{x}(t) \in P_{T_\Omega(x(t))}\Big(-\varphi(x(t))\Big).$$

The following result gives the existence of PDS (see [72]).

Theorem 1.3.1. *Let $\Omega \subset \mathbb{R}^n$ be a polyhedron. Suppose that $x^0 \in \Omega$, and assume that $\varphi : \Omega \to \mathbb{R}^n$ is a vector field with linear growth, namely, there exists $M > 0$ so that for all $x \in \Omega$, $\|\varphi(x)\| \leq M(1 + \|x\|)$. Then, the initial value problem* (1.13) *has unique absolutely continuous solution on the interval* $[0, \infty[$.

I note that Lipschitz continuity implies the linear growth assumption and, hence, it is a sufficient condition for the existence of a unique solution to locally projected dynamical systems.

1.4 Stability of solutions

In this section, I focus my attention on the stability of solutions under perturbations; see [40, 156, 164]. In the theory of PDS, monotonicity concept and its extensions are connected to stability. In fact, monotonicity describes the behavior of perturbed equilibria and show the existence of periodic cycles.

I consider variational inequality (1.10) and the associated locally projected dynamical system

$$\dot{X} = \Pi_{\mathcal{K}}(X, -F(X)), \quad X(0) = X^0 \in \mathcal{K}. \tag{1.15}$$

Definition 1.4.1. *A mapping $F : \mathcal{K} \to \mathbb{R}^{mn+m}$ is said to be*

- *monotone if*

$$\langle F(X) - F(Y), X - Y\rangle \geq 0, \forall X, Y \in \mathcal{K}.$$

- *strictly monotone if*

$$\langle F(X) - F(Y), X - Y\rangle > 0, \forall X, Y \in \mathcal{K}, X \neq Y.$$

- *strongly monotone if there exists $\mu > 0$ such that*

$$\langle F(X) - F(Y), X - Y\rangle \geq \mu\|X - Y\|^2, \forall X, Y \in \mathcal{K}.$$

In the following, $B(X^*, \delta)$ denotes the open ball centered at X^* with radius δ. I now recall some definitions; see [177] for further discussions and examples.

Definition 1.4.2. *Let X^* be a critical point of (1.15).*

- *X^* is called monotone attractor if there exists $\delta > 0$ such that, for every solution $X(t)$ with $X(0) \in B(X^*, \delta) \cap \mathcal{K}$, $\|X(t) - X^*\|$ is a non increasing function of t.*
- *X^* is a strictly monotone attractor if $\|X(t) - X^*\|$ is decreasing to 0 in t.*
- *X^* is a strictly global monotone attractor if the above property holds for any solution $X(t)$ such that $X(0) \in \mathcal{K}$.*
- *X^* is exponentially stable if the solutions starting from points close to X^* are convergent to X^* with exponential rate, namely, if there is $\delta > 0$ and two constants $b > 0$ and $C > 0$ such that for every solution $X(t)$, with $X(0) \in B(X^*, \delta) \cap \mathcal{K}$, it results*

$$\|X(t) - X^*\| \leq C\|X(0) - X^*\|e^{-bt}, \quad \forall t \geq 0.$$

- *X^* is globally exponentially stable if the above property holds for all solutions $X(t)$ such that $X(0) \in \mathcal{K}$.*

I also recall a stability theorem; see [164].

Theorem 1.4.1. *Suppose that X^* solves* (1.10).

(i) If F is monotone, then X^* is a global monotone attractor for the content diffusion dynamics.

(ii) If F is strictly monotone, then X^* is a strictly global monotone attractor for the content diffusion dynamics.

(iii) If F is strongly monotone, then X^* is globally exponentially stable for the content diffusion dynamics.

Definition 1.4.3. *For each provider i, the production cost $f_i(Q, q_i)$ is said to be additive if*

$$f_i(Q, q_i) = f_i^1(Q_i) + f_i^2(Q_{-i}) + f_i^3(q_i),$$

where Q_{-i} denotes the views of the rivals of provider i.
For each viewer j, the evaluation function $E_j(Q, q)$ is said to be additive if

$$E_j(Q, q) = \tilde{E}_j(Q) + E_j^1(q_1) + \cdots + E_j^m(q_m).$$

Theorem 1.4.2. *The operator F of the variational inequality* (1.10) *is strictly monotone if the production cost f_i, $i = 1, \ldots, m$, are additive, f_i^l are strictly convex, $i = 1, \ldots, m$, $l = 1, 2, 3$, $E_j(Q, q)$, $j = 1, \ldots, n$, are additive, $-E(Q, q) = (-E_j(Q, q))_j$, $j = 1, \ldots, n$, are strictly monotone with respect to Q, $\tilde{E}_j(Q) = \tilde{E}_j \sum_{i=1}^m Q_{ij}$, with $\tilde{E}_j < 0$, $j = 1, \ldots, n$, and $-E_j^i(q_i) \cdot Q_{ij}$, $i = 1, \ldots, m$, $j = 1, \ldots, n$, are strictly convex functions with respect to q_i.*

Proof. Let $X' = (Q', q'), X'' = (Q'', q''), X \neq Y$. I consider

$$\begin{aligned}
&\langle F(X') - F(X''), X' - X'' \rangle \\
&= \sum_{i=1}^{m} \sum_{j=1}^{n} \left[\frac{\partial f_i(Q', q_i')}{\partial Q_{ij}} - \frac{\partial f_i(Q'', q_i'')}{\partial Q_{ij}} \right] \times (Q_{ij}' - Q_{ij}'') \\
&- \sum_{i=1}^{m} \sum_{j=1}^{n} \left[E_j(Q', q') + \sum_{k=1}^{n} \frac{\partial E_k(Q', q')}{\partial Q_{ij}} \cdot Q_{ik}' - E_j(Q'', q'') \right. \\
&\left. - \sum_{k=1}^{n} \frac{\partial E_k(Q'', q'')}{\partial Q_{ij}} \cdot Q_{ik}'' \right] \times (Q_{ij}' - Q_{ij}'') \\
&+ \sum_{i=1}^{m} \left[\frac{\partial f_i(Q', q_i')}{\partial q_i} - \frac{\partial f_i(Q'', q_i'')}{\partial q_i} \right] \times (q_i' - q_i'') \\
&- \sum_{i=1}^{m} \left[\sum_{k=1}^{n} \frac{\partial E_k(Q', q')}{\partial q_i} \cdot Q_{ik}' - \frac{\partial E_k(Q'', q'')}{\partial q_i} \cdot Q_{ik}'' \right] \times (q_i' - q_i'').
\end{aligned}$$

Since f_i, $i = 1, \ldots, m$, are additive, and f_i^l are strictly convex functions, $i = 1, \ldots, m$, $l = 1, 2, 3$, I have

$$\begin{aligned}
&\sum_{i=1}^{m} \sum_{j=1}^{n} \left[\frac{\partial f_i(Q', q_i')}{\partial Q_{ij}} - \frac{\partial f_i(Q'', q_i'')}{\partial Q_{ij}} \right] \times (Q_{ij}' - Q_{ij}'') \\
&+ \sum_{i=1}^{m} \left[\frac{\partial f_i(Q', q_i')}{\partial q_i} - \frac{\partial f_i(Q'', q_i'')}{\partial q_i} \right] \times (q_i' - q_i'') \\
&= \sum_{i=1}^{m} \sum_{j=1}^{n} \left[\frac{\partial f_i^1(Q')}{\partial Q_{ij}} - \frac{\partial f_i^1(Q'')}{\partial Q_{ij}} \right] \times (Q_{ij}' - Q_{ij}'') \\
&+ \sum_{i=1}^{m} \left[\frac{\partial f_i^3(q_i')}{\partial q_i} - \frac{\partial f_i^3(q_i'')}{\partial q_i} \right] \times (q_i' - q_i'') > 0.
\end{aligned}$$

Due to strict monotonicity of $-E(Q, q)$ with respect to Q, I have

$$- \sum_{i=1}^{m} \sum_{j=1}^{n} \left[E_j(Q', q') - E_j(Q'', q'') \right] \times (Q_{ij}' - Q_{ij}'') > 0.$$

Moreover, $E_j(Q, q)$, $j = 1, \ldots, n$ are additive, and $\tilde{E}_j(Q) = \tilde{E}_j \sum_{i=1}^{m} Q_{ij}$, with

$\tilde{E}_j < 0$, $j = 1, \ldots, n$, then I find

$$
\begin{aligned}
&- \sum_{i=1}^{m} \sum_{j=1}^{n} \left[\sum_{k=1}^{n} \frac{\partial E_k(Q', q')}{\partial Q_{ij}} \cdot Q'_{ik} - \sum_{k=1}^{n} \frac{\partial E_k(Q'', q'')}{\partial Q_{ij}} \cdot Q''_{ik} \right] \times (Q'_{ij} - Q''_{ij}) \\
&= - \sum_{i=1}^{m} \sum_{j=1}^{n} \left[\sum_{k=1}^{n} \frac{\partial \tilde{E}_k(Q')}{\partial Q_{ij}} \cdot Q'_{ik} - \sum_{k=1}^{n} \frac{\partial \tilde{E}_k(Q'')}{\partial Q_{ij}} \cdot Q''_{ik} \right] \times (Q'_{ij} - Q''_{ij}) \\
&= - \sum_{i=1}^{m} \sum_{j=1}^{n} \tilde{E}_j \left(Q'_{ij} - Q''_{ij} \right)^2 > 0.
\end{aligned}
$$

Finally, $-E^i_j(q_i) \cdot Q_{ij}$, $i = 1, \ldots, m$, $j = 1, \ldots, n$ are strictly convex functions with respect to q_i, then I have

$$
\begin{aligned}
&- \sum_{i=1}^{m} \left[\sum_{k=1}^{n} \frac{\partial E_k(Q', q')}{\partial q_i} \cdot Q'_{ik} - \frac{\partial E_k(Q'', q'')}{\partial q_i} \cdot Q''_{ik} \right] \times (q'_i - q''_i) \\
&= - \sum_{i=1}^{m} \left[\sum_{k=1}^{n} \frac{\partial E^i_k(q'_i)}{\partial q_i} \cdot Q'_{ik} - \frac{\partial E^i_k(q''_i)}{\partial q_i} \cdot Q''_{ik} \right] \times (q'_i - q''_i) > 0.
\end{aligned}
$$

Thus, I conclude that F is strictly monotone. □

Now, I am able to state the following result.

Theorem 1.4.3. *Under the assumption of Theorem* 1.4.2*, the variational inequality* (1.10) *has at most one solution, which is a global strictly monotone attractor for the content diffusion dynamics.*

1.5 Dynamics of contents diffusion

I now propose a dynamic adjustment process for the evolution of content providers' views and quality levels. I consider the locally projected dynamical system associated with variational inequality (1.9)

$$
\dot{X} = \frac{dX(t)}{dt} = \Pi_{\mathcal{K}}(X, -F(X)) = P_{T_{\mathcal{K}}(X)}(-F(X)).
$$

By Theorem 1.4.3 and inclusion (1.14), the unique optimal strategy for my game is $X^* \in \mathcal{K}$, where X^* is the solution of the inclusion $-F(X) \in N_{\mathcal{K}}(X)$.

I note that the strategy set $\mathcal{K}$ can be written into the form $\mathcal{K} = \mathcal{K}^1 \times \mathcal{K}^2$, where

$$\mathcal{K}^1 = \left\{ Q \in \mathbb{R}^{mn} : \ Q_{ij} \geq 0, \forall i, j; \sum_{j=1}^{n} Q_{ij} \geq s, \forall i; \sum_{i=1}^{m} Q_{ij} \leq d_j, \forall j \right\},$$

$$\mathcal{K}^2 = \left\{ q \in \mathbb{R}^m : \underline{q}_i \leq q_i \leq \overline{q}_i, \forall i \right\}.$$

Therefore, $N_{\mathcal{K}}(X) = N_{\mathcal{K}}(Q, q) = N_{\mathcal{K}^1}(Q) \times N_{\mathcal{K}^2}(q)$.

Under the additivity assumptions as in Definition 1.4.3, for all i, j, I set

$$\tilde{F}^1_{ij}(Q, q) = c_i + \frac{\partial f^1_i(Q)}{\partial Q_{ij}} - p_i - E_j(Q, q) - \sum_{k=1}^{n} \frac{\partial \tilde{E}_k(Q)}{\partial Q_{ij}} \cdot Q_{ik},$$

$$\tilde{F}^2_i(Q, q) = \frac{\partial f^3_i(q_i)}{\partial q_i} - \sum_{k=1}^{n} \frac{\partial E^i_k(q)}{\partial q_i} \cdot Q_{ik}.$$

If X^* solves the inclusion $-F(X) \in N_{\mathcal{K}}(X)$, then

$$-\tilde{F}^1(Q^*, q^*) = \left(-\tilde{F}^1_{ij}(Q, q) \right)_{i,j} \in N_{\mathcal{K}^1}(Q^*),$$

$$-\tilde{F}^2(Q^*, q^*) = \left(-\tilde{F}^2_i(Q, q) \right)_i \in N_{\mathcal{K}^2}(q^*).$$

Moreover, I note that $N_{\mathcal{K}^2}(q^*) = N_{[\underline{q}_1, \overline{q}_1]}(q^*_1) \times \cdots \times N_{[\underline{q}_m, \overline{q}_m]}(q^*_m)$.

I now focus on some combinations of active and non-active constraints that are more interesting to my purposes.

1. If $\sum_{j=1}^{n} Q^*_{ij} = s$ for all i, the normal cone is generated by vectors with negative components; hence, $-\tilde{F}^1(Q^*, q^*) < 0$.

2. If $\sum_{i=1}^{m} Q^*_{ij} = d_j$, for all j, the normal cone is generated by vectors with positive components; hence, $-\tilde{F}^1(Q^*, q^*) > 0$.

3. If $\sum_{i=1}^{m} Q_{ij}^* < d_j$, for all j, and $\sum_{j=1}^{n} Q_{ij}^* > s$, for all i, then $N_{\mathcal{K}^1}(Q^*) = \{0\}$; hence, $\tilde{F}^1(Q^*, q^*) = 0$.

4. If $q_i^* = \underline{q}_i$, for all i,$N_{[\underline{q}_i, \overline{q}_i]}(\underline{q}_i)$ contains vectors with negative components; hence $-\tilde{F}^2(Q^*, q^*) < 0$.

5. If $q_i^* = \overline{q}_i$, for all i, $N_{[\underline{q}_i, \overline{q}_i]}(\overline{q}_i)$ contains vectors with positive components; hence $-\tilde{F}^2(Q^*, q^*) > 0$.

6. If $\underline{q}_i < q_i^* < \overline{q}_i$, for all i, $N_{[\underline{q}_i, \overline{q}_i]}(q_i^*) = \{0\}$; hence, $\tilde{F}^2(Q^*, q^*) = 0$.

I now discuss the main scenarios:

Case 1.5.1. *The game can be monotonically attracted to $X^* = (Q^*, q^*)$, with $\sum_{j=1}^{n} Q_{ij}^* = s$ for all i and $q^* = \underline{q}$. This means that $-\tilde{F}^1(Q^*, q^*) < 0$, namely, the marginal profit with respect to views is negative. In addition, $-\tilde{F}^2(Q^*, q^*) < 0$, namely, the marginal profit with respect to quality level is negative. As a consequence, the investment in acceleration mechanisms is not advantageous for the content providers. The quality level is low as well as the views, there is no successful strategy to increase profits.*

Case 1.5.2. *The game can be monotonically attracted to $X^* = (Q^*, q^*)$, with $\sum_{j=1}^{n} Q_{ij}^* = s$ for all i and $q^* = \overline{q}$. This means that $-\tilde{F}^1(Q^*, q^*) < 0$, that is, the marginal profit view-wise is negative. Moreover, $-\tilde{F}^2(Q^*, q^*) > 0$, that is, the marginal profit quality-wise is positive. The content is very good, but still unpopular to make investments in acceleration mechanisms be profitable.*

Case 1.5.3. *The game can be monotonically attracted to $X^* = (Q^*, q^*)$, with $\sum_{j=1}^{n} Q_{ij}^* = s$ for all i and $\underline{q} < q^* < \overline{q}$. Thus, $-\tilde{F}^1(Q^*, q^*) < 0$, namely, the marginal profit view-wise is negative. I also have $\tilde{F}^2(Q^*, q^*) = 0$, namely, the*

total marginal revenue equals the total marginal cost quality-wise. Thus, there is no incentive to invest in acceleration mechanisms. Providers are indifferent to improving quality level.

Case 1.5.4. *The game can be monotonically attracted to* $X^* = (Q^*, q^*)$*, with* $\sum_{i=1}^{m} Q_{ij}^* = d_j$ *for all* j *and* $q^* = \underline{q}$*; this means that* $-\tilde{F}^1(Q^*, q^*) > 0$*, namely, the marginal profit view-wise is positive. In addition,* $-\tilde{F}^2(Q^*, q^*) < 0$*, namely, the marginal profit quality-wise is negative. Investments in acceleration mechanisms can be profitable. The contents reached their lifetime, hence, improving quality level is not convenient.*

Case 1.5.5. *The game can be monotonically attracted to* $X^* = (Q^*, q^*)$*, with* $\sum_{i=1}^{m} Q_{ij}^* = d_j$ *for all* j *and* $q^* = \overline{q}$*. This means that* $-\tilde{F}^1(Q^*, q^*) > 0$*, that is, the marginal profit view-wise is positive. Moreover,* $-\tilde{F}^2(Q^*, q^*) > 0$*, that is, the marginal profit quality-wise is positive. Investing in both acceleration mechanisms and quality improvement is a successful strategy, even if the contents reached their lifetime.*

Case 1.5.6. *The game can be monotonically attracted to* $X^* = (Q^*, q^*)$*, with* $\sum_{i=1}^{m} Q_{ij}^* = d_j$ *for all* j *and* $\underline{q} < q^* < \overline{q}$*. Thus,* $-\tilde{F}^1(Q^*, q^*) > 0$*, namely, the marginal profit view-wise is positive. I also have* $\tilde{F}^2(Q^*, q^*) = 0$*. Thus, investing in acceleration mechanisms can be profitable. Providers are indifferent to improving quality level.*

Case 1.5.7. *The game can be monotonically attracted to* $X^* = (Q^*, q^*)$*, with* $\sum_{i=1}^{m} Q_{ij}^* < d_j$*, for all* j*,* $\sum_{j=1}^{n} Q_{ij}^* > s$*, for all* i*, and* $\underline{q} < q^* < \overline{q}$*. In this case,* $\tilde{F}^1(Q^*, q^*) = \tilde{F}^2(Q^*, q^*) = 0$*, and, hence, the marginal revenues equal the marginal costs. Providers are indifferent to both investing in acceleration*

mechanisms and improving quality level.

1.6 Numerical examples

Youtube is now the world's second biggest search engine with more than 1,8 billion people registered on the site to watch daily 5 billion videos. Every 60 seconds more than 300 hours of HD quality video are uploaded to YouTube to generate the massive collection of 1,300,000,000 videos. The major structure unit that YouTube is built on is a channel. There are hundreds of thousands channels; some have very few subscribers and some are very popular.

One of the main features of Youtube, is that people, as well as video contents published may become very popular. A large number of viewers allows video creators to profit from the volume of traffic that their videos generates. On YouTube, video creators can take part in the YouTube Partner Program (in short, YTPP), see [1], and monetize contents through a variety of ways including advertisements, paid subscriptions, and merchandise. Specific terms to these agreements are often reserved, but it is known that Google keeps 45% of YouTube advertising revenue. The advertising can take the form of a banner advertisement, a pre-video commercial, or an in-video box advertisement. The system monitors video views, ad clicks, and other metrics that convert the videos' popularity into a monetary value that can be charged to advertisers and then shared with partners of YTPP. The key to attracting advertisers is having good contents that are able to capture a large number of viewers and subscribers.

The revenue for content's owner is based on the cost per mille (CPM) system or

[1] https://support.google.com/youtube/answer/72851?hl=en - V,v., A,a.: What is the YouTube Partner Program?, GOOGLE

on a cost per click (CPC) system. The CPM system assigns an advertisement cost per one thousand views; whereas the CPC assigns an advertisement cost per each view. Recently, YouTube has tightened the rules around the YTPP and applies new eligibility policy to all existing channels, so that channels that fail to meet the threshold will no longer be able to make income from advertisement.

I now apply the achievements to some numerical examples. Even if the examples are of small dimensions, my setting is not restrictive, since my aim is to show the feasibility of my model and the effectiveness of my approach. I consider a population of users divided into social groups, each having a different characteristic according to a certain criterion (for instance, hobbies, age, education, etc...). Therefore, viewers of the same group are aggregated together and represented as a single viewer. The variational solutions of the examples are implemented as an M-script file of MatLab and are solved by applying the extragradient method with constant steplength as in [128] (see also [167] for further discussions on efficient computational procedures).

Example 1 I consider two channel creators who post one video each, and two groups of aggregated viewers. I assume that both YouTubers are eligible for the YTPP. The data for this example were constructed for easy interpretation purposes. The production cost functions are assumed to be:

$$f_1(Q, q_1) = 0.2Q_{11}^2 + 0.2Q_{12}^2 + q_1^2,$$
$$f_2(Q, q_2) = 0.2Q_{21}^2 + 0.5Q_{22}^2 + 0.5q_2^2.$$

The evaluation functions for each viewer are:

$$E_1(Q, q) = -0.1(Q_{11} + Q_{21})^4 + 0.5(q_1 + q_2) + 58,$$
$$E_2(Q, q) = -0.1(Q_{12} + Q_{22})^4 + 0.5(q_1 + q_2) + 126.$$

I consider Q_{ij} in the order of tens of thousand. I assume that the advertiser pays 6$ every click to YouTuber 1 and 7$ to YouTuber 2. Moreover, YouTube takes the 45% of the advertisement payment; hence, YouTuber 1 pays 2.7$ every view and YouTuber 2 pays 3.15$ every view.

I set: $p_1 = 6, c_1 = 2.7, p_2 = 7, c_2 = 3.15, d_1 = 5, d_2 = 4$.

The assumptions of Theorem 1.4.2 are verified; hence, the variational inequality associated with the GNE problem has at most one solution, which is a global strictly monotone attractor for the content diffusion dynamics. I first seek for variational solutions. Assuming that the shared constraints are satisfied as equalities, I find the equilibrium solution

$$Q_{11}^* = 2.49454;\ Q_{12}^* = 3.00577;\ Q_{21}^* = 2.50546;\ Q_{22}^* = 2.99423;$$

$$q_1^* = 1.37509;\ q_2^* = 2.74987.$$

I observe that, even if the second content is better than the first one, the viewcount for YouTuber 1 (55, 003 views) is very close to that of YouTuber 2 (54, 996 views). The reason could be that the first YouTuber is more popular than the second one, and his followers access his contents even if the quality is not high. The total profit of YouTuber 1 is 25, 067.5 $, and the total profit of YouTuber 2 is 9, 439.44$. Thus, the advertisement strategy for YouTuber 1 is more profitable.

I can also consider non variational solutions, applying KKT conditions to the

optimization problems of the YouTubers. I find

$$
\begin{aligned}
Q_{11}^* &= 1.27778 + 0.555556\lambda_1 + 3.88889\lambda_2,\\
Q_{12}^* &= 3.61111 + 1.22222\lambda_1 + 0.555556\lambda_2,\\
Q_{21}^* &= 3.72222 - 0.555556\lambda_1 - 3.88889\lambda_2,\\
Q_{22}^* &= 2.38889 - 1.22222\lambda_1 - 0.555556\lambda_2,\\
q_1^* &= 1.22222 + 0.444444\lambda_1 + 1.11111\lambda_2,\\
q_2^* &= 3.05556 - 0.888889\lambda_1 - 2.22222\lambda_2.
\end{aligned}
$$

where λ_1, λ_2 are the Lagrange multipliers attached to the shared constraints and can be opportunely chosen. For instance, I may have

$$
\begin{aligned}
&-0.125 < \lambda_1 \leq 0.5\\
&3.58932 \cdot 10^{-30}(-5.57209 \cdot 10^{28} - 1.11442 \cdot 10^{29}\lambda_1) \leq \lambda_2\\
&\leq 1.31148 \cdot 10^{-29}(7.05309 \cdot 10^{28} - 3.04999 \cdot 10^{28}\lambda_1)
\end{aligned}
$$

It is worth noting that under the assumption that the shared constraints are equalities, the game results in a Pseudo-Nash equilibrium problem, and all the solutions can be obtained by solving a suitable variational inequality. I address the interested reader to [11].

Example 2 I consider the case of two YouTubers and six aggregated viewers. The production cost functions are:

$$
\begin{aligned}
f_1(Q, q_1) &= 0.00089(Q_{14} + Q_{15} + Q_{16})^2 + 0.5Q_{13}^2 + 0.4Q_{12}^2 + 0.5Q_{11}^2 + q_1^2,\\
f_2(Q, q_2) &= 0.00089(Q_{21} + Q_{22} + Q_{23})^2 + 0.3Q_{26}^2 + 0.2Q_{24}^2 + 0.4Q_{25}^2 + 1.2q_2^2.
\end{aligned}
$$

The evaluation functions of each viewer are:

$$E_1(Q,q) = -3(Q_{11}+Q_{21}) + 0.5(q_1+q_2) + 10,$$
$$E_2(Q,q) = -2(Q_{12}+Q_{22}) + 0.5(q_1+q_2) + 9,$$
$$E_3(Q,q) = -1.5(Q_{13}+Q_{23}) + 0.5(q_1+q_2) + 7,$$
$$E_4(Q,q) = -3(Q_{14}+Q_{24}) + 0.5(q_1+q_2) + 6,$$
$$E_5(Q,q) = -2.5(Q_{15}+Q_{25}) + 0.5(q_1+q_2) + 8.5,$$
$$E_6(Q,q) = -3.5(Q_{16}+Q_{26}) + 0.5(q_1+q_2) + 7.5.$$

I set: $p_1 = 6$, $c_1 = 2.7$, $p_2 = 7$, $c_2 = 3.15$, $s = 0.5$, $d_1 = 5$, $d_2 = 7$, $d_3 = 8$, $d_4 = 4$, $d_5 = 5$, and $d_6 = 4$.

The assumptions of Theorem 1.4.2 are verified, and the variational inequality associated with this game has at most one solution, which is a global strictly monotone attractor for the content diffusion dynamics.

The variational solutions with active shared constraints are:

$Q_{11} = 2.0674$; $Q_{12} = 2.80663$; $Q_{13} = 2.86795$; $Q_{14} = 2.03715$; $Q_{15} = 2.74789$; $Q_{16} = 2.08392$; $Q_{21} = 2.9326$; $Q_{22} = 4.19337$; $Q_{23} = 5.13205$; $Q_{24} = 1.96285$; $Q_{25} = 2.25211$; $Q_{26} = 1.91608$; $q_1 = 3.65274$; $q_2 = 3.83105$.

In this case, the second content is slightly better than the first one and the viewcount for YouTuber 2 (183, 890 views) is more than that of YouTuber 1 (146, 109 views). YouTuber 2 earns 234, 307.7 \$, whereas YouTuber 1 earns 46, 338.8 \$. Thus, for YouTuber 2 the advertisement strategy is more profitable.

Obviously, the above examples are highly stylized, however they show the efficacy of the model. One can now conduct numerous simulations by altering the data as well as adding decision-makers with their associated functions.

1.7 Conclusions

In this chapter, I introduced a dynamic network game theory model of online contents' competition, with a known and fixed limit to the number of times each viewer could access a content. This requirement generated shared constraints for all the providers. The model resulted in a GNE problem because both the providers' profit functions and their feasible sets depend on the rival players' strategies. Due to the common constraints, I proposed a variational inequality formulation, rather than a quasi-variational inequality one. I then provided a continuous-time adjustment process, guaranteed existence and uniqueness of the dynamic trajectories, and gave conditions for the stability analysis, using a monotonicity approach. The results in this work add to the growing literature on modeling and analysis of UGC platforms. As further research issues, I could study the connection with potential games, see [79, 196]. Moreover, in order to incorporate the viewers in the model, I could investigate a bilevel formulation of the problem in which the viewers are followers and the providers are leaders, see [133].

Chapter 2

Time-Dependent Generalized Nash Equilibria in Social Media Platforms

2.1 Introduction

Nowadays, due to the development of new technologies, smartphones and internet connectivity devices are becoming cheaper and easier to access, thus expanding the possibilities to approach other people. Every year, there is an increasing number of people signing up for social media. In 2019, there were around 2.77 billion people using social media, and, in 2021, more than 3 billion people were using social media. Of course, the rising popularity boosts social media company profits. YouTube is the largest video-sharing social media site in the world. Users may upload videos on the platform, view videos from other users, and interact with them. In 2019, it had an average of 2.3 billion monthly active users. YouTube users spend an average of 23.2 hours per month on the Android app watching videos on the platform. In this paper, I study the competition among the creators of user generated contents posted on a social media platform. Specifically, I consider

a two-layer dynamic network consisting of creators and viewers. Each creator seeks to determine the optimal views and likes, so as to maximize the profit. I assume that there is a known and fixed upper bound on the total amount of views and, hence, I formulate the competitive interaction of creators as a time-dependent generalized Nash equilibrium. Generalized Nash equilibrium problems (GNEPs) are non-cooperative games where the strategy of each player may depend on the strategies of the rivals. A large class of problems can be formulated as GNEPs, such as oligopolies, transportation networks, and electricity market models. In [194], Rosen introduced a case of GNEPs where the players have to share some constraints. For this class of problems, in [76] the authors showed that in finite dimensional spaces, certain solutions can be computed by solving a variational inequality and that the KKT multipliers of all players are equal. An infinite dimensional formulation of GNEPs was studied in [12], where the formulation of the GNEP as an evolutionary variational inequality problem is proved in the general setting of quasi convex functions. In [83], the authors extended the result in [76] to an infinite-dimensional functional setting. In [147], the authors studied GNEPs in Lebesgue spaces by means of a family of variational inequalities parameterized by an L^∞ vector. Other contributions to the search of non variational solutions are given in [11, 80]. Motivated by all the above analysis, I construct a dynamic equilibrium model of the competition among creators on a social media platform. Our contribution consists in improving the models in [85, 89] by considering time-varying data. In addition, I consider as our decision variables the views, given by a fraction of the number of subscribers, and the likes. Then, the problem is modelled as a time-dependent generalized Nash equilibrium, and, using the concept of variational equilibrium, I derive an evolutionary variational

inequality formulation. This gives rise to challenging problems in both theory and computations (see [54]). Moreover, following [36] I formulate the competition problem as a dynamic game, derived from an infinitely repeated simultaneous game. Therefore, I propose a unified approach and provide a differential game formulation for the dynamic generalized Nash equilibrium model. The paper is organized as follows. In Section 2.2, I introduce the game theory model, and give the related optimization problem. In Section 2.3, I characterize the GNEP as a solution of an evolutionary variational inequality. Moreover, I discuss a differential game approach. In Section 2.4, I provide an illustrative example, and, finally, Section 2.5 is dedicated to the conclusions.

2.2 The time-dependent game theory model of digital content competition

In this section, I present a dynamic game theory model of the competition among digital creators. I consider a network that consists of m creators and n groups of viewers with homogeneous interests, feelings and age. Each creator posts a content in the planning horizon $[0, \mathcal{T}]$. The topology of the network of this model is the same in $[0, \mathcal{T}]$. Each creator $i \in \{1, \dots, m\}$ posts a content at time t, that can be accessed by each group $j \in \{1, \dots, n\}$. In order to express the time dependence, I choose as our functional setting the Hilbert space $L^2([0, \mathcal{T}], \mathbb{R}^k)$ of square-integrable functions defined in the closed interval $I = [0, \mathcal{T}]$, endowed with the scalar product $\langle \cdot, \cdot \rangle_{L^2} = \int_0^{\mathcal{T}} \langle \cdot, \cdot \rangle dt$ and the usual associated norm $\| \cdot \|_{L^2}$. In particular, I suppose that the functional space for the trajectories of views is $L^2(I, \mathbb{R}^{mn})$, while for the trajectories of likes is $L^2(I, \mathbb{R}^m)$.

Let $v_{ij}(t)$ denote the views given by the fraction of subscribers who have accessed to the content generated by i at time $t \in I$. I group the $\{v_{ij}\}$ elements for all j into the vector $v_i \in L^2(I, \mathbb{R}^n_+)$ and then I group all the vectors v_i for all i into the vector $v \in L^2(I, \mathbb{R}^{mn}_+)$. In addition, $\ell_i(t)$ denotes the percentage of likes of content i at time t, and takes value in the interval $[0, 1]$. I group the likes of all creators into the vector $\ell \in L^2(I, [0, 1]^m)$.

Usually, a content must reach a minimum amount of accesses to raise the interest of viewers and enter the competition with the other contents. I denote this threshold by $s > 0$. Thus, for each posted content i, the views must satisfy the condition

$$\sum_{j=1}^{n} v_{ij}(t) \geq s, \quad i = 1, \ldots, m, \ \text{ a.e. } t \in I. \tag{2.1}$$

In addition, since each content has a lifetime, I denote by $\bar{v}_j(t)$ the upper bound on the total amount of views at time t in each group j. I also assume $\bar{v}_j(t)$ to be known and fixed, and the following condition must hold:

$$\sum_{i=1}^{m} v_{ij}(t) \leq \bar{v}_j(t), \quad j = 1, \ldots, n, \ \text{ a.e. } t \in I. \tag{2.2}$$

Each creator i incurs a production cost $\pi_i(v, \ell_i)$, $i = 1, \ldots, m$. I assume that the production cost of i may depend upon the entire amount of views and on its own likes. I also assume that creators may accelerate the viewcount by paying a fee for the advertisement service in the social media platform. Hence, for each creator i, I introduce the advertisement cost function

$$c_i(t) \sum_{j=1}^{n} v_{ij}(t), \quad i = 1, \ldots, m, \ \text{ a.e. } t \in I, \tag{2.3}$$

with $c_i(t) \geq 0, i = 1, \ldots, m$, a.e $t \in I$. Similarly, the revenue of creator i, deriving from hosting advertisements and benefits from firms, is given by

$$p_i(t) \sum_{j=1}^{n} v_{ij}(t), \quad i = 1, \ldots, m, \ \text{ a.e. } t \in I, \tag{2.4}$$

with $p_i(t) \geq 0$, $i = 1, \ldots, m$, a.e $t \in I$. The advertisements hosted in the videos can be of several types, i.e. the creator can decide to insert a small advertising spot, shot by himself, during his video or to interrupt the video by broadcasting advertisements managed by the YouTube platform.

I associate to each group of viewers j the feedback function $f_j(t, v, \ell)$, that represents the evaluation of the contents and depends upon the entire amount of views and likes. Now, I define the popularity function of creator i as the function

$$\sum_{j=1}^{n} f_j(t, v, \ell) v_{ij}, \quad i = 1, \ldots, m, \ \text{ a.e. } t \in I. \tag{2.5}$$

I consider the content diffusion model as a game where players are the creators, who compete for the diffusion of their contents. Strategic variables are content views v and likes ℓ. The profit for player i, denoted by $U_i(t, v, \ell)$, $i = 1, \ldots, m$, is the difference between total revenue and total costs, namely, for a.e. $t \in I$

$$U_i(t, v, \ell) = \sum_{j=1}^{n} f_j(t, v, \ell) v_{ij}(t) + p_i(t) \sum_{j=1}^{n} v_{ij}(t) - \pi_i(t, v, \ell_i) - c_i(t) \sum_{j=1}^{n} v_{ij}(t). \tag{2.6}$$

Thus, the set of strategies of creator i is given by

$$\mathbb{K}_i = \left\{ (v_i, \ell_i) \in L^2(I, \mathbb{R}^{n+1}) : \ v_{ij}(t) \geq 0, \forall j; \sum_{j=1}^{n} v_{ij}(t) \geq s; 0 \leq \ell_i \leq 1, \text{ a.e. in } I \right\}.$$

I also define $\mathbb{K} = \prod_{i=1}^{m} \mathbb{K}_i$.

In addition, players have to satisfy the shared constraints (1.2). Hence, I define the set $\mathcal{S}$ as follows:

$$\mathcal{S} = \left\{ v \in L^2(I, \mathbb{R}^{mn+m}) : \sum_{i=1}^{m} v_{ij}(t) \leq \bar{v}_j(t), j = 1, \ldots, n, \text{ a.e. in } I \right\}.$$

I suppose that the production cost function $\pi_i(t, v, \ell_i)$, $\forall i$, is defined on $I \times \mathbb{R}^{mn} \times \mathbb{R} \to \mathbb{R}_+$, it is measurable in t and continuous with respect to v and ℓ_i. Moreover,

I assume that $\frac{\partial \pi_i}{v_{ij}}$ and $\frac{\partial \pi_i}{\ell_i}$ exist and that they are measurable in t and continuous with respect to v and ℓ_i. I also require that the feedback function $f_j(t, v, \ell)$, $\forall j$, is defined on $I \times \mathbb{R}^{mn} \times \mathbb{R}^m \to \mathbb{R}_+$, it is measurable in t and continuous with respect to v and ℓ. In addition, I assume that $\frac{\partial f_j}{v_{ij}}$ and $\frac{\partial f_j}{\ell_i}$ exist and that they are measurable in t and continuous with respect to v and ℓ. Further, I set $u_i = (v, \ell_i)$, $u = (v, \ell)$, and require the following growth conditions, $\forall i, j$ and a.e. in I:

$$\left|\pi_i(t,u)\right| \leq \alpha_1(1 + \|u_i\|), \forall \ell, \quad \left|f_j(t,u)\right| \leq \alpha_2(1 + \|u\|), \forall v, \ell, \tag{2.7}$$

$$\left|\frac{\partial \pi_i}{\partial v_{ij}}\right| \leq \beta_1(1 + \|v\|), \forall v, \quad \left|\frac{\partial \pi_i}{\partial l_i}\right| \leq \beta_2(1 + \|\ell\|), \forall \ell, \tag{2.8}$$

$$\left|\frac{\partial f_j}{\partial v_{ij}}\right| \leq \beta_3(1 + \|v\|), \forall v, \quad \left|\frac{\partial f_j}{\partial l_i}\right| \leq \beta_4(1 + \|\ell\|), \forall \ell, \tag{2.9}$$

with $\alpha_1, \alpha_2, \beta_1, \beta_2, \beta_3, \beta_4 > 0$.

The above conditions will be useful in the following, since they ensure that problem (2.12) is well-defined.In fact, if $(v_i, \ell_i, v_{-i}, \ell_{-i}) \in L^2(I, \mathbb{R}^{mn+m})$ and conditions (2.7)-(2.9) hold, then $U_i(t, v_i, \ell_i, v_{-i}, \ell_{-i}) \in L^2(I, \mathbb{R})$.

2.3 The Generalized Nash Equilibrium Formulation

In our model, the creators behave in a non-cooperative fashion, each one trying to maximize her profit. Since players have to satisfy the shared constraints (2.2), each player's strategy vector (v_i, ℓ_i) belongs to the set $\mathbb{K}_i$, but depends also on the rival players' strategies through the constraints $v \in \mathcal{S}$. Therefore, the underlying equilibrium concept will be that of a time-dependent generalized Nash equilibrium; see [12, 76, 83, 147]. I use the notation (v_{-i}, ℓ_{-i}) to indicate the variables for all players except i. So that for any $t \in I$, $(v_{-i}(t), \ell_{-i}(t))$ is the vector formed by

all players' decision variables except the player i at time $t \in I$. Following [12, 194], the strategy profile is chosen in a common subset K and thus the admissible strategy set of each player is defined as

$$K_i(v_{-i}, \ell_{-i}) = \{(v_i, \ell_i) \in L^2(I, \mathbb{R}^{m+1}) \ : \ (v_i, \ell_i, v_{-i}, \ell_{-i}) \in K\}. \tag{2.10}$$

Definition 2.3.1. *Let $U_i : L^2(I, \mathbb{R}^{m+1}) \to \mathbb{R}$ be the profit function for player i. A strategy $(v^*, \ell^*) \in K \subseteq L^2(I, \mathbb{R}^{mn+n})$ is a time-dependent generalized Nash equilibrium if and only if for each player i, I have $(v_i^*, \ell_i^*) \in K_i(v_{-i}^*, \ell_{-i}^*)$ and*

$$U_i(t, v^*, \ell^*) \leq U_i(t, v_i^*, \ell_i^*, v_{-i}^*, \ell_{-i}^*), \quad \forall (v_i, \ell_i) \in K_i(v_{-i}^*, \ell_{-i}^*). \tag{2.11}$$

This means that $(v^*, \ell^*) \in K \subseteq L^2(I, \mathbb{R}^{mn+n})$ is a time-dependent generalized Nash equilibrium if, for all creators i, $(v_i^*, \ell_i^*) \in L^2([0, T], \mathbb{R}^{m+1})$ solves the following optimization problem

$$\min_{(v_i, \ell_i) \in K_i(v_{-i}^*, \ell_{-i}^*)} \int_I U_i(t, v_i, \ell_i, v_{-i}^*, \ell_{-i}^*) dt. \tag{2.12}$$

Since the convex sets $K_i(v_{-i}^*, \ell_{-i}^*)$, $\forall i$, depend on the solution, the GNEP can be formulated as a quasi-variational inequality. However, following [83, 194], considering the structure of the feasible strategies, I am allowed to reduce the problem to a variational inequality.

Definition 2.3.2. *Let us assume that for each creator i the profit function $U_i(t, v, \ell)$ is concave with respect to the variables $(v_{i1}, \ldots, v_{in})$, and ℓ_i, continuously differentiable, and the growth conditions* (2.7)-(2.9) *hold. A variational inequality approach to finding a GNE is to define the set $\mathcal{K} = \mathbb{K} \cap \mathcal{S}$, and to solve the evolutionary variational inequality*

Find $(v^*, \ell^*) \in \mathcal{K}$:

$$\int_0^{\mathcal{T}} \Bigg\{ - \sum_{i=1}^{m} \sum_{j=1}^{n} \frac{\partial U_i(t, v^*, \ell^*)}{\partial v_{ij}} \times \Big(v_{ij}(t) - v_{ij}^*(t) \Big) \\ - \sum_{i=1}^{m} \frac{\partial U_i(t, v^*, \ell^*)}{\partial \ell_i} \times \big(\ell_i(t) - \ell_i^*(t) \big) \Bigg\} dt \geq 0, \forall (v, \ell) \in \mathcal{K}. \tag{2.13}$$

For a discussion on the existence of solutions, I address the reader to [148]. As in [76, 83], I have the following result.

Theorem 2.3.1. *Every solution of variational inequality* (2.13) *is a solution of GNEP.*

2.3.1 A differential Game Model

In contrast to the differential game approach as in [6], the evolution of the state in our model is not governed by differential equations. In fact, I present the competition problem of creators as an evolutionary variational inequality. Thus, I am able to describe how creators adapt the choice of contents to be posted, and the acceleration mechanisms in response to the reactions of viewers in the time horizon. However, I may provide a unified approach and present a differential game formulation for the dynamic generalized Nash equilibrium model. The model presented in this work can be regarded as an infinitely repeated simultaneous move game. In the repeated games, the same static game, called the stage game, is repeated a finite or infinite number of times, and the result of each stage is observed by all the players before the new stage starts. In our case, the competitive game represents the stage game that is repeated and played almost at the same way at all the instants t. In fact, at each repetition the game is slightly different, since creators adjust their strategies according to the demands that change over time. I also

emphasize that all the creators make their decisions simultaneously at the beginning of the game and such simultaneous moves are repeated indefinitely. Therefore, each creator chooses his decisions without any knowledge of the decisions taken by the other creators.

Now, I focus on differential games, where time evolves continuously and the state evolution can be modelled by a set of differential equations given by

$$\dot{x}(t) = g(x(t), z_1(t), \ldots, z_n(t)),\ x(0) = x_0,$$

where $x(t)$ is the state, $z_1(t), \ldots, z_n(t)$ are the controls and t is the time.

I can transform the digital content competition game into a problem that can be approached as a differential game. Nevertheless, I emphasize that the game itself is not a differential game. I set:

$$\Psi_i(t, v(t), \ell(t)) = \sum_{j=1}^{n} \frac{\partial U_i(t, v^*, \ell^*)}{\partial v_{ij}} \times \left(v_{ij}(t) - v_{ij}^*(t)\right) - \frac{\partial U_i(t, v^*, \ell^*)}{\partial \ell_i} \times \left(\ell_i(t) - \ell_i^*(t)\right)$$

and observe that the competition problem of creator i is equivalent to

$$\min_{(v,\ell)\in\mathcal{K}} \int_0^{\mathcal{T}} \Psi_i(t, v(t), \ell(t))dt.$$

Now, I introduce the profit of creator i over the interval $[0, t]$:

$$\int_0^t \Psi_i(\tau, v(\tau), \ell(\tau))d\tau = G_i(t).$$

Then, the problem of creator i becomes

$$\begin{aligned} &\min G_i(\mathcal{T}) \\ &\text{subject to } \frac{dG_i(t)}{dt} = \Psi_i(t, v(t), \ell(t)),\ G_i(0) = 0, \end{aligned}$$

and the constraints in $\mathcal{K}$. In the above formulation, $G_i(t)$ represents the state, whereas $v(t)$ and $\ell(t)$ are the controls.

2.4 An Illustrative Example

In this section, I present a numerical example. Even if the problem could be solved using optimal control tools, I will adopt a variational inequality approach. I focus on an example in which I consider two creators and one group of viewers who have the same preferences about the contents. The steps that I use to solve the example are the following: Firstly, I use a discretization procedure and select discrete points in the time interval (see [41, 42]). Then, I reduce our problem to solve a static variational inequality at each discrete point. Finally, I solve each static variational inequality using the extragradient method as in [128]. This procedure can be performed if the continuity of the solutions is guaranteed, see [17].
I consider the production cost functions as:

$$\pi_1(v_{11}(t), \ell_1(t)) = 43v_{11}(t)^2 + v_{21}(t) + 25\ell_1(t)^2 + 3,$$

$$\pi_2(v_{21}(t), \ell_2(t)) = 160v_{21}(t)^2 + 400v_{11}(t) + 50\ell_2(t)^2 + 6;$$

the evaluation function for the group of viewers as:

$$f_1(v_{11}(t), v_{21}(t), \ell_1(t), \ell_2(t)) = -(v_{11}(t) + v_{21}(t)) + 0.4\ell_1(t) + 0.5\ell_2(t).$$

All functions are chosen so as to guarantee the existence, uniqueness, and continuity of the solution. I also emphasize that all the functions are expressed in a form widely used in relevant literature, see for instance [41, 42, 54]. I suppose that creator 1 earns from advertisement 16400$ per 10000 views, otherwise creator 2 earns from advertisement 40000$ per 10000 views. This means that creator 2 has brands, as advertising partner, that are more famous than the brand advertised by the creator 1. Moreover, for each creator, the coefficients of the cost functions and the revenue functions are: $p_1 = 16400$, $c_1 = 7380$, $p_2 = 40000$, $c_2 = 18000$.

Following the policy of YouTube, the cost parameter c_i is the 45% of the revenue parameter p_i, for $i = 1, 2$. I set $s = 0.5$, $\bar{v}_1 = 30t$. Our aim is to investigate only the first six minutes after that the video has been posted, and analyze the impact of the video on the subscribers of the channel at the time when the video has been released. Thus, I set $t = 0, \dots 6$. I observe that Fig.2.1 represents the views made by the analyzed user group. It can be seen from the plot that creator 1 has less views when the video is posted, but after a few instants of time it exceeds the views of the video of creator 2, which has more or less a constant trend of the number of views over time. The same trend of the equilibrium solutions as regards the views can also be observed from the Fig.2.4. It represents a heat map, where the x-axis and the y-axis are the creators for $i = 1, 2$ and the time interval from the starting point until the sixth minute after that the video has been posted, respectively. Fig.2.2 shows the total percentage of likes that the group of viewers gives to the video for each instant of time. I note that the video of creator 2 has a small increase over time, whereas the other creator has a significant increase. Indeed, this confirms once again that video 1 is more appreciated by the audience. As a consequence, this appreciation is also reflected in Fig.2.1, where the number of views of video 1 is greater than the number of views of video 2. The same trend of the equilibrium solutions concerning the percentage of likes, i.e. ℓ_i, can also be observed from the Fig.2.5. It represents a heat map, where the x-axis and the y-axis are the creators for $i = 1, 2$ and the time interval from the starting point until the sixth minute after that the video has been posted, respectively. Fig.2.7 shows that obtaining a percentage of likes and a number of views with a slight increase over time brings a greater profit U_2 than U_1, in the first six minutes after that the video has been posted. As I can observe in Fig.2.3-2.6, the strategies of creator 1

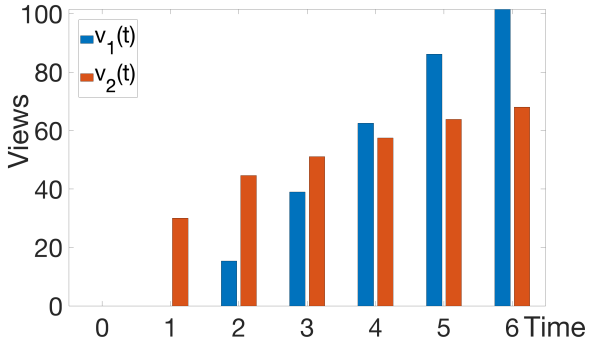

Figure 2.1: Number of views for each creator

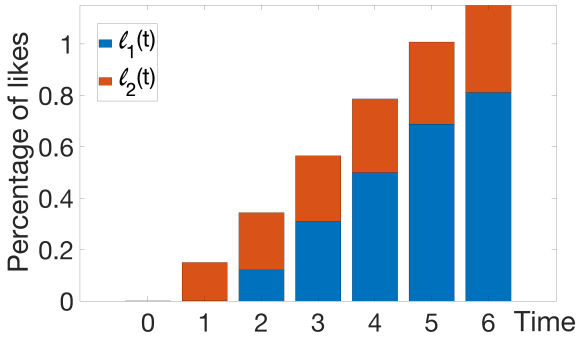

Figure 2.2: Percentage of likes for each creator

Figure 2.3: Total number of views and total percentage of likes for each creator for each time $t \in \{0, \ldots, 6\}$

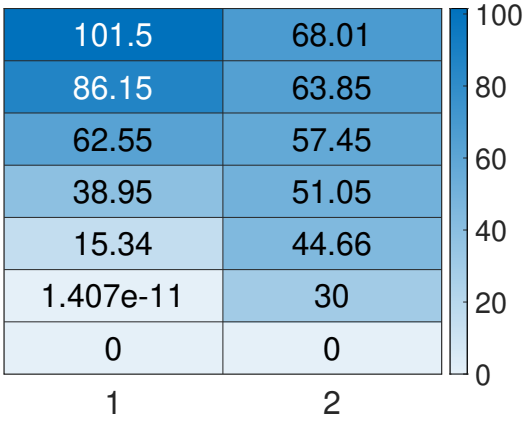

Figure 2.4: Number of views $v_{ij}(t)$

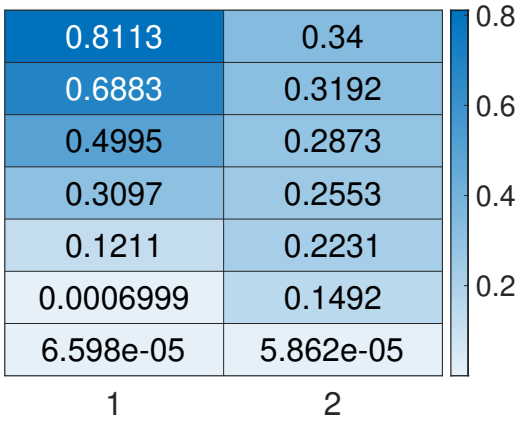

Figure 2.5: Percentage of likes $\ell_i(t)$

Figure 2.6: Equilibrium solutions of the number of views and the percentage of likes over time $t \in \{0, \ldots, 6\}$ for all creator $i = 1, 2$ and for the group of viewers $j = 1$

could pay off over time respect to the strategies of creator 2, despite that the profit of the second creator remains higher than the profit of the first one in the first six minutes. In Fig.2.7, I characterize the net profit of each creator with dotted lines. The difference between the net and the gross profit depends on the profit that a content earns from advertisement. Indeed, only the 15% of the views counts as a profit from advertisement strategies, because the only views that make creator earn money are those in which viewers have watched the advertisement for at least 30 seconds, or half advertisement for a very short video.

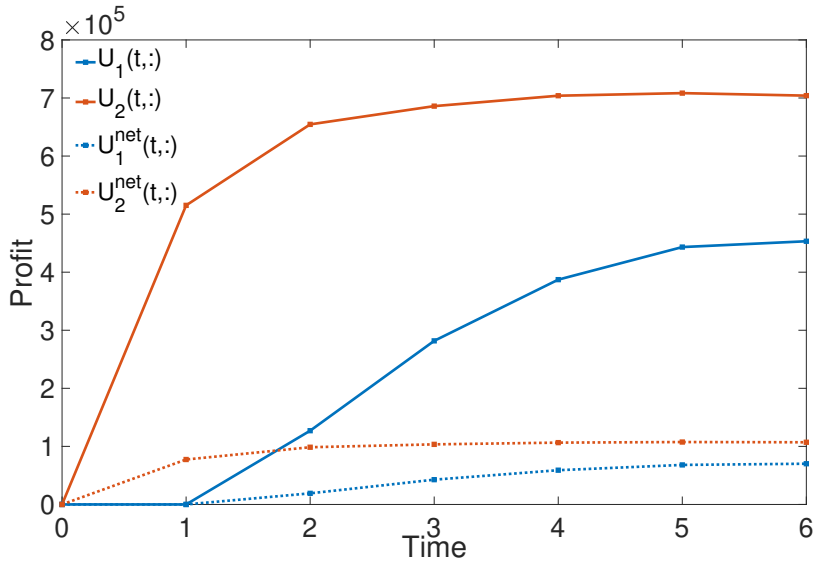

Figure 2.7: The net profit, i.e. $U_i^{net}(t, v_{ij}(t), \ell_i(t))$, and gross profit, i.e. $U_i(t, v_{ij}(t), \ell_i(t))$, considering the net and the gross viewcount at each time $t \in \{0, \ldots, 6\}$ for all creators

2.5 Conclusions

In this Chapter, I focused on a dynamic network model that allowed us to describe the complex social media platform mechanisms and the evolution of views over

time. I showed that the underlying generalized Nash equilibrium problem can be represented by means of an evolutionary variational inequality. This may give the opportunity to use the powerful variational inequality theory for existence results, stability and sensitivity of solutions, and computational procedures. Moreover, I remark that a static approach is not suitable to follow the behavior of phenomena evolving in time, whereas a dynamic approach is more efficient and desirable. Finally, I suggested a possible differential game formulation, so as to unify GNEPs, variational inequalities and differential games. As a future research issue, I could conduct a Lagrange analysis of the multipliers to assess the role of the constraints.

Chapter 3

Closed-Loop Supply Chain Network Equilibrium with online second-hand trading

3.1 Introduction

Reverse logistics aims at improving the exploitation of used products through recycling or re-manufacturing and leads to a reduction in environmental damage. Products may reverse direction in the supply chain for several motivations, such as manufacturing returns, product recalls, warranty or service returns, end-of-use returns, and end-of-life returns. Reverse logistics and, in particular, second-hand trading has received large interest for the opportunity of sustainable consumption, extending the life span of products and reducing adverse environmental impacts due to the purchase of new goods. Recently, the increasing use of the Internet and trading platforms, such as eBay or Vinted, has completely changed the market conditions. In the U.S., the e-commerce sales have reached $876 billion in the

first quarter of 2021, up 38% year-over-year. Moreover, the speculative buying of limited edition goods has become a real business. In fact, people may gain profit from selling high-uniqueness goods at a price much higher than the original one to potential consumers when the goods get scarce over time.

Due to several advantages, closed-loop supply chains (CLSCs) have been extensively studied in recent years. Many researchers have investigated the network structure of the CLSC, which includes competitive manufacturers, competitive retailers and consumer markets. For example, Nagurney and Toyasaki [163] develop a network model for supply chain decision-making with environmental criteria. In [197], the authors explore a reverse supply chain network model using variational inequality. In [203], Shen et al. examine the sale of second-hand products through an online platform on a supply chain consisting of contributors, one second-hand online platform, and one supplier. Different scenarios in terms of CLSC structure and block-chain use are considered. In [220], Wang et al. study the waste of electrical and electronic equipment and provide a variational inequality to model the CLSC network. In [234], the authors examine a CLSC network equilibrium problem in multiperiod planning horizons, with consideration to product lifetime and carbon emission constraints. By variational inequalities and complementary theory, the governing CLSC network equilibrium model is established.

Motivated by all the above analysis, this paper establishes a CLSC network equilibrium model with online second-hand trading of high-uniqueness products. I consider a CLSC network consisting of manufacturers, retailers, demand markets, and one online platform, in which the consumers purchase new products and collect them. Then, collectors sell the goods to consumers through the online platform. By variational inequalities, the optimal behaviors of all the decision-makers

are modeled, and, in turn, the governing CLSC network equilibrium model is given. The main contributions of this paper are: the modeling of the second-hand market in a reverse logistics setting, and the study of the horizontal competition among the members of the same tiers as well as the vertical one between adjacent tiers. I describe the forward and the reverse logistics, taking into account capacity constraints of manufacturers and retailers, as well as consumers' risk-aversion to purchasing second-hand goods, and platform's risk-aversion to transacting with collectors.

The paper is organized as follows. In Section 3.2, I develop the CLSC model by describing the manufacturers' and the retailers' competitive behavior, and the interactions with the demand markets and the online platform. I then provide a variational inequality formulation of the optimal behavior of decision-makers. In Section 3.3, I state that the governing equilibrium conditions of the CLSC network. I summarize our results and present our conclusions in Section 3.4.

3.2 The closed-loop supply chain network

I consider a CLSC network consisting of multiple manufacturers, multiple retailers, and multiple demand markets, in which the consumers purchase new products and collect them. Collectors distribute the used goods through an online platform for the aim of gaining profit on the resale. The criterion of each player in the network is the total profit maximization.

Let M be the set of manufacturers (I denote by m the typical manufacturer), R be the set of retailers (I denote by r the typical retailer), K be the set of demand markets (I denote by k the typical demand market) and I consider a single online platform as eBay, Marketplace by Facebook, Vinted etc... Abusing notation, without risk

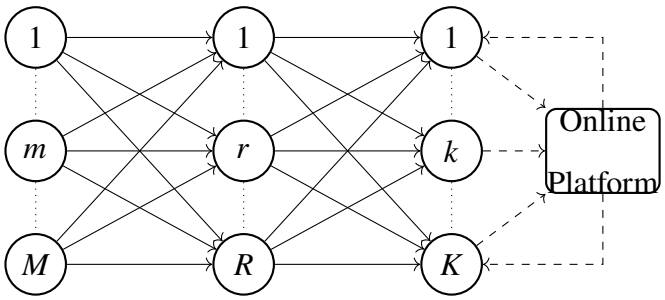

Figure 3.1: The closed-loop supply chain network

of confusion, I use the same symbols here to denote the sets M, R, K and their cardinalities. Furthermore, I introduce the set of collectors K^c, with $|K^c| \leq K$, that represents the set of consumers who decide to resell their collectibles. The network can be divided into two parts: the forward chain, formed by manufacturers, retailers and consumers, and the reverse chain, formed by collectors, the online platform and consumers. The collectors and the online platform make it possible to connect the forward and the reverse chains and form the closed-loop network. I consider two different types of items: the new ones denoted by index $n = 1, \ldots N$ and the used ones indicated by index $u = 1 \ldots U$. The model network can be represented as in Figure 3.1. The solid lines represent the forward transactions and the dashed lines refer to the reverse ones.

I first focus on the manufacturers. I then turn to the retailers, to the consumers, and, finally, to the platform. The complete equilibrium model is then constructed as a variational inequality.

3.2.1 The Optimal Behavior of the Manufacturers

Let x^n_{mr} be the quantity of new item n sold by manufacturer m to retailer r. I group all the n and r elements into the vector $x_m \in \mathbb{R}^{NR}$, and then I group all the

vectors (x_m) for all m into the vector $x^M \in \mathbb{R}^{NMR}$. I denote by x_m^{max} the production capacity of manufacturer m.

In the forward logistics, a manufacturer incurs production costs and transaction costs. In order to maximize his own profit, each manufacturer m must decide the quantity x_{mr}^n of new item n to be sold to retailer r. I associate with each manufacturer production cost, c_m, and assume that it can depend, in general, on the entire vector of production outputs, namely, $c_m = c_m(x^M)$. I denote by $t_{mr}(x_{mr}^n)$ the transaction cost from manufacturer m to retailer r. Moreover, I assume that $c_m(x^M)$ and $t_{mr}(x_{mr}^n)$ are continuous, differentiable and convex functions. Finally, I consider p_{mr}^n as the selling price of a new product. Given the above notation, each manufacturer m wishes to maximize the profit as follows:

$$\max \sum_{n\in N}\sum_{r\in R} p_{mr}^n x_{mr}^n - c_m(x^M) - t_{mr}(x_{mr}^n) \tag{3.1}$$

$$\sum_{n\in N}\sum_{r\in R} x_{mr}^n \leq x_m^{max}, \quad x_{mr}^n \geq 0, \forall n, r. \tag{3.2}$$

The objective function (3.1) maximizes the profit, which equals sales revenue minus costs associated with production and transaction. The first constraint in (3.2) expresses the production capacity of manufacturer m. All the manufactures compete in a non-cooperative fashion, and each manufacturer seeks to maximize his profit given other manufacturers' decisions. Thus, the optimality conditions of all the manufacturers can be described by the following variational inequality, see [155]:

$$\sum_{n\in N}\sum_{m\in M}\sum_{r\in R}\left(\frac{\partial c_m(x^{*M})}{\partial x_{mr}^n} + \frac{\partial t_{mr}(x_{mr}^{*n})}{\partial x_{mr}^n} - p_{mr}^n\right)(x_{mr}^n - x_{mr}^{*n}) \geq 0, \forall x^M \in S^M, \tag{3.3}$$

$$S^M = \left\{x^M \in \mathbb{R}_+^{NMR} : \sum_{n\in N}\sum_{r\in R} x_{mr}^n \leq x_m^{max}, \forall m \in M\right\}. \tag{3.4}$$

3.2.2 The Optimal Behavior of Retailers

The retailers interact with manufacturers and consumers. Specifically, they decide the amount of products to order from the manufactures, so as to transact with the demand markets, while seeking to maximize their profit. The product shipment of new good n between retailer r and consumer k is denoted by x_{rk}^n; the product shipments x_{rk}^n for all n and k are then grouped into the column vector $x_r \in \mathbb{R}^{NK}$ and, further, into the vector $x^R \in \mathbb{R}^{NRK}$.

Each retailer r has associated management cost c_r related to the items in stock. I assume that it depends on the amounts of the product held by other retailers, that is, $c_r = c_r(x^M)$. Let $\hat{c}_{mr}^n(x_{mr}^n)$, be the transportation cost from m for new items and let p_{rk}^n be the sale price associated with a new item. Moreover , retailers incur transaction costs $t_{rk}^n(x_{rk}^n)$, when selling new products to consumers. Finally, I assume that $c_r(x_{mr}^n)$, $\hat{c}_{mr}^n(x^M)$, and $t_{rk}(x_{rk}^N)$ are continuous, differentiable and convex functions.

Each retailer r seeks to maximize his profit function as follows:

$$\max \sum_{n\in N}\left(\sum_{k\in K} p_{rk}^n x_{rk}^n - \sum_{m\in M}\hat{c}_{mr}^n(x_{mr}^n) - \sum_{k\in K} t_{rk}^n(x_{rk}^n) - \sum_{m\in M} p_{mr}^n x_{mr}^n\right) - c_r(x^M) \tag{3.5}$$

$$\sum_{n\in N}\sum_{k\in K} x_{rk}^n \leq \sum_{n\in N}\sum_{m\in M} x_{mr}^n, \quad x_{mr}^n \geq 0,\ x_{rk}^n \geq 0, \forall n, m, k. \tag{3.6}$$

Objective function (3.5) expresses that the profit of the retailer is equal to sales revenues minus costs associated with the management, the transportation, the transaction and the payout to the manufacturers. The first constraint in (3.6) states that consumers cannot purchase more from a retailer than is held in stock. Since all the retailers compete in a non-cooperative fashion, the optimality conditions for all retailers can be expressed as the variational inequality:

$$\sum_{n\in N}\sum_{r\in R}\sum_{k\in K}\left(\frac{\partial t_{rk}(x^{*n}_{rk})}{\partial x^{n}_{rk}} - p^{n}_{rk}\right)(x^{n}_{rk} - x^{*n}_{rk})$$
$$+\sum_{n\in N}\sum_{m\in M}\sum_{r\in R}\left(p^{n}_{mr} + \frac{\partial c_r(x^{*n}_{mr})}{\partial x^{n}_{mr}} + \frac{\partial \hat{c}^{n}_{mr}(x^{*M})}{\partial x^{n}_{mr}}\right)(x^{n}_{mr} - x^{*n}_{mr}) \geq 0,$$
$$\forall (x^R, x^M) \in S^R, \tag{3.7}$$
$$S^R = \left\{(x^R, x^M) \in \mathbb{R}^{NRK+NMR}_{+} : \sum_{n\in N}\sum_{k\in K} x^{n}_{rk} \leq \sum_{n\in N}\sum_{m\in M} x^{n}_{mr}, \forall r \in R\right\}. \tag{3.8}$$

3.2.3 The Optimal Behavior of the Consumers

The consumers at demand markets transact with the retailers as well as the online platform. Specifically, in the forward supply chain, consumers purchase new products; in the reverse supply chain, consumers act as collectors and sell their goods on the online platform, that are then purchased by consumers at demand markets. I analyze these situations separately.

The Consumers in the Forward Logistics

Let $\hat{c}^{n}_{rk}(x^{n}_{rk})$ be the transportation cost for new product n sold by retailer r to demand market k. Moreover, let d^{n}_{k} be the demand of new item n at demand market k and be p^{n}_{k} the price of new product n at demand market k. The equilibrium conditions for consumers at demand market k are (see [158, 163, 162, 161, 157]):

$$p^{*n}_{rk} + \hat{c}^{n}_{rk}(x^{*n}_{rk}) \begin{cases} = p^{*n}_{k} & \text{if } x^{*n}_{rk} > 0, \\ \geq p^{*n}_{k} & \text{if } x^{*n}_{rk} = 0, \end{cases} \qquad \forall r, k, n. \tag{3.9}$$

$$d^{n}_{k}(p^{*n}_{k}) \begin{cases} = \sum_{r\in R} x^{*n}_{rk} & \text{if } p^{*n}_{k} > 0, \\ \leq \sum_{r\in R} x^{*n}_{rk} & \text{if } p^{*n}_{k} = 0, \end{cases} \qquad \forall k, n. \tag{3.10}$$

Inequality (3.9) states that if the consumers at demand market k purchase the products from retailer r, then the price charged by the retailer for the product plus the transportation cost undertaken by the consumers does not exceed the price that the consumers are willing to pay. Equation (3.10) states that if the equilibrium price that the consumers are willing to pay for the new products at the demand market is positive, then the quantities purchased of new goods from the retailers will be exactly equal to the demand. These conditions correspond to the well-known spatial price equilibrium conditions, see [155].

The Consumers in the Reverse Logistics

In the reverse supply chain, some consumers resell collectible items to the demand market through the online platform. The product shipment of second-hand good u between collector k_c and consumer k, using the platform, is denoted by $x^u_{k_c k}$. The product shipments $x^u_{k_c k}$, for all u and k, are then grouped into the column vector $x_{k_c} \in \mathbb{R}^{UK}$ and, further, into the vector $x^U \in \mathbb{R}^{UK^c K}$. I set Q_{k_c} as the amount of items in the collection of collector k_c. Let $p^u_{k_c}$ be the price charged by the collector k_c for second-hand items. I note that selling on the online platform can give higher visibility to the products and, as a consequence, it can be more profitable, even if the platform retains a portion of the sale price. For instance, on eBay the transaction price amounts to the 10% of the selling price, indicated by the coefficient γ. Let $c_{k_c}(x_{k_c})$ be the maintenance and restoring cost of the collector k_c, depending on the amount of items that he resells on the online platform. Let $\hat{c}^n_{rk_c}(x^R)$, be the transportation cost from r for new item n to collector k_c. I assume that $c_{k_c}(x_{k_c})$ and $\hat{c}^n_{rk_c}(x^R)$ are continuous, differentiable and convex functions. I denote by $\mu_{k_c} \in (0, 1]$ the portion of second-hand goods that collector $k_c \in K^c$

decides to sell on the platform.

Each collector $k_c \in K^c$ seeks to maximize his profit function as follows:

$$\max \sum_{u\in U}\sum_{k\in K}(1-\gamma)p^{*u}_{k_c}x^u_{k_ck} - c_{k_c}(x_{k_c}) - \sum_{n\in N}\sum_{r\in R}\left(p^n_{rk_c}x^n_{rk_c} - \hat{c}^n_{rk_c}(x^R)\right) \quad (3.11)$$

$$\sum_{u\in U}\sum_{k\in K}x^u_{k_ck} \le \mu_{k_c}Q_{k_c}, \quad x^u_{k_ck}, x^n_{rk_c} \ge 0, \quad \forall n,u,r,k. \quad (3.12)$$

Objective function (3.11) expresses that the profit of the collector is equal to sales revenues minus costs associated with restoring, purchasing and transportation. The first constraint in (3.12) states that the amount of products collector k_c decides to sell should be less than or equal to the amount of collectibles in k_c's collection. I now examine the transactions between the platform and the demand market k. Let $\hat{c}^u_{k_ck}(x^U)$ be the transportation cost from collector k_c to consumer k for used product u purchased on the platform. Furthermore, let d^u_k be the demand of second-hand items at demand market k, and ρ^u_k be the willingness to pay second-hand items at demand market k. I group all these ρ^u_k into a column vector $\rho_k \in \mathbb{R}^U$, and then into the vector $\rho^U \in \mathbb{R}^{UK}$. I also consider a risk associated with purchasing second-hand items from the trading platform. Therefore, each consumer exhibits risk aversion that may be dependent on flows controlled by other demand markets. Hence, the risk aversion function can be expressed as the continuous function $\pi_k(x^U)$, [161]. The equilibrium conditions for consumers at demand market k in the reverse supply chain are

$$p^{*u}_{k_c} + \hat{c}^u_{k_ck}(x^{*U}) + \pi_k(x^{*U}) \begin{cases} = \rho^{*u}_k & \text{if } x^{*u}_{k_ck} > 0, \\ \ge \rho^{*u}_k & \text{if } x^{*u}_{k_ck} = 0, \end{cases} \quad \forall k_c, u. \quad (3.13)$$

$$d^u_k(\rho^{*U}) \begin{cases} = x^{*u}_{k_ck} & \text{if } \rho^{*u}_k > 0, \\ \le x^{*u}_{k_ck} & \text{if } \rho^{*u}_k = 0, \end{cases} \qquad p^{*n}_{rk} - \rho^{*u}_k \begin{cases} < 0 & \text{if } x^{*n}_{rk} = 0, \\ \ge 0 & \text{if } x^{*n}_{rk} > 0, \end{cases} \quad \forall r,k,u,n. \quad (3.14)$$

Equality (3.13) states that if the consumers at demand market k purchase the product on the online platform, then the price charged by the collector k_c for second-hand items plus the transportation cost plus the risk undertaken by the consumer is equal to the price that the consumer is willing to pay. The first condition in (3.14) states that if the equilibrium price the consumers at demand market k are willing to pay for the second-hand product is positive, then the amount purchased of second-hand product should exactly be equal to the demand of this second-hand item. The second condition in (3.14) means that the unitary price of a second-hand collectible is higher than the unitary price of a new collectible that is totally sold out.

The Consumers' Equilibrium Conditions

Combining consumer behaviors in both forward and reverse supply chain, the equilibrium conditions for all the demand markets can be expressed as the following variational inequality, see [158, 163, 162, 161, 157]:

$$\begin{aligned}
&\sum_{n\in N}\sum_{k\in K}\left(\sum_{r\in R} x^n_{rk} - d^{*n}_k(p^{*n}_k)\right)(p^n_k - p^{*n}_k)\\
&+\sum_{u\in U}\sum_{k_c\in K^c}\left(\frac{\partial c_{k_c}(x_{k_c})}{\partial x^u_{k_c k}} + \gamma p^{*u}_{k_c} + \hat{c}^u(x^{*u}_{k_c k}) + \pi_k(x^{*U}) - \rho^{*u}_k\right)(x^u_{k_c k} - x^{*u}_{k_c k})\\
&+\sum_{u\in U}\sum_{k\in K}\left(x^{*u}_{k_c k} - d^u_k(\rho^{*U})\right)(\rho^u_k - \rho^{*u}_k)\\
&+\sum_{n\in N}\sum_{r\in R}\sum_{k\in K}\left(p^{*n}_{rk} + \hat{c}^n_{rk}(x^{*n}_{rk}) - p^{*n}_k + p^{*n}_{rk} - \sum_{u\in U}\rho^{*u}_k - \frac{\partial \hat{c}^n_{rk_c}(x^R)}{\partial x^n_{rk}}\right)(x^n_{rk} - x^{*n}_{rk}),\\
&+\sum_{n\in N}\sum_{r\in R} p^n_{rk_c}(x^n_{rk_c} - x^{*n}_{rk_c}) \geq 0, \quad \forall (p^N, x^{UK}, \rho^U, x^U, x^R) \in S^K, \qquad (3.15)
\end{aligned}$$

$$S^K = \left\{(p^N, x^{UK}, \rho^U, x^U, x^R) \in \mathbb{R}^{KN+2UK+UK^cK+NRK}_+ : \sum_{u\in U}\sum_{k\in K} x^u_{k_c k} \leq \mu_{k_c} Q_{kc}\right\}.$$

3.2.4 The Behavior of the Online Platform

Now, I present the behavior of the online platform as an intermediary that matches consumers and collectors. As an intermediary, the platform is involved in transactions both with the collectors, as well as with the consumers at the demand markets.

Collectors resell items on the platform and determine the unitary price p_k^u of second-hand goods. Let $C^u(x^U)$ be the management costs of second-hand product u, including processing and advertisement, and let $\hat{t}_k^u(x_k^u)$ be the transaction cost function between the platform and demand market k, where $x_k^u = \sum_{k_c} x_{k_c k}^u$. Since the platform has no decision-making power on the choice of products that will be sold, it takes the risk of owning false objects or with descriptions that do not correspond to the real conditions of the item. As a consequence, the intermediary may have risk associated with transacting with the various collectors and with the demand markets. Let $\pi(x^U)$ denote the risk function associated with online platform. I assume that $C(x^U)$, $\hat{t}_k^u(x_k^u)$ and $\pi(x^U)$ are continuous, differentiable and convex. Let μ_{k_c} the portion of second-hand goods that collector k_c decides to sell on the platform, and satisfies $\mu_{k_c} \in (0, 1]$. I define $Q^u \in R^U$ as the total amount of item u on the online platform. Each online platform makes his optimal decisions based on maximizing the following profit function:

$$\max \sum_{u \in U} \Big(\sum_{k_c \in K^c} \sum_{k \in K} \gamma p_{k_c}^u x_{k_c k}^u - C^u(x^U) - \sum_{k \in K} \hat{t}_k^u(x_k^u) - \pi(x^U) \Big). \tag{3.16}$$

$$\sum_{k \in K} x_k^u \leq Q^u, \qquad x_k^u, x_{k_c k}^u \geq 0, \ \forall u, \forall k. \tag{3.17}$$

Objective function (3.16) expresses that the profit of the online platform is equal to a percentage of the profit of sale of the product minus the management, transaction

costs and teh risk. The first constraint in (3.17) states that the total amount of each second-hand item bought by all consumers k on platform should be less or equal than the availability of item u.

Under my assumptions, the optimality conditions for the online platform can be expressed as the variational inequality:

$$\sum_{u\in U}\sum_{k_c\in K^c}\sum_{k\in K}\left(\frac{\partial C^u(x^{*U})}{\partial x^u_{k_c k}}-\frac{\partial \pi^u(x^{*U})}{\partial x^u_{k_c k}}-\gamma p^{*u}_k\right)(x^u_{k_c k}-x^{*u}_{k_c k}) \tag{3.18}$$

$$+\sum_{u\in U}\sum_{k\in K}\left(\frac{\partial \hat{t}^u_k(x^u_k)}{\partial x^u_k}\right)(x^u_k-x^{*u}_k)\geq 0,\ \forall (x^U,x^{K^c})\in S^P \tag{3.19}$$

$$S^P=\left\{(x^U,x^{K^c})\in\mathbb{R}^{UK^cK+UK}_+ : \sum_{k\in K}x^u_k\leq Q^u,\forall u\in U\right\}. \tag{3.20}$$

3.3 The Equilibrium Conditions of the CLSC Network

In equilibrium state, the optimality conditions for all suppliers, manufacturers, retailers, demand markets and online platform must be satisfied simultaneously. I now define the CLSC network equilibrium and give an equivalent variational inequality formulation.

Definition 3.3.1. *The CLSC network is at equilibrium if the forward and reverse flows between the tiers of the decision-makers coincide and the product flows and prices satisfy the sum of optimal conditions in* (3.3)*,* (3.7)*,* (3.15)*, and* (3.19)*.*

Using standard arguments, it can be prove that the equilibrium conditions governing the CLSC network model with competition are equivalent to solve a single variational inequality problem. I can establish the following theorem:

Theorem 3.3.1. *The equilibrium conditions governing the CLSC network model with competition are equivalent to solve a single variational inequality problem, given by the sum of problems* (3.3)*,* (3.7)*,* (3.15)*, and* (3.19)*.*

3.4 Conclusions

This study presents an equilibrium model of a CLSC network consisting of manufacturers, retailers, demand markets, and one online platform, in which the consumers purchase new products and collect them. Then, collectors sell the goods to consumers through the online platform. I take into consideration capacity constraints of manufacturers and retailers, as well as consumers' risk-aversion to purchasing second-hand goods, and platform's risk-aversion to transacting with collectors. I model the optimal behaviors of all the decision-makers as variational inequality problems and provide the governing CLSC network equilibrium conditions.

Future research can explore the equilibrium problem in multi-period planning horizons, and the introduction of some random factors in the demand functions. Notwithstanding its limitations, this study may suggest some valuable insights for the market trend.

Chapter 4

A multi-stage integer linear programming problem for personnel and patient scheduling for a therapy centre

4.1 Introduction

The nurse scheduling problem is one of the main issues in healthcare system. It aims to assign a number of nurses to a number of shifts in order to satisfy hospital demand [217]. Scheduling in healthcare is often planned manually and it is time-consuming. Therefore, the automatic assignment of shifts can lead to improvements in efficiency, personnel and patient satisfaction, and staff workload. This research aims at presenting the multi-stage integer linear programming problem for determining the proper scheduling of speech-language pathologists. The model is tested on a case study conducted in a speech therapy centre in *Acireale*

(*Catania, Italy*), where qualified therapists are involved in conventional treatments as well as in Augmentative Alternative Communication (for simplicity, AAC) therapies. In addition, all the therapists, apart from the therapy sessions at the centre, have to provide rehabilitation services in patients' homes. In this paper, I deal with the following problems encountered by the personnel and patients of the speech therapy centre:

1. selection of patients for AAC therapy according to their priority levels;

2. assignment of therapists' shifts (for conventional and AAC therapies) to optimize their workload;

3. planning of the routes/reducing time for the delivery of home-based therapy.

Therefore, I propose a hierarchical approach that breaks the problem into three sub-problems: the selection of the maximum number of patients for AAC therapies, the achievement of an equitable distribution of therapists' workload, and decrease in the transfer time of therapists, who have to change location during the working day, respectively [173]. The first sub-problem is to determine the maximum number of patients benefiting from AAC therapies, with respect to predetermined staff capacity. Because of the extremely high demand of this service, selection of patients must be done before the scheduling. In this step, the selection of patients for AAC treatment among the total number of patients is made according to their priority decided by doctors. In the second sub-problem, I minimize the penalty of each soft constraint and, in particular, I find the optimal assignment of therapists' shifts on weekdays from Monday to Saturday. Thus, the important goal of this study is to provide a balanced schedule for every speech therapist. The AAC therapy is scheduled throughout a week, in order to replicate what really

happens in the centre I analyzed. Finally, in the third sub-problem, I determine the minimum cost on the journeys made by therapists so as to minimize their travel time. The remainder of this paper is organized as follows. Section 4.2 is devoted to the related literature. Section 4.3 presents the proposed methodology which encompasses parameters, model formulation, and solution method. Section 4.4 describes the case study and the numerical experiment results. Finally, Section 4.5 draws the conclusions and illustrates further research issues.

4.2 Related Work

The problem addressed in this work relates to a model described in [173], where a hierarchical mathematical programming problem is proposed to generate weekly staff scheduling. The model is decomposed into three hierarchical stages: the selection of patients, the assignment of patients to the staff, and the scheduling of patients throughout a day.

In the past years, several approaches were proposed, such as tabu search [30], genetic algorithms [2], learning methodologies [1, 75], scatter search [29], and mathematical programming [174, 224, 221]. The approach used is to penalize the violation of the constraints in the objective function. In real applications, it is often difficult to find feasible solutions. In [137], the authors study the scheduling process for two types of nursing teams, regular teams from care units and the float team that covers for shortages in the hospital. The corresponding multi-objective model and heuristics are presented. In [73], the authors study a nurse scheduling problem to minimize the overall hospital cost, and maximize nurses' preferences, while taking into consideration the governmental rules and hospital standards. The mathematical model presented is based on multi-commodity network flow

model. In [23, 24], a multi-objective approach is introduced that differentiates between hard and soft constraints. In [216], a non-optimal solution is generated by solving the mathematical model, and a post-optimization phase using tabu search is performed. In [225], the authors solve the nurse scheduling problem in a Hong Kong emergency department with a two-phase heuristic implemented in Excel. In [201], the authors present an algorithm for supporting weekly planning of therapists. In particular, it allows one to match patient demand with therapist skills while minimizing treatment, travel, administrative and mileage reimbursement costs. Solutions are found with a parallel Greedy Randomized Adaptive Search Procedure (GRASP) that exploits a novel decomposition scheme and employs a number of benefit measures that explicitly address the trade-off between feasibility and solution quality.

This study is builds on the work of [173], but with the following extensions: 1) in this model all the patients receive basic treatments at the centre and some of them are eligible for the AAC therapy program; 2) only some therapists in the centre are qualified to deliver AAC therapies; 3) AAC qualified therapists may also deliver conventional treatments; 4) some patients (AAC and not) receive home-based rehabilitation services.

4.3 Proposed Methodology

This section presents the assumption of the model and the formulation. The assumptions of the model are defined as below:

- the number of patients eligible to start the AAC program is known and fixed;
- the number of therapists in the speech centre is known and constant;

- the velocity of the vehicles used for delivering home-based therapy is constant, and the traffic conditions are not taken into consideration.

The overall problem was broken down into three hierarchical sub-problems, since it was rather difficult to solve the entire problem within an acceptable time for even small size problem instances [174]. The first sub-problem, called "AAC patient selection" aims to get the list of patients whose AAC therapy will be scheduled for the following weeks. These patients receive special therapies only from qualified AAC therapists, while continuing with conventional treatments delivered by the other therapists. The second stage called "Shift assignment" aims to get the weekly shifts for both AAC and basic therapists. Lastly, the third stage called "Travelling therapist problem" aims to get the best route of therapists for delivering home-based sessions during a working day. Mathematical programming models corresponding to each stage are explained in detail in the following subsections.

4.3.1 Problem I: Augmentative Alternative Communication Patient Selection

The purpose of this stage is to select patients that will be scheduled for the following weeks from the candidate list, considering therapists' capacity and priority of patients. The first step of the process is then to determine the maximum number of patients benefiting from the AAC therapy, with respect to the predetermined staff capacity. Moreover, patients may have different priority levels. This difference must be included in an efficient scheduling plan. Priority of patients are categorized into three levels as high, normal, and low according to specialized doctors. In addition, AAC therapy sessions are longer than conventional ones; hence, it is important to balance the distribution of patients among therapists.

Indices and Parameters

- P: number of patients;
- p: patients index;
- w_p: priority level of patients;
- t_p^b: basic treatment time of pth patient;
- t_p^{AAC}: AAC treatment time of pth patient;
- H: total weekly hours;
- T^{AAC}: total weekly hours of AAC sessions.

Decision variables Decision variables at this stage are defined as followed;

$$x_p = \begin{cases} 1 & \text{if } p\text{th patient is selected,} \\ 0 & \text{otherwise.} \end{cases}$$

Objective function Problem I In the objective function (4.1), total number of selected patients is maximized considering priority factor of patients.

$$\max \sum_{p=1}^{P} w_p x_p \tag{4.1}$$

Subject to:

$$\sum_{p=1}^{P} x_p (t_p^b + t_p^{AAC}) \leq H; \tag{4.2}$$

$$t_p^b x_p \leq 1.5, \quad \forall p \in P; \tag{4.3}$$

$$\sum_{p=1}^{P} t_p^{AAC} x_p \leq T^{AAC}; \tag{4.4}$$

Constraint (4.2) ensures that the total sum of the therapy times for all patients must not exceed the total time available in a working week. Inequality (4.3) expresses that each patient does an hour and a half weekly each basic treatment. Finally, inequality (4.4) establishes that the sum over all the time for all AAC patients is less or equal than the total hours devote to AAC sessions per week. I remark that when patients complete the AAC program, it is necessary to update the list of eligible ones, and a new optimal selection is performed.

4.3.2 Problem II: Shift Assignment

In this section, I present the second sub-problem in which I focus on the planning of the shifts. The assignment of shifts is based on the schedules and the availability of the therapy centre to which I am referring. In particular, I differentiate the shifts in the following way: the morning shift, the afternoon shift and the shift for AAC therapy, during the working week from Monday to Saturday, excluding Saturday afternoon. The shift assignment is going to be the same and is repeated for each week. Some patients change as the weeks change but the number of patients in the first sub-problem can be catered for every week. The aim of this sub-problem is to minimize the sum of all the deviations of the soft constraints, multiplied each by an appropriate weight.

Indices

- $C = \{1, \ldots, c\}$ set of therapists working for the AAC program.
- $T = \{c + 1, \ldots, t\}$ set of shift workers.
- $I = C \cup T = \{1, \ldots i, \ldots, t\}$ set of the total number of therapists in the centre.

- $L = \{1, 2, 3\}$ set of shifts, with the typical element of the set denoted by l, where
  - $l = 1 = M$: morning shift;
  - $l = 2 = A$: afternoon shift;
  - $l = 3 = AAC$: AAC shift.
- $J = \{1, \ldots, j, \ldots, 6\}$ set of working days.
  The days will be identified as follows:
  - $j = 1$: Monday;
  - $j = 2$: Tuesday;
  - $j = 3$: Wednesday;
  - $j = 4$: Thursday;
  - $j = 5$: Friday;
  - $j = 6$: Saturday.
- S: set of soft constraints;
- W_s: weight parameter $\forall s \in S$ assigned to each violation of soft constraints.

Decision variables

$$X_{ijl} = \begin{cases} 1 & \text{if the therapist } i \text{ is assigned to the shift } l \\ & \text{on the day } j, \\ 0 & \text{otherwise.} \end{cases}$$

Hard Constraints

$$\sum_{i \in C} X_{ij3} = 2, \quad j = 2, 4; \tag{4.5}$$

$$\sum_{i \in I} X_{i22} \geq 3; \tag{4.6}$$

$$\sum_{i \in I} X_{i51} \geq 1; \tag{4.7}$$

$$\sum_{l \in L} X_{ijl} = 1, \quad \forall i \in C,\ j \in J; \tag{4.8}$$

$$X_{ij1} + X_{ij2} = 1, \quad \forall i \in T,\ j \in J; \tag{4.9}$$

$$X_{i62} = 0, \quad \forall i \in I; \tag{4.10}$$

$$X_{ij2} = 0, \quad \forall i \in C,\ j = 2, 4; \tag{4.11}$$

$$X_{ij3} = 0, \quad \forall i \in T, \forall j \in J \tag{4.12}$$

$$X_{ij3} = 0, \quad \forall i \in C,\ j = 1, 3, 5; \tag{4.13}$$

$$6 \sum_{j \in J} X_{ij3} \geq T^{AAC}, \quad \forall i \in C; \tag{4.14}$$

Constraint (4.5),(4.6) and (4.7) ensure that two therapists are required for AAC shifts, three therapists are required for Tuesday afternoons and one for Friday mornings, respectively. Constraints (4.8) and (4.9) state that each therapist only has to do one shift a day. Constraint (4.10) specifies that the centre is closed on Saturday afternoon. Constraints (4.11) and (4.13) state that each AAC therapist has not to do afternoon shift on Tuesday and Thursday, and has not to do AAC shift on Monday, Wednesday and Friday. Constraint (4.12) ensures that shift workers have not to do AAC shift. Finally, inequality (4.14) establishes that the therapists have to do at least T^{AAC} hours per week. I emphasize that I set the constraints according to the specific centre under consideration. They can be modified as needed and adapted to other situations.

Soft Constraint Now, I present the soft constraints and introduce the variables that take into account the deviations of the constraints from their predetermined goals. These variables will then be minimized in the objective function in order to obtain the best possible solution, trying to reduce the deviations from these constraints. I denoted by $d^+_{si} \geq 0$, $d^+_{sij} \geq 0$ and $d^+_{sij} \geq 0$, $d^-_{si} \leq 0$ the positive and the negative deviations, respectively, associated to the soft constraint $s \in S$, $i \in I$ and $j \in J$.

The soft constraints are the following:

$$6 \sum_{j \in J} (X_{ij2} + X_{ij2}) + 6 \sum_{j \in J} X_{ij3} + d^+_{1i} \geq 36, \quad \forall i \in C; \tag{4.15}$$

$$6 \sum_{j \in J} X_{ij3} - d^-_{2i} \leq 18, \quad \forall i \in C; \tag{4.16}$$

$$6 \sum_{j \in J} (X_{ij2} + X_{ij1}) + d^+_{3i} \geq 36, \quad \forall i \in T; \tag{4.17}$$

$$X_{ij3} + X_{i(j+1)1} - (d^+_{4ij} + d^-_{4ij}) = 1, \quad \forall i \in C,\ j \in J \tag{4.18}$$

$$X_{ij2} + X_{i(j+1)2} - (d^+_{5ij} + d^-_{5ij}) = 1, \quad \forall i \in T,\ j \in J \tag{4.19}$$

$$X_{ij1} + X_{i(j+1)1} - (d^+_{6ij} + d^-_{6ij}) = 1, \quad \forall i \in T,\ j \in J \tag{4.20}$$

Constraint (4.15) and (4.16) establish that it is preferable that the therapists do at least thirty six hours a week. Constraint (4.18) states that is preferable that the therapists do no more than eighteen hours per week of AAC sessions. Finally, equalities (4.17), (4.19) and (4.20) ensure that is preferable that they do not have two consecutive mornings or afternoons.

Objective function Problem II The overall objective function to be minimized is given by the sum of all the deviations of the soft constraints described above, each multiplied by an appropriate weight, chosen on the basis of the importance

of the violated constraint.

$$\min\Big(W_1 \sum_{i \in C} d^+_{1i} + W_2 \sum_{i \in C} -d^-_{2i} + W_3 \sum_{i \in T} d^+_{3i} + W_4 \sum_{i \in C} \sum_{j \in J} (d^+_{4ij} - d^-_{4ij}) + W_5 \sum_{i \in T} \sum_{j \in J} (d^+_{5ij} - d^-_{5ij}) + W_6 \sum_{i \in T} \sum_{j \in J} (d^+_{6ij} - d^-_{6ij})\Big); \tag{4.21}$$

The minimization of the objective function, subject to the constraints already described, guarantees a solution that satisfies all the hard constraints and violates the soft constraints as little as possible.

4.3.3 Problem III: Travelling therapist problem

In this section, I optimize the routing from one location to another one during the working day. The problem can be defined as an asymmetric multiple Traveling Salesman Problem with Time Windows (mTSPTW) [21], and additional constraints, such as an upper bounded variable of the number of therapists, and the maximum traveling time or distance of each therapist. I also include time window at each location. Usually, the mTSP is specified as an integer programming formulation.

Sets and Parameters

- $G = (V, E)$;
- $V = \{v_1, \ldots v_h, \ldots, v_k, \ldots, v_n\}$ set of vertices;
- $E = \{(v_h, v_k)\}$ set of edges, which satisfy the symmetric property;
- $I = \{1, \ldots i, \ldots, t\}$ set of the total number of therapists in the centre, where i is the general one;

- TW indicates the time window. It is important to remark the role of this parameter as each therapist takes at least 2 hours for home-based therapies (considering transfer time and therapy session), before leaving for a new destination. Morevoer, the daily working hours are limited.

- $\hat{c}_{hk}$, where $\hat{c}_{hk} = c_{hk} + c_k^{TW}$ is the total cost considered;

- c_{hk} ordinary cost (distance or duration) associated with E. The costs could be symmetric if $c_{hk} = c_{kh}, \forall (v_h, v_k) \in E$ and asymmetric otherwise;

- c_k^{TW} cost of the time window TW, where every therapist has to do the therapy in each location, which takes about 2 hours;

- $\bar{I}$ upper bound of the therapist i, namely, the actual number of therapist used, i.e. the number of available therapists;

- c_i cost of the involvement of a therapist $i \in I$, i.e a fixed cost aiming to minimize their number;

- D maximum length of any tour in the solution.

Decision variables

$$y_{hki} = \begin{cases} 1 & \text{if therapist } i \text{ chooses the edge}(v_h, v_k), \\ 0 & \text{otherwise.} \end{cases}$$

Objective function Stage III

$$\min \sum_{h=0}^{n} \sum_{k=0}^{n} \hat{c}_{hk} \sum_{i=1}^{t} y_{hki} + t \cdot c_i \tag{4.22}$$

Subject to

$$\sum_{h=0}^{n} \sum_{i=1}^{t} y_{hki} = 1, \quad \forall k = 1, \ldots, n, \tag{4.23}$$

$$\sum_{k=0}^{n} \sum_{i=1}^{t} y_{hki} = 1, \quad \forall h = 1, \ldots, n, \tag{4.24}$$

$$\sum_{h=1}^{n} \sum_{i=1}^{t} y_{1ki} = t, \quad \forall k = 1, \ldots, n, \tag{4.25}$$

$$\sum_{k=1}^{n} \sum_{i=1}^{t} y_{h1i} = t, \quad \forall h = 1, \ldots, n, \tag{4.26}$$

$$\sum_{h=1}^{n} \sum_{k=1}^{n} c_{hk} \cdot y_{hki} \leq D, \quad \forall i \in I \tag{4.27}$$

$$+ \text{ sub tour elimination constraints} \tag{4.28}$$

The objective function (4.22) represents the minimization of the cost of the journey, where $\hat{c}_{hk}$ is expressed as a weight on each edge, based on the distance or the cost of the journey, and c_i is the cost of involvement of the therapist i. Constraints (4.23) and (4.24) state that in each node v_h only one edge enters and exits $\forall h, k = 1, \ldots n$. Constraints (4.25) and (4.26) are the usual assignment constraints for the starting and the ending point, using the binary variable. Constraints (4.27) ensures that the tour length of each therapist is under the specified bound D.

4.4 Case Study

In order to apply my models, a data set of the speech therapy centre of *Acireale*, *Sicily* (*Italy*) is used. In this centre, there are two therapists assigned to work on

the AAC project and six conventional therapists, who are working 6 days a week for 6 hours a day. To solve the mathematical models, AMPL and CPLEX solver for the first and the second problem and GA Matlab code for the third problem were used.

4.4.1 Problem I

In this stage, priority of patients, which was categorized into three levels as high, medium, and low, according to specialized doctors' view, is reflected in the model. Determination of these weights (w_p) for each priority level depends on the decision maker's preferences. The difference between the weights for different levels of priorities should be selected large enough to maintain a certain hierarchy between priorities. The selection of weights is just a case for an illustration of the model. I fixed $w_p = 0.8$, $w_p = 0.5$ and $w_p = 0.2$ for high, medium and low level, respectively. I considered the number of patients equal to 50, ($P = 50$), who ask to participate in the AAC program in addition to basic therapy. This particular therapy can only be carried out by some therapists because the staff must be qualified for this additional therapy. In fact, Table 4.1 shows that only 21 patients were selected among those who asked to participate in the special AAC program, as a consequence the following Table 4.1 represents the patients that are selected for the AAC treatment, considering only the two therapists who are involved in the AAC shift. Unselected patients are not ignored, but will continue to be followed through basic therapy, because they do not have severe language difficulties and do not urgently need additional therapy.

In this case study, the treatment time was classified into two categories; t_p^b and t_p^{AAC} were assigned to symbolize basic treatment (45 min) and AAC treatment

Weight	Patient i	Selected
	1	0
$w_i = 0.2$	⋮	⋮
	15	0
	16	1
	⋮	⋮
	26	1
$w_i = 0.5$	27	0
	⋮	⋮
	40	0
	41	1
$w_i = 0.8$	⋮	⋮
	50	1

Table 4.1: Selected Patients Number

($\geq$ 60 min), respectively. Finally, I fixed 24 weekly hours dedicated to basic therapy by each AAC therapist and 12 hours carried out simultaneously by both AAC therapists. Therefore the total hours available to AAC therapists is $H = 60$.

4.4.2 Problem II

In this stage, I considered two therapists $i = 1, 2$ who perform both basic shifts and AAC treatments and six shift workers, $i = 3, \ldots 8$. In the centre under study, the weekly work is structured from Monday to Friday, morning (M) and afternoon (A), and on Saturday only in the morning. In particular, the AAC treatment is carried

out only on Tuesday, Thursday and Saturday mornings, indicated with the index $l = 3$. I remind that the centre is closed on Saturday afternoons. In the objective function (4.21), I fixed $W_1 = 0.84$, $W_2 = 0.3$, $W_3 = 0.58$, $W_4 = 0.88$, $W_5 = 0.67$, $W_6 = 0.68$, which represent the weight associated with the soft constraint. The greater the weight, the greater the importance of the soft constraint. I fixed $t_p = 0.75$ and $t_p^{AAC} = 2$ to define the following constraint:

$$0.75x_p \leq 1.5, \quad \forall p \in P; \tag{4.29}$$

$$2\sum_{p=1}^{P} x_p \leq 12. \tag{4.30}$$

In Table 4.2, I provide the shifts for the eight therapists that I have considered.

	Morning	Afternoon	AAC
Mon	4, 7, 8	1, 2, 3, 5, 6	
Tue	3, 5, 6	4, 7, 8	1, 2
Wed	7, 8	1, 2, 3, 4, 5, 6	
Thu	3, 4, 5, 6	7, 8	1, 2
Fri	7, 8	1, 2, 3, 4, 5, 6	
Sat	3, 4, 5, 6, 7, 8	*closed*	1, 2

Table 4.2: Therapists' shifts

4.4.3 Problem III

In this subsection I investigate the problem of moving from one location to another one considering fixed time windows. In fact, during the working day, therapists have to move from one therapy centre to another one, from one centre to another

location to deliver home-based rehabilitation services, or from one house to another one. I considered $\bar{I} = 8$ therapists, who have the starting point at the centre of *Acireale* and I supposed that patients' houses are in the other locations considered, to simulate that some therapies are carried out directly at home. The corresponding multiple traveling salesmen problem was implemented using the genetic algorithm with multi-chromosome representation as in [127]. The algorithm considers that each therapist starts at the first location, and ends at the first location, but travels to a unique set of cities in between. I assume that the first location is the central location placed in *Acireale, Italy*, then each therapist has her own patients in different places. As a consequence, except for the starting point, each location is visited by exactly one therapist. The algorithm uses a special, so-called multi-chromosome genetic representation to code solutions into individuals. Special genetic operators (even complex ones) are used. The number of therapists that every day have to travel from one location to another is minimized during the algorithm. The algorithm also considers additional constraints, such as the minimum number of locations that the therapists visit and the maximum distance travelled by each therapist. I fixed $D = 80$ kilometers as the maximum tour length for each therapist, since a working day lasts only six hours. I considered the objective function (4.22), where the weights, considered as distances and costs, associated with the edges, are defined as

$$c_{hk} = \sqrt{(x_h - x_k)^2 + (y_h - y_k)^2}, \quad \forall v_h, v_k \in V. \tag{4.31}$$

I solved this problem using a genetic algorithm (GA), implemented in Matlab [127], tested on MacBook Air (2021), processor Apple M1 8 Core, 3.2 GHz, RAM 8 GB.

For instance, I obtained the total distance traveled by all the therapists equal to

379 kilometers, obtained by 474 number of iterations and 19 time in milliseconds until the solution was given. The following plots explain better the solution reached. Figure 4.1 represents the different 40 locations chosen in the example.

Figure 4.1: City Locations

It is necessary that therapists move from one location to another, because some therapies, especially on younger people, are carried out in places where they spend a lot of their life, for example at home or in parks or even at school.

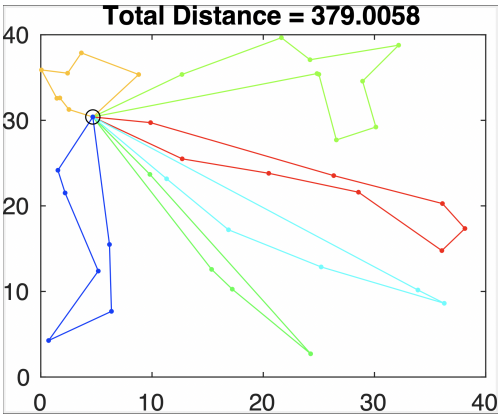

Figure 4.2: Total Distance

Figure 4.2 shows the routes solution of each therapist. As a conclusion, I underline that the minimum number of therapists needed to reach all the 40 locations in one

day is six. As a consequence of the six hours a day of each therapist, the time spent for travel influence the number of patients that could be treated. The Figure 4.2 underlines that some therapists are forced to face even long distances on a daily basis to satisfy the request of their patients.

4.5 Conclusions

This work presented a multi-stage integer linear programming problem to solve the scheduling of speech-language pathologists involved in conventional treatments as well as Augmentative Alternative Communication therapies. In order to reduce the complexity of this problem, I developed a mathematical model based on a hierarchical approach. Thus, the problem was broken down into three sub-problems. The aims were: the selection of the maximum number of patients, who can use the Augmentative Alternative Communication therapy program in addition to basic therapy; the achievement of an equitable distribution of therapists' workload to optimize work shifts and distribute them optimally during the week; the decrease of the time-wasting of therapists during transfers, who have to move for home-based therapies and have to change location during the working day. The model was tested on a therapy centre and the solution time was acceptable for the hierarchical implementation, with AMPL optimization package and Genetic Algorithm implementation in Matlab to find the solution in a faster way and to avoid the limitations of AMPL software. The model presented has some limitations that encourage us to further investigate the problem and improve my achievements. In fact, I did not take into consideration the preferences of therapists about their shifts, and the staggered entry times due to COVID-19 pandemic. As a future research, I can also explore the model with a higher number of therapists and patients.

Chapter 5

A two-stage variational inequality for medical supply in emergency management

5.1 Introduction

In recent years, emergencies and natural disasters have significantly affected our social and economic progress. Therefore, emergency management has become one of the most important and challenging issues. Moreover, emergency resource storage and distribution have led to strong competition for medical supplies among healthcare institutions.

In this paper, I investigate hospital competition for medical supplies as a generalized Nash equilibrium problem, and propose a stochastic programming model to describe the behaviour of each demand location. Thus, I am able to obtain the optimal amount of medical items from warehouses to hospitals, in order to minimize both the purchasing cost and the transportation costs. Following [220], I consider

real-time information spreading and up-to-date disaster evaluation. Therefore, I provide a two-stage stochastic programming model based on disaster scenarios that takes into account the unmet demand at the first stage, and the consequent penalty, see [138]. In particular, in the first stage, hospitals receive the early warning information about the emergency and decide the medical item procurement planning; however, they are not aware of the real situation. Subsequently, accurate real-time information is observed and the process reaches the second-stage, where the decision relies on the first-stage solution and on the observed scenario. Moreover, I introduce a penalty function for the unmet demand of medical supplies in the second stage decision, see also [90]. The problem is then formulated as a two-stage stochastic variational inequality (see [138]).

The importance of an efficient approach to emergency management and medical supply planning has been investigated in several papers. For instance, in [72] the authors construct a generalized Nash equilibrium model with stochastic demand to analyse competition among organizations for medical supplies. The problem is then formulated as a variational inequality, using the concept of variational equilibrium. In [155], Nagurney et al. present a stochastic generalized Nash equilibrium model for disaster relief. Each humanitarian organization solves a two-stage stochastic optimization problem, and the model is formulated as a finite-dimensional variational inequality. In [197], Nagurney and Salarpour introduce a variational inequality formulation of a two-stage stochastic game theory model in order to examine the behavior of national governments during Covid-19 pandemic and their competition for essential medical supplies. In [138], the authors develop a stochastic programming model to select the storage locations of medical supplies and required inventory levels for each type of medical supply. The resulting model

captures the information updating making use of disaster scenarios. In [53], the authors present an optimization model consisting of a dynamic supply chain network for personal protective equipment, and study the related evolutionary variational inequality in the presence of a delay function.

Recently, two-stage stochastic variational inequalities have been introduced, where one seeks a decision vector before the stochastic variables are known, and a decision vector after the scenario has been realized. In [38], the authors propose a two-stage stochastic variational inequality model to deal with random variables in variational inequalities, and formulate this model as a two-stage stochastic programming with recourse. In [138], the authors investigate the transformation of a general two-stage stochastic programming problem to a two-stage stochastic variational inequality. In [192], Rockafellar and Wets discuss the multistage stochastic variational inequality. In [190], the authors develop progressive hedging methods for solving multistage convex stochastic programming, see also [189].

In this paper, I extend the model in [72] in two directions. First, I tackle the medical item procurement planning problem as a two-stage stochastic programming problem. Then, I describe the model as a generalized Nash equilibrium problem. Our second improvement is the characterization as a two-stage variational inequality. This approach allows us to decompose the problem in two lower dimensional variational inequalities, instead of solving a unique large-scale variational inequality. I also present an alternative formulation based on Lagrangian relaxation approximation, that makes it possible to investigate the role of Lagrange multipliers in the market behavior.

The structure of this paper is as follows. In Section 5.2, I introduce the two-stage stochastic model. In Section 5.3, I model the competition among healthcare

institutions as a generalized Nash equilibrium problem, and provide a two-stage variational inequality formulation. I also present an alternative two-stage variational inequality based on the Lagrangian relaxation approach. Finally, in Section 5.4, I draw our conclusions and present further research issues.

5.2 Two-Stage Stochastic Model of the Competition for Medical Supply

In this section, I present a two-stage stochastic model for the medical supply competition. Let $\mathcal{W}$ denote the set of warehouses, with typical warehouse denoted by w; let $\mathcal{H}$ denote the set of hospitals, with typical hospital denoted by h; let $\mathcal{K}$ denote the set of medical supply type, with typical type denoted by k, and let $\mathcal{M}$ denote the set of transportation modes, with typical mode denoted by m. I consider a network representation as in Figure 5.1. The links between the levels

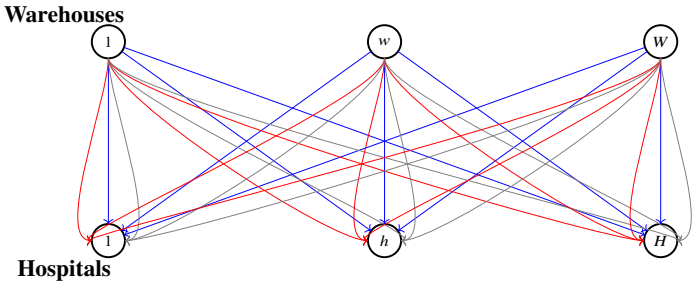

Figure 5.1: The Network representation of Warehouses and Hospitals

of the network represent all the possible connections between warehouses and hospitals. Multiple links between each warehouse and each hospital depict the possibility of alternative modes of transportation. I note that the choice of the transportation mode is due to the distance between supply and demand locations.

For example, for long distances airplanes are preferred to transportation by truck or train. The choice of the transportation mode may also depend on the type of medical item or on the severity of the emergency.

I denote by Q_w^k the amount of medical item of type k in warehouse w, and by $Q_w = \sum_{k\in\mathcal{K}} Q_w^k$ the total amount of medical items in warehouse w.

Now, let x_{wh}^k be the amount of medical item of type k from warehouse w to hospital h, and let ρ_w^k be the unitary price of medical item k at warehouse w. Let x_{wh} denote the total amount delivered from warehouse w to hospital h, where

$$x_{wh} = \sum_{k\in\mathcal{K}} x_{wh}^k.$$

I further group the x_{wh} into the $WH-$dimensional column vector x.

In addition, I introduce the transportation time t_{wh}^m from warehouse w to hospital h with mode m and assume that it depends on the amount x_{wh}, namely, $t_{wh}^m = t_{wh}^m(x_{wh})$.

Table 5.1 summarizes the relevant notations used in the model formulation.

I consider a pre-event policy, in which each demand location (hospital) seeks to minimize the purchasing cost of medical items and the transportation time from the first stage, and a recourse decision process to optimize the transportation costs from the second stage, in response to each disaster scenario. Let $(\Omega, \mathcal{F}, P)$ be a probability space, where the random parameter $\omega \in \Omega$ represents the typical disaster scenario. For each $\omega \in \Omega$, I denote by $\xi : \Omega \to \mathbb{R}^{WHK+HK}$ a finite dimensional random vector and by $\mathbb{E}_\xi$ the mathematical expectation with respect to ξ. In order to formulate the two-stage stochastic model, I introduce two types of decision variables. The first-stage decision variable x_{wh}^k is used to represent the quantity of medical supplies of type k from warehouse w to hospital h. The second-stage decision variables are $y_{wh}^k(\omega)$ and $z_h^k(\omega)$. The variable $y_{wh}^k(\omega)$ represents

Symbols	Definitions
$\mathcal{W}$	set of warehouses, with typical warehouse denoted by w, $card(\mathcal{W}) = W$
$\mathcal{H}$	set of hospitals, with typical hospital denoted by h, $card(\mathcal{H}) = H$
$\mathcal{K}$	set of different medical items, with typical item denoted by k, $card(\mathcal{K}) = K$
$\mathcal{M}$	set of transportation modes, with typical mode denoted by m, $card(\mathcal{M}) = M$
d_h^k	demand of medical item k of hospital h in stage one
$d_h^k(\omega)$	demand of medical item k of hospital h in stage two under scenario ω
x_{wh}^k	amount of medical item k from warehouse w to hospital h in stage one
x_{wh}	amount of medical items delivered from warehouse w to hospital h in stage one
x	amount of total medical items from all warehouses to all hospitals in stage one
Q_w^k	the amount of the medical item k in warehouse w
$Q_w = \sum_{k\in\mathcal{K}} Q_w^k$	the total amount of the medical items in warehouse w
e_k	maximum amount available of medical item k
ρ_w^k	unitary price of medical item k at warehouse w
$t_{wh}^m(x_{wh})$	transportation time from warehouse w to hospital h with mode m
$y_{wh}(\omega)$	amount of medical items to be delivered from warehouse w to hospital h in stage two under scenario ω
$z_h^k(\omega)$	amount of unfulfilled demand at hospital h of medical supply item k under scenario ω
$c_{wh}^m(y_{wh}(\omega), \omega)$	transportation cost from warehouse w to hospital h with mode m under scenario ω
$\pi_h^k(z_h^k(\omega), \omega)$	penalty for unfulfilled demand at hospital h of medical supply item k under scenario ω

Table 5.1: The notation for the two-stage stochastic model

the quantity of medical supplies of type k to be delivered from warehouse w to hospital h under scenario ω. The variable $z_h^k(\omega)$ is the unfulfilled demand at hospital h of medical item k under scenario ω. I penalize the amount of unfulfilled demand $z_h^k(\omega)$ by function $\pi_h^k = \pi_h^k(z_h^k(\omega), \omega)$. From the perspective of demand locations, x_{wh}^k is chosen before a realization of ξ is revealed and later $y_{wh}^k(\omega)$ and $z_h^k(\omega)$ are selected with known realization. Finally, I introduce the transportation cost c_{wh}^m from warehouse w to hospital h with mode m and assume that it depends on the amount $y_{wh}(\omega) = \sum_{k\in\mathcal{K}} y_{wh}^k(\omega)$, namely, $c_{wh}^m = c_{wh}^m(y_{wh}(\omega), \omega)$.

Our aim is to obtain an efficient plan of medical item procurement of each demand location in the first stage by the evaluation of adaptive plans in the second stage.

5.2.1 First-Stage Problem

For each hospital h, I minimize the purchasing cost and the transportation time of the first stage with the expected overall costs and the penalty for the prior plan. Therefore, the first-stage problem is given by:

$$\min \sum_{w \in \mathcal{W}} \left(\sum_{k \in \mathcal{K}} \rho_w^k x_{wh}^k + \sum_{m \in \mathcal{M}} t_{wh}^m(x_{wh}) \right) + \mathbb{E}_\xi(\Phi_h(x, \xi(\omega))) \tag{5.1}$$

subject to

$$\sum_{h \in \mathcal{H}} \sum_{k \in \mathcal{K}} x_{wh}^k \leq Q_w, \ \forall w \in \mathcal{W}, \tag{5.2}$$

$$\sum_{w \in \mathcal{W}} x_{wh}^k = d_h^k, \ \forall k \in \mathcal{K}, \tag{5.3}$$

$$\sum_{w \in \mathcal{W}} x_{wh}^k \leq e_k, \ \forall k \in \mathcal{K}, \tag{5.4}$$

$$x_{wh}^k \geq 0, \ \forall w \in \mathcal{W}, \ \forall k \in \mathcal{K}. \tag{5.5}$$

The objective function (5.1) minimizes the sum of the purchasing cost for early supply plan, the transportation time, and the expected value of costs of hospital h in the second stage with respect to disaster scenarios. Constraint (5.2) ensures that the storage capacity of warehouse w is satisfied. It is a shared constraint and realizes that hospitals compete for medical items available at the warehouses at a maximum supply. Constraint (5.3) states that the amount of delivered medical items of type k has to satisfy the requirement of hospital h; constraint (5.4) is the maximum availability constraint of medical item k; constraint (5.5) is the non-negativity requirement on variables. I require that $d_h^k \leq e_k, \forall h, k$. Finally, I assume that $t_{wh}^m(\cdot)$ is continuously differentiable and convex for all w, h, m.

5.2.2 Second-Stage Problem

The second stage is the evaluation of the first stage to obtain the optimal medical supply procurement.

For a given realization $\omega \in \Omega$, the second-stage problem of hospital h is given as:

$$\Phi_h(x, \xi(\omega)) = \min \sum_{w \in \mathcal{W}} \sum_{m \in \mathcal{M}} c^m_{wh}(y_{wh}(\omega), \omega) + \sum_{k \in \mathcal{K}} \pi^k_h(z^k_h(\omega), \omega) \tag{5.6}$$

subject to

$$\sum_{h \in \mathcal{H}} \sum_{k \in K} y^k_{wh}(\omega) \leq Q_w(\omega) - \sum_{h \in \mathcal{H}} \sum_{k \in \mathcal{K}} x^k_{wh}, \ \forall w \in \mathcal{W}, P\text{-}a.s., \tag{5.7}$$

$$\sum_{w \in \mathcal{W}} y^k_{wh}(\omega) + z^k_h(\omega) = d^k_h(\omega), \ \forall k \in \mathcal{K}, P\text{-}a.s., \tag{5.8}$$

$$\sum_{w \in \mathcal{W}} y^k_{wh}(\omega) \leq e_k(\omega), \ \forall k \in \mathcal{K}, P\text{-}a.s., \tag{5.9}$$

$$y^k_{wh}(\omega) \geq 0, z^k_h(\omega) \geq 0 \ \forall w \in \mathcal{W}, \ \forall k \in \mathcal{K}, P\text{-}a.s. \tag{5.10}$$

Thus, $\Phi_h(x, \xi(\omega))$ is the optimal value of the second-stage problem (5.6)-(5.10), where the constraints hold almost surely (P-a.s.). The objective function (5.6) minimizes the total cost and the penalty for the unmet demand at the second stage. Constraint (5.7) is the warehouse storage capacity which takes into account the quantity of medical items already delivered. Constraint (5.8) is a balance constraint, and states that the supply at the second stage plus the unmet demand should be equal to the demand at the second stage. Constraint (5.9) is the maximum availability constraint of medical supply of type k at the second stage. Finally, (5.10) is the non-negativity constraint. I emphasize that the connection between stage-wise decision variables x and y is captured by coupling constraint (5.7). It is the linking factor between the first and second stage, and communicates the first-stage decisions to the second one.

I assume that:

a) $c^m_{wh}(\cdot, \omega)$, $\pi^k_h(\cdot, \omega)$, a.e. in Ω, are continuously differentiable and convex for all w, h, k, m;

b) for each $u \in \mathbb{R}^{WH}$, $c^m_{wh}(u, \cdot)$ is measurable with respect to the random parameter in Ω for all w, h, m;

c) for each $v \in \mathbb{R}^{HK}$, $\pi^k_h(v, \cdot)$ is measurable with respect to the random parameter in Ω for all h, k;

d) $y^k_{wh} : \Omega \to \mathbb{R}$ and $z^k_h : \Omega \to \mathbb{R}$ are measurable mappings for all w, h, k;

e) $d^k_h : \Omega \to \mathbb{R}$ is a measurable mapping for all h and all k.

Finally, I require that $d^k_h(\omega) \leq e_k(\omega)$, $\forall h, k$ and for all scenario ω.

If the random parameter $\omega \in \Omega$ follows a discrete distribution with finite support $\Omega = \{\omega_1, \ldots, \omega_r\}$ and probabilities $p(\omega_r)$ associated with each realization ω_r, $r \in \mathcal{R} = \{1, \ldots, R\}$, then the two-stage problem of hospital h can be formulated

as the unique large scale problem:

$$\min \sum_{w\in\mathcal{W}} \left(\sum_{k\in\mathcal{K}} \rho_{wh}^k x_{wh}^k + \sum_{m\in\mathcal{M}} t_{wh}^m(x_{wh}) \right)$$
$$+ \sum_{r\in\mathcal{R}} p(\omega_r) \left(\sum_{w\in\mathcal{W}} \sum_{m\in\mathcal{M}} c_{wh}^m(y_{wh}(\omega_r), \omega_r) + \sum_{k\in\mathcal{K}} \pi_h^k(z_h^k(\omega_r), \omega_r) \right) \tag{5.11}$$

subject to

$$\sum_{h\in\mathcal{H}} \sum_{k\in\mathcal{K}} x_{wh}^k \leq Q_w, \ \forall w \in \mathcal{W}, \tag{5.12}$$

$$\sum_{w\in\mathcal{W}} x_{wh}^k = d_h^k, \ \forall k \in \mathcal{K}, \tag{5.13}$$

$$\sum_{w\in\mathcal{W}} x_{wh}^k \leq e_k, \ \forall k \in \mathcal{K}, \tag{5.14}$$

$$\sum_{h\in\mathcal{H}} \sum_{k\in\mathcal{K}} y_{wh}^k(\omega_r) \leq Q_w(\omega_r) - \sum_{h\in\mathcal{H}} \sum_{k\in\mathcal{K}} x_{wh}^k, \ \forall w \in \mathcal{W}, \forall r \in \mathcal{R}, \tag{5.15}$$

$$\sum_{w\in\mathcal{W}} y_{wh}^k(\omega_r) + z_h^k(\omega_r) = d_h^k(\omega_r), \ \forall k \in \mathcal{K}, \forall r \in \mathcal{R}, \tag{5.16}$$

$$\sum_{w\in\mathcal{W}} y_{wh}^k(\omega_r) \leq e_k(\omega_r), \ \forall k \in \mathcal{K}, \forall r \in \mathcal{R}, \tag{5.17}$$

$$x_{wh}^k \geq 0, \ \forall w \in \mathcal{W}, \ \forall k \in \mathcal{K}, \tag{5.18}$$

$$y_{wh}^k(\omega_r) \geq 0, \ \forall w \in \mathcal{W}, \ \forall k \in \mathcal{K}, \forall r \in \mathcal{R}, \tag{5.19}$$

$$z_h^k(\omega_r) \geq 0, \ \forall k \in \mathcal{K}, \forall r \in \mathcal{R}. \tag{5.20}$$

5.3 Stochastic generalized Nash equilibrium

Competition for medical supplies among hospitals can be studied also as a game. The underlying equilibrium concept is then that of a stochastic generalized Nash equilibrium (SGNE), namely, a Nash equilibrium when the functions are expected value functions, and the players are subject to shared constraints.

I define the sets:

$$S_h = \left\{ x_h = (x^k_{wh})_{w,k} \in \mathbb{R}^{WK} : (5.3) - (5.5) \text{ hold} \right\},$$

$$X = \{ x = (x_h)_h \in \mathbb{R}^H : x \text{ satisfies (5.2)} \},$$

$$T_h = \left\{ (y_h(\omega), z_h(\omega)) = \left((y^k_{wh}(\omega))_{w,k}, (z^k_h(\omega))_k \right) \in \mathbb{R}^{WK+K} : \right.$$

$$\left. (5.8) - (5.10) \text{ hold, } P\text{-a.s.} \right\},$$

$$V = \{ (y(\omega), z(\omega)) = (y_h(\omega), z_h(\omega))_h \in \mathbb{R}^{2H} : (5.7) \text{ holds, } P\text{-a.s.} \}.$$

I also define $S = \prod_h S_h$ and $T = \prod_h T_h$.

I refer to the objective function (5.1) for $h \in \mathcal{H}$ as the function:

$$\mathbb{J}_h(x_h, x_{-h}) = \sum_{w \in \mathcal{W}} \left(\sum_{k \in \mathcal{K}} \rho^k_{wh} x^k_{wh} + \sum_{m \in \mathcal{M}} t^m_{wh}(x_{wh}) \right) + \mathbb{E}_\xi(\Phi_h(x_h, x_{-h}, \xi(\omega))),$$

where x_{-h} denotes the amount of medical items required by all hospitals except for h.

Definition 5.3.1. *A vector of medical items $x^* = (x^*_h, x^*_{-h}) \in S \cap X$ is a stochastic generalized Nash equilibrium of the first-stage if for each $h \in \mathcal{H}$*

$$\mathbb{J}_h(x^*_h, x^*_{-h}) \leq \mathbb{J}_h(x_h, x^*_{-h}), \quad \forall x_h \in S_h, \forall x \in X.$$

Analogoysly, I can define the SGNE for the second stage. A solution of such a problem can be found solving a quasi-variational inequality; see [112]. I point out that this problem can also be solved in the form of a variational inequality, using the concept of variational equilibrium; see [76, 131]. However, I note that it is not possible to obtain a full characterization of the solutions of a SGNE problem as solutions of a variational inequality. For this reason, recently, some authors focused on the computation of non-variational equilibria; see [80, 153].

5.3.1 Two-Stage Variational Inequality Formulation

I now adopt a variational equilibrium approach to my SGNE problem. The two-stage stochastic problem is then equivalent to a two-stage variational inequality (see [126, 155] for theoretical aspects and applications on variational inequality theory).

I restrict my attention to the case of discrete probability distribution.

Theorem 5.3.1. *The vector* $(x^*, y^*(\omega_r), z^*(\omega_r))$, $\forall \omega_r, r \in \mathcal{R}$, *is an optimal solution of the medical item procurement planning if and only if:*

1. *the vector* $x^* = (x_h^*, x_{-h}^*) \in S \cap X$ *is a solution of the variational inequality*

$$\sum_{w\in\mathcal{W}}\sum_{h\in\mathcal{H}}\sum_{k\in\mathcal{K}}\left(\rho_{wh}^k + \sum_{m\in\mathcal{M}}\frac{\partial t_{wh}^m(x_{wh}^*)}{\partial x_{wh}^k} + \sum_{r\in\mathcal{R}} p(\omega_r)\frac{\partial \Phi_h(x^*, \xi(\omega_r))}{\partial x_{wh}^k}\right) \times (x_{wh}^k - x_{wh}^{*k}) \geq 0, \forall x \in S \cap X; \tag{5.21}$$

2. *the vector* $(y^*(\omega_r), z^*(\omega_r)) \in T \cap V$, $\forall \omega_r, r \in \mathcal{R}$, *is a solution of the variational inequality*

$$\sum_{r\in\mathcal{R}} p(\omega_r)\sum_{w\in\mathcal{W}}\sum_{h\in\mathcal{H}}\sum_{k\in\mathcal{K}}\left(\sum_{m\in\mathcal{M}}\frac{\partial c_{wh}^m(y_{wh}^*(\omega_r), \omega_r)}{\partial y_{wh}^k(\omega_r)}\right) \times (y_{wh}^k(\omega_r) - y_{wh}^{*k}(\omega_r)) + \sum_{r\in\mathcal{R}} p(\omega_r)\sum_{h\in\mathcal{H}}\sum_{k\in\mathcal{K}}\frac{\partial \pi_h^k(z_h^{*k}(\omega_r), \omega_r)}{\partial z_h^k(\omega_r)} \times (z_h^k(\omega_r) - z_h^{*k}(\omega_r)) \geq 0, \quad \forall (y(\omega_r), z(\omega_r)) \in V \cap T. \tag{5.22}$$

In order to ensure the existence of solutions to (5.21), I note that the set $S \cap X$ is compact and convex, and the operator that enters (5.21) is continuous. Thus, a solution exists from the standard theory of variational inequalities; see [126]. A similar reasoning ensures the existence of solutions to (5.22).

5.3.2 Lagrangian Relaxation Approach

In the following, I provide an alternative two-stage variational inequality, that leads to a lower bound to the optimal value of the initial model. I relax constraints (5.2) and (5.7) into their respective objective functions by Lagrangian relaxation approach (see [22, 138]). I associate a non-negative Lagrange multiplier $\lambda_w \geq 0$ to constraint (5.2), for each $w \in \mathcal{W}$. I group all the Lagrange multipliers into the vector $\lambda \in \mathbb{R}_+^W$. Analogously, I associate a non-negative Lagrange multiplier $\mu_w(\omega_r) \geq 0$ to constraint (5.7), for each $w \in \mathcal{W}$ and $r \in \mathcal{R}$. I group all the Lagrange multipliers into the vector $\mu(\omega_r) \in \mathbb{R}_+^W$, $\forall r \in \mathcal{R}$. Thus, I find the following two-stage variational inequality:

1. Find $x^* = (x_h^*, x_{-h}^*) \in S$ and $\lambda^* \in \mathbb{R}_+^W$ such that

$$\sum_{w\in\mathcal{W}}\sum_{h\in\mathcal{H}}\sum_{k\in\mathcal{K}}\left(\rho_{wh}^k + \sum_{m\in\mathcal{M}}\frac{\partial t_{wh}^m(x_{wh}^*)}{\partial x_{wh}^k} + \sum_{r\in\mathcal{R}} p(\omega_r)\frac{\partial \Phi_h(x^*, \xi(\omega_r))}{\partial x_{wh}^k} + \lambda_w\right)$$
$$\times (x_{wh}^k - x_{wh}^{*k})$$
$$+ \sum_{w\in\mathcal{W}}\left(Q_w - \sum_{h\in\mathcal{H}}\sum_{k\in\mathcal{K}} x_{wh}^{*k}\right) \times (\lambda_w - \lambda_w^*) \geq 0, \forall x \in S, \lambda \in \mathbb{R}_+^W. \qquad (5.23)$$

2. Find $(y^*(\omega_r), z^*(\omega_r)) \in T$ and $\mu^*(\omega_r) \in \mathbb{R}_+^W$, $\forall \omega_r, r \in \mathcal{R}$, such that

$$\begin{aligned}
&\sum_{r\in\mathcal{R}} p(\omega_r) \sum_{w\in\mathcal{W}} \sum_{h\in\mathcal{H}} \sum_{k\in\mathcal{K}} \sum_{m\in\mathcal{M}} \left(\frac{\partial c_{wh}^m(y_{wh}^*(\omega_r), \omega_r)}{\partial y_{wh}^k(\omega_r)} + \mu_w(\omega_r) \right) \\
&\times (y_{wh}^k(\omega_r) - y_{wh}^{*k}(\omega_r)) \\
&+ \sum_{r\in\mathcal{R}} p(\omega_r) \sum_{h\in\mathcal{H}} \sum_{k\in\mathcal{K}} \frac{\partial \pi_h^k(z_h^{*k}(\omega_r), \omega_r)}{\partial z_h^k(\omega_r)} \times (z_h^k(\omega_r) - z_h^{*k}(\omega_r)) \\
&+ \sum_{r\in\mathcal{R}} p(\omega_r) \sum_{w\in\mathcal{W}} \left(Q_w(\omega_r) - \sum_{h\in\mathcal{H}} \sum_{k\in\mathcal{K}} (x_{wh}^k + y_{wh}^{*k}(\omega_r)) \right) \\
&\times (\mu_w(\omega_r) - \mu_w^*(\omega_r)) \geq 0 \\
&\forall (y(\omega_r), z(\omega_r)) \in T, \forall \mu(\omega_r) \in \mathbb{R}_+^W. \qquad (5.24)
\end{aligned}$$

The operator in (5.23) can be obtained applying Karush-Kuhn-Tucker conditions to the Lagrangian relaxation of the problem (5.1)-(5.5), with dual variable λ_w, for all $w \in \mathcal{W}$. Thus, the first term is the stationarity condition of each optimization problem (5.1)-(5.5); while the second term is the complementarity condition. Analogously, I can construct the operator in (5.24).

I emphasize that variational inequalities (5.23)-(5.24) are expressed in terms of Lagrange variables λ_w and $\mu_w(\omega_r)$, that have a fundamental role in regulating the medical item procurement. In fact, λ_w is a control variable on the item availability level; whereas $\mu_w(\omega_r)$ is a control variable on the second-stage warehouse storage capacity. Therefore, the above formulation can be advantageous since allows us to to gain a deeper understanding of the market behavior.

5.4 Conclusions

In this Chapter, I present a stochastic generalized Nash equilibrium model for a medical supply network. Specifically, I consider a two-layer network that consists

of warehouses and hospitals with multiple medical items and multiple transportation modes. Each hospital solves a two-stage stochastic optimization problem: in the first stage, he seeks to minimize the purchasing cost of medical items and the transportation time; in the second stage, he adopts a recourse decision process to optimize the expected overall costs and the penalty, for the prior plan for each possible disaster scenario. The hospitals simultaneously solve their own stochastic optimization problems and reach a stable state given by the stochastic generalized Nash equilibrium concept. The model is formulated as a two-stage variational inequality. By Lagrangian relaxation approximation, an alternative two-stage variational inequality based on the Lagrange multipliers is given. I highlight that dual variables play a fundamental role in investigating the market behavior.

Further research issues are the study of the two-stage stochastic problem in the case of general probability distribution with the associated infinite-dimensional variational inequality, and a characterization of the second-stage equilibrium by means of infinite-dimensional Lagrange duality tools. Partial results in these directions have already been achieved.

Chapter 6

A Stochastic Nash Equilibrium Problem for Medical Supply Competition

6.1 Introduction

Emergencies resulting from man-made or natural events strongly affect our social and economic life. Depending on the type of emergency different hazards may occur in the emergency locations. Thus, emergency management has raised increasing interest. In particular, businesses require special measures to protect their activities from any potential dangerous effect of an emergency. Therefore, it is important to establish a plan before the occurrence of these events to be prepared in case an emergency happens. A business continuity plan defines how a company will continue operating, even in the case of a natural disaster, IT failure or a cyber attack. The end goal is to preserve profitability and market position [82].

In this paper, I focus on a plan for the storage and distribution of medical supplies

among healthcare institutions in emergencies caused by natural disasters. In particular, I model the competition among hospitals as a Nash equilibrium problem, and introduce a stochastic programming model to design and evaluate the behaviour of each demand location. Inspired by [138, 220], I provide a two-stage stochastic programming model based on disaster scenarios that introduces the unmet demand at the first stage, and the consequent penalty at the second stage, see also [90]. Thus, I consider a pre-event policy, in which each healthcare institution minimize both the purchasing cost of medical items and the transportation time from the first stage. Then, I present a post-event policy through a recourse decision process to optimize the expected overall costs, and the penalty for the preassigned plan, in response to each possible disaster scenario of the second stage. Institutions simultaneously solve their own two-stage stochastic optimization problems and reach a stable state governed by the stochastic Nash equilibrium concept, that is formulated as a large-scale variational inequality. In addition, in the case of a general probability distribution, I define the stochastic Nash equilibrium as a random variational inequality in a Hilbert space setting. Then, I give the first order optimality conditions for the second-stage problem in terms of Lagrange multipliers, using a separation assumption, called *Assumption S*, as a constraint qualification [55, 58, 57, 117]. This condition results to be a necessary and sufficient condition for strong duality to hold. In infinite dimensional spaces, the classical theorems, which prove strong duality and existence of multipliers, require that the interior of the ordering cone be nonempty [120]. However, in most infinite dimensional cases, where the functional space is L^2 or a Sobolev space, the ordering cone has the empty interior. Therefore, I aim at proving that the second-stage problem verifies the *Assumption S*. As a result, I ensure

the existence of Lagrange multipliers and give an alternative formulation of the two-stage problem. Moreover, I show that the dual variables regulate the medical item procurement. In fact, they represent the control variables on the first-stage demand, on the second-stage demand, and on the unfulfilled demand.

The importance of an efficient approach to emergency management and medical supply planning has been investigated in several papers. As an example, in [138], the authors presented a stochastic programming model, in which they selected the storage locations of medical supplies and use inventory levels for medical items. In the model they captured the information updating during disaster scenarios. In [155], Nagurney et al. developed a stochastic generalized Nash equilibrium model consisting of multiple purchase locations for the disaster relief items, multiple humanitarian organizations, multiple freight service provision options and multiple hubs for storage to multiple points of demand. In [72] the authors presented a generalized Nash equilibrium model with stochastic demand to analyse competition among organizations at demand points for medical supplies. In [197], Nagurney and Salarpour introduced a two-stage stochastic game theory model in order to examine the behavior of national governments during Covid-19 pandemic, and their competition for essential medical supplies in both the preparation and response phases. All the problems presented in [155], [72], [197] were solved as variational inequalities, using the concept of variational equilibrium. I remark that our model differs from the treatment in [138] as I develop a variational inequality approach. In addition, although the problems introduced in [155], [72], [197] have similarities, they are all restricted to the case of discrete probability distribution; whereas our model is valid also for general probability distribution. This poses challenges for both theory and computations.

Recently, two-stage stochastic variational inequalities have been introduced to model cases where one looks for a decision vector before the real situation is known, and a new one after the scenario has been realized. In [38], the authors formulated the two-stage stochastic variational inequality as a two-stage stochastic programming problem with recourse. In [138], Li and Zhang studied the transformation of a general two-stage stochastic programming problem to a two-stage stochastic variational inequality. In [87], the authors presented an evacuation model where a population had to be evacuated from crisis areas to shelters, and, due to the uncertainty in the size of the population to be evacuated, a two-stage stochastic variational inequality model was given. In [192], Rockafellar and Wets discussed the multistage stochastic variational inequality. In [190], the authors developed progressive hedging methods for solving multistage convex stochastic programming, see also [189].

In [106], Gwinner and Raciti studied the random variational inequality and general random equilibrium problems. In particular, they worked on a class of linear random variational inequalities on random sets, with results on measurability, existence and uniqueness in a Hilbert space. Furthermore, they provided an approximation procedure in a special case. Then, in [107], the same authors carried out the theory of random variational inequalities to study a class of random equilibrium problems on networks in the linear case, and in [108] they studied the application to nonlinear random traffic equilibrium problem. A valuable additional contribution of the same authors is the book in [105]. In [81], the authors formulated the multicriteria spatial price network equilibrium problem as a random variational inequality, in which the consumers weight, using random fluctuations, transportation cost and the transportation time associated with the

shipment of a given item. In [59, 56], the authors applied a general random traffic equilibrium problem, featuring the random Wardrop equilibrium distribution using random variational inequality. In [119], Jadamba and Raciti explored stochastic Nash equilibrium problems using monotone variational inequalities in probabilistic Lebesgue spaces. Their results are applied to a class of oligopolistic market equilibrium problems.

Inspired by the above works, in this paper, I provide a variational inequality formulation of the two-stage stochastic optimization problem describing the competition of healthcare institutions in case an emergency happens. The main contributions of our work are:

- Modeling a medical supply network that involves warehouses and hospitals with multiple medical items and multiple transportation modes.
- Providing a two-stage stochastic programming model based on disaster scenarios that considers the unmet demand at the first stage, and the consequent penalty at the second stage.
- Deriving a variational inequality formulation in both the discrete and general probability cases.
- Characterizing the second-stage equilibrium, in the case of general probability distribution, by means of infinite-dimensional Lagrange duality.
- Testing the equilibrium model with numerical illustrations with realistic data.

An analysis of the Lagrange multipliers is also performed and, hence, this paper adds to the literature on the study of marginal utilities in the more challenging setting of stochastic programming problems.

This paper is organized as follows. In Section 6.2, I introduce the two-stage stochastic model for the medical supply competition. In Section 6.3, I present the stochastic Nash equilibrium concept underlying our model and the equivalent variational inequality formulation. The cases of discrete and general probability distribution are discussed. In Section 6.4, I recall some infinite-dimensional duality tools, and, in Section 6.5, I present an alternative formulation of the second-stage problem. The progressive hedging algorithm is then applied to some numerical examples in Section 6.6. I summarize our results and draw our conclusions in Section 6.7.

6.2 The Two-Stage Stochastic Model

In this section, I present my two-stage stochastic model for the medical supply competition. Let $\mathcal{W}$ be the set of warehouses, with typical warehouse denoted by w; let $\mathcal{H}$ be the set of hospitals, with typical hospital denoted by h; let $\mathcal{K}$ be the set of medical supply type, with typical type denoted by k, and let $\mathcal{M}$ be the set of transportation modes, with typical mode denoted by m. I consider a network model as in Figure 6.1. The links between the nodes of the network represent all

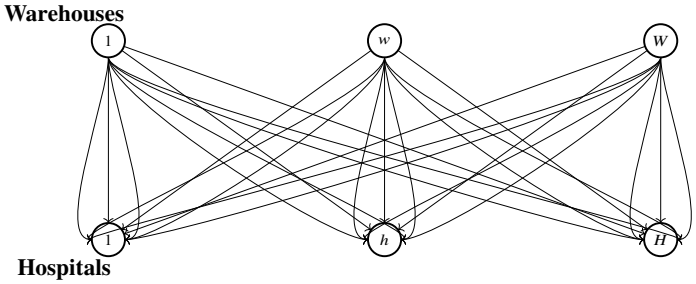

Figure 6.1: The Network representation of Warehouses and Hospitals

the possible connections between the warehouses and the hospitals. Multiple links

between each warehouse and each hospital describe the possibility of alternative modes of transportation. I note that the suitable transportation mode is often connected to the distance between supply and demand locations. Thus, for long distances airplanes are preferred to transportation by truck or train. The choice of the transportation mode may also depend on the type of medical item or on the severity of the emergency.

Let x_{wh}^k be the amount of medical item of type k from warehouse w to hospital h, and let ρ_w^k be the unitary price of medical item k at warehouse w. Let x_{wh} denote the total amount delivered from warehouse w to hospital h, where

$$x_{wh} = \sum_{k \in \mathcal{K}} x_{wh}^k.$$

I further group the x_{wh} into the $WH-$dimensional column vector x.

Moreover, I introduce the transportation time t_{wh}^m from warehouse w to hospital h with mode m and assume that it depends on the total amount x, namely, $t_{wh}^m = t_{wh}^m(x)$. I consider two stages, where one corresponds to the preparedness phase and the other represents the response phase. In the first phase, each demand location, namely the hospital, looks for minimizing the purchasing cost of medical items and the transportation time from the first stage; in the second one, a recourse decision process is developed to optimize the transportation costs from the second stage, in response to each disaster scenario. Let $(\Omega, \mathcal{F}, P)$ be a probability space, where the random parameter $\omega \in \Omega$ represents the typical disaster scenario. For each $\omega \in \Omega$, I denote by $\xi : \Omega \to \mathbb{R}^{WHK+HK}$ a finite dimensional random vector and by $\mathbb{E}_\xi$ the mathematical expectation with respect to ξ. In order to formulate the two-stage stochastic model, I introduce two types of decision variables. The first-stage decision variable x_{wh}^k is used to represent the quantity of medical supplies of type k from warehouse w to hospital h in stage one. The second-stage decision

variables are $y^k_{wh}(\omega)$ and $z^k_h(\omega)$. The variable $y^k_{wh}(\omega)$ represents the quantity of medical supplies of type k to be delivered from warehouse w to hospital h under scenario ω. The variable $z^k_h(\omega)$ is the unfulfilled demand at hospital h of medical supply item k under scenario ω. The amount of unfulfilled demand $z^k_h(\omega)$ is penalized by the penalty function $\pi^k_h = \pi^k_h(\omega, z^k_h(\omega))$. I note that x^k_{wh} is chosen before a realization of ξ is revealed and later $y^k_{wh}(\omega)$ and $z^k_h(\omega)$ are selected with known realization. I set $y_{wh}(\omega) = \sum_{k\in\mathcal{K}} y^k_{wh}(\omega)$. I further group the $y_{wh}(\omega)$ into the $WH-$dimensional column vector $y(\omega)$. Finally, I introduce the transportation cost c^m_{wh} from warehouse w to hospital h with mode m and assume that it depends on the total amount $y(\omega)$, namely, $c^m_{wh} = c^m_{wh}(\omega, y(\omega))$. Table 6.1 summarizes the relevant notations used in the model formulation. I aim at obtaining an efficient

Symbols	**Definitions**
$\mathcal{W}$	set of warehouses, with typical warehouse denoted by w, $card(\mathcal{W}) = W$
$\mathcal{H}$	set of hospitals, with typical hospital denoted by h, $card(\mathcal{H}) = H$
$\mathcal{K}$	set of different medical items, with typical item denoted by k, $card(\mathcal{K}) = K$
$\mathcal{M}$	set of transportation modes, with typical mode denoted by m, $card(\mathcal{M}) = M$
d^k_h	demand of medical item k of hospital h in stage one
$d^k_h(\omega)$	demand of medical item k of hospital h in stage two under scenario ω
x^k_{wh}	amount of medical item k from warehouse w to hospital h in stage one
x_{wh}	amount of medical items delivered from warehouse w to hospital h in stage one
x	amount of total medical items from all warehouses to all hospitals in stage one
e_k	maximum amount available of medical item k
ρ^k_w	unitary price of medical item k at warehouse w
$t^m_{wh}(x)$	transportation time from warehouse w to hospital h with mode m
$y_{wh}(\omega)$	amount of medical items to be delivedered from warehouse w to hospital h in stage two under scenario ω
$y(\omega)$	amount of medical items to be delivedered from all warehouses to all hospitals in stage two under scenario ω
$z^k_h(\omega)$	amount of unfulfilled demand at hospital h of medical supply item k under scenario ω
$c^m_{wh}(\omega, y(\omega))$	transportation cost from warehouse w to hospital h with mode m under scenario ω
$\pi^k_h(\omega, z^k_h(\omega))$	penalty for unfulfilled demand at hospital h of medical supply item k under scenario ω

Table 6.1: The notation for the two-stage stochastic model

plan of medical item procurement of each demand location in the first stage by

the evaluation of adaptive plans in the second stage. Thus, for each hospital, I minimize the purchasing cost and the transportation time of the first stage with the expected overall costs and the penalty for the prior plan. For each hospital, a two-stage procurement planning model in a random environment is formulated. I first present the hospital's problem as a two-stage stochastic programming problem and then define the stochastic Nash equilibrium describing the competition of all hospitals.

For each hospital h, the first-stage problem is given by

$$\min \sum_{w\in\mathcal{W}} \left(\sum_{k\in\mathcal{K}} \rho_w^k x_{wh}^k + \sum_{m\in\mathcal{M}} t_{wh}^m(x) \right) + \mathbb{E}_\xi(\Phi_h(x, \xi(\omega))) \tag{6.1}$$

$$\sum_{w\in\mathcal{W}} x_{wh}^k \geq d_h^k, \ \forall k \in \mathcal{K}, \tag{6.2}$$

$$\sum_{w\in\mathcal{W}} x_{wh}^k \leq e_k, \ \forall k \in \mathcal{K}, \tag{6.3}$$

$$x_{wh}^k \geq 0, \ \forall w \in \mathcal{W}, \ \forall k \in \mathcal{K}. \tag{6.4}$$

The objective function (6.1) minimizes the sum of the purchasing cost for early supply plan, the transportation time, and the expected value of the second stage solution, with respect to disaster scenario, $\Phi_h(x, \xi(\omega))$. Constraint (6.2) states that hospital h receives at least the needed amount of medical items; constraint (6.3) is the maximum availability constraint of each medical supply type k; constraint (6.4) is the non-negativity requirement on variables. In order to ensure that the constraint set is nonempty, I require that $d_h^k \leq e_k, \forall h, k$.

For a given realization $\omega \in \Omega$, $\Phi_h(x, \xi(\omega))$ is given by

$$\Phi_h(x, \xi(\omega)) = \min \sum_{w \in \mathcal{W}} \sum_{m \in \mathcal{M}} c^m_{wh}(\omega, y(\omega)) + \sum_{k \in \mathcal{K}} \pi^k_h(\omega, z^k_h(\omega)) \tag{6.5}$$

subject to

$$\sum_{w \in \mathcal{W}} y^k_{wh}(\omega) + z^k_h(\omega) \geq d^k_h(\omega), \ \forall k \in \mathcal{K}, P\text{-a.s.}, \tag{6.6}$$

$$\sum_{w \in \mathcal{W}} y^k_{wh}(\omega) + \sum_{w \in \mathcal{W}} x^k_{wh} \leq e_k(\omega), \ \forall k \in \mathcal{K}, P\text{-a.s.}, \tag{6.7}$$

$$y^k_{wh}(\omega) \geq 0, z^k_h(\omega) \geq 0, z^k_h(\omega) \leq \alpha \, d^k_h, \forall w \in \mathcal{W}, \ \forall k \in \mathcal{K}, P\text{-a.s.} \tag{6.8}$$

Thus, $\Phi_h(x, \xi(\omega))$ is the optimal value of the second-stage problem (6.5)-(6.8) associated with hospital h, where the constraints hold almost surely (P-a.s.). I remark that $\Phi_h(x, \xi(\omega))$ depends on x via constraint (6.7). The objective function (6.5) minimizes the total cost and the penalty for unmet demand at the second stage. Constraint (6.6) states that the supply at the second stage plus the unmet demand should be at least as much as the demand at the second stage. Constraint (6.7) is the maximum availability constraint of each medical supply of type k. I emphasize that the connection between stage-wise decision variables x and y is captured by constraint (6.7). It is the linking factor between the first and second stage, and communicates the first-stage decisions to the second one. Constraint (6.8) is the non-negativity requirement on variables. I also assume that $z^k_h(\omega) \leq \alpha \, d^k_h$, $\alpha \in]0, 1]$, *P-a.s.*, namely, the unmet demand cannot exceed a fixed percentage of the first stage demand.

In order to ensure that the constraint set of the second stage is nonempty, it suffices to require that

$$d^k_h(\omega) \leq \min \left\{ e_k(\omega), \frac{d^k_h}{\alpha} \right\}, \ \forall h, k, P\text{-a.s.}$$

I assume that:

a) $t^m_{wh}(\cdot)$ is continuously differentiable and convex for all w, h, k;

b) $c^m_{wh}(\omega, \cdot)$, $\pi^k_h(\omega, \cdot)$, a.e. in Ω, are continuously differentiable and convex for all w, h, k, m;

c) for each $u \in \mathbb{R}^{WH}$, $c^m_{wh}(\cdot, u)$ is measurable with respect to the random parameter in Ω for all w, h, m;

d) for each $v \in \mathbb{R}^{HK}$, $\pi^k_h(\cdot, v)$ is measurable with respect to the random parameter in Ω for all h, k;

e) $\frac{\partial c^m_{wh}(\omega, y(\omega))}{\partial y^k_{wh}}$, $\frac{\partial \pi^k_h(\omega, z^k_h(\omega))}{\partial z^k_h}$ are measurable in ω and continuous in y and z;

f) $y^k_{wh} : \Omega \to \mathbb{R}$ and $z^k_h : \Omega \to \mathbb{R}$ are measurable mappings for all w, h, k;

g) $d^k_h : \Omega \to \mathbb{R}$ is a measurable mapping for all h and all k.

The two-stage problem of hospital h can be also formulated as the unique large scale problem:

$$\min \sum_{w \in \mathcal{W}} \left(\sum_{k \in \mathcal{K}} \rho_{wh}^{k} x_{wh}^{k} + \sum_{m \in \mathcal{M}} t_{wh}^{m}(x) \right) + \mathbb{E}_{\xi}(\Phi_h(x, \xi(\omega))) \tag{6.9}$$

subject to

$$\sum_{w \in \mathcal{W}} x_{wh}^{k} \geq d_h^{k}, \ \forall k \in \mathcal{K}, P\text{-a.s.}, \tag{6.10}$$

$$\sum_{w \in \mathcal{W}} x_{wh}^{k} \leq e_k, \ \forall k \in \mathcal{K}, P\text{-a.s.}, \tag{6.11}$$

$$\sum_{w \in \mathcal{W}} y_{wh}^{k}(\omega) + z_h^{k}(\omega) \geq d_h^{k}(\omega), \ \forall k \in \mathcal{K}, P\text{-a.s.}, \tag{6.12}$$

$$\sum_{w \in \mathcal{W}} y_{wh}^{k}(\omega) + \sum_{w \in \mathcal{W}} x_{wh}^{k} \leq e_k(\omega), \ \forall k \in \mathcal{K}, P\text{-a.s.}, \tag{6.13}$$

$$x_{wh}^{k} \geq 0, \ \forall w \in \mathcal{W}, \ \forall k \in \mathcal{K}, P\text{-a.s.}, \tag{6.14}$$

$$y_{wh}^{k}(\omega) \geq 0, \ \forall w \in \mathcal{W}, \ \forall k \in \mathcal{K}, P\text{-a.s.}, \tag{6.15}$$

$$z_h^{k}(\omega) \geq 0, \ \forall k \in \mathcal{K}, P\text{-a.s.}, \tag{6.16}$$

$$z_h^{k}(\omega) \leq \alpha \, d_h^{k}, \ \forall k \in \mathcal{K}, P\text{-a.s.} \tag{6.17}$$

6.3 Stochastic Nash Equilibrium Problem

In this section, I present the equilibrium concept underlying my model and the equivalent variational inequality formulation. Both the cases of discrete and general probability distribution are discussed.

Each hospital minimizes the deterministic costs and the expected costs for all the scenarios. Then, the hospitals simultaneously solve their own optimization problems and reach a stable state governed by the Nash equilibrium concept.

I define the sets:

$$S_h = \Big\{x_h = (x_{wh})_w \in \mathbb{R}^W : (6.10) - (6.11), (6.14) \text{ hold}\Big\},$$

$$T_h = \Big\{(y_h, z_h) = (y_{wh}(\omega), z_{hk}(\omega))_{w,k} \in \mathbb{R}^{W+K} :$$

$$(6.12) - (6.13), (6.15) - (6.17) \text{ hold, } P\text{-a.s.}\Big\},$$

$$S = \prod_h S_h,$$

$$T = \prod_h T_h.$$

I will refer to the objective function (6.9) as the function $\mathbb{J}_h(\omega, x, y(\omega), z(\omega))$, namely

$$\mathbb{J}_h(\omega, x, y(\omega), z(\omega)) = \sum_{w\in\mathcal{W}} \left(\sum_{k\in\mathcal{K}} \rho^k_{wh} x^k_{wh} + \sum_{m\in\mathcal{M}} t^m_{wh}(x) \right) + \mathbb{E}_\xi(\Phi_h(x, \xi(\omega))).$$

Definition 6.3.1. *A vector of medical items* $(x^*, y^*, z^*) \in S \times T$ *is a stochastic Nash equilibrium if for each* $h \in \mathcal{H}$

$$\mathbb{J}_h(\omega, x^*_h, y^*_h(\omega), z^*_h(\omega), x^*_{-h}, y^*_{-h}(\omega), z^*_{-h}(\omega)) \leq \mathbb{J}_h(\omega, x_h, y_h(\omega), z_h(\omega), x^*_{-h}, y^*_{-h}(\omega), z^*_{-h}(\omega)),$$

$$\forall (x_h, y_h(\omega), z_h(\omega)) \in S_h \times T_h, \text{ P-a.s.},$$

where $x_{-h}, y_{-h}(\omega), z_{-h}(\omega)$ *denotes the amount of medical items and the unmet demands of all hospitals except for h.*

According to the above definition, a Nash equilibrium is established if no hospital can unilaterally improve upon his profit by choosing an alternative medical item flow pattern, given other hospitals' decision strategies.

6.3.1 Discrete Probability Distribution

If the random parameter $\omega \in \Omega$ follows a discrete distribution with finite support $\Omega = \{\omega_1, \ldots, \omega_r\}$ and probabilities $p(\omega_r)$ associated with each realization ω_r,

$r \in \mathcal{R} = \{1, \ldots, R\}$, then the objective function (6.9) for $h \in \mathcal{H}$ becomes

$$\mathbb{J}_h(\omega, x, y(\omega), z(\omega)) = \sum_{w \in \mathcal{W}} \left(\sum_{k \in \mathcal{K}} \rho_{wh}^k x_{wh}^k + \sum_{m \in \mathcal{M}} t_{wh}^m(x) \right) + \sum_{r \in \mathcal{R}} p(\omega_r) \left(\sum_{w \in \mathcal{W}} \sum_{m \in \mathcal{M}} c_{wh}^m(\omega_r, y(\omega_r)) + \sum_{k \in \mathcal{K}} \pi_h^k(\omega_r, z_h^k(\omega_r)) \right), \tag{6.18}$$

and the cost minimization problem for $h \in \mathcal{H}$ is given by

$$\min \mathbb{J}_h(\omega, x, y(\omega), z(\omega)) \tag{6.19}$$

$$\sum_{w \in \mathcal{W}} x_{wh}^k \geq d_h^k, \ \forall k \in \mathcal{K}, \tag{6.20}$$

$$\sum_{w \in \mathcal{W}} x_{wh}^k \leq e_k, \ \forall k \in \mathcal{K}, \tag{6.21}$$

$$\sum_{w \in \mathcal{W}} y_{wh}^k(\omega_r) + z_h^k(\omega_r) \geq d_h^k(\omega_r), \ \forall k \in \mathcal{K}, \forall r \in \mathcal{R}, \tag{6.22}$$

$$\sum_{w \in \mathcal{W}} y_{wh}^k(\omega_r) + \sum_{w \in \mathcal{W}} x_{wh}^k \leq e_k(\omega_r), \ \forall k \in \mathcal{K}, \forall r \in \mathcal{R}, \tag{6.23}$$

$$x_{wh}^k \geq 0, \ \forall w \in \mathcal{W}, \ \forall k \in \mathcal{K}, \tag{6.24}$$

$$y_{wh}^k(\omega_r) \geq 0, \ \forall w \in \mathcal{W}, \ \forall k \in \mathcal{K}, \forall r \in \mathcal{R}, \tag{6.25}$$

$$z_h^k(\omega_r) \geq 0, \ \forall k \in \mathcal{K}, \forall r \in \mathcal{R}, \tag{6.26}$$

$$z_h^k(\omega_r) \leq \alpha \, d_h^k, \ \forall k \in \mathcal{K}, \forall r \in \mathcal{R}. \tag{6.27}$$

It is well known that a Nash equilibrium can be characterized as a solution to a variational inequality problem (see [126, 158] for theory and applications on variational inequalities). Thus, the competition among hospitals under the Nash criterion is described by the following variational inequality:

$$\sum_{w\in\mathcal{W}}\sum_{h\in\mathcal{H}}\sum_{k\in\mathcal{K}}\left(\rho^k_{wh}+\sum_{m\in\mathcal{M}}\frac{\partial t^m_{wh}(x^*)}{\partial x^k_{wh}}\right)\times(x^k_{wh}-x^{*k}_{wh})$$
$$+\sum_{r\in\mathcal{R}}p(\omega_r)\sum_{w\in\mathcal{W}}\sum_{h\in\mathcal{H}}\sum_{k\in\mathcal{K}}\left(\sum_{m\in\mathcal{M}}\frac{\partial c^m_{wh}(\omega_r,y^*(\omega_r))}{\partial y^k_{wh}}\right)\times(y^k_{wh}(\omega_r)-y^{*k}_{wh}(\omega_r))$$
$$+\sum_{r\in\mathcal{R}}p(\omega_r)\sum_{h\in\mathcal{H}}\sum_{k\in\mathcal{K}}\frac{\partial\pi^k_h(\omega_r,z^{*k}_h(\omega_r))}{\partial z^k_h}\times(z^k_h(\omega_r)-z^{*k}_h(\omega_r))\geq 0,$$
$$\forall(x,y(\omega_r),z(\omega_r))\in S\times T,\forall r\in\mathcal{R}. \tag{6.28}$$

I note that the set S, and the set T, $\forall r\in\mathcal{R}$, are nonempty, compact and convex, and the operator entering (6.28) is continuous. Therefore, a solution to the above problem exists from the standard theory of variational inequalities [126].

6.3.2 General Probability Distribution

In the case of a general probability space $(\Omega,\mathcal{F},P)$, studying the optimality conditions can be very hard, as one should state the order of the decision process explicitly. For this reason, I choose as my functional setting a Hilbert space and assume that $y\in L^2(\Omega,P,\mathbb{R}^{WH})$, $z\in L^2(\Omega,P,\mathbb{R}^{HK})$, $d\in L^2(\Omega,P,\mathbb{R}^{HK})$. $L^2(\Omega,P,\mathbb{R}^{WH})$ denotes the class of $\mathbb{R}^{WH}$-valued functions defined in Ω, that are square integrable with respect to the probability measure P. Analogous meaning has the space $L^2(\Omega,P,\mathbb{R}^{HK})$.

Moreover, I require the following growth conditions, $\forall m,w,h,k$:

$$\left|c_{wh}^{m}(\omega, y)\right| \leq \beta_{wh}^{1m}(\omega)(1 + \|y\|), \forall y \in \mathbb{R}^{WH}, \tag{6.29}$$

$$\left|\pi_{h}^{k}(\omega, z)\right| \leq \beta_{h}^{2k}(\omega)(1 + \|z\|), \forall z \in \mathbb{R}^{HK}, \ P\text{-a.s.}, \tag{6.30}$$

$$\left|\frac{\partial c_{wh}^{m}(\omega, y)}{\partial y_{wh}^{k}}\right| \leq \beta_{wh}^{3m}(\omega)(1 + \|y\|), \forall y \in \mathbb{R}^{WH}, \tag{6.31}$$

$$\left|\frac{\partial \pi_{h}^{k}(\omega, z_h)}{\partial z_{h}^{k}}\right| \leq \beta_{h}^{4k}(\omega)(1 + \|z\|), \forall z \in \mathbb{R}^{HK}, \ P\text{-a.s.}, \tag{6.32}$$

where $\beta_{wh}^{1m}, \beta_{h}^{2k}, \beta_{wh}^{3m}, \beta_{h}^{4k}$ are non-negative functions of $L^{\infty}(\Omega)$.

Theorem 6.3.1. *Under assumptions* a)-g) *and conditions* (6.29)-(6.32)*, a vector* $(x^*, y^*, z^*) \in S \times T$ *is an optimal solution of the medical supply problem if and only if it is a solution of the following variational inequality:*

$$\begin{aligned}
&\sum_{w\in\mathcal{W}}\sum_{h\in\mathcal{H}}\sum_{k\in\mathcal{K}}\left(\rho_{wh}^{k} + \sum_{m\in\mathcal{M}}\frac{\partial t_{wh}^{m}(x^*)}{\partial x_{wh}^{k}}\right) \times (x_{wh}^{k} - x_{wh}^{*k}) \\
&+ \sum_{h\in\mathcal{H}}\sum_{k\in\mathcal{K}}\int_{\Omega}\left[\sum_{w\in\mathcal{W}}\left(\sum_{m\in\mathcal{M}}\frac{\partial c_{wh}^{m}(\omega, y^*(\omega))}{\partial y_{wh}^{k}}\right) \times (y_{wh}^{k}(\omega) - y_{wh}^{*k}(\omega))\right. \\
&\left. + \frac{\partial \pi_{h}^{k}(\omega, z_{h}^{*k}(\omega))}{\partial z_{h}^{k}} \times (z_{h}^{k}(\omega) - z_{h}^{*k}(\omega))\right] dP(\omega) \geq 0, \quad \forall (x, y, z) \in S \times T.
\end{aligned} \tag{6.33}$$

Proof. The proof procceds as in [16]. □

Ensure the existence of solutions, I may apply the results in [148]. I first recall some definitions.

Let E be a reflexive Banach space with dual space E^* and $K \subset E$ a closed convex set.

Definition 6.3.2. *A mapping* $A : K \mapsto E^*$ *is called pseudomonotone in the sense of Brezis if and only if*

- *for each sequence u_n weakly converging to u in K and such that*

$$\limsup_n \langle Au_n, u_n - u\rangle \leq 0$$

it results

$$\liminf_n \langle Au_n, u_n - v \geq \langle Au, u - v\rangle, \quad \forall v \in K;$$

- *for each $v \in K$ the function $u \mapsto \langle Au, u - v\rangle$ is lower bounded on the bounded subsets of K.*

Definition 6.3.3. *A mapping $A : K \mapsto E^*$ is hemicontinuous in the sense of Fan if and only if for all $v \in K$ the function $u \mapsto \langle Au, u - v\rangle$ is weakly lower semicontinuous on K.*

Definition 6.3.4. *The map $A : K \to E^*$ is said to be lower hemicontinuous along line segments, if and only if the function:*

$$\xi \mapsto \langle A\xi, u - v\rangle$$

is lower semicontinuous for all $u, v \in K$ on the line segments $[u, v]$.

Definition 6.3.5. *The map $A : K \to E^*$ is said to be pseudomonotone in the sense of Karamardian if and only if for all $u, v \in K$*

$$\langle Av, u - v\rangle \geq 0 \to \langle Au, u - v\rangle \geq 0.$$

Theorem 6.3.2. *Let us assume that the map $A : K \mapsto E^*$ be B-pseudomonotone or F-hemicontinuous and there exist $u_0 \in K$ and $R > \|u_0\|$ such that*

$$\langle Av, v - u_0\rangle \geq 0, \quad \forall v \in K \cap \{v \in E : \|v\| = R\}. \tag{6.34}$$

Then, the variational inequality $\langle Au, v - u\rangle, \forall v \in K$ admits solutions.

Theorem 6.3.3. *Let $A : K \mapsto E^*$ be a K-pseudomonotone map which is lower hemicontinuous along line segments. Let us assume that condition* (6.34) *holds true. Then, variational inequality $\langle Au, v - u\rangle, \forall v \in K$ admits solutions.*

I recall that condition (6.34) is satisfied if the coercivity condition is verified:

$$\lim_{\substack{\|u\|\to\infty \\ u\in K}} \frac{\langle Au, u - u_0\rangle}{\|u\|} = +\infty. \tag{6.35}$$

I can apply Theorem 6.3.2 and Theorem 6.3.3, assuming that the operator of the variational inequality is B-pseudomonotone or F-hemicontinuous and (6.34) or (6.35) holds true, or assuming that it is K-pseudomonotone, conditions (6.29)-(6.32) are verified, and (6.34) or (6.35) holds true. I also recall that condition (6.32) is sufficient to guarantee that the operator is lower hemicontinuous along line segments (see [77]).

6.4 Duality Theory

I now present some infinite dimensional Lagrange duality results as in [55, 58, 57, 117]. For reader's convenience, I first recall some typical concepts in duality theory [120]. Let X denote a real normed space and X^* the topological dual of all continuous linear functionals on X. Given C, a nonempty subset of X, and an element $x \in X$, the set

$$T_C(x) := \Big\{ h \in X : h = \lim_{n\to\infty} \lambda_n(x_n - x), \lambda_n \in \mathbb{R}, \lambda_n > 0 \; \forall n \in \mathbb{N},$$
$$x_n \in C \; \forall n \in \mathbb{N}, \; \lim_{n\to\infty} x_n = x \Big\}$$

is called the contingent cone to C at x. Of course, if $T_C(x) \neq \emptyset$, then x belongs to the closure of C, denoted by cl C. If C is convex, then [120]

$$T_C(x) = \text{cl cone}(C - \{x\}), \text{where cone}(C) := \{\lambda x : x \in C, \lambda \in \mathbb{R}, \lambda \geq 0\}.$$

I now present the statement of Theorem 3.2 in [149]. Let X be a real normed space real and S be a nonempty subset of X; let $(Y, \|\cdot\|)$ be a real normed space, partially ordered by a convex cone C. Let $f : S \to \mathbb{R}$ and $g : S \to Y$ be two convex functions. Let us consider the primal problem

$$\min_{x \in K} f(x), \quad K := \{x \in S : g(x) \in -C\}, \tag{6.36}$$

and the dual problem

$$\max_{u \in C^*} \inf_{x \in S} \{f(x) + \langle u, g(x)\rangle\}, \quad C^* := \left\{u \in Y^* : \langle u, v\rangle \geq 0, \forall v \in C\right\}, \tag{6.37}$$

where C^* is the dual cone of C.

I say that *Assumption S* is fulfilled at a point $x_0 \in K$ if and only if it results:

$$T_{\widetilde{M}}(f(x_0), 0_Y) \cap]-\infty, 0[\times \{0_Y\} = \emptyset,$$

where

$$\widetilde{M} := \left\{(f(x) - f(x_0) + \gamma, g(x) + v) : x \in S \setminus K, \alpha \geq 0, v, y \in C\right\}.$$

Then, in [149] the following theorem is proved.

Theorem 6.4.1. *Under the above assumptions, if problem* (6.36) *is solvable and Assumption S is fulfilled at the extremal solution $x_0 \in K$, then also problem* (6.37) *is solvable, the extreme values of both problems are equal and, denoted by $\overline{u}$ the optimal solution of* (6.37)*, it results that $\langle \overline{u}, g(x_0)\rangle = 0$.*

The following result entitles us to characterize a solution of problem (6.36) as a saddle point of the Lagrange function [55].

Theorem 6.4.2. *Let us assume that assumptions of Theorem* 6.4.1 *be satisfied. Then, $x_0 \in K$ is a minimal solution to problem* (6.36) *if and only if there exists $\overline{u} \in C^*$ such that $(x_0, \overline{u})$ is a saddle point of the Lagrange function, namely,*

$$\mathcal{L}(x_0, u) \leq \mathcal{L}(x_0, \overline{u}) \leq \mathcal{L}(x, \overline{u}), \forall x \in S, u \in C^*, \quad \langle \overline{u}, g(x_0) \rangle = 0.$$

I now apply the duality framework in [55, 58, 57] to the second stage problem (6.5)-(6.8). First, I note problem (6.5)-(6.8) is equivalent to a variational inequality, see [16].

Theorem 6.4.3. *The vector $(y_h^*, z_h^*) \in T_h$, for all $h \in \mathcal{H}$, is an optimal solution of the second-stage problem* (6.5)-(6.8) *if and only if $(y_h^*, z_h^*) \in T_h$ solves the variational inequality*

$$\sum_{k \in \mathcal{K}} \int_{\Omega} \left[\sum_{w \in \mathcal{W}} \left(\sum_{m \in \mathcal{M}} \frac{\partial c_{wh}^m(\omega, y^*(\omega))}{\partial y_{wh}^k} \right) \times (y_{wh}^k(\omega) - y_{wh}^{*k}(\omega)) \right.$$
$$\left. + \frac{\partial \pi_h^k(\omega, z_h^{*k}(\omega))}{\partial z_h^k} \times (z_h^k(\omega) - z_h^{*k}(\omega)) \right] dP(\omega) \geq 0, \forall (y_h, z_h)) \in T_h. \quad (6.38)$$

Now, I give two preliminary results.

Lemma 6.4.1. *Let $(y_h^*, z_h^*) \in T_h$ be a solution to* (6.38)*. Let us introduce, a.e. in* Ω*,*

$$\nu_h^1(\omega) = \min\left\{\sum_{m\in\mathcal{M}} \frac{\partial c_{wh}^m(\omega, y^*(\omega))}{\partial y_{wh}^k} : w \in \mathcal{W}, k \in \mathcal{K}\right\},$$
$$\nu_h^2(\omega) = \min\left\{\frac{\partial \pi_h^k(\omega, z_h^{*k}(\omega))}{\partial z_h^k} : k \in \mathcal{K}\right\}$$
$$\Omega_w^{1k} = \left\{\omega \in \Omega : \sum_{m\in\mathcal{M}} \frac{\partial c_{wh}^m(\omega, y^*(\omega))}{\partial y_{wh}^k} = \nu_h^1(\omega)\right\}, w \in \mathcal{W}, k \in \mathcal{K}$$
$$\Omega_w^{2k} = \left\{\omega \in \Omega : \sum_{m\in\mathcal{M}} \frac{\partial c_{wh}^m(\omega, y^*(\omega))}{\partial y_{wh}^k} > \nu_h^1(\omega)\right\}, w \in \mathcal{W}, k \in \mathcal{K}$$
$$\Omega^{3k} = \left\{\omega \in \Omega : \frac{\partial \pi_h^k(\omega, z_h^{*k}(\omega))}{\partial z_h^k} = \nu_h^2(\omega)\right\}, k \in \mathcal{K},$$
$$\Omega^{4k} = \left\{\omega \in \Omega : \frac{\partial \pi_h^k(\omega, z_h^{*k}(\omega))}{\partial z_h^k} > \nu_h^2(\omega)\right\}, k \in \mathcal{K}.$$

Then,

$$\omega \in \Omega_w^{1k} \Rightarrow y_{wh}^k(\omega) \geq 0, \omega \in \Omega_w^{2k} \Rightarrow y_{wh}^k(\omega) = 0, \tag{6.39}$$
$$\omega \in \Omega^{3k} \Rightarrow z_h^k(\omega) \geq 0, \omega \in \Omega^{4k} \Rightarrow z_h^k(\omega) = 0. \tag{6.40}$$

Vice versa, if there exist two functions $\nu_h^1, \nu_h^2 \in L^2(\Omega, P, \mathbb{R})$ *such that* (6.39)-(6.40) *hold, then* $(y_h^*, z_h^*) \in T_h$ *solves* (6.38).

Proof. I assume that $(y_h^*, z_h^*) \in T_h$ is a solution to (6.38). Following [16], I prove that if there exist w_1, k_1, w_2, k_2 such that

$$\sum_{m\in\mathcal{M}} \frac{\partial c_{w_1h}^m(\omega, y^*(\omega))}{\partial y_{w_1h}^{k_1}} < \sum_{m\in\mathcal{M}} \frac{\partial c_{w_2h}^m(\omega, y^*(\omega))}{\partial y_{w_2h}^{k2}}, \tag{6.41}$$

then $y_{w_2h}^{k2} = 0$. By contradiction, suppose that there exists a set $E \subseteq \Omega$, with

positive measure, such that $y^{k2}_{w_2h} > 0$, for all $\omega \in E$ and (6.41) holds. Let us set

$$y^k_{wh} = \begin{cases} y^{*k}_{wh} & \text{in } \Omega \setminus E, \\ y^{*k}_{wh} & \text{if } w \neq w_1, w_2, k \neq k_1, k_2, \text{in } E, \\ y^{*k_1}_{w_1h} + y^{*k_2}_{w_2h} & \text{if } w = w_1, k = k_1, \text{in } E, \\ 0 & \text{if } w = w_2, k = k_2, \text{in } E, \end{cases}$$

with $\sum_{w\in\mathcal{W}} x^k_{wh} \geq d^k_h$, $\sum_{w\in\mathcal{W}} x^k_{wh} \leq e_k$, $x^k_{wh} \geq 0, \forall w \in \mathcal{W}$, $\forall k \in \mathcal{K}$ and $z^k_h(\omega) = z^{*k}_h(\omega)$, $\forall k \in \mathcal{K}$. Variational inequality (6.38) becomes

$$\begin{aligned}
&\sum_{k\in\mathcal{K}} \int_{\Omega\setminus E} \left[\sum_{w\in\mathcal{W}} \left(\sum_{m\in\mathcal{M}} \frac{\partial c^m_{wh}(\omega, y^*(\omega))}{\partial y^k_{wh}} \right) \times (y^k_{wh}(\omega) - y^{*k}_{wh}(\omega)) \right] dP(\omega) \\
&+ \sum_{\substack{k\in\mathcal{K} \\ k\neq k_1,k_2}} \int_E \left[\sum_{\substack{w\in\mathcal{W} \\ w\neq w_1,w_2}} \left(\sum_{m\in\mathcal{M}} \frac{\partial c^m_{wh}(\omega, y^*(\omega))}{\partial y^k_{wh}} \right) \times (y^k_{wh}(\omega) - y^{*k}_{wh}(\omega)) \right] dP(\omega) \\
&+ \int_E \left(\sum_{m\in\mathcal{M}} \frac{\partial c^m_{w_1h}(\omega, y^*(\omega))}{\partial y^{k_1}_{w_1h}} \right) \times (y^{k_1}_{w_1h}(\omega) - y^{*k_1}_{w_1h}(\omega)) dP(\omega) \\
&+ \int_E \left(\sum_{m\in\mathcal{M}} \frac{\partial c^m_{w_2h}(\omega, y^*(\omega))}{\partial y^{k_2}_{w_2h}} \right) \times (y^{k_2}_{w_2h}(\omega) - y^{*k_2}_{w_2h}(\omega)) dP(\omega) \\
&= \int_E \left(\sum_{m\in\mathcal{M}} \frac{\partial c^m_{w_1h}(\omega, y^*(\omega))}{\partial y^{k_1}_{w_1h}} - \sum_{m\in\mathcal{M}} \frac{\partial c^m_{w_2h}(\omega, y^*(\omega))}{\partial y^{k_2}_{w_2h}} \right) y^{k_2}_{w_2h}(\omega) dP(\omega) < 0.
\end{aligned}$$

This contradics variational inequality (6.38). Thus, I have

$$\begin{aligned}
\sum_{m\in\mathcal{M}} \frac{\partial c^m_{wh}(\omega, y^*(\omega))}{\partial y^k_{wh}} = \nu^1_h(\omega) &\Rightarrow y^{*k}_{wh}(\omega) \geq 0, \\
\sum_{m\in\mathcal{M}} \frac{\partial c^m_{wh}(\omega, y^*(\omega))}{\partial y^k_{wh}} > \nu^1_h(\omega) &\Rightarrow y^{*k}_{wh}(\omega) = 0.
\end{aligned}$$

Analogously, I find

$$\frac{\partial \pi_h^k(\omega, z_h^{*k}(\omega))}{\partial z_h^k} = \nu_h^2(\omega) \Rightarrow z_h^{*k}(\omega) \geq 0,$$
$$\frac{\partial \pi_h^k(\omega, z_h^{*k}(\omega))}{\partial z_h^k} > \nu_h^2(\omega) \Rightarrow z_h^{*k}(\omega) = 0.$$

Now, I suppose that there exist two functions $\nu_h^1, \nu_h^2 \in L^2(\Omega, P, \mathbb{R})$ such that (6.39)-(6.40) hold. Variational inequality (6.38) becomes

$$\begin{aligned}
&\sum_{k\in\mathcal{K}} \int_\Omega \left[\sum_{w\in\mathcal{W}} \left(\sum_{m\in\mathcal{M}} \frac{\partial c_{wh}^m(\omega, y^*(\omega))}{\partial y_{wh}^k} \right) \times (y_{wh}^k(\omega) - y_{wh}^{*k}(\omega)) \right. \\
&\left. + \frac{\partial \pi_h^k(\omega, z_h^{*k}(\omega))}{\partial z_h^k} \times (z_h^k(\omega) - z_h^{*k}(\omega)) \right] dP(\omega) \\
&= \sum_{w\in\mathcal{W}} \sum_{k\in\mathcal{K}} \int_{\Omega_w^{1k}} \nu_h^1(\omega)(y_{wh}^k(\omega) - y_{wh}^{*k}(\omega)) dP(\omega) \\
&+ \sum_{w\in\mathcal{W}} \sum_{k\in\mathcal{K}} \int_{\Omega_w^{2k}} \sum_{w\in\mathcal{W}} \left(\sum_{m\in\mathcal{M}} \frac{\partial c_{wh}^m(\omega, y^*(\omega))}{\partial y_{wh}^k} \right) (y_{wh}^k(\omega) - y_{wh}^{*k}(\omega)) dP(\omega) \\
&+ \sum_{w\in\mathcal{W}} \sum_{k\in\mathcal{K}} \int_{\Omega^{3k}} \nu_h^2(\omega)(z_h^k(\omega) - z_h^{*k}(\omega)) dP(\omega) \\
&+ \sum_{w\in\mathcal{W}} \sum_{k\in\mathcal{K}} \int_{\Omega^{4k}} \sum_{w\in\mathcal{W}} \left(\frac{\partial \pi_h^k(\omega, z_h^{*k}(\omega))}{\partial z_h^k} \right) (z_h^k(\omega) - z_h^{*k}(\omega)) dP(\omega) \\
&\geq \sum_{w\in\mathcal{W}} \sum_{k\in\mathcal{K}} \int_{\Omega_w^{1k}} \nu_h^1(\omega)(y_{wh}^k(\omega) - y_{wh}^{*k}(\omega)) dP(\omega) \\
&+ \sum_{w\in\mathcal{W}} \sum_{k\in\mathcal{K}} \int_{\Omega_w^{2k}} \nu_h^1(\omega)(y_{wh}^k(\omega) - y_{wh}^{*k}(\omega)) dP(\omega) \\
&+ \sum_{w\in\mathcal{W}} \sum_{k\in\mathcal{K}} \int_{\Omega^{3k}} \nu_h^2(\omega)(z_h^k(\omega) - z_h^{*k}(\omega)) dP(\omega) \\
&+ \sum_{w\in\mathcal{W}} \sum_{k\in\mathcal{K}} \int_{\Omega^{4k}} \nu_h^2(\omega)(z_h^k(\omega) - z_h^{*k}(\omega)) dP(\omega) = 0.
\end{aligned}$$

Therefore, variational inequality (6.38) is satisfied. □

Now, I prove that *Assumption S* is verified.

Theorem 6.4.4. *Problem* (6.38) *verifies Assumption S at the optimal solution* $(y_h^*, z_h^*) \in T_h$.

Proof. I suppose that $(y_h^*, z_h^*) \in T_h$ is a solution to (6.38), and prove that *Assumption S* is verified at $(y_h^*, z_h^*) \in T_h$. I set $Y = L^2(\Omega, P, \mathbb{R}^{WK})$, $Z = L^2(\Omega, P, \mathbb{R}^K)$, and prove that if $(l, \theta_Y, \theta_Y, \theta_Y, \theta_Z, \theta_Z)$ is such that

$$l = \lim_n \lambda_n \Bigg\{ \sum_{k\in\mathcal{K}} \int_\Omega \Bigg[\sum_{w\in\mathcal{W}} \Bigg(\sum_{m\in\mathcal{M}} \frac{\partial c_{wh}^m(\omega, y^*(\omega))}{\partial y_{wh}^k} \Bigg) \times (y_{wh}^k(\omega) - y_{wh}^{*k}(\omega)) \tag{6.42}$$

$$+ \frac{\partial \pi_h^k(\omega, z_h^{*k}(\omega))}{\partial z_h^k} \times (z_h^k(\omega) - z_h^{*k}(\omega)) \Bigg] dP(\omega) + \gamma_n \Bigg\}, \tag{6.43}$$

$$\theta_Y = \lim_n \lambda_n \Big(d_h^k(\omega) - \sum_{w\in\mathcal{W}} y_{wh}^k(\omega) - z_h^k(\omega) + u_n^1 \Big),$$

$$\theta_Y = \lim_n \lambda_n \Big(\sum_{w\in\mathcal{W}} y_{wh}^k(\omega) + \sum_{w\in\mathcal{W}} x_{wh}^k - e_k(\omega) + u_n^2 \Big), \tag{6.44}$$

$$\theta_Y = \lim_n \lambda_n \Big(- y_{wh}^k(\omega) + u_n^3 \Big),$$

$$\theta_Z = \lim_n \lambda_n \Big(- z_h^k(\omega) + u_n^4 \Big), \tag{6.45}$$

$$\theta_Z = \lim_n \lambda_n \Big(z_h^k(\omega) - \alpha d_h^k + u_n^5 \Big), \tag{6.46}$$

with $\gamma_n \geq 0$, $\lambda_n > 0$, $u_n^i \geq 0$, $i = 1, \ldots, 5$, and

$$\lim_n \left\{ \sum_{k \in \mathcal{K}} \int_\Omega \left[\sum_{w \in \mathcal{W}} \left(\sum_{m \in \mathcal{M}} \frac{\partial c_{wh}^m(\omega, y^*(\omega))}{\partial y_{wh}^k} \right) \times (y_{wh}^k(\omega) - y_{wh}^{*k}(\omega)) \right.\right.$$
$$\left.\left. + \frac{\partial \pi_h^k(\omega, z_h^{*k}(\omega))}{\partial z_h^k} \times (z_h^k(\omega) - z_h^{*k}(\omega)) \right] dP(\omega) + \gamma_n \right\} = 0,$$
$$\lim_n \left(d_h^k(\omega) - \sum_{w \in \mathcal{W}} y_{wh}^k(\omega) - z_h^k(\omega) + u_n^1 \right) = \theta_Y,$$
$$\lim_n \left(\sum_{w \in \mathcal{W}} y_{wh}^k(\omega) + \sum_{w \in \mathcal{W}} x_{wh}^k - e_k(\omega) + u_n^2 \right) = \theta_Y,$$
$$\lim_n \left(- y_{wh}^k(\omega) + u_n^3 \right) = \theta_Y,$$
$$\lim_n \left(- z_h^k(\omega) + u_n^4 \right) = \theta_Z, \lim_n \lambda_n \left(z_h^k(\omega) - \alpha d_h^k + u_n^5 \right) = \theta_Z,$$

then l must be nonnegative. I prove that every term in (6.42)-(6.43) tends to zero. I first considers only the terms in y:

$$
\begin{aligned}
&\lambda_n \Bigg\{ \sum_{k\in\mathcal{K}} \int_\Omega \Bigg[\sum_{w\in\mathcal{W}} \Bigg(\sum_{m\in\mathcal{M}} \frac{\partial c^m_{wh}(\omega, y^*(\omega))}{\partial y^k_{wh}} \Bigg) \times \Big(y^k_{wh}(\omega) - y^{*k}_{wh}(\omega) \Big) \Bigg\} \\
&= \lambda_n \Bigg\{ \sum_{w\in\mathcal{W}} \sum_{k\in\mathcal{K}} \int_{\Omega^{1k}_w} \nu^1_h(\omega) \Big(y^k_{wh}(\omega) - y^{*k}_{wh}(\omega) \Big) dP(\omega) \\
&+ \sum_{k\in\mathcal{K}} \int_{\Omega^{2k}_w} \sum_{w\in\mathcal{W}} \Bigg(\sum_{m\in\mathcal{M}} \frac{\partial c^m_{wh}(\omega, y^*(\omega))}{\partial y^k_{wh}} \Bigg) (y^k_{wh}(\omega) - y^{*k}_{wh}(\omega)) dP(\omega) \Bigg\} \\
&\geq \lambda_n \Bigg\{ \sum_{w\in\mathcal{W}} \sum_{k\in\mathcal{K}} \int_{\Omega^{1k}_w} \nu^1_h(\omega) \Big(y^k_{wh}(\omega) - y^{*k}_{wh}(\omega) \Big) dP(\omega) \\
&+ \sum_{w\in\mathcal{W}} \sum_{k\in\mathcal{K}} \int_{\Omega^{2k}_w} \nu^1_h(\omega) \Big(y^k_{wh}(\omega) - y^{*k}_{wh}(\omega) \Big) dP(\omega) \Bigg\} \\
&= \lambda_n \Bigg\{ \sum_{w\in\mathcal{W}} \sum_{k\in\mathcal{K}} \int_{\Omega} \nu^1_h(\omega) \Big(y^k_{wh}(\omega) - y^{*k}_{wh}(\omega) \Big) dP(\omega) \Bigg\} \\
&= \lambda_n \Bigg\{ \sum_{k\in\mathcal{K}} \int_\Omega \nu^1_h(\omega) \Big(\sum_{w\in\mathcal{W}} y^k_{wh}(\omega) + \sum_{w\in\mathcal{W}} x^k_{wh} - e_k(\omega) + u^2_n \Big) dP(\omega) \\
&+ \sum_{k\in\mathcal{K}} \int_\Omega \nu^1_h(\omega) \Big(- \sum_{w\in\mathcal{W}} x^k_{wh} + e_k(\omega) - \sum_{w\in\mathcal{W}} y^{*k}_{wh}(\omega) \Big) dP(\omega) \Bigg\}.
\end{aligned}
$$

Taking into account that $\sum_{w\in\mathcal{W}} y^{*k}_{wh}(\omega) = -\sum_{w\in\mathcal{W}} x^k_{wh} + e_k(\omega)$, all the terms tends to zero. Analogously, I can prove that the other terms tends to zero. □ □

6.5 Application of the Infinite-Dimensional Duality to the Second-Stage Problem

In this section, I prove that variational inequality (6.38) can be expressed in terms of Lagrange variables. As a consequence, the second-stage problem can be replaced by optimality conditions and the large scale problem (6.9)-(6.17) can be reformulated.

Theorem 6.5.1. $(y_h^*, z_h^*) \in T_h$ *is a solution to* (6.38) *if and only if there exist* $\lambda_h^{1k}, \lambda_h^{2k}, \mu_w^{1k}, \mu_w^{2k}, \mu_w^{3k} \in L^2(\Omega, P, \mathbb{R}_+)$*, such that*

$$\sum_{m\in\mathcal{M}} \frac{\partial c_{wh}^m(\omega, y^*(\omega))}{\partial y_{wh}^k} - \lambda_h^{*1k}(\omega) + \lambda_h^{*2k}(\omega) - \mu^{*1k}(\omega) = 0, \ P\text{-a.s.}$$

$$\frac{\partial \pi_h^k(\omega, z_h^{*k}(\omega))}{\partial z_h^k} - \mu^{*2k}(\omega) + \mu^{*3k}(\omega) = 0, \ P\text{-a.s.}$$

$$\lambda_h^{1k}(\omega)\Big(d_h^k(\omega) - \sum_{w\in\mathcal{W}} y_{wh}^k(\omega) - z_h^k(\omega)\Big) = 0, \ P\text{-a.s.}$$

$$\lambda_h^{2k}(\omega)\Big(\sum_{w\in\mathcal{W}} y_{wh}^k(\omega) + \sum_{w\in\mathcal{W}} x_{wh}^k - e_k(\omega)\Big) = 0, \ P\text{-a.s.}$$

$$\mu_w^{1k}(\omega) y_{wh}^k(\omega) = 0, \ \mu_w^{2k}(\omega) z_h^k(\omega) = 0, \ P\text{-a.s.}$$

$$\mu_w^{3k}(\omega)\Big(z_h^k(\omega) - \alpha d_h^k\Big) = 0, \ P\text{-a.s.}$$

Proof. I assume that $(y_h^*, z_h^*) \in T_h$ is a solution to (6.38). For $h = 1, \ldots, H$ and for given $x \in S$, I set:

$$\Psi_h(x, y, z) = \sum_{k\in\mathcal{K}} \int_\Omega \Bigg[\sum_{w\in\mathcal{W}} \Bigg(\sum_{m\in\mathcal{M}} \frac{\partial c_{wh}^m(\omega, y^*(\omega))}{\partial y_{wh}^k} \Bigg) \times (y_{wh}^k(\omega) - y_{wh}^{*k}(\omega)) + \frac{\partial \pi_h^k(\omega, z_h^{*k}(\omega))}{\partial z_h^k} \times (z_h^k(\omega) - z_h^{*k}(\omega)) \Bigg] dP(\omega) \geq 0, \forall (y_h, z_h) \in T_h$$

and observe that variational inequality (6.38) is equivalent to the minimization problem

$$\min_{y,z\in T} \Psi_h(x, y, z) = \Psi_h(x, y^*, z^*) = 0. \tag{6.47}$$

For $h = 1, \ldots, H$, I consider the Lagrange function associated with optimization

problem (6.47):

$$\begin{aligned}
&\mathcal{L}_h(x, y, z, \lambda, \mu) = \Psi_h(x, y, z) + \\
&+ \int_0^T \sum_{k\in\mathcal{K}} \lambda_h^{1k}(\omega)\Big(d_h^k(\omega) - \sum_{w\in\mathcal{W}} y_{wh}^k(\omega) - z_h^k(\omega)\Big)dP(\omega) + \\
&+ \int_0^T \sum_{k\in\mathcal{K}} \lambda_h^{2k}(\omega)\Big(\sum_{w\in\mathcal{W}} y_{wh}^k(\omega) + \sum_{w\in\mathcal{W}} x_{wh}^k - e_k(\omega)\Big)dP(\omega), \\
&- \int_0^T \sum_{k\in\mathcal{K}}\sum_{w\in\mathcal{W}} \mu_w^{1k}(\omega) y_{wh}^k(\omega)dP(\omega) - \int_0^T \sum_{k\in\mathcal{K}} \mu_w^{2k}(\omega) z_h^k(\omega)dP(\omega) + \\
&+ \int_0^T \sum_{k\in\mathcal{K}} \mu_w^{3k}(\omega)\Big(z_h^k(\omega) - \alpha d_h^k\Big)dP(\omega), \qquad (6.48)
\end{aligned}$$

$\forall y \in L^2(\Omega, P, \mathbb{R}^{WH})$, $z \in L^2(\Omega, P, \mathbb{R}^{HK})$, $\lambda_h^{1k}, \lambda_h^{2k}, \mu_w^{1k}, \mu_w^{2k}, \mu_w^{3k} \in L^2(\Omega, P, \mathbb{R}_+)$. Then, applying results in [58, 57], since I proved *Assumption S*, there exist $\lambda_h^{*1k}(\omega), \lambda_h^{*2k}(\omega), \mu_w^{*1k}(\omega), \mu_w^{*2k}(\omega), \mu_w^{*3k}(\omega) \geq 0$, P.a.s. such that

$$(y_h, z_h, \lambda_h^{*1k}, \lambda_h^{*2k}, \mu_w^{*1k}, \mu_w^{*2k}, \mu_w^{*3k})$$

is a saddle point of the Lagrange functional

$$\begin{aligned}
&\mathcal{L}_h(x, y^*, z^*, \lambda, \mu) \leq \mathcal{L}_h(x, y^*, z^*, \lambda^*, \mu^*) \leq \mathcal{L}_h(x, y, z, \lambda^*, \mu^*) \\
&\forall (y_h, z_h) \in T_h, \forall \lambda_h^{1k}(\omega), \lambda_h^{2k}(\omega), \mu_w^{1k}(\omega), \mu_w^{2k}(\omega), \mu_w^{3k}(\omega) \geq 0, P.a.s. \\
&\lambda_h^{*1k}(\omega)\Big(d_h^k(\omega) - \sum_{w\in\mathcal{W}} y_{wh}^{*k}(\omega) - z_h^{*k}(\omega)\Big) = 0, \ P\text{-a.s.} \\
&\lambda_h^{*2k}(\omega)\Big(\sum_{w\in\mathcal{W}} y_{wh}^{*k}(\omega) + \sum_{w\in\mathcal{W}} x_{wh}^k - e_k(\omega)\Big) = 0, \ P\text{-a.s.} \\
&\mu_w^{*1k}(\omega) y_{wh}^{*k}(\omega) = 0, \ \mu_w^{*2k}(\omega) z_h^{*k}(\omega) = 0, \ P\text{-a.s.} \\
&\mu_w^{*3k}(\omega)\Big(z_h^{*k}(\omega) - \alpha d_h^k\Big) = 0, \ P\text{-a.s.}
\end{aligned}$$

Thus, I find

$$0 = \mathcal{L}_h(x, y^*, z^*, \lambda^*, \mu^*) \leq \mathcal{L}_h(x, y, z, \lambda^*, \mu^*)$$
$$= \sum_{k\in\mathcal{K}} \int_\Omega \Bigg[\sum_{w\in\mathcal{W}} \Bigg(\sum_{m\in\mathcal{M}} \frac{\partial c^m_{wh}(\omega, y^*(\omega))}{\partial y^k_{wh}} - \lambda^{*1k}_h(\omega) + \lambda^{*2k}_h(\omega) - \mu^{*1k}(\omega) \Bigg) \times$$
$$(y^k_{wh}(\omega) - y^{*k}_{wh}(\omega)) \Bigg(\frac{\partial \pi^k_h(\omega, z^{*k}_h(\omega))}{\partial z^k_h} - \mu^{*2k}(\omega) + \mu^{*3k}(\omega) \Bigg) \times (z^k_h(\omega) - z^{*k}_h(\omega)) \Bigg] dP(\omega)$$

Setting $y^k_{wh}(\omega) = y^{*k}_{wh}(\omega) \pm \epsilon_1(\omega)$, and then $z^k_h(\omega) = z^{*k}_h(\omega) \pm \epsilon_2(\omega)$, I find that

$$\sum_{m\in\mathcal{M}} \frac{\partial c^m_{wh}(\omega, y^*(\omega))}{\partial y^k_{wh}} - \lambda^{*1k}_h(\omega) + \lambda^{*2k}_h(\omega) - \mu^{*1k}(\omega) = 0, \ P\text{-a.s.}$$
$$\frac{\partial \pi^k_h(\omega, z^{*k}_h(\omega))}{\partial z^k_h} - \mu^{*2k}(\omega) + \mu^{*3k}(\omega) = 0, \ P\text{-a.s.}$$

The converse is easily achieved. □

Therefore, the two-stage problem can be reformulated as follow

$$\min \sum_{w\in\mathcal{W}} \Bigg(\sum_{k\in\mathcal{K}} \rho^k_w x^k_{wh} + \sum_{m\in\mathcal{M}} t^m_{wh}(x) \Bigg) + \int_\Omega \Phi_h(x, \xi(\omega)) dP(\omega)$$
$$\sum_{w\in\mathcal{W}} x^k_{wh} \geq d^k_h, \ \forall k \in \mathcal{K},$$
$$\sum_{w\in\mathcal{W}} x^k_{wh} \leq e_k, \ \forall k \in \mathcal{K},$$
$$x^k_{wh} \geq 0, \ \forall w \in \mathcal{W}, \ \forall k \in \mathcal{K},$$
$$\sum_{m\in\mathcal{M}} \frac{\partial c^m_{wh}(\omega, y^*(\omega))}{\partial y^k_{wh}} - \lambda^{*1k}_h(\omega) + \lambda^{*2k}_h(\omega) \geq 0, \ P\text{-a.s.}$$
$$\frac{\partial \pi^k_h(\omega, z^{*k}_h(\omega))}{\partial z^k_h} + \mu^{*3k}(\omega) \geq 0, \ P\text{-a.s.}$$
$$\lambda^{1k}_h(\omega) \Big(d^k_h(\omega) - \sum_{w\in\mathcal{W}} y^k_{wh}(\omega) - z^k_h(\omega) \Big) = 0, \ P\text{-a.s.}$$
$$\lambda^{2k}_h(\omega) \Big(\sum_{w\in\mathcal{W}} y^k_{wh}(\omega) + \sum_{w\in\mathcal{W}} x^k_{wh} - e_k(\omega) \Big) = 0, \ P\text{-a.s.}$$
$$\mu^{3k}_w(\omega) \Big(z^k_h(\omega) - \alpha d^k_h \Big) = 0, \ P\text{-a.s.}$$

I now describe some relevant consequences that gives an insights into the market behavior with respect to the product shipment. Dual variables λ_h^{1k}, λ_h^{2k}, μ_w^{1k}, μ_w^{2k}, μ_w^{3k} regulate the medical item procurement. In particular, λ_h^{1k} is a control variable on the first-stage demand; λ_h^{2k} is a control variable on the item availability level; μ_w^{1k} is a control variable on the second-stage demand; μ_w^{2k} and μ_w^{3k} are control variables on the unfulfilled demand. I discuss some cases, considering active and non-active constraints. I have:

$$\sum_{m\in\mathcal{M}} \frac{\partial c_{wh}^m(\omega, y^*(\omega))}{\partial y_{wh}^k} - \lambda_h^{*1k}(\omega) + \lambda_h^{*2k}(\omega) - \mu^{*1k}(\omega) = 0, \ P\text{-}a.s.$$

If $y_{wh}^{*k}(\omega) > 0$, then $\mu_w^{1k}(\omega) = 0, \ P\text{-}a.s.$, and

$$\sum_{m\in\mathcal{M}} \frac{\partial c_{wh}^m(\omega, y^*(\omega))}{\partial y_{wh}^k} = \lambda_h^{*1k}(\omega) - \lambda_h^{*2k}(\omega), \ P\text{-}a.s.$$

namely, the marginal cost is equal to the difference of the control variables on demand and market item availability. Moreover, if $\lambda_h^{*1k}(\omega) = 0$, $\lambda_h^{*2k}(\omega) > 0$, $P\text{-}a.s.$, I find $\sum_{m\in\mathcal{M}} \frac{\partial c_{wh}^m(\omega, y^*(\omega))}{\partial y_{wh}^k} = -\lambda_h^{*2k}(\omega)$, $P\text{-}a.s.$, and the marginal cost decreases. If $\lambda_h^{*2k}(\omega) = 0$, $\lambda_h^{*1k}(\omega) > 0, \ P\text{-}a.s.$, I find thet $\sum_{m\in\mathcal{M}} \frac{\partial c_{wh}^m(\omega, y^*(\omega))}{\partial y_{wh}^k} = \lambda_h^{*1k}(\omega), \ P\text{-}a.s.$, and the marginal cost increases.

From

$$\frac{\partial \pi_h^k(\omega, z_h^{*k}(\omega))}{\partial z_h^k} = \mu^{*2k}(\omega) - \mu^{*3k}(\omega), \ P\text{-}a.s.,$$

I note that the marginal penalty is equal to the difference between the control variables on the unfulfilled demand. If $0 < z_h^{*k}(\omega) < \alpha d_h^k, \ P\text{-}a.s.$, then $\mu^{*2k}(\omega) = \mu^{*3k}(\omega) = 0$, and $\frac{\partial \pi_h^k(\omega, z_h^{*k}(\omega))}{\partial z_h^k} = 0, \ P\text{-}a.s.$, namely, the marginal penalty is equal to zero. If $\mu^{*2k}(\omega) > 0$, then $z_h^{*k}(\omega) = 0, \ P\text{-}a.s.$ This is the case of an effective emergency plan, in which hospital does not incur in any unmet demand. If $\mu^{*3k}(\omega) > 0$, then $\mu^{*2k}(\omega) = 0, \ P\text{-}a.s.$, and $\frac{\partial \pi_h^k(\omega, z_h^{*k}(\omega))}{\partial z_h^k} = -\mu^{*3k}(\omega), \ P\text{-}a.s.$, namely, the marginal penalty decreases.

6.6 Numerical Example

In this section, I present two small numerical examples for illustrative purposes. I consider two warehouses ($w = 2$), two hospitals ($h = 2$), three different items ($k = 3$), one transportation mode ($m = 1$) and five scenarios. The economic data mainly come from [4]. For the calculation of transportation costs, I apply the Product & Distance-based calculation rule, which computes the transportation costs based on the coefficients for transportation costs (that include all the different terms, e.g. fuel price, tolls, etc.) for national shipments assumed to be $0.19€/km * m^3$. For transportation time from warehouses to hospitals, I consider hourly cost set, that includes the time spending for the loading process, the route to go and the unloading process. Penalty costs, concerning the unfulfilled demand, depends on the number of items that are not delivered in one day.

The numerical simulations are solved applying the Progressive Hedging Method (PHM) [191]. This is a well-known algorithm that has been recently extended to multistage SVI and multistage stochastic Lagrangian variational inequalities [190, 189]. In [8], the authors presented a new framework that shows how PHM can be utilized, while guaranteeing convergence, to globally optimal solutions of mixed-integer stochastic convex programs. I now briefly present the Progressive Hedging Algorithm for a two-stage stochastic optimization problem.
I consider the problem:

$$\min_{x \in X} f(x) + \mathbb{E}_{\xi}(\Phi_h(x, \xi(\omega))),$$

where

$$f(x) = \sum_{w\in\mathcal{W}} \left(\sum_{k\in\mathcal{K}} \rho_w^k x_{wh}^k + \sum_{m\in\mathcal{M}} t_{wh}^m(x) \right)$$

is convex in x and $\Phi_h(x, \xi(\omega))$ is the recourse function, defined as the second-stage optimal value function

$$\Phi_h(x, \xi(\omega)) = \min_{y(\xi)\in Y(x,\xi)} g(x, y(\xi), \xi(\omega)),$$

where

$$g(x, y(\xi), \xi(\omega)) = \sum_{w\in\mathcal{W}} \sum_{m\in\mathcal{M}} c_{wh}^m(\omega, y(\omega)) + \sum_{k\in\mathcal{K}} \pi_h^k(\omega, z_h^k(\omega)),$$

$c_{wh}^m(\omega, \cdot)$ and $\pi_h^k(\omega, \cdot)$ are convex function for all w, h, k, m. I emphasize that the

Algorithm 1 Pseudo-code of PHM for two-stage stochastic programming.

Initial. $x^0(\xi) = 0$, $y^0(\xi) = 0$ and $w^0(\xi) = 0\,\forall\xi$, $r > 0, v = 1$.

Step 1. For each ξ, obtain $\hat{x}^v(\xi)$ and $\hat{y}^v(\xi)$ by solving subproblem:

$\min f(x(\xi)) + g(x(\xi), y(\xi), \xi) + \langle x(\xi), w^v(\xi)\rangle + \frac{r}{2}||x(\xi) - x^v(\xi)||^2$,

s.t. $x(\xi) \in X$, $y(\xi) \in Y(x(\xi), \xi)$;

Step 2. Update $x^{v+1} = \mathbb{E}_\xi[\hat{x}^v(\xi)]$, $y^{v+1}(\xi) = \hat{y}^v(\xi)\,\forall\xi$,

$w^{v+1}(\xi) = w^v(\xi) - r(\hat{x}^v(\xi) - x^{v+1}(\xi))\,\forall\xi$;

$v := v + 1$, **repeat**.

convergence of PHM to global optimal solution is ensured for convex stochastic programs if the involved function in the corresponding variational inequality is strongly monotone, [190, 189].

All the codes were written in MATLAB and run in MATLAB R2020a (derived data supporting the findings of this study are available from the corresponding author upon request.). Following a discrete approximation scheme as in [138], I choose $|R| = 5$ realizations of random variable ξ with probability $1/R$. I note

that hospital medical items are generally purchased as multiple packs into boxes. In my examples I consider two different cases. In the first example I consider some indispensable items; hence, I use a high penalty of unfulfilled demand, and I consider all cost referred to a single pack. In the second example I consider a box as a unit of measurement, which contains thousand packs and a low penalty of unfulfilled demand.

Numerical Example 1: In this numerical example, the items are collected in multiple packages, and the coefficients of the cost functions are related to a single package. I have considered high penalty functions, since not satisfying the demand for a particular item would cause severe discomfort. It can be noted that, given the danger of the penalty, at equilibrium I get zero penalties as it is likely that hospitals pay more attention to some indispensable items. The matrix of the cost functions is given by

$$\begin{pmatrix} 2,6 & 2,9 & 3,5 & 7,2 & 0,00019 & 0,00029 & 0,00038 & 0,00023 & 1800 & 1600 \\ 2,7 & 2,5 & 1,7 & 2,2 & 0,00025 & 0,00031 & 0,00024 & 0,00018 & 1500 & 1400 \\ 1,6 & 1,9 & 1,02 & 2,03 & 0,00021 & 0,00036 & 0,00032 & 0,00028 & 1300 & 1500 \end{pmatrix}. \tag{6.49}$$

First of all, I focus my attention on the flows x^k_{wh} of the first stage. I find

$$\begin{aligned} &x^1_{11} = 3,00; \quad x^1_{12} = 3,40; \quad x^1_{21} = 0,00; \quad x^1_{22} = 0,00; \\ &x^2_{11} = 0,00; \quad x^2_{12} = 0,00; \quad x^2_{21} = 0,00; \quad x^2_{22} = 0,00; \\ &x^3_{11} = 0,00; \quad x^3_{12} = 1,50; \quad x^3_{21} = 1,00; \quad x^3_{22} = 0,00. \end{aligned} \tag{6.50}$$

From the numerical result of the first example [see (6.50),Tab.6.2], I notice that in a condition without emergency, each hospital prefers to choose his trusted warehouse. In particular,

- All hospitals decide to buy the medical item one ($k = 1$) from warehouse one ($w = 1$);
- All hospitals decide not to buy the medical item two ($k = 2$) from warehouse one ($w = 1$) or two ($w = 2$);
- For medical item three ($k = 3$), hospital two ($h = 2$) decides to rely on warehouse one ($w = 1$) and hospital one ($h = 1$) on warehouse two ($w = 2$).

In the second stage, namely, in an emergency situation, the usual choice is no longer the optimal one, but demand must always be satisfied by minimizing costs. Furthermore, the penalties are fortunately null for each hospital and for each item. The results are shown in Table 6.2.

Numerical Example 2: In this numerical example, the items are treated as boxes and the coefficients of the cost functions are related to boxes which contain thousand packages. I have considered low penalty functions, since not satisfying the demand for a particular item would not cause severe discomfort. In this case, the amount of unfulfilled demand at hospital h of medical supply item k under scenario ω, for all h, k are not null. This is a consequence of the fact that for these items it is not necessary to satisfy fully the daily demand. Another difference with the first numerical example, is that all hospitals use all warehouses, without choosing the trusted warehouses.

The coefficient matrix of the cost functions is represented by (6.51).

$$\begin{pmatrix} 2,41 & 2,44 & 2,47 & 2,42 & 1,90 & 2,85 & 3,80 & 2,28 & 0,05 & 0,04 \\ 2,81 & 2,84 & 2,87 & 2,82 & 2,54 & 3,10 & 2,42 & 1,83 & 0,07 & 0,03 \\ 1,76 & 1,79 & 1,82 & 1,77 & 2,10 & 3,63 & 3,21 & 2,82 & 0,02 & 0,08 \end{pmatrix} \times 10^{-3}. \tag{6.51}$$

The flows x^k_{wh} of the first stage (6.52) are given by

$$\begin{aligned} &x^1_{11} = 1,65; \quad x^1_{12} = 1,71; \quad x^1_{21} = 1,44; \quad x^1_{22} = 1,78; \\ &x^2_{11} = 1,14; \quad x^2_{12} = 1,11; \quad x^2_{21} = 0,94; \quad x^2_{22} = 1,17; \\ &x^3_{11} = 0,64; \quad x^3_{12} = 0,79; \quad x^3_{21} = 0,52; \quad x^3_{22} = 0,85. \end{aligned} \tag{6.52}$$

In the following Table 6.3, I group all variables for the second stage, under scenario ω.

6.7 Conclusions

In this chapter, I constructed a stochastic Nash equilibrium model for a medical supply network that consists of warehouses and hospitals with multiple medical items and multiple transportation modes. Each hospital solves a two-stage stochastic optimization problem, where, in the first stage, seeks to minimize the purchasing cost of medical items and the transportation time. Then, I introduced a recourse decision process to optimize the expected overall costs and the penalty for the prior plan, in response to each possible disaster scenario of the second stage. The hospitals simultaneously solve their own stochastic optimization problems and reach a stable state given by the stochastic Nash equilibrium concept. Specific features of the model include: the uncertainty of the scenarios, the supply availability of medical items, the penalty for unmet demand and the fluctuating costs. The model is formulated as a variational inequality. In the case of general probability distribution, I characterized the Nash equilibrium of the problem as a solution to an infinite-dimensional variational inequality in the Hilbert space L^2. The associated Lagrange function was studied and a strong duality result was provided. Finally, I presented some numerical illustrations solved applying the progressive hedging algorithm.

The results reveal that hospitals are able to re-arrange timely their requests in order to satisfy the need for medical items. In emergencies, uncertainty plays a fundamental role in the success of disaster management; hence, health institutions must be ready to adjust the request of medical items. My contributions to the literature lie in advancing the state-of-the-art of stochastic programming for disaster management as well as applications of variational inequalities and strong duality. I

also emphasize that to-date there has been limited work on stochastic programming problems under general probability distribution.

This model could be extended in future research. For example, I could incorporate additional details to the model and solve examples using data from real situations. The extension to a multi-stage problem where I consider different stages of information is another future research opportunity.

Items	Flows	Scenario1	Scenario2	Scenario3	Scenario4	Scenario5
$k=1$	$y_{11}(\omega)$	1,21	1,56	1,66	1,82	2,04
	$y_{12}(\omega)$	1,12	1,12	1,31	1,41	1,57
	$y_{21}(\omega)$	0,79	0,64	0,85	0,99	1,03
	$y_{22}(\omega)$	1,29	1,49	1,58	1,68	1,91
$k=2$	$y_{11}(\omega)$	0,51	0,62	0,77	0,91	1,01
	$y_{12}(\omega)$	0,56	0,57	0,73	0,81	0,85
	$y_{21}(\omega)$	0,51	0,65	0,81	0,94	1,06
	$y_{22}(\omega)$	0,65	1,00	1,16	1,28	1,42
$k=3$	$y_{11}(\omega)$	0,34	1,25	0,48	0,57	0,79
	$y_{12}(\omega)$	0,44	0,46	0,54	0,58	0,64
	$y_{21}(\omega)$	0,31	0,27	0,37	0,40	0,41
	$y_{22}(\omega)$	0,48	0,55	0,66	0,72	0,87
$k=1$	$z_1(\omega)$	0,00	0,00	0,00	0,00	0,00
	$z_2(\omega)$	0,00	0,00	0,00	0,00	0,00
$k=2$	$z_1(\omega)$	0,00	0,00	0,00	0,00	0,00
	$z_2(\omega)$	0,00	0,00	0,00	0,00	0,00
$k=3$	$z_1(\omega)$	0,00	0,00	0,00	0,00	0,00
	$z_2(\omega)$	0,00	0,00	0,00	0,00	0,00

Table 6.2: Numerical results solved by PHM about indispensable items

Items	Flows	Scenario1	Scenario2	Scenario3	Scenario4	Scenario5
$k = 1$	$y_{11}(\omega)$	1,25	1,47	1,77	2,07	2,22
	$y_{12}(\omega)$	0,44	0,51	0,46	0,51	0,42
	$y_{21}(\omega)$	0,21	0,15	0,15	0,15	0,21
	$y_{22}(\omega)$	1,25	1,38	1,63	1,79	2,32
$k = 2$	$y_{11}(\omega)$	0,34	0,39	0,51	0,63	0,70
	$y_{12}(\omega)$	0,10	0,20	0,21	0,21	0,24
	$y_{21}(\omega)$	0,41	0,46	0,64	0,80	0,94
	$y_{22}(\omega)$	0,75	0,94	1,22	1,41	1,57
$k = 3$	$y_{11}(\omega)$	0,37	0,44	0,52	0,62	0,72
	$y_{12}(\omega)$	0,19	0,23	0,25	0,28	0,23
	$y_{21}(\omega)$	0,14	0,17	0,19	0,19	0,22
	$y_{22}(\omega)$	0,50	0,52	0,69	0,75	0,96
$k = 1$	$z_1(\omega)$	0,65	0,68	0,67	0,67	0,68
	$z_2(\omega)$	0,79	0,78	0,79	0,78	0,77
$k = 2$	$z_1(\omega)$	0,40	0,44	0,44	0,44	0,44
	$z_2(\omega)$	0,47	0,47	0,48	0,48	0,48
$k = 3$	$z_1(\omega)$	0,21	0,20	0,20	0,20	0,19
	$z_2(\omega)$	0,32	0,32	0,33	0,33	0,34

Table 6.3: Numerical result solved by PHM with unfulfilled demand

Chapter 7

Optimal Emergency Evacuation with Uncertainty

7.1 Introduction

Natural disasters (earthquakes, hurricanes, landslides, etc.) as well as unnatural ones (wars, terrorist attacks, etc.) are a serious threat for the humankind. Evacuation of the disaster region is the most used strategy to save people affected by a disaster. Generally, disasters cannot be predicted, and it is extremely difficult to estimate their intensity and damages; hence, evacuation planning must be done under uncertainty. For this reason, it is generally formulated as a stochastic programming problem (see [202]). Incomplete information may regard different factors, such as evacuation demand, link capacity, disruption in the road network or how much infrastructures may be impacted by disasters.

In this paper, I propose a scenario-based evacuation planning model that provides the optimal flows of evacuees from crisis areas to shelters, in order to minimize both the transportation cost and the transportation time, under uncertainty on the

evacuation demand and the link capacities. Inspired by [220], I admit real-time information availability, which makes the evacuation process be divided into two stages. In the first stage, people at risk receive the early warning information about the disaster and escape from the crisis areas; however, they cannot obtain the exact information of disaster intensity. After a certain time period, accurate real-time information is observed and the process reaches the second-stage, where the decision relies on the first-stage solution and on the observed scenario. Moreover, I introduce a penalty to the unmet demand of evacuation which will affect the second stage decision.

The importance of an efficient approach to emergency management and evacuation planning has been emphasized in several papers.

In [47] the authors model an escape situation in a labyrinth, where people are agents that act as two different kinds of ant colonies. Payoff values in both the competitive and the cooperative framework are studied, merging a game theoretical approach and Ant Colony Optimization.

In [18] the authors present a two-stage stochastic programming model to plan the transportation of vital first-aid commodities to disaster-affected areas during emergency response. A multi-commodity, multi-modal network flow formulation is then developed. Since it is difficult to predict the timing and magnitude of any disaster, uncertainty and information asymmetry naturally arise. The authors introduce randomness as a finite sample of scenarios for capacity, supply and demand.

In [20], the authors propose a scenario-based two-stage stochastic evacuation planning model that optimally chooses shelter sites, and assigns evacuees to nearest shelters within a tolerance degree to minimize the expected total evacuation time.

The model takes into account the uncertainty in the evacuation demand and the disruption in the road network and shelter sites.

In [184], the authors develop a stochastic optimization model that determines the order in which patients should be evacuated over time, based on the evolution of the storm by considering a weighted sum of the expected risk and the expected cost of evacuation.

In [199], a bi-objective optimization model is proposed, which study critical management before and after the disaster. The first level investigates the locations of shelters and warehouses before the disaster, and maximizes the weights of the sites selected for construction of shelters. The second level minimizes the distances from warehouses to the shelters and the distances from crisis areas to the shelters.

In [220], the authors study the regional emergency resources storage, and, in particular, the region division. A two-stage stochastic programming model is proposed to solve the region division problem.

Recently, two-stage stochastic variational inequalities were introduced, where one seeks a decision vector before the stochastic variables are known, and a decision vector after the scenario has been realized. In [192], Rockafellar and Wets proposed the multistage stochastic variational inequality. In [190], the authors develop progressive hedging methods for solving multistage convex stochastic programming, see also [189]. In [38], the authors formulate the two-stage stochastic variational inequality as a two-stage stochastic programming problem with recourse.

In this paper, I present a two-stage stochastic programming problem for the evacuation planning and give an equivalent formulation as a two-stage stochastic variational inequality, using the Lagrangian relaxation approach. I also discuss the qualitative properties of the two-stage stochastic variational inequality.

The structure of this paper is as follows. In Section 7.2, we present the deterministic evacuation model and derive an equivalent variational inequality formulation. In Section 7.3, I present the two-stage stochastic model. In Section 7.4, I propose an equivalent two-stage variational inequality formulation. In Section 7.5, I provide a numerical example, and, finally, I present our conclusions in Section 7.6.

7.2 The deterministic model

I assume that a population of N individuals is located in some crisis areas and must be evacuated to some shelters. Different modes of transportation are considered to enhance node accessibility. I denote by A the set of crisis areas, with typical area denoted by i, by S the set of shelters, with typical shelter denoted by j, and by M the set of transportation modes, with typical mode denoted by m. I consider a network representation as in Figure 7.1. The links between the levels of the network represent all the possible connections between the crisis areas and the shelters. Multiple links between each area and each shelter depict the possibility of alternative modes of transportation.

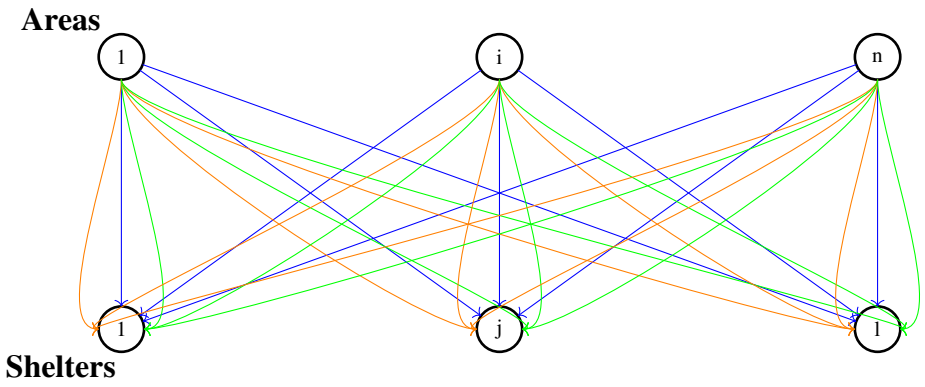

Figure 7.1: The Network representation of Areas and Shelters

Let d_i^m be the demand of crisis area i for evacuation with mode m, namely, the number of people to be evacuated from area i with mode m, where $\sum_{i\in A}\sum_{m\in M} d_i^m \leq N$. I denote by $d_i = \sum_{m\in M} d_i^m$ the demand of area i on all modes. Moreover, let x_{ij} the flows of evacuees from area i to shelter j. I also assume that K_j is maximum number of people that can be hosted in shelter j, and k_j is the minimum number of people required to open shelter j. Thus, the following conditions have to be satisfied:

$$\sum_{i\in A} x_{ij} \leq K_j, \forall j \in S, \quad \sum_{i\in A} x_{ij} \geq k_j, \forall j \in S.$$

I group the flows x_{ij} into a column vector $x \in \mathbb{R}^{nl}$. In addition, I introduce the transportation cost c_{ij}^m from area i to shelter j with mode m and assume that it depends on the flow x_{ij}, namely, $c_{ij}^m = c_{ij}^m(x_{ij})$. Analogously, I define the transportation time t_{ij}^m from area i to shelter j with mode m and assume that it depends on the flow x_{ij}, namely, $t_{ij}^m = t_{ij}^m(x_{ij})$.

I summarize the relevant notations used in the mathematical formulation in Table 7.1.

I introduce the total evacuation cost C_{ij}^m given by

$$C_{ij}^m(x_{ij}) = w\, c_{ij}^m(x_{ij}) + (1-w)\, t_{ij}^m(x_{ij}), \quad \forall i \in A\,, j \in S\,, m \in M.$$

Our aim is to minimize the total evacuation costs; hence, I seek to solve the following optimization problem:

Symbols	Definitions
A	set of crisis areas, with typical area denoted by i, $card(A) = n$
S	set of shelters, with typical shelter denoted by j, $card(S) = l$
M	set of transportation modes, with typical mode denoted by m, $card(M) = \bar{m}$
d_i^m	demand of crisis area i for evacuation with mode m
$d_i = \sum_{m \in M} d_i^m$	the demand of area i on all modes
K_j	maximum number of people that can be hosted in shelter j
k_j	recommended number of people to open shelter j
w	weight in $[0, 1]$
ε	positive balance tolerance
μ_{ij}	flow capacity on link (i, j)
$\mu = (\mu_{ij})_{i,j}$	total flow capacity
x_{ij}	flow of evacuees from area i to shelter j
$x = (x_{ij})_{i,j}$	total flow of evacuees
$c_{ij}^m(x_{ij})$	transportation cost from area i to shelter j with mode m
$t_{ij}^m(x_{ij})$	transportation time from area i to shelter j with mode m

Table 7.1: The notation for the deterministic model

$$\min \sum_{i \in A} \sum_{j \in S} \sum_{m \in M} C_{ij}^m(x_{ij}) \tag{7.1}$$

$$\sum_{i \in A} x_{ij} \leq K_j, \ \forall j \in S, \tag{7.2}$$

$$\sum_{i \in A} x_{ij} \geq k_j, \ \forall j \in S, \tag{7.3}$$

$$x_{ij} \leq \mu_{ij}, \ \forall i \in A, \ j \in S, \tag{7.4}$$

$$\frac{\sum_{i \in A} x_{ij}}{K_j} - \frac{\sum_{i \in A} x_{ij'}}{K'_j} \leq \varepsilon, \ \forall j, \ j' \in S, \tag{7.5}$$

$$\sum_{j \in S} x_{ij} \leq d_i, \ \forall i \in A, \tag{7.6}$$

$$x_{ij} \geq 0, \ \forall i \in A \, , j \in S. \tag{7.7}$$

The objective function (7.1) is the weighted sum of transportation cost and transportation time, where $w \in [0,1]$. Constraint (7.2) ensures that the capacity of each shelter j is not exceeded. Constraint (7.3) guarantees that each shelter j is used. Constraint (7.4) requires that the flow on link (i,j) must satisfy the flow capacity on that link. Constraint (7.5) states that the number of evacuees is balanced amongst the shelters. Constraint (7.6) establishes that for each area i the evacuation demand d_i on all modes is satisfied, and, finally, (7.7) represents the non-negativity requirement on flows.

I now introduce the set of feasible flows

$$X = \Big\{ x \in \mathbb{R}^{nl} : x_{ij} \geq 0, \forall i,j \,; \sum_{i \in A} x_{ij} \leq K_j, \; \forall j; \sum_{i \in A} x_{ij} \geq k_j, \; \forall j;$$
$$x_{ij} \leq \mu_{ij}, \; \forall i,j, \,; \frac{\sum_{i \in A} x_{ij}}{K_j} - \frac{\sum_{i \in A} x_{ij'}}{K'_j} \leq \varepsilon, \; \forall j, \; j'; \; \sum_{j \in S} x_{ij} \leq d_i, \; \forall i \Big\}.$$

I assume that the transportation cost and the transportation time functions are continuously differentiable and convex. In addition, since the set X is closed, bounded and convex, I can apply the classical theory on variational inequalities (see, for instance, [78], [126] or [158]) and formulate problem (7.1)-(7.7) as the following variational inequality:

$$\text{Find } x^* \in X :$$
$$\sum_{i \in A} \sum_{j \in S} \sum_{m \in M} \left[w \frac{\partial c_{ij}^m(x_{ij}^*)}{\partial x_{ij}} + (1-w) \frac{\partial t_{ij}^m(x_{ij}^*)}{\partial x_{ij}} \right] \times \left(x_{ij} - x_{ij}^* \right), \; \forall x \in X.$$

The above variational inequality can be put in standard form as follows (see [158]):

$$\text{Find } x^* \in X \text{ such that } \langle F(x^*), x - x^* \rangle \geq 0, \quad \forall x \in X, \tag{7.8}$$

where $\langle \cdot, \cdot \rangle$ denotes the inner product in the (nl)-dimensional Euclidean space and

$$F(x^*) = \left[w \frac{\partial c_{ij}^m(x_{ij}^*)}{\partial x_{ij}} + (1-w) \frac{\partial t_{ij}^m(x_{ij}^*)}{\partial x_{ij}} \right]_{\substack{i \in A \\ j \in S \\ m \in M}} .$$

Under the assumptions on the feasible set X and the objective function, I can ensure the existence of at least one solution to (7.8) (see [126]). Moreover, if the function $F(x)$ in (7.8) is strictly monotone on X, namely

$$\langle F(x^1) - F(x^2), x^1 - x^2 \rangle > 0 \quad \forall x^1, x^2 \in X,\ x^1 \neq x^2,$$

then variational inequality (7.8) admits a unique solution.

7.3 Two-stage stochastic evacuation model

In this section, I present a scenario-based stochastic optimization model to represent the evacuation process after an earthquake. At the occurrence of the disaster event, affected people receive the early warning information and escape from the crisis areas. After the event, accurate information is available, for instance due to technological communication tools. Since the initial response will depend on a number of disaster scenarios, I propose a two-stage stochastic programming model with recourse, where both the first stage and the second stage arise in different time phases in the same evacuation network. I remark that the first-stage decision is taken before the realization of the disaster scenario is observed. After that this information is accessible, the decision process reaches the second-stage, where the decision depends on the first-stage solution and on the observed scenario.

As it is very hard to estimate exactly the impact of a natural disaster, I allow for uncertainty in the modeling assumptions, and introduce some random parameters.

In particular, since the effects of disasters naturally randomizes the number of people who survive, I consider random evacuation demands at the emergency sites. Moreover, I take into account possible disruptions on network links, and deal with random capacities on links.

I note that, in the first stage, the evacuation demand and the link capacities are known only from a probabilistic point of view. Thus, in the first stage, people at risk must be evacuated from crisis areas before observing the real data. Instead, in the second stage, the evacuation plan will be obtained with the realization of the evacuation demand and the link capacities.

The aim is to formulate the random evacuation problem as a two-stage optimization problem. In the first stage, I seek for the optimal flows to minimize the penalty cost generated by the decisions taken before the acquisition of the information plus the recourse cost for the disaster scenario. In the second stage, another optimization problem is solved, based on a given realization of each scenario.

Let $(\Omega, \mathcal{F}, P)$ be a probability space, where the random parameter $\omega \in \Omega$ represents the typical disaster scenario. For each $\omega \in \Omega$, I denote by $\xi : \Omega \to \mathbb{R}^K$ a finite dimensional random vector and by $\mathbb{E}_\xi$ the mathematical expectation with respect to ξ.

In order to formulate the two stage stochastic evacuation model, I introduce two types of decision variables. In the first stage, the decision variable x_{ij} is used to represent the flow of evacuees from area i to shelter j in stage one. The second-stage decision variable $y_{ij}(\omega)$ represents the flow of evacuees from area i to shelter j in stage two under scenario ω. From the perspective of the entire system, the decision planner chooses x_{ij} before a realization of ξ is revealed and later selects $y(\omega)$ with known realization.

Table 7.2 summarizes the relevant notations used in the model formulation.

Symbols	**Definitions**
μ_{ij}	flow capacity on link (i, j) in stage one
$\mu_{ij}(\omega)$	random flow capacity in stage two
d_i^m	evacuation demand of crisis area i with mode m in stage one
$d_i = \sum_{m \in M} d_i^m$	demand of area i on all modes in stage one
$d_i^m(\omega)$	evacuation demand of crisis area i with mode m in stage two
$d_i(\omega) = \sum_{m \in M} d_i^m(\omega)$	demand of area i on all modes in stage two
$\xi(\omega)$	random parameters in stage two resulting from decisions made in stage one according to ω
x_{ij}	flow of evacuees from area i to shelter j in stage one
$y_{ij}(\omega)$	flow of evacuees from area i to shelter j in stage two under scenario ω
$\pi_{ij}(x_{ij})$	the penalty cost on link (i, j)

Table 7.2: The notation for the two-stage stochastic model

I denote by $\pi_{ij} = \pi_{ij}(x_{ij})$ the penalty cost generated by the decisions taken before obtaining the information. In order to minimize the penalty for the prior evacuation plan and the expected total evacuation expenses (time and cost) for each scenario, I formulate the following two-stage evacuation problem.

$$\min \sum_{i\in A}\sum_{j\in S}\sum_{m\in M} \pi_{ij}(x_{ij}) + \mathbb{E}_{\xi}(\Phi(x,\xi(\omega))) \tag{7.9}$$

subject to

$$\sum_{i\in A} x_{ij} \le K_j,\ \forall j \in S, \tag{7.10}$$

$$\sum_{i\in A} x_{ij} \ge k_j,\ \forall j \in S, \tag{7.11}$$

$$x_{ij} \le \mu_{ij},\ \forall i \in A,\ j \in S, \tag{7.12}$$

$$\frac{\sum_{i\in A} x_{ij}}{K_j} - \frac{\sum_{i\in A} x_{ij'}}{K'_j} \le \varepsilon,\ \forall j,\ j' \in S, \tag{7.13}$$

$$\sum_{j\in S} x_{ij} \le d_i,\ \forall i \in A, \tag{7.14}$$

$$x_{ij} \ge 0,\ \forall i \in A,\ j \in S, \tag{7.15}$$

where

$$\Phi(x,\xi(\omega)) = \min \sum_{i\in A}\sum_{j\in S} \Big(w\, c^m_{ij}(y_{ij}(\omega)) + (1-w)\, t^m_{ij}(y_{ij}(\omega)) \Big) \tag{7.16}$$

subject to

$$\sum_{i\in A} y_{ij}(\omega) \le K_j,\ \forall j \in S,\ P\text{-a.s.}, \tag{7.17}$$

$$\sum_{i\in A} y^m_{ij}(\omega) \ge k_j,\ \forall j \in S, P\text{-a.s.}, \tag{7.18}$$

$$y_{ij}(\omega) \le \mu_{ij}(\omega),\ \forall i \in A,\ j \in S, P\text{-a.s.}, \tag{7.19}$$

$$\frac{\sum_{i\in A} y_{ij}(\omega)}{K_j} - \frac{\sum_{i\in A} y_{ij'}(\omega)}{K'_j} \le \varepsilon,\ \forall j,\ j' \in S,\ P\text{-a.s.}, \tag{7.20}$$

$$\sum_{j\in S} y_{ij}(\omega) + \big(d_i - \sum_j x_{ij}\big) \le d_i(\omega),\ \forall i \in A,\ P\text{-a.s.}, \tag{7.21}$$

$$y_{ij}(\omega) \ge 0,\ \forall i \in A,\ j \in S,\ P\text{-a.s.} \tag{7.22}$$

Problem (7.9)-(7.15) is the first-stage problem. The objective function (7.9) minimizes the sum of the penalty for early evacuation plan and the recourse cost

$\Phi(x, \xi(\omega))$. Constraints (7.10)-(7.11) ensure that the capacity of each shelter j is satisfied. Constraint (7.12) is the link flow capacity, constraint (7.13) is the balance constraint amongst the shelters, constraint (7.14) states that for each area i the number of evacuees cannot exceed the number of affected people. Finally, (7.15) is the non-negativity requirements on flows.

For a given realization $\omega \in \Omega$, $\Phi(x, \xi(\omega))$ is the optimal value of the second-stage problem (7.16)-(7.22), where the constraints hold almost surely (P-a.s.). The objective function (7.16) minimizes the total evacuation cost and the transportation time in the second stage. Constraints (7.17)-(7.18) are the shelter capacities, constraint (7.19) is the flow capacity, constraint (7.20) is the balance constraint amongst the shelters. Constraint (7.21) establishes that the number of evacuees at the second stage plus the unmet demand of evacuation at the first stage, given by $d_i - \sum_{j \in S} x_{ij}$, cannot exceed the two-stage demand of people at risk $d_i(\omega)$. I emphasize that the connections between stage-wise decision variables x and y are captured by constraint (7.21). It is the linking factor between the first and second stage, and communicates the first-stage decisions to the second one. Finally, (7.22) is the non-negativity constraint.

I assume that:

1. $\pi_{ij}(\cdot)$, is continuously differentiable and convex for all i, j;

2. $c_{ij}^m(\cdot, \omega)$, $t_{ij}^m(\cdot, \omega)$, a.e. in Ω, are continuously differentiable and convex for all i, j;

3. for each $u \in \mathbb{R}^{pq}$, $c_{ij}^m(u, \cdot)$, $t_{ij}^m(u, \cdot)$ are measurable with respect to the random parameter in Ω for all i, j;

4. $y_{ij} : \Omega \to \mathbb{R}$ and $\mu_{ij} : \Omega \to \mathbb{R}$ are measurable mappings for all i, j;

5. $d_i^m : \Omega \to \mathbb{R}$ is a measurable mapping for all i and all m.

Now, I set

$$Y = \Big\{ y(\omega) \in \mathbb{R}^{nl} : y_{ij}(\omega) \geq 0, \forall i,\ j\,; \sum_{i \in A} y_{ij}(\omega) \leq K_j,\ \forall j; \sum_{i \in A} y_{ij}(\omega) \geq k_j,\ \forall j;$$
$$y_{ij}(\omega) \leq \mu_{ij}(\omega),\ \forall i,\ j; \frac{\sum_{i \in A} y_{ij}(\omega)}{K_j} - \frac{\sum_{i \in A} y_{ij'}(\omega)}{K'_j} \leq \varepsilon,\ \forall j,\ j',\ P\text{-a.s.} \Big\},$$

which is a closed, convex and bounded subset of $\mathbb{R}^{pq}$.

Thus, the two-stage stochastic problem can be stated in a more compact form as

$$\min_{x \in X} \sum_{i \in A} \sum_{j \in S} \pi_{ij}(x_{ij}) + \mathbb{E}_{\xi}(F(x, \xi(\omega))), \tag{7.23}$$

$$\Phi(x, \xi(\omega)) = \min_{y(\omega) \in Y} \sum_{i \in A} \sum_{j \in S} \sum_{m \in M} \Big(w\, c_{ij}^m(y_{ij}(\omega)) + (1 - w)\, t_{ij}^m(y_{ij}(\omega)) \Big) \tag{7.24}$$

$$\sum_{j \in S} y_{ij}(\omega) + (d_i - \sum_j x_{ij}) \leq d_i(\omega),\ \forall i \in A,\ P\text{-a.s.} \tag{7.25}$$

If the random parameter $\omega \in \Omega$ follows a discrete distribution with finite support $\Omega = \{\omega_1, \ldots, \omega_{\bar{r}}\}$ and probabilities $p(\omega_1), \ldots, p(\omega_{\bar{r}})$ associated with each realization $\omega_1, \ldots, \omega_{\bar{r}}$, then the two-stage problem can be formulated as the unique large scale problem

$$\min \pi_{ij}(x_{ij}) + \sum_{r\in R} p(\omega_r) \sum_{i\in A} \sum_{j\in S} \sum_{m\in M} \left(w\, c_{ij}^m(y_{ij}(\omega_r)) + (1-w)\, t_{ij}^m(y_{ij}(\omega_r)) \right)$$

$$\sum_{i\in A} x_{ij} \leq K_j, \forall j \in S,$$

$$\sum_{i\in A} x_{ij} \geq k_j, \forall j \in S,$$

$$x_{ij} \leq \mu_{ij}, \forall i \in A,\ j \in S,$$

$$\frac{\sum_{i\in A} x_{ij}}{K_j} - \frac{\sum_{i\in A} x_{ij'}}{K'_j} \leq \varepsilon,\ \forall j,\ j' \in S,$$

$$\sum_{j\in S} x_{ijr} \leq d_i,\ \forall i \in A,$$

$$\sum_{i\in A} y_{ij}(\omega_r) \leq K_j, \forall j \in S,\ r \in R,$$

$$\sum_{i\in A} y_{ij}(\omega_r) \geq k_j, \forall j \in S,\ r \in R,$$

$$y_{ij}(\omega_r) \leq \mu_{ij}(\omega_r), \forall i \in A,\ j \in S,\ r \in R,$$

$$\frac{\sum_{i\in A} y_{ij}(\omega_r)}{K_j} - \frac{\sum_{i\in A} y_{ij'}(\omega_r)}{K'_j} \leq \varepsilon,\ \forall j,\ j' \in S,\ r \in R,$$

$$\sum_{j\in S} y_{ij}(\omega_r) + d_i - \sum_{j\in S} x_{ij} \leq d_i(\omega_t),\ \forall i \in A,\ r \in R,$$

$$x_{ij} \geq 0, \forall i \in A,\ j \in S,$$

$$y_{ij}(\omega_r) \geq 0, \forall i \in A,\ j \in S,\ r \in R,$$

where $R = \{1, \ldots, \bar{r}\}$. If the number of scenarios is not excessive, then a possible approach is to solve directly the linear programming problem using a solver such as CPLEX. In the next section, I suggest an alternative approach that decomposes the original problem into two variational inequality subproblems.

7.4 Two-stage variational inequality formulation

In this section, I propose an equivalent two-stage variational inequality formulation, using the Lagrangian relaxation approach.

I note that the second-stage problem (7.24)-(7.25), due to constraint (7.25), contains the variable x that is not yet known at that stage. For this reason, the problem is not easy to solve. Thus, I suggest to relax (7.25) into the objective function by Lagrangian relaxation approach (see [22, 122, 138]). As a consequence, I decompose the original problem into two sub-problems, that can be easily solved, and provide a lower bound of the optimal value of the initial model (7.9)-(7.22).

Now, I focus on the second stage problem and give its Lagrangian formulation. I introduce the Lagrange multiplier vector $\lambda : \Omega \to \mathbb{R}^n$, with $\lambda_i(\omega) \geq 0$ i.e. $\omega \in \Omega$, for all $i \in A$, and consider the relaxed constraints

$$\sum_{i \in A} \lambda_i(\omega) \Big(\sum_{j \in S} y_{ij}(\omega) + d_i - \sum_{j \in S} x_{ij} - d_i(\omega) \Big).$$

Lagrange multiplier $\lambda_i(\omega)$ represents the price or disutility deriving from the unmet demand at the first stage. Therefore, the Lagrangian of the second-stage problem with general probability distribution is

$$L(x, y(\omega), \lambda(\omega), \omega) = \sum_{i \in A} \sum_{j \in S} \sum_{m \in M} \Big(w\, c_{ij}^m(y_{ij}(\omega)) + (1 - w)\, t_{ij}^m(y_{ij}(\omega)) \Big)$$
$$+ \sum_{i \in A} \lambda_i(\omega) \Big(\sum_{j \in S} y_{ij}(\omega) + d_i - \sum_{j \in S} x_{ij} - d_i(\omega) \Big).$$

I have

$$\inf_{y\in Y} L(x, y(\omega), \lambda(\omega), \omega) = \sum_{i\in A} \lambda_i(\omega)\Big(d_i - \sum_{j\in S} x_{ij} - d_i(\omega)\Big)$$
$$+ \inf_{y\in Y} \Big(\sum_{i\in A}\sum_{j\in S}\sum_{m\in M} \Big(w\, c_{ij}^m(y_{ij}(\omega)) + (1-w)\, t_{ij}^m(y_{ij}(\omega))\Big) + \sum_{i\in A} \lambda_i(\omega) \sum_{j\in S} y_{ij}(\omega)\Big).$$

Then, the dual problem is

$$\max_{\lambda\geq 0} \Bigg(\sum_{i\in A} \lambda_i(\omega)\Big(d_i - \sum_{j\in S} x_{ij} - d_i(\omega)\Big) \tag{7.26}$$
$$+ \inf_{y\in Y} \Big(\sum_{i\in A}\sum_{j\in S}\sum_{m\in M} \Big(w\, c_{ij}^m(y_{ij}(\omega)) + (1-w)\, t_{ij}^m(y_{ij}(\omega))\Big) + \sum_{i\in A} \lambda_i(\omega) \sum_{j\in S} y_{ij}(\omega)\Big)\Bigg).$$
(7.27)

Thus, the two-stage problem becomes

$$\min_{x\in X} \sum_{i\in A}\sum_{j\in S}\sum_{m\in M} \pi_{ij}^m(x_{ij}) + \mathbb{E}_\xi(\Phi^1(x, \xi(\omega))),$$
$$\Phi^1(x, \xi(\omega)) = \max_{\lambda\geq 0} \inf_{y\in Y} L(x, y(\omega), \lambda(\omega), \omega).$$

Under the assumption of discrete probability space, I find

$$\mathbb{E}_\xi(\Phi^1(x, \xi(\omega))) = \sum_{r\in R} p(\omega_r)\Phi^1(x, \xi(\omega_r)),\ \nabla_x \mathbb{E}_\xi(\Phi^1(x, \xi(\omega))) =$$
$$= \mathbb{E}_\xi(-\lambda(\omega)) = -\sum_{r\in R} p(\omega_r)\lambda(\omega_r).$$

Theorem 7.4.1. *The pair $(x^*, y^*(\omega))$, where $x^* \in \mathbb{R}^{nl}$ and $y^* : \Omega \to \mathbb{R}^{nl}$ is a measurable map, is an optimal solution of the two-stage problem if and only if there exists $\lambda^* : \Omega \to \mathbb{R}^n$ measurable such that*

1. *x^* is a solution of the variational inequality*

$$\sum_{i\in A}\sum_{j\in S}\left(\sum_{m\in M}\frac{\partial \pi^m_{ij}(x^*_{ij})}{\partial x_{ij}} - \sum_{r\in R} p(\omega_r)\lambda^*_i(\omega_r)\right)\times(x_{ij}-x^*_{ij}) \geq 0, \quad \forall x\in X. \tag{7.28}$$

2. *$(y^*(\omega_r), \lambda^*(\omega_r))$ is a solution of the parametric variational inequality*

$$\begin{aligned}&\sum_{r\in R}\sum_{i\in A}\sum_{j\in S} p(\omega_r)\Bigg(w\sum_{m\in M}\frac{\partial c^m_{ij}(y^*_{ij}(\omega_r))}{\partial y_{ij}}+\\ &+(1-w)\sum_{m\in M}\frac{\partial t^m_{ij}(y^*_{ij}(\omega_r))}{\partial y_{ij}}+\lambda_i(\omega_r)\Bigg)\times(y_{ij}(\omega_r)-y^*_{ij}(\omega_r))+\\ &+\sum_{r\in R} p(\omega_r)\sum_{i\in A}\Big(\sum_{j\in S}x^*_{ij}-\sum_{j\in S}y^*_{ij}(\omega_r)-d_i+d_i(\omega_r)\Big)\times(\lambda_i(\omega_r)-\lambda^*_i(\omega_r))\geq 0,\\ &\forall y(\omega_r)\in Y, \forall\lambda_i(\omega_r)\geq 0.\end{aligned} \tag{7.29}$$

Proof. Function $\Phi^1(x,\xi(\omega_r))$ is linear w.r.t. x, and, hence, is convex for all $\omega_r\in\Omega$. This implies the convexity of the expectation function $\mathbb{E}_\xi(\Phi^1(x,\xi(\omega_r)))$. Since Ω is finite, for any $x_0\in\cap_{r\in R}\Phi^1(x,\xi(\omega_r))$, the expectation function is differentiable at x_0. Then, by interchangeability of the gradient and the expectation operators, and by classical variational inequality theory, I conclude that the first stage problem (7.23) is equivalent to variational inequality (7.28). Finally, from the optimality conditions of the dual problem (7.27), then it is easy to see that $\lambda^*(\omega_r)$ implies the existence of $y^*(\omega_r)$ such that $(y^*(\omega_r),\lambda^*(\omega_r))$ satisfies (7.29) . □

I observe that problem (7.28)-(7.29) can be put in the standard form variational inequality,

$$\langle G(z^*), z-z^*\rangle \geq 0, \quad \forall z\in X\times Y\times\mathbb{R}^n_+, \tag{7.30}$$

where

$$z = \begin{bmatrix} x \\ y \\ \lambda \end{bmatrix},$$

$$G(z) = \begin{bmatrix} \sum_{m\in M} \frac{\partial \pi_{ij}^m(x_{ij})}{\partial x_{ij}} - \sum_{r\in R} p(\omega_r)\lambda_i(\omega_r) \\ \sum_{r\in R} p(\omega_r)\left(w \sum_{m\in M} \frac{\partial c_{ij}^m(y_{ij}(\omega_r))}{\partial y_{ij}} + (1-w) \sum_{m\in M} \frac{\partial t_{ij}^m(y_{ij}(\omega_r))}{\partial y_{ij}} + \lambda_i(\omega_r)\right) \\ p(\omega_r)\Big(\sum_{j\in S} x_{ij} - \sum_{j\in S} y_{ij}(\omega_r) - d_i + d_i(\omega_r)\Big) \end{bmatrix}_{\substack{r\in R \\ i\in A \\ j\in S}}.$$

In virtue of Theorem 7.4.1, variational inequality (7.30) represents the optimality conditions of the decision planner that is faced with the two-stage stochastic optimization problem (7.23)-(7.25). I now highlight the economic interpretation of these conditions. From variational inequality (7.28), I can infer that, if there is a positive evacuation flow between area i and shelter j in the first stage, then the expected price $p(\omega_r)\lambda_r(\omega_r)$ is equal to the marginal penalty cost of the unmet demand at the first stage. From the first term in inequality (7.29), I have that, if there is a positive evacuation flow between area i and shelter j in the second stage, then the marginal evacuation costs plus the price $\lambda(\omega_r)$ must be null. From the second term, I also note that if no flow is positive, then sum of the marginal evacuation costs plus the price $\lambda(\omega_r)$ can be positive. Finally, from the second term in inequality (7.29), I see that the price $\lambda(\omega_r)$ serves as the price to balance the system.

I now discuss some qualitative properties of (7.30). Since the feasible set underlying the variational inequality problem is not compact we cannot derive existence of a solution simply from the assumption of continuity of the functions. Instead, I could require some coercivity conditions (see, for instance, [78]). It is well-known that the uniqueness of the solution to the above variational inequality is ensured by the strict monotonicity of mapping $G(z)$. The theorem below presents the

sufficient conditions for the uniqueness.

Theorem 7.4.2. *Let us assume that functions $\pi_{ij}^m(x_{ij})$ are strictly convex in x_{ij}, $c_{ij}^m(y_{ij})$ and $t_{ij}^m(y_{ij})$ are strictly convex in y_{ij}. Then, the vector function G involved in the variational inequality* (7.30) *is strictly monotone, that is,*

$$\langle G(\bar{z}) - G(\tilde{z}), \bar{z} - \tilde{z}\rangle > 0, \forall \bar{z}, \tilde{z} \in X \times Y \times \mathbb{R}_+^n, \bar{z} \neq \tilde{z}.$$

Proof. For any $\bar{z} = (\bar{x}^T, \bar{y}^T, \bar{\lambda}^T)^T, \tilde{z} = (\tilde{x}^T, \tilde{y}^T, \tilde{\lambda}^T)^T \in X \times Y \times \mathbb{R}_+^n$, and using the linearity of constraint (7.21) (see [138], Theorem 2), direct computations lead to

$$\begin{aligned}\langle (G(\bar{z}) - G(\tilde{z})), \bar{z} - \tilde{z}\rangle = &\sum_{i\in A}\sum_{j\in S}\sum_{m\in M}\left(\frac{\partial \pi_{ij}^m(\bar{x}_{ij})}{\partial x_{ij}} - \frac{\partial \pi_{ij}^m(\tilde{x}_{ij})}{\partial x_{ij}}\right)(\bar{x}_{ij} - \tilde{x}_{ij})\\ &+\sum_{r\in R}\sum_{i\in A}\sum_{j\in S} p(\omega_r)\Bigg(w\sum_{m\in M}\left(\frac{\partial c_{ij}^m(\bar{y}_{ij}(\omega_r))}{\partial y_{ij}} - \frac{\partial c_{ij}^m(\tilde{y}_{ij}(\omega_r))}{\partial y_{ij}}\right)\\ &+(1-w)\sum_{m\in M}\left(\frac{\partial t_{ij}^m(\bar{y}_{ij}(\omega_r))}{\partial y_{ij}} - \frac{\partial t_{ij}^m(\tilde{y}_{ij}(\omega_r))}{\partial y_{ij}}\right)\Bigg)(\bar{y}_{ij} - \tilde{y}_{ij}).\end{aligned}$$

Since $\pi_{ij}^m, c_{ij}^m, t_{ij}^m$ are strictly convex functions, the matrices of the second derivatives of those functions are positive definite, and the functions are strictly monotone. Thus, $G(z)$ is strict monotone if and only if $\bar{z} \neq \tilde{z}$. □

7.5 Numerical results

In this section, I introduce a numerical example for the aim of validating my approach.

For simplicity, I consider only a single mode of transportation between each crisis area and each shelter ($m = 1$). Moreover, I set $w = 0.6$, $\varepsilon = 0.01$, $\bar{r} = 100$. Then, I choose the random parameter $\omega_r \in [0, 1]$, and fix the following parameters for $i = 1, 2,\ j = 1, 2$ and $r = 1, \ldots, 100$, as follows:

- the probabilities $p(\omega_r) = \frac{1}{100}$ associated with each realization ω_r, randomly taken in $[0, 1]$;

- the recommended number and the maximum number of people that can be hosted in shelter:

$$k_1 = 4, \qquad k_2 = 3,$$
$$K_1 = 40, \qquad K_2 = 40;$$

- capacity of flows in stage one and random flow capacity in stage two:

$$\mu_{ij} = 50 \quad \forall i = 1, 2,\ j = 1, 2;$$

- evacuation demand in stage one and random evacuation demand in stage two:

$$d_1 = 50, \qquad d_1(\omega_r) = 50\omega_r;$$
$$d_2 = 60, \qquad d_2(\omega_r) = 60\omega_r.$$

I now describe the two-stage variational inequality formulation, based on Lagrangian relaxation approach. The procedure is structured in two steps:

1. I first solve the second-stage parametric variational inequality, and find the solution $(y^*(x, \omega), \lambda^*(\omega))$;

2. I write the operator $\sum_{m\in M} \sum_{i\in A} \sum_{j\in S} \pi_{ij}^m(x_{ij}^*) + \mathbb{E}_\xi(F(x^*, \xi(\omega)))$, solve the first-stage variational inequality, and find x^*.
   I obtain the solution $(x^*, y^*(\omega), \lambda^*(\omega))$. I remark that $\sum_{m\in M} \sum_{i\in A} \sum_{j\in S} \pi_{ij}^m x_{ij}^*$ $+\mathbb{E}_\xi(F(x^*, \xi(\omega)))$ is a lower bound of the optimal value of the original problem.

I apply the extragradient method (see [128]) to compute solutions to my numerical problem and implement it as M-script files of MatLab.
The first step of this approach consists in solving the second-stage parametric variational inequality, using the Lagrangian approach. The profit function F_{ij} for each area $i = 1, 2$ and shelter $j = 1, 2$ are given by

$$F_{11} = \sum_{r=1}^{100} p(\omega_r)\Big(w(20y_{11}(\omega_r)^2 - 90y_{11}(\omega_r) + 200) + (1-w)(20y_{11}(\omega_r)^2 - 180y_{11}(\omega_r) + 600)$$
$$+ \lambda_1(y_{11}(\omega_r) + y_{12}(\omega_r) + 50 - x_{11} - x_{12} - 50\omega_r)\Big) + \frac{2x_{11}^2 + x_{12}^2 - 5x_{11}}{2},$$
$$F_{12} = \sum_{r=1}^{100} p(\omega_r)\Big(w(45y_{12}(\omega_r)^2 - 105y_{12}(\omega_r) + 225) + (1-w)(60y_{12}(\omega_r)^2 - 180y_{12}(\omega_r) + 900)$$
$$+ \lambda_1(y_{11}(\omega_r) + y_{12}(\omega_r) + 50 - x_{11} - x_{12} - 50\omega_r)\Big) + \frac{x_{11}^2 + 1.5x_{12}^2 - 5.4x_{12}}{2},$$
$$F_{21} = \sum_{r=1}^{100} p(\omega_r)\Big(w(80y_{21}(\omega_r)^2 - 200y_{21}(\omega_r) + 300) + (1-w)(45y_{21}(\omega_r)^2 - 120y_{21}(\omega_r) + 450)$$
$$+ \lambda_2(y_{21}(\omega_r) + y_{22}(\omega_r) + 60 - x_{21} - x_{22} - 60\omega_r)\Big) + \frac{x_{22}^2 + 3x_{21}^2 - 7.4x_{21}}{2},$$
$$F_{22} = \sum_{r=1}^{100} p(\omega_r)\Big(w(30y_{22}(\omega_r)^2 - 110y_{22}(\omega_r) + 350) + (1-w)(54y_{22}(\omega_r)^2 - 168y_{22}(\omega_r) + 675)$$
$$+ \lambda_2(y_{21}(\omega_r) + y_{22}(\omega_r) + 60 - x_{21} - x_{22} - 60\omega_r)\Big) + \frac{2x_{22}^2 + x_{21}^2 - 6.2x_{22}}{2}.$$

I obtain the following solutions

$$y_{11} = -35.9789 + 35.9155\omega_r + 0.71831x_{11} + 0.71831x_{12},$$
$$y_{12} = -14.0211 + 14.0845\omega_r + 0.28169x_{11} + 0.28169x_{12},$$
$$y_{21} = -22.375 + 22.5\omega_r + 0.375x_{21} + 0.375x_{22},$$
$$y_{22} = -37.625 + 37.5\omega_r + 0.625x_{21} + 0.625x_{22},$$
$$\lambda_1 = 156515 - 143662\omega_r - 2873.24x_{11} - 2873.24x_{12},$$
$$\lambda_2 = 312150 - 297000\omega_r - 4950x_{21} - 4950x_{22}.$$

For all i and j, each flow y_{ij} and the corresponding Lagrange multipliers λ_i depend

on x_{ij} and ω_r, for $r = 1, \ldots, 100$.

The second step consists in calculating x_{ij} using the profit function of the first stage F_{ij}; hence, I obtain the flows of the first and the second stage and the Lagrange multipliers of the second-stage, which depend on ω_r. I find

$$x_{11}(\omega_r) = 32.9972 - 30.8684\omega_r,$$
$$x_{12}(\omega_r) = 18.3999 - 16.1403\omega_r,$$
$$x_{21}(\omega_r) = 17.6953 - 16.3862\omega_r,$$
$$x_{22}(\omega_r) = 42.7048 - 40.9655\omega_r.$$

$$y_{11}(\omega_r) = 0.940151 + 2.14868\omega_r,$$
$$y_{12}(\omega_r) = 0.456949 + 0.842619\omega_r,$$
$$y_{21}(\omega_r) = 0.275037 + 0.993113\omega_r,$$
$$y_{22}(\omega_r) = 0.125063 + 1.65519\omega_r,$$
$$\lambda_1(\omega_r) = 8838.8 - 8594.72\omega_r,$$
$$\lambda_2(\omega_r) = 13169.5 - 13109.1\omega_r.$$

Thus, the average values of profit functions F_{ij}, for $i = 1, 2$, $j = 1, 2$ and $\omega_1, \ldots, \omega_{100}$, are

$$F_{11} = 39602, \qquad F_{12} = 25789,$$
$$F_{21} = 43715, \qquad F_{22} = 60095.$$

In the following Table 7.3, I present the average value of flows x_{ij}, y_{ij}, and the multipliers λ_{ij}.

In order to verify the effectiveness of the proposed model, we compare the deterministic model and the Lagrange relaxation approach.

(i, j)	$(1, 1)$	$(1, 2)$	$(2, 1)$	$(2, 2)$
$\bar{x}_{ij}$	17.6921	10.3973	9.5707	22.3934
$\bar{\lambda}_{ij}$	4577.4	4577.4	6669.8	6669.8
$\bar{y}_{ij}$	2.0055	0.8747	0.7674	0.9457

Table 7.3: Average of flows x_{ij}, y_{ij}, and multipliers λ_{ij} in each scenarios and the total profit function F_{ij}

In the deterministic case, using the same data, I find the solutions:

$$x_{11} = 2.82246, \qquad x_{12} = 1.47495,$$
$$x_{21} = 1.177549, \qquad x_{22} = 2.12505.$$

The values of the deterministic profit functions F_{ij}, $i = 1, 2,\ j = 1, 2$, are then:

$$F_{11} = 163.696, \qquad F_{12} = 406.831,$$
$$F_{21} = 253.689, \qquad F_{22} = 357.92.$$

I note that the values of the deterministic profit functions F_{ij} are greater than the respective values of the Lagrange relaxation approach. This observation implies that the stochastic framework and the real-time updating of information allow one to evaluate more precisely the situation, and to lower evacuation costs. Of course, for small dimensional models the two-stage stochastic evacuation problem can be directly solved.

Thus, I consider the two-stage evacuation model without the Lagrange relaxation.

I define F_{ij} for $i = 1, 2,$ and $j = 1, 2$ as

$$F_{11} = \sum_{r=1}^{100} p(\omega_r)\Big(w(20y_{11}(\omega_r)^2 - 90y_{11}(\omega_r) + 200) + (1-w)(20y_{11}(\omega_r)^2 - 180y_{11}(\omega_r) + 600)\Big) + \frac{2x_{11}^2 + x_{12}^2 - 5x_{11}}{2},$$

$$F_{12} = \sum_{r=1}^{100} p(\omega_r)\Big(w(45y_{12}(\omega_r)^2 - 105y_{12}(\omega_r) + 225) + (1-w)(60y_{12}(\omega_r)^2 - 180y_{12}(\omega_r) + 900)\Big) + \frac{x_{11}^2 + 1.5x_{12}^2 - 5.4x_{12}}{2},$$

$$F_{21} = \sum_{r=1}^{100} p(\omega_r)\Big(w(80y_{21}(\omega_r)^2 - 200y_{21}(\omega_r) + 300) + (1-w)(45y_{21}(\omega_r)^2 - 120y_{21}(\omega_r) + 450)\Big) + \frac{x_{22}^2 + 3x_{21}^2 - 7.4x_{21}}{2},$$

$$F_{22} = \sum_{r=1}^{100} p(\omega_r)\Big(w(30y_{22}(\omega_r)^2 - 110y_{22}(\omega_r) + 350) + (1-w)(54y_{22}(\omega_r)^2 - 168y_{22}(\omega_r) + 675)\Big) + \frac{2x_{22}^2 + x_{21}^2 - 6.2x_{22}}{2}.$$

I obtain the following average of the flows of the first and second stage over $r = 1, \ldots, 100$, respectively

$$\bar{x}_{11} = 13.69769, \qquad \bar{y}_{11} = 3.15,$$
$$\bar{x}_{12} = 13.59372, \qquad \bar{y}_{12} = 1.32,$$
$$\bar{x}_{21} = 12.85349, \qquad \bar{y}_{21} = 1.27,$$
$$\bar{x}_{22} = 16.96938, \qquad \bar{y}_{22} = 1.78.$$

As a consequence the value of profit functions F_{ij}, for $i = 1, 2$, $j = 1, 2$ and $\omega_1, \ldots, \omega_{100}$, are:

$$F_{11} = 43343, \qquad F_{12} = 62724,$$
$$F_{21} = 72244, \qquad F_{22} = 74621.$$

As expected, the values of the deterministic profit functions F_{ij}, for all i, j, are

greater than the respective values of the two-stage evacuation model without the Lagrange relaxation. This confirms the efficiency of the stochastic approach.

7.6 Conclusions

In this Chapter, I introduced a two-stage stochastic programming model for the emergency evacuation problem. I proposed a scenario-based evacuation planning model able to provide the optimal flows of evacuees from crisis areas to shelters, in order to minimize both the transportation cost and the transportation time, and under uncertainty on the evacuation demand and the link capacities.

I then proposed a variational inequality formulation of the model; in particular, I reduced my problem to a two-stage stochastic variational inequality, using the Lagrangian relaxation approach. I also discussed the qualitative properties of the two-stage stochastic variational inequality. In addition, I analyzed the role of Lagrange multipliers associated with the relaxed constraints. Finally, in order to show the applicability and effectiveness of my model, I provided a numerical example. Future research may include extending this framework to multistage stochastic models.

Chapter 8

A Game Theory Approach for Crowd Evacuation Modelling

8.1 Introduction

Throughout history, humans have been interested in natural disasters and the topic of evacuation, because optimizing the evacuation's strategies has vital importance in reducing the human and social harm, and saving the aid time. During evacuation, there are more than a few decisions which have to be made in a very short period of time, and in the most appropriate way. Significant research efforts have been made in the literature, (see [129]), to deal with evacuation optimization on the basis of deterministic optimization model, nevertheless the cooperative or non-cooperative behavior's aspects of real-world evacuation have not been taken into account comprehensively. In [93] the authors focused their ideas on the evacuation routes; whereas, in our work I focused on the minimum path and also on the behavior of the crowd. A suitable way to find optimum evacuation routes, during an emergency, is using Ant Colony Optimization (ACO) algorithms [232, 109, 113]. Indeed,

humans have faced complex optimization problems such as finding the shortest path between various points, evacuation simulations and optimization, allocating the optimum amount of resources, determining the optimum sequence of the processes in a production line, among others. Ant Colony Optimization algorithms are approximate techniques, belonging to the Swarm Intelligence methods, which imitate the cooperative behavior of real ants to solve optimization problems. Each artificial ant is inspired by the behavior of a real ant and can be seen as an agent of a multi-agent system. Real ants are eusocial insects and use collective behavior to achieve complex task, such as finding shortest paths between food sources and their nest. Using a simple communication mechanism like a chemical trail (pheromone), an ant colony is able to find the shortest path between two points. Initially, ant colony optimization algorithms have been applied to many combinatorial optimization problems, achieving good results in solving different problems, such as graph coloring [44], scheduling [236, 187] and assignment problems [31]. Nowadays, ACO algorithms have also been applied to problems belonging to the class of dynamic optimization problems, in which topology and costs can change during the execution of the algorithm. Routing in telecommunications networks is an example of such a problem [115]. Game theory has been widely used in the research of various scientific disciplines, from biological systems to economic and social networks [89].With the help of game theory, researchers can conduct extensive studies on the pedestrian and evacuation dynamics [68, 239]. However, game-theoretical models are focused on the study of the crowd's behavior in evacuation process. Indeed, in [238] the authors study a game-theoretical model to underline the relationship between cooperative and competitive agents in a crowd. Also, [181] discusses the basic principles of multiple robot cooperative

system using Game Theory and Ant Colony Algorithms. The aim of this research work is to study and analyse the collective behavior of a little social group that tries to escape from a disaster situation, such as earthquakes, volcanic eruptions, and/or hurricanes, trying to reach a safe location in the shortest possible time. Therefore, an ACO algorithm has been taken into account to study the behavior of different agents in strictly dynamic situations. Specifically, two different agents have been considered, which act differently: cooperative and non-cooperative agents. Ants colonies are recognized to be the best organized and cooperative social system, able to make their social community work at the best, and able to perform complex tasks, such as, for instance, discovering the shortest path between food and anthill, or defend the own anthill from attack by predators [171]. Moreover, any action of any ant, is related only to its local environment, local interactions with other ants, simple social rules, and in total absence of centralized decisions. These last features, that I find own in catastrophic situations, convinced us to consider ACO as the simulation model suitable for our study, because a sophisticated collective behavior based on local interactions, social rules, and in absence of centralized decisions, becomes crucial in reaching safe locations. Finally, the relationship between ACO and Game Theory aims to find a good solution in the case where agents with different ideas and strategies have to share a particular situation. As happens in an emergency scenario for the crowd, the same happens with a group of ants that tries to achieve the exit as safe as possible.

8.2 The Model

The Ant Colony Optimization algorithm is a well-known procedure that takes inspiration from the ants' behavior, when they look for a path between any food

source and their anthill. It has been observed that they can identify the shortest path, and communicate it to the others through chemical signals released along the path, called pheromones. In recent years, this behavior has been translated into mathematical and computer language and used to solve different kinds of optimization problems through different versions of the algorithm itself. Despite the different contexts where it has been applied, the mathematical description of the algorithm is quite the same for most of the problems. In particular, the ant's environment is considered as a graph $G = (N, L)$, where N is the set of nodes and L is the set of links. A generic ant k is supposed to be placed on a node i, and she must choose a destination node according to her behavior in real life; that is, preferring a path with some pheromone traces. However, this behavior is not deterministic so a proportional transition rule $p_{ij}^k(t)$ is defined as in Eq. (8.1). It states that an ant k, on a node i and at a time t will choose a destination node j with a probability that is proportional to the quantity of pheromone on the link connecting i with j, if the link j belongs to the set of possible displacements for k. The probability is 0 otherwise. In formulas, I have:

$$p_{ij}^k(t) = \begin{cases} \frac{\tau_{ij}(t)^\alpha \cdot \eta_{ij}^\beta}{\sum_{l \in J_i^k} \tau_{il}(t)^\alpha \cdot \eta_{il}^\beta} & \text{if } j \in J_i^k \\ 0 & \text{if } j \notin J_i^k. \end{cases} \tag{8.1}$$

As said previously, J_i^k is the set of possible movements of the ant k. Moreover, η_{ij} is the visibility of node j (defined as the inverse of the distance between two nodes), $\tau_{ij}(t)$ is the pheromone intensity on a path at a given iteration, while α and β are two parameters that determine the importance of pheromone intensity with respect to the visibility of a path. Once the ant k arrives at a destination node j, she updates the pheromone trace by releasing at a time t an amount of it proportional to the inverse of the length of the path $L^k(t)$ (eventually multiplied

by a Q-factor) if the link (i, j) belongs to the path $T^k(t)$ of the ant at time t. It is 0 otherwise. In this way, the greater the length of a path is, the less pheromone will be present on it. This feature is described by Eq. (8.2) in which $\Delta\tau_{ij}^k(t)$ represents the amount of pheromone deposited by the ant k.

$$\Delta\tau_{ij}^k(t) = \begin{cases} \frac{Q}{L^k(t)} & \text{if } (i,j) \in T^k(t) \\ 0 & \text{if } (i,j) \notin T^k(t). \end{cases} \tag{8.2}$$

Finally, a global updating rule $\tau_{ij}(t+1)$ is applied as in Eq. (8.3). It states that the intensity of pheromone will be updated considering the intensity $\tau_{ij}(t)$ of it at a previous step, and decreasing it with an evaporation factor ρ.

$$\tau_{ij}(t+1) = (1-\rho) \cdot \tau_{ij}(t) + \sum_{k=1}^{m} \Delta\tau_{ij}^k(t). \tag{8.3}$$

Now, starting from this procedure I have modified and extended ACO rules to fit them in my model. In particular, I have tried to mix concepts of game theory with concepts of optimization, to explore and highlight some novel features still not completely understood. To do this, I have imagined a generic risk situation like the one a group of ants is forced to live if it must solve a labyrinth. In other words, I assume that ants must find the exit of the labyrinth from a certain entrance as soon as possible to survive. I have modelled this escape situation like a game in which every ant can adopt two different strategies to exit from the labyrinth. I have chosen a labyrinth structure, since it generalizes and makes more interesting and challenging the optimization problem of finding the shortest path in a graph. I have realized this model using *NetLogo* [222], an agent-based model software that allowed us not only to build materially the structure of the labyrinth itself and implement the algorithm, but also to see what was happening during the simulation thanks to an opportune dedicate tab. I have built the labyrinth

modifying an existing model proposed in [209]. I have fixed the seed of the random numbers to regenerate, at each run, the same labyrinth. Then, I have created a network underneath the labyrinth and realized more complex labyrinths by strictly modifying the procedure proposed in [209]. This upgraded version can add other links between some nodes with at least two first neighbors and other nodes with at least two first neighbors, in order to prevent the loss of the dead ends. I have repeated this procedure for different kinds of labyrinths with different sets of nodes and links, and grouped them in order to increase complexity. Finally, I have selected for all of them one node on the left part of the labyrinth to be the entrance, and one node on the right part to be the exit. I underline that the entrance and the exit are chosen on the left and on the right, respectively, to give an example to focus on a sample of the labyrinth. In order to generalize the problem, I can put the exit wherever I want or I can rotate the labyrinth, as suitably as I need. Then, I have created two different kinds of ants that act differently, and each of them follow a different strategy to escape from the labyrinth. In particular, I have imagined what would happen if some ants acted cooperatively, while other ants acted non cooperatively. Thus, at first I initialize the set of the whole colony and then, by means of a cooperation parameter f, I establish the fraction of ants who will act cooperatively. It follows that the remaining fraction $(1 - f)$ of ants will act non cooperatively. In detail, I set the two strategies, that cannot be changed once the fraction of cooperative ants is defined, as follows:

- Non-Cooperative: they block a random node of their path. In Fig. 8.1, non-cooperative ants are colored in blue, while a blocked node is represented as a fire.

- Cooperative: if they find a damaged node close to their path, they repair it.

In Fig. 8.1, cooperative ants are colored in red.

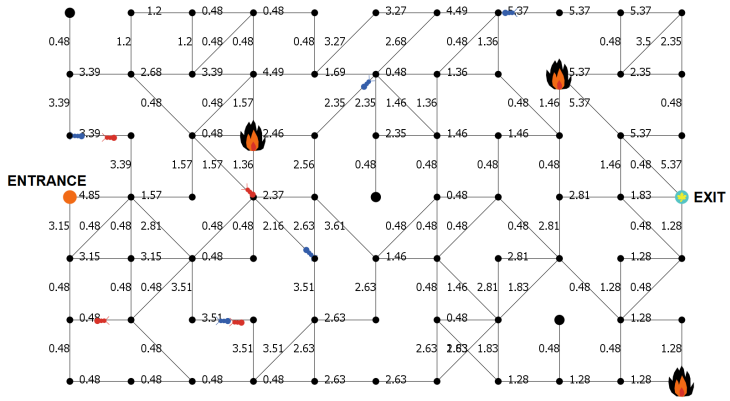

Figure 8.1: In this model the entrance is fixed (always on the left part of the labyrinth), whilst the exit changes, in any position of the labyrinth, in according to the number of prizes on it. Bigger black nodes represent end nodes, i.e. dead ends roads; fires indicate the damaged nodes by the non-cooperative ants; and the black labels on the edges indicate the intensity of pheromone on that route. With red are showed the cooperative ants, and in blue the non-cooperative ones.

Both of them become safe if and only they arrive at the exit. Every kind of ant is ”equipped” with the same transition rule. In other words, each ant chooses the next target node according to the same rule, even if it belongs to different families and acts differently. In particular, the transition rule in (8.4) defines the probability $p_{ij}^{k}(t)$ of an ant to go from a starting node i to a destination node j as follows: during the first iteration, the ants explore randomly the labyrinth. They choose to visit a link according to the intensity of pheromone on it that, in the first iteration, is equal to 1 for all the links of the labyrinth.

The first ant of each kind that arrives at the exit releases a trace of pheromone $\Delta\tau_{ij}$ along every link of her path. For simplicity, in my model, the intensity of pheromone released by each ant on every link of her path is $\Delta\tau_{ij} = 1.5$. After that,

the other ants of the same kind die, the global updating rule (8.5) is applied and a new generation is launched. In formulas, I define the transition rule as:

$$p_{ij}^{k}(t) = \begin{cases} \frac{\tau_{ij}(t)}{\sum_{l \in J_i^k} \tau_{il}(t)} & \text{if } j \in J_i^k \\ 0 & \text{otherwise,} \end{cases} \tag{8.4}$$

with τ_{ij} intensity of pheromone on the link (i, j) and J_i^k is the set of allowed links. Finally, the global updating rule is defined as:

$$\tau_{ij}(t+1) = (1-\alpha) \cdot \tau_{ij}(t) + \Delta\tau_{ij}, \tag{8.5}$$

where α is the evaporation rate, τ_{ij} is the pheromone intensity on the link (i, j) at the previous step and $\Delta\tau_{ij}$ is the amount of deposited pheromone by the winning ant, at each turn, on the same link. In this model, I have also imposed that, once the quantity of pheromone falls below a certain threshold, it remains fixed and does not decrease further. This choice is to prevent the stagnation of the algorithm around a local optimum. Thus, within this situation, I want to analyze how two different strategies evolve in time during a critical situation, namely, in finding the shortest path from the entrance to the exit in the shortest possible time. In the next section, I will discuss about some game theory definitions used in the model. I decide not to consider the gain of a single link, but the aim of one ant is to reach the exit as soon as possible. In fact, the exit, or in my case the shelter, has a capacity that in the algorithm is represented by a prize in the exit. If there are no more prizes on the exit, i.e. capacity in the shelter, the exit will move (with the same budget of prizes) to another edge node of the graph, except the ones on the left part of the labyrinth. I am ruling out the possibility that the exit and the entrance are on the same side of the graph. It is a dynamic case in which not only the ants must be able to find the exit from the maze through the shortest path, but

from time to time, they must also have the ability to organize themselves for a new objective that gives the opportunity to collect prizes.

8.2.1 Evacuees' game

Game theory allows one to define how much an agent can gain from its actions and decisions. Indeed, agents are defined to be rational and intelligent and try to reach the highest value of the profit function. In game theory, the profit function models reality so as to give a value to the emotional or economic gain to the agent who adopts a certain strategy. A strategy space for a player is the set of all possible strategies of a player; whereas, a strategy is a complete plan of action for every stage of the game. Formally, I define a payoff function for a player as a map from the cross-product of players' strategy spaces to reals, i.e. the payoff function of a player takes as its input a strategy profile and yields a representation of payoff as its output.

In this model, I consider an N-players game ($N \geq 2$). The evacuees represent the players of the game, who have to reach a safe area. I suppose that evacuees can choose either to cooperate (C) or not to cooperate (NC), when attempting to arrive a desired safe area after or during a disaster. Each player starts from the same node and tries to reach an exit using the minimum path. A little group of evacuees tries to arrive in a safe area, which has a capacity K, but only one member of the group can reach that place. When the shelter is full or is not enough safe, I consider a new shelter, placed in another node of the graph, which the evacuees have to reach. Let $G = (V, L)$ be the graph associated with the game, where V is the set of vertices and L the set of links. The payoff of the player that finally reaches the safe area depends on a parameter, the pheromone τ_{ij} on the edge (i, j) used in the

Ant Colony Algorithm. According to the strategies I define two different payoff functions, which depend on the strategy that an agent chooses. As a consequence, I define the payoff function of an agent k, who chooses the cooperative strategy a_k^C:

$$u_k(a_k^C, a_{-k}) = \frac{f \cdot \sum_{i,j} \tau_{ij}}{n}, \quad 0 < f \leq 1. \tag{8.6}$$

I define the payoff function of an agent k, who chooses the non-cooperative strategy a_k^{NC}:

$$u_k(a_k^{NC}, a_{-k}) = \frac{(1-f) \cdot \sum_{i,j} \tau_{ij}}{n}, \quad 0 \leq f < 1. \tag{8.7}$$

I denote f as the percentage of cooperative players and n as the number of evacuees of a group. I consider $\sum_{i,j} \tau_{ij}$ as the sum of the pheromone on the links of the agent path. I underline that a_k is a generic strategy, that an agent k can choose from (C) or (NC) and I denote a_{-k} the strategies of all agents, except k.
I group for all k, the cooperative (C) and the non-cooperative ants (NC) respectively, as:

$$u^C = f \cdot \sum_{i,j} \tau_{ij}, \quad 0 < f \leq 1; \qquad u^{NC} = (1-f) \cdot \sum_{i,j} \tau_{ij}, \quad 0 \leq f < 1.$$

Finally, I denote the profit function of the game as the sum of the payoff of all cooperative ants plus the payoff of all non-cooperative ants, i.e. $U = u^C + u^{NC}$.

8.3 Experiments and Results

In my simulations, I use ant shape agents according to the implemented algorithm, but this is just a graphic feature that doesn't affect the correctness of the procedure. It follows that a generation of ants represents a group of people who try to arrive at a shelter or a safe area. At the end of each generation, only one ant of each

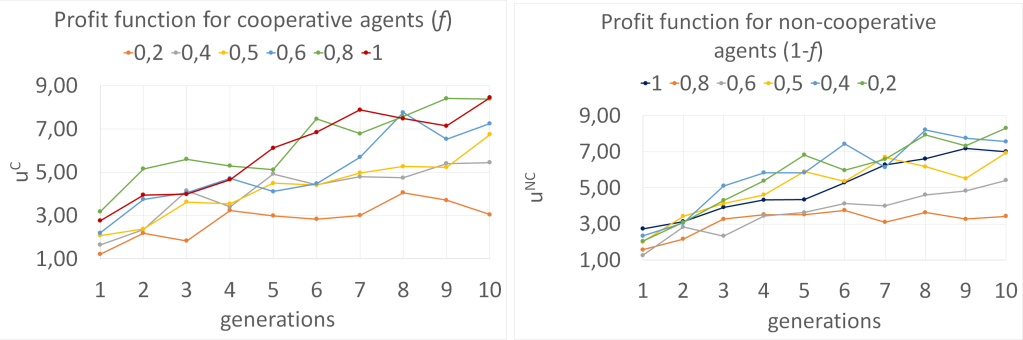

(a) (b)

Figure 8.2: Comparison of the average profit obtained by cooperative agents (plot (a)), compared to obtained one by non-cooperatives (plot (b)).

kind survives. After several preliminary experiments, I choose a set of $n = 10$ agents and perform 10 different simulations for different values of f, starting from $f = 0$ to $f = 1$ and increasing f at a regular interval of 0.20. For my purposes, I consider the trend of ten generations. Figure 8.2 shows the trend of the average profit function over 10 simulations at different values of f (and correspondingly $(1 - f)$). In each plot, the x-axis indicates the generations number, while in the y-axis are displayed the average profits obtained, respectively, by the cooperative agents (Fig. 8.2a) and by the non-cooperative ones (Fig. 8.2b). In particular, the figure represents the comparison of the values of the profit function for each evacuee referred to the percentage of cooperative agents (f). I notice that when the number of cooperative agents increases, the value of profit function increases too, following a linear trend. Furthermore, for $f = 0.8$ and $f = 1.0$, after a few generations, the average profit function grows similarly, reaching the same value after 10 generations. This suggests that a non-cooperative behavior of a few agents can increase the profit of the other ones. In the same way, the plot in Fig. 8.2b

shows that a non-cooperative strategy is good if and only if a lot of agents choose that particular strategy. Also, in this case, the average profit function reaches the best values for $f = 0.2$ and $f = 0.4$, leading to the same evaluation of the previous case.

In Fig. 8.3 I can see the average profit function comparison for $f = 0.2$ and $f = 0.8$, both for cooperative evacuees and non-cooperative evacuees. In Fig. 8.3a, I find the value of f for which are present 2 cooperative evacuees and 8 non-cooperative evacuees, and in Fig. 8.3e the symmetric situation. The same distinction is present also in Fig. 8.3 for $f = 0.4$ in Fig. 8.3b, and $f = 0.6$ in Fig. 8.3d, but with 4 and 6 different kinds of evacuees in two symmetric situations. For these plots, the average profit function is higher for the larger groups (non-cooperative for $f < 0.5$ and cooperative for $f > 0.5$). This can be explained because these plots are calculated for a percentage of cooperation less than $f = 0.5$. In fact, at $f = 0.5$ something special happens. In Fig. 8.3c the trend of the average profit function for cooperative evacuees starts to be lower than the one for the non-cooperative evacuees, but as the generations increase, the two functions tend to reach the same value.

The *Chicken Game* supports my considerations. Indeed, the main feature of this game is that players try to avoid appearing as a ”chicken”. So each player taunts the others to increase the risk of shame in giving up. However, when a player surrenders, the conflict is avoided and the game is mostly over. Furthermore, the fact that the profit function is the same when half of the population is cooperative and the other is not, leads to compare the *Chicken Game* with the particular case $f = 0.5$. In fact, the balance of the game is obtained when one player chooses strategy (C) and the other the strategy (NC), that is the opposite strategy. In this

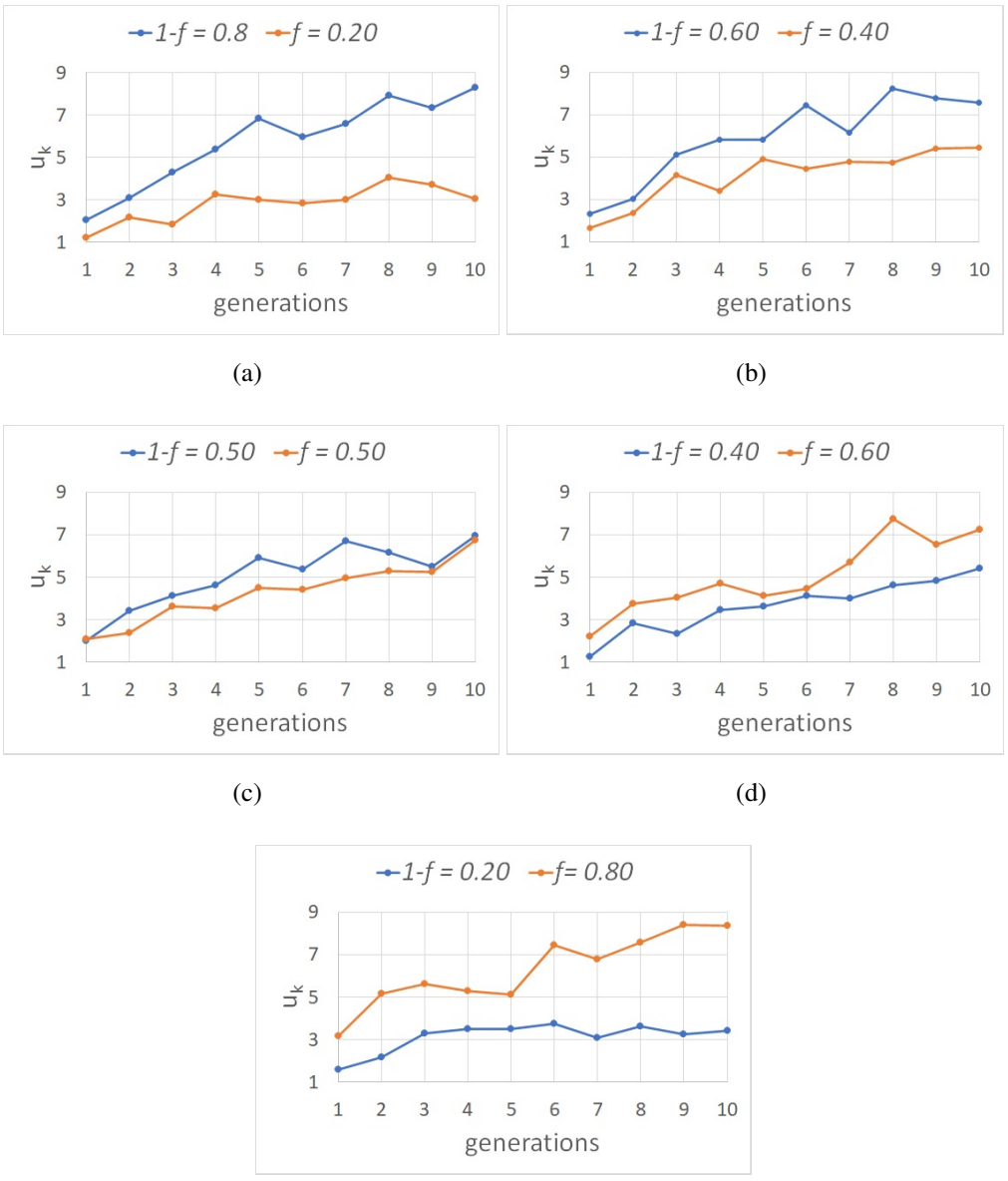

(a) (b)

(c) (d)

(e)

Figure 8.3: Average profit function comparison obtained by the cooperative and non-cooperative agents, at different values of f and $(1 - f)$.

situation, no player is considered a ”chicken” until the moment when the value of f decreases, and hence the competitive strategy takes advantage. I observe,

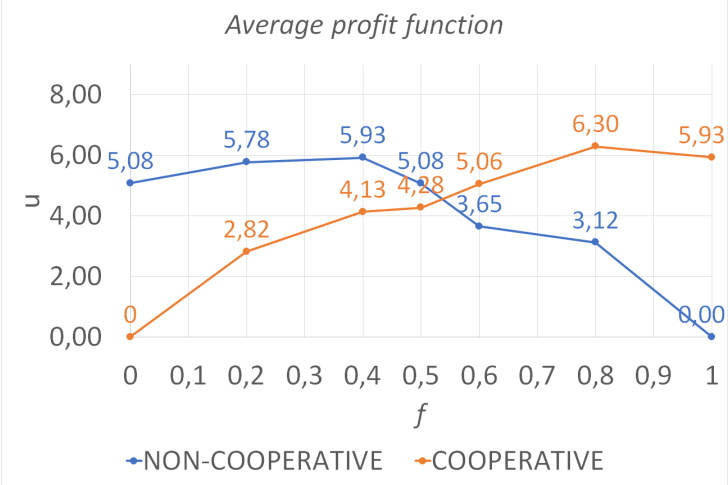

Figure 8.4: Average profit function comparison over 10 simulations and over 10 generations for cooperative and non-cooperative evacuees.

however, that the game of chicken is considered as a social dilemma [144].

To better investigate the meaning of these data, I calculate the average values of the profit function over 10 simulations for each group of evacuees and for each value of f. Fig. 8.4 shows what I have obtained. As I can see, as the percentage of f increases, the average value of the profit function has two different trends. The one for cooperative evacuees increases as f increases. The one for non-cooperative evacuees decreases. In particular, the average value of the profit function for $f \geq 0.50$ is higher than the ones for $f \leq 0.50$. This means that the average values calculated for two opposite and symmetric configurations are not the same. In fact, the two curves are not symmetrical because they are the outcome of different dynamic scenarios, where the two kinds of agents (cooperative and non-cooperative) act differently. Of course, these effects are strongly affected by the number of the former compared to the latter, and in particular, higher values of the profit function (u) are strictly related to higher values of the parameter f. This,

in general, is not a surprising result since is quite common that cooperation means, in most cases, better performances. It is important to say that in game theory there are several examples in which players can choose whether to adopt a more or less cooperative strategy. Let's consider the classic game of hawks and doves as an example. These sample-animals represent couples of the same type of animals and same population that fly on a prey. Each animal can choose to behave like a hawk or a dove: hawk (strategy H) or dove (strategy D) behavior indicates aggressive or peaceful behavior, respectively. In this example, if the players choose the same strategy then they divide the loot, otherwise, if they both choose the same strategy, one will get the maximum profit the other the minimum profit. From this example I can see how in situations where there is total collaboration, a greater profit is obtained than in a situation in which only one can obtain a good profit. However, in this context, I imagine that better performances can be linked or explained with one evacuee's willing to improve its profit. It is presumable that in real-life escape situations people tend to act in the same way that is, trying to improve their profit function. Therefore, my results suggest that to do this they should prefer a cooperative strategy.

8.4 Conclusions

In this chapter, I analyse the affinity between the behavior of ants and people in a particular situation. Indeed, in an emergency situation, a crowd seems to move in a messy way but inside the crowd there are little groups that try to decide their behavior inside that group. As a consequence, I investigate the cooperative or non-cooperative agents' choice inside each single group. This original approach consists of correlation between ants and people, that give us the possibility to

underline some interesting factors, as the importance of using the sum of the pheromone into the profit function. The payoff's values, for each agent, lead to significant observations regarding the cooperative and competitive behaviors of the agents, in a difficult situation, where an evacuee has to decide as fast as he can. Furthermore, the idea to insert the percentage of cooperative agents in the profit function represents another innovative aspect that allows us to better understand both the behavior of the agents and the profit they may have as I explain in Section 8.3. In fact, for the first time is used a game theory approach to an evacuation model using an ACO algorithm, to find the solution of the profit function of the game. The quality and safety of the chosen path is directly proportional to the sum of the pheromone along this path. This leads to a profit function that reflects the safety and efficiency of the path chosen by the evacuees. Moreover, during the comparison over 10 simulations and over 10 generations for cooperative and non-cooperative evacuees, I notice that if a lot of evacuees choose cooperative strategies, then the value of the function is higher than the same number of evacuees can gain playing a competitive strategy. The results presented in this work are just a small part of a bigger study that is still under work. Further studies and simulations have to be made. Especially because this model considers just one winner at each run, which is not a desirable situation in real life.

Chapter 9

An agent-based model to evaluate strategies in a crowd evacuation

9.1 Introduction

Modeling and understanding crowds' behaviour has become one of the most engaging and challenging topics of the last decades in different disciplines ,such as establishing evacuation plans after an emergency [141, 180, 235], optimal architectural design [206, 205, 200], or even for entertainment purposes [230, 118]. All these fields are based on one key point: the comprehension of human behaviour. It is well known that how people act and react to different situations may positively or negatively affect the overall outcome, especially in emergencies and evacuations, where understanding the human behaviour becomes a primary issue to optimize evacuation plans [207]. However, the common problem encountered in these studies is the lack of human and social behavioural data [175]. For this reason, modeling and studying human behaviour is became one of the main purposes for many research areas [207]. Indeed, different models o crowd behaviour

exist nowadays, each of which however focuses on different aspects of the problem depending on the framework used. Evacuation models can be classified into three main categories: (1) *macroscopic models* [67, 90, 114, 111], which consider the crowd's dynamics as a flow; (2) *microscopic models* [139, 151, 110], which consider individual behaviour; and (3) *hybrid models* [19, 37, 103], which are a combination of both. Macroscopic models are mostly used to evaluate evacuation flow but can not describe emergent crowd behaviour. Microscopic models, on the other hand, are used to investigate how small changes in the individual's characteristics affect the whole behaviour but are inefficient in large scenarios due to their computational cost. The main advantage in using hybrid models is that by combining macroscopic and microscopic methods, or even methods from different areas, one can exploit the best aspects of both or different approaches. Following the guidelines proposed in [207], in this paper an agent-based model is presented to evaluate whether and how different agent behaviours affect the collective behavior of the whole group in a crowd simulation. In particular, a hybrid model has been developed in which agent-based models, which are one of the most powerful techniques to model individual-decision making and social behaviour, are combined to the features and dynamics of swarm intelligence methods. It consists of a set of agents that must reach a specific location, named *exit*, starting from a chosen point, adopting two different behavioral strategies: (i) the collaborative one, that is share information about the paths and/or repair destroyed paths; and (ii) defector that, on the other hand, doesn't share any information, can destroy some paths and/or nodes, but in any case exploits the help of the collaborative agents. Regardless of their behavior, the goal of each agent is to reach the exit point. In this context, swarm intelligence algorithms, are useful not only for optimization purposes [125]

but also to model the dynamics of the crowd [116, 241, 219, 47], since they are capable to show the collective behaviours of the system under investigation. In the presented model, the Ant Colony Optimization (ACO) algorithm's principles and dynamics are considered to simulate the agents' behaviour and the environment setup. In particular, the agents are equipped with movement and decision rules that take inspiration from the ones used in ACO. The aim is to understand whether and how their behaviours, collaboratives and defectors, affect the whole behaviour of the crowd. The investigation has been conducted by comparing simultaneously three evaluation metrics: (i) number of agents that have reached the exit; (ii) exit times, and (iii) cost of the paths to reach the exit. Using these metrics, the best expected performances are, therefore, the ones for which the number of outgoing agents is the highest possible, while the exit time and the path cost are the lowest possible.

9.2 The mathematical model

The idea of taking inspiration from the Ant Colony Optimization algorithm (ACO) to model the agents' behaviour comes from the observation that people in a crowd and ants seem to share some characteristics. Both of them, indeed, seem to behave following unwritten social rules. For instance, ants are able to find the shortest route from their anthill to a source of food and share it with the rest of the colony using some chemical signs called pheromones. This kind of communication is undirected because ants do not really communicate with each other but release their pheromones along their path, and these pheromones act as roads to follow for the rest of the colony. The colony is able to find the best route thanks to this kind of communication and the finding itself is an example of emergent behaviour that

is something indescribable if looking at the colony as a sum of single elements, the ants. On the other hand in some contexts, for instance, in exiting and evacuation processes, people manifest the same local interactions, like ants do, since they take decisions following what their neighbours do, and they do it in absence of centralized decisions. Think for instance about how many times in a social context people find the exit of a place just by following the crowd. There is no one that guides the crowd and the success of the process depends on how people are able to share information, directly by communicating with each other or indirectly by seeing what others do. In our model, the agents' behaviours take inspiration from the ones of the ants. The agents may be able to find promising routes in an unknown environment by communicating with each other in an indirect way. In addition, they may adopt an alternative behaviour of not sharing information about the path and destroying a part of it. The environment in which the agents move is represented as a weighted undirected graph $G = (V, E, w)$, where V is the set of vertices, $E \subseteq V \times V$ is the set of edges and $w : V \times V \to \mathbb{R}^+$ is a *weighted* function that assigns to each edge of the graph a positive cost. The *weighted* function highlights how hard is crossing a edge. Let define $A_i = \{j \in V : (i, j) \in E\}$ as the set of vertices adjacent to vertex i and $\pi^k(t) = (\pi_1, \pi_2, \ldots, \pi_t)$ as a non-empty sequence of vertices, with repetitions, visited by an agent k at the timestep t, where $(\pi_i, \pi_{i+1}) \in E$ for $i = 1, \ldots, t-1$. Starting from a prefixed point, a population of N agents explore the environment trying to reach a destination point as quick as possible, through a path that has a lower cost. This population of agents is divided in Γ groups, each of which begins its exploration at regular intervals. For instance, it can be considered a simplified version of a delayed evacuation strategy, as the authors in [207] mention in their survey. Indeed, it is supposed

that in some contexts, people do not evacuate all at the same time but organize themselves to evacuate in the ordered possible manner, for instance, in schools, public offices, and especially in recent pandemic plans to avoid Covid-19 diffusion. I have modeled this situation by establishing that each group starts its tour after a fixed time. At a specific time t, an agent k placed on a vertex i chooses as destination one of its neighbour vertices j, with a probability $p_{ij}^k(t)$ defined as the proportional transition rule defined in [69]:

$$p_{ij}^k(t) = \begin{cases} \frac{\tau_{ij}(t)^\alpha \cdot \eta_{ij}(t)^\beta}{\sum_{l \in J_i^k} \tau_{il}(t)^\alpha \cdot \eta_{il}(t)^\beta} & \text{if } j \in J_i^k \\ 0 & \text{otherwise,} \end{cases} \tag{9.1}$$

where $J_i^k = A_i \setminus \{\pi_{t-1}^k\}$ are all the possible displacements of the agent k from vertex i, $\tau_{ij}(t)$ is the trace intensity on the edge (i, j) and $\eta_{ij}(t)$ is the desirability of the edge (i, j) at a given time t, while α and β are two parameters that determine the importance of trace intensity with respect to the desirability of an edge. The trace intensity τ_{ij} on the edge (i, j) is a data that manifest how many times an edge is crossed by the agents and can help new agents to make a decision based on the actions of other agents. It is the equivalent of the pheromone in ACO algorithm. This value is a passive information, because the agents leave it unintentionally and after each movement the trace $\tau_{ij}(t)$ is increased by a constant quantity K, that is:

$$\tau_{ij}(t+1) = \tau_{ij}(t) + K, \tag{9.2}$$

where K is a user-defined parameter. Equation 9.2 is the equivalent of the reinforcement rule of the ACO algorithm. This rule is so called because at each step, the amount of pheromone on a path (i, j) is augmented by the ants of a quantity that may be constant or not. In other words, every agent leave a constant trace after

crossing an edge (i, j). On the other hand, every T ticks[1] the amount of trace on the edges decays according to the global updating rule, which is also in this case the same present in ACO procedure. In ACO algorithm, the global updating rule states that the amount of pheromone present in the environment is not fixed but it decays in time:

$$\tau_{ij}(t+1) = (1-\rho)\tau_{ij}(t), \tag{9.3}$$

where ρ is the evaporation decay parameter.

The desirability $\eta_{ij}(t)$ in Equation 10.1, at a given time t, establish how much an edge (i, j) is promising. This information is not known a priory and it is released intentionally by an agent on a vertex after crossing an edge. In particular, $\eta_{ij}(t)$ is related to the discovered information by the agent k after crossing the edge (j, i). Its value depends on the inverse of the weight of the edge (i, j), that is:

$$\eta_{ij}(t) = 1/w(i, j). \tag{9.4}$$

It is important to note that the desirability is asymmetric because this information is present on the vertices, that is $\eta_{ij}(t) \leq \eta_{ji}(t)$ at a given time t. Lower the cost to cross an edge is, greater the desirability and the probability to follow a promising path is; vice versa, higher is the cost to cross an edge, lower is the desirability.

The agents are divided in two categories, each with its specific behaviour:

- **collaborators** C: they *leave* an information $\eta_{ij}(t)$ after crossing an edge (j, i) to help other agents during the escape and may *repair* a destroyed edge and/or a destroyed vertex before performing his movement, with a probability P_e^C and P_v^C respectively.

[1]The time unit used that corresponds to a single movement of all agents.

- **defectors** D: they *not leave* any information after crossing an edge and may *destroy* an edge and/or a vertex after performing his movement, with probability P_e^D and P_v^D respectively. A node or an edge destroyed is one no more traversable by other agents.

In other words, collaborators mainly perform actions that somehow help all the other agents to reach the rescue point as quick as possible. I can assume that they cross an edge or vertex in a cautious way, taking care not only to not destroy it, but also engaging themselves to repairing it if destroyed by a defector. Moreover, they leave an information $\eta_{ij}(t)$ about how hard is to cross a particular edge, so that the other agents can exploit in their own strategies. This increases the possibility to discover a more promising path toward the rescue point. To focus on a real situation, one can imagine leaving information to the other agent as, for example, a written message, a color mark or a simple indication. On the other hand, the defectors mainly act in a hasty way, carrying out actions that can destroy the surrounding environment. Indeed, after crossing a node or an edge, and with a certain probability, they may destroy it decreasing the possibility of the other agents exploring the environment. This action may influence not only the cooperatives but also themselves especially if the destroyed path is an important one that is crucial to reach the location. The defectors' behaviour can be seen as a consequence of a stress and panic situation in which the agents like real people, due to this, are unable to be aware of their actions. They only try to find a good path by following the others and not informing the rest of the group about what they have found.

To evaluate how these two different behaviour strategies influence the performance of all agents, the model takes into account as comparison metrics (i) the path

Variable	*Description*
$w(i, j)$	weight of an edge
$p_{ij}^{k}(t)$	transition probability of the agents
$\tau_{ij}(t)$	trace intensity on the edge
$\eta_{ij}(t)$	desirability of an edge
$P_{e,v}$	destruction/repair probability of a node and/or edge

Table 9.1: Table of the variables and constants used.

cost, (ii) the exit time, and (iii) the number of agents that successfully reach the destination point. These three quantities have been considered together because the action of destroying/repair of nodes and/or edges makes the environment a dynamic environment. To clarify: once a simulation is launched, and if the population of agents is mixed with both kinds of agents, it may happen that one or more defectors cross an edge and/or a node and destroy it. Within the same simulation, it may also happen that one or more collaborator, approach the same nodes and/or edges destroyed by the defectors and may decide to repair them. Since a destroyed node and/or edge is no more traversable, it follows that these two actions change, from time to time, the structure of the environment, making the scenario dynamic. For this reason, considering just one of the three evaluation metrics mentioned above would have been incorrect because a promising path may not be the best in terms of cost, or just in terms of the success rate of the agents, or just in terms of exit time. A good path is one that minimizes its cost and exit time and, at the same time, maximizes the number of agents exiting that path.

Mathematically, the cost of a generic path $\pi(t) = (\pi_1, \pi_2, \ldots, \pi_t)$ is calculated as:

$$\sum_{i=1}^{t-1} w(\pi_i, \pi_{i+1}), \tag{9.5}$$

where π_1 and π_t are the starting and destination points, respectively. Since every tick all agents in the environment perform a single movement (from one vertex to another one), the exit time is calculated as the number of moves that an agent makes in its exploration and corresponds to the length of the path $\pi(t)$. All variables of interest are listed in Table 9.1.

9.3 NetLogo Model

The results are obtained using **NetLogo** [222], a multi-agent programmable modeling environment. As said in Section 9.2, the environments have been modelled as graphs with a topology similar to grid graphs, where each node can be connected with its 8-neighbours. The connectivity of a node with its neighbours is controlled by two parameters: $0 \leq p_1 \leq 1$, that represents the probability to create horizontal and vertical edges, and $0 \leq p_2 \leq 1$, that represents the probability to create oblique edges. The weight of each edge is a real value assigned with a uniform distribution in the range $[1, 100]$. Two different scenarios have been considered for the experiments:

- scenario **A** with $|V| = 100$ and $|E| = 213$, generated with $p_1 = 0.6$, $p_2 = 0.2$;
- scenario **B** with $|V| = 225$ and $|E| = 348$, generated with $p_1 = 0.6$, $p_2 = 0.0$.

They are both represented in Fig. 9.1.

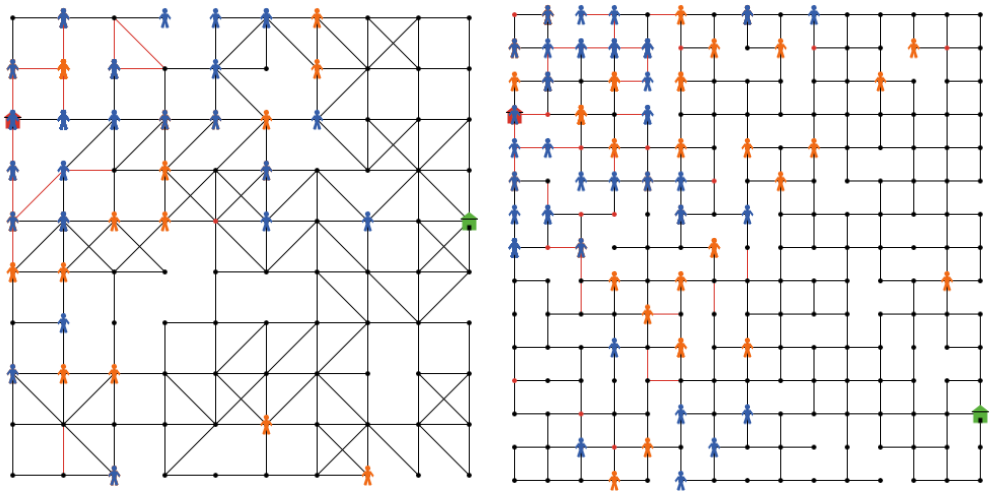

(a) (b)

Figure 9.1: Examples of networks used for the simulations in scenario **A** (Fig. 9.1a) and in scenario **B** (Fig. 9.1b). The starting point is represented by the house-shaped red node on the left of the network, while the exit point is the house-shaped green node on the right. Red nodes and edges represent the destroyed nodes by the defectors. The defectors themselves are represented by human-shaped blue agents, while the collaborators are of the same shape but in orange.

9.4 Experimental Results

As the first step of this investigation, in both scenarios, have been considered $N = 1000$ agents divided into $\Gamma = 10$ groups. These values was chosen since 1000 agents represent a common number of people involved in a crowd, and 10 groups to better distribute the agents during the simulations. Depending on the value of the parameter $f \in [0, 1]$, user-defined and named *collaborative factor*, in each group there will be f collaborative agents, and $(1 - f)$ defectors. Therefore, in each group may be present both, or just one type of agent. In particular, if

$f = 0.0$ groups with only defectors are considered; if $f = 0.5$ (for instance) each group is formed by half collaborative and half defectors; while for $f = 1.0$ only collaborative groups are generated.

Each group begins its exploration at different times, and precisely after a given time T_e from the group that precedes it, excepts the first group that obviously starts at the time 0. In general, then, the i-th group will begin its exploration at the time $(T_e \times (i - 1))$. Note that the value to assign to T_e is related to the vertices number of the scenario considered ($T_e = |V|$). Therefore at every T_e ticks, a new group starts its journey, having however a maximum time within which the agents must reach the exit. Let T_{max} the overall maximum time allowed to reach the exit, given by:

$$T_{max} = 2 \times \Gamma \times T_e, \tag{9.6}$$

where Γ is the number of the groups, and 2 is a fixed parameter. It follows therefore that the time window within which each agent must reach the exit is from the begins of its exploration to the overall maximum time T_{max}, that is:

$$T_{max} - (T_e \times (i - 1)), \tag{9.7}$$

where i is the agent belonging group.

Analysing the Equations 9.6 and 9.7 one can note that the first groups have more time to explore the environment compared to the others. This is due because the groups begin their exploration even if in the environment are still present agents belonging to the previous groups. This means also that agents belonging to the same group can exit at different times (always within their time window) and those belonging to the first groups benefit more time to find the exit. It is important to highlight that the trace left by the collaborators along their path degrades over time with a evaporation interval fixed at $T_d = 50$. This means, then,

that to every T_d ticks the global updating rule defined in Equation 9.3 is applied with evaporation rate $\rho = 0.10$. Note that initially the trace on all edges is set to $\tau_{ij}(0) = 1.0$. Moreover, the parameters that regulate the importance of the trace and desirability in Equation 10.1, i.e. α and β, are both set to 1.0. The destruction-repair probabilities on a vertex and an edge are $P_e^C = P_e^D = 0.02$ and $P_v^C = P_v^D = 0.02$, respectively and they are the same for both kinds of agents.

Finally, to evaluate the effects of the two behaviours, collaboratives and defectors, I have carried out experiments varying the collaborative factor f, that is the percentage of collaborators among the population of agents. For each value of f, from 0.0 to 1.0 with step of 0.1, I have performed 100 independent simulations. The exit time (Fig. 9.2) and path cost (Fig. 9.3) plots, have been normalized with respect to the group success rate, that is the percentage of agents in a group, which successfully reach the exit point. Lower these values are, the better performances of the agents are. In both scenarios, the exit time decreases, so gets better, with respect to the collaborative factor, indicating that the more collaborative the agents are, faster their exit will be. This seems true except for $f = 1.0$, i.e. when all agents are collaboratives, where the performances of each group are worst than the previous values of f. The groups are indicated by different colored lines and it also seems that the exit time decreases with respect to the group number, indicating that the groups that evacuate later, even if they have less allowed time, in some way, exploit the information left by those who have previously evacuated. In fact, looking for instance at group 1, in both scenarios, one can see how it has worse performances for low values of f, and better performances for high values of f. It means that the agents of this group are able to exploit better the information about the path especially when the crowd is composed mainly of collaborative agents.

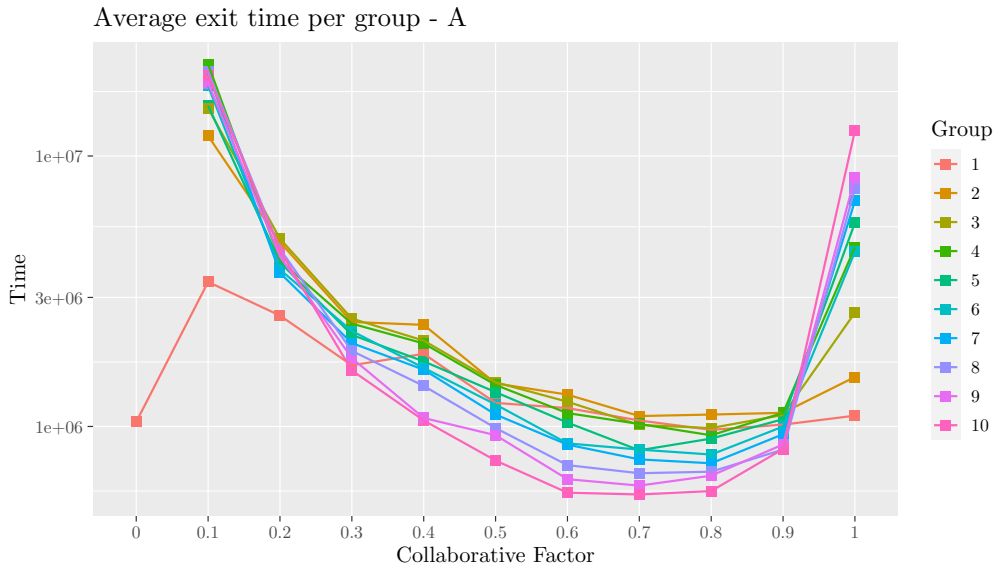

(a)

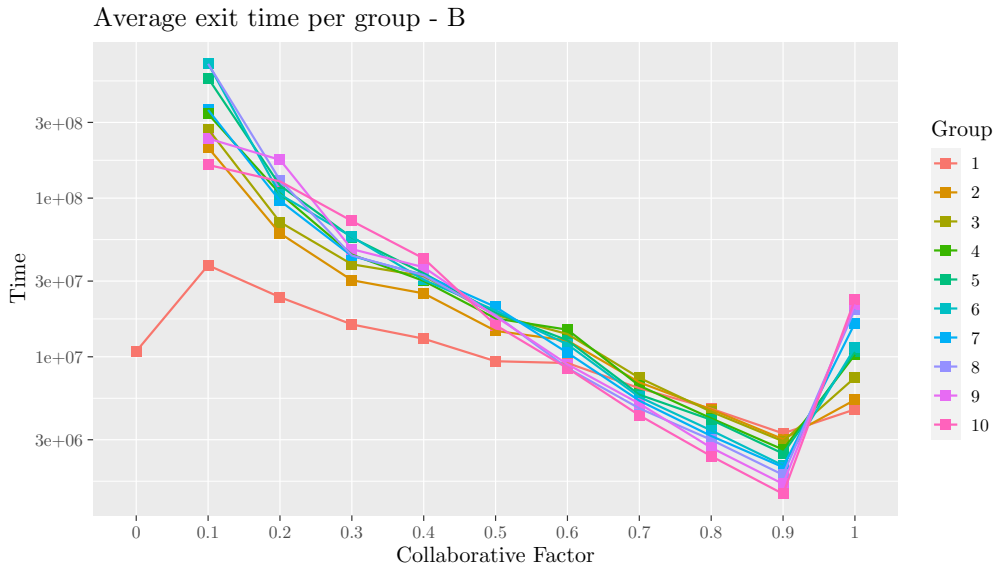

(b)

Figure 9.2: The exit time for (a) scenario **A** and (b) scenario **B**.

Do not be confused by the fact that the same group has good performance even for the lowest value of the collaborative factor f, because for that value, as it will

be shown later, few agents find the exit from the environment and so, considering both metrics (the exit time and the number of agents exited) it can be concluded that it is not a significant result. On the other hand, by looking at group 10, in both scenarios, its performances improve with f, except for $f = 1.0$. This indicates that the last group can exploit better the information about the path when the crowd is composed mainly, but not totally, of collaborative agents. Same conclusions can be done for the path cost in Fig. 9.3, that decreases with respect to the collaborative factor and the group number. This is true for every value of f except for $f = 1.0$. This indicates, as above, that the more collaborative the agents are, the better path they will find, but if the collaboration is absolute, it seems to not work.

The heat maps in Figs. 9.4a and 9.5a represent the number of agents that reached the exit and they are normalized with respect to the exit time available for each group. They represent how many agents have been evacuated in one unit of time (that is how many agents have been evacuated at each tick). The higher this value is, the better the performances of the agents are. It is present the same trend, but opposite in value, observed for the exit time and the path cost: it seems that the number of exited agents increases with the collaborative factor except, also in this case, for $f = 1.0$, value for which few agents reach the exit. The performances of the agents are better not when all of them are collaborative but, oddly, when some of them act in a different way as defectors. The same quantity seems to increase with respect to the group number, indicating that the last groups benefit from the first ones, especially in scenario **A**.

Figs. 9.4b and 9.5b represent the total number of exited agents for the **A** scenario and for the **B** scenario. Even without considering the group number, one can come to the same conclusions as above: the number of agents, that reaches the

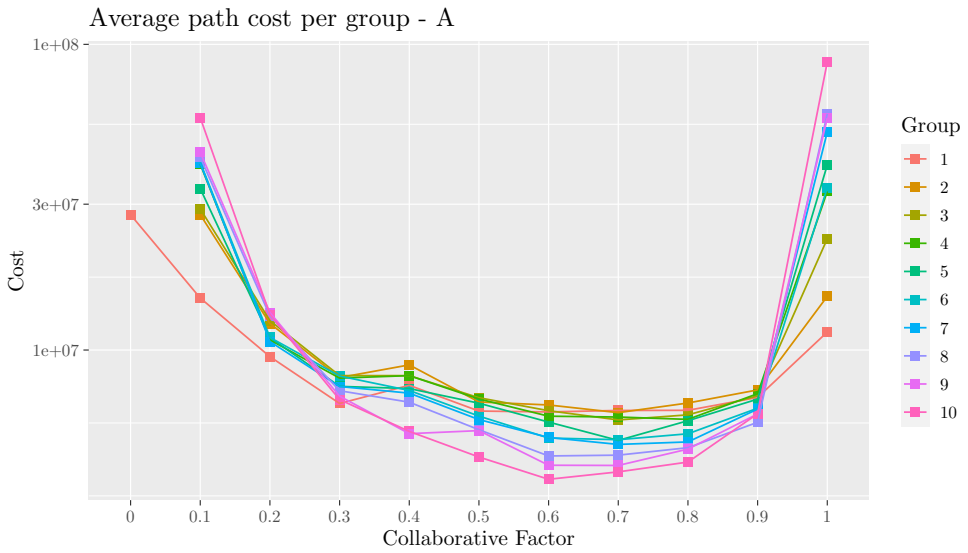

(a)

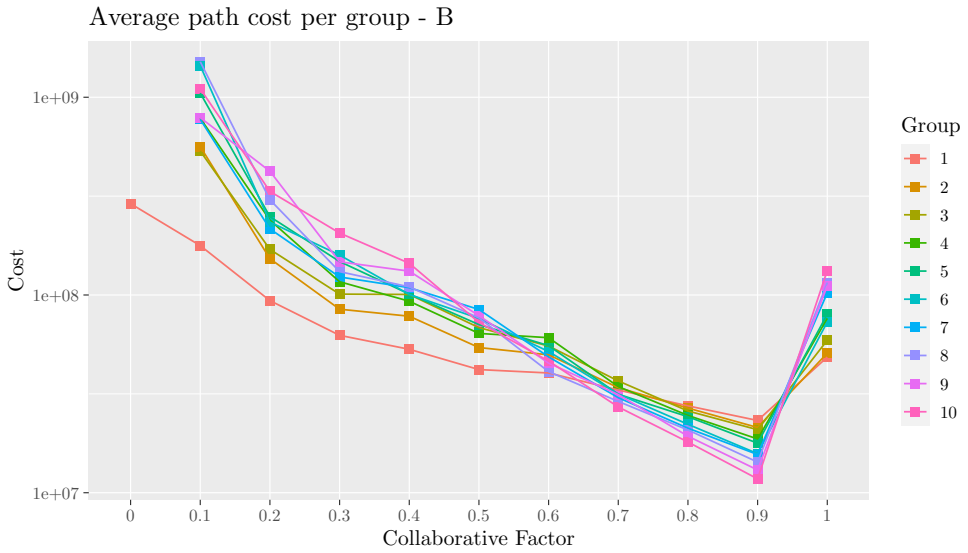

(b)

Figure 9.3: The path cost for (a) scenario **A** and (b) scenario **B**.

exit, increases with respect to the collaborative factor and one can better observe the collective behaviour of the simulated crowd. The maximum number of exited

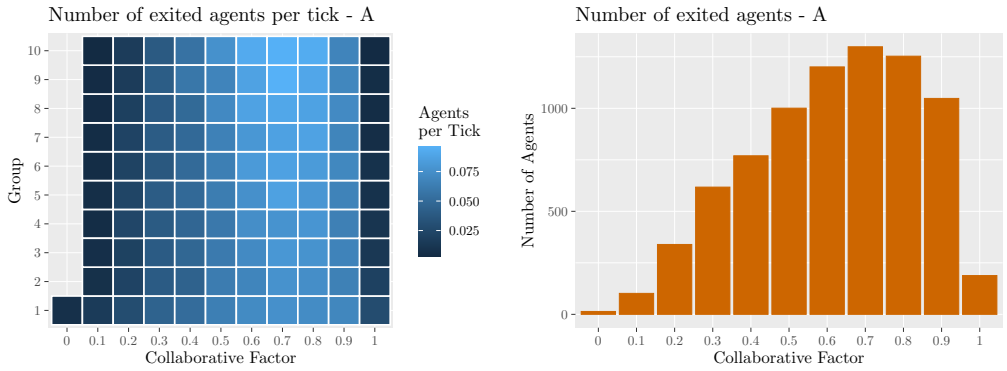

(a) (b)

Figure 9.4: The number of agents for the scenario **A**.

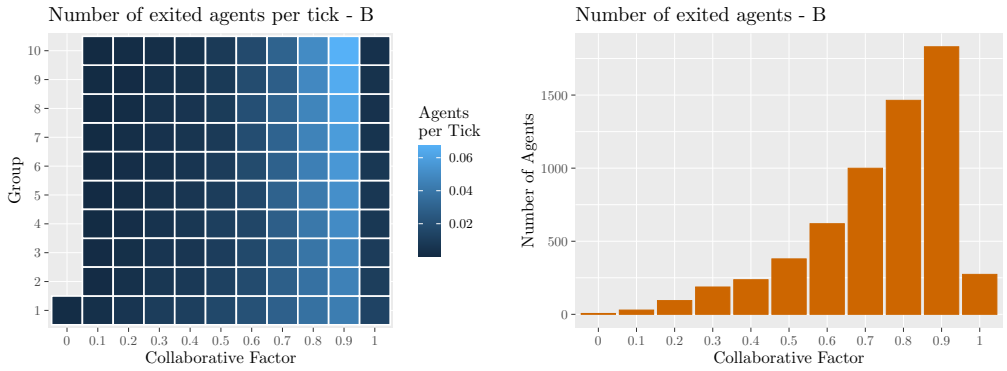

(a) (b)

Figure 9.5: The number of agents for the scenario **B**.

agents is obtained for $f = 0.7$ for scenario **A** and for $f = 0.9$ for scenario **B**. Considering the overall trend of the metrics used (the number of agents that reaches the exit, the path cost, and the exit time) it is possible to observe that the best performances of the agents are not when the entire group is composed only of collaborative agents, but when some of them are defectors. In other words, the crowd seems to perform better when some agents act differently and, in general,

when there is a condition of mixed strategy among the agents.

9.5 Conclusions

In this work, I proposed an agent-based model to evaluate the effects of two different behaviours in a crowd simulation: a collaborative and a defector one. Each strategy corresponds to different actions performed by the agents. The metrics used to evaluate the strategies are the number of exited agents, the path cost, and the exit time. From the results presented I can conclude that:

- a completely collaborative crowd has, in general, bad performances because it exits spending more time, by a more expensive path and does not maximize the number of agents that reach the exit point;
- a mixed crowd in which are present both behaviours is more efficient not only in obtaining the best values of the metrics used but also in the transmission of the information from one group to another;
- the results are confirmed for two scenarios with different characteristics, indicating that they may be generalized to more complex ones.

Future works include simulations with more complex scenarios, more starting points and end points and, a sensitivity analysis of the parameters used.

Chapter 10

How a Different Ant Behavior Affects on the Performances of the Whole Colony

10.1 Introduction

Ant Colony Optimization (ACO) is a well-known optimization procedure and represents nowadays the most representative methodology into the Swarm Intelligence family as it was successfully applied in many hard combinatorial optimization problems [70]. ACO is a metaheuristic that takes inspiration from observing foraging behavior of natural ant colonies since they can find exactly the shortest path from their nest to source of food, and they communicate with each other through chemical signals called pheromones. Thanks to these properties, it has become powerful optimization techniques for solving different kinds of complex combinatorial optimization problems [182], such as scheduling and routing problems [63, 121], coloring [44, 92], the robot path planning to patrol areas where humans

cannot get there [26, 3, 233], transportation problems [123], and feature selection [179]. Ant colonies are also recognized to be the best organized and cooperative system, able to make its community work at its best, and able to perform complex tasks [171]: any action of each ant is related only to its local environment, local interactions with other ants, simple social rules, and in the total absence of centralized decisions. It is known that it is not the single ant that finds the best solution but its cooperation and interaction with the environment and the rest of the colony that produces the desired result. These features have been implemented in ACO algorithms to solve not only the previously mentioned problems but also to evaluate how they affect the efficiency of the algorithm [48] and to investigate and analyze crowds' behavior [47]. This research paper proposes an analysis of what happens if in an ACO algorithm some ants act in a different way from the rest of the colony. In particular, the presented study consists of analyse two different kinds of ants, which act in different way: *Low Performing Ants* (LPAs) that can accidentally destroy some nodes or links of the network, therefore making them not crossable; and *High Performing Ants* (HPAs) that instead repair them. These different actions performed by the ants make the network dynamics in the sense that both actions (destroy or repair) change instantaneously the environment, modifying consequently the network topology. This means that a node or a link can be not crossable in the timestep t, but becoming crossable just after $(t + 1)$. Both kinds of ants must find the exit point of the network, starting from a given entrance, with the overall goal to maximize the number of ants that reach the exit, and minimize the path cost and the resolution time. The problem studied is a general path problem, however, the shortest path, in this case, is not a good evaluation metric due to the dynamism of the network. Moreover, thinking about a possible

application of this study in the field of swarm robotics, it is desirable that if there are some robots exploring unknown environments, the same robots will be able to come out from them in the maximum possible number. Two different complex networks have been considered to analyze how the presence of LPA affects the performance of the entire colony at different levels of available information: *high trace*, i.e. high amount of pheromone released, and *low trace*, low amount of pheromone released. Analyzing the investigation conducted on entire colony from an optimization point of view, emerges that the presence of a group of LPA helps and stimulates the rest of the colony to work better, especially when the amount of trace shared is high. Indeed, the disturbing actions performed by LPAs force the rest of the colony to change its behavior, and, consequently, to explore new paths.

10.2 The Model

The presented model has been realized using the software NetLogo [222], and the environment in which the ants move is a weighted network defined mathematically as a graph $G = (V, E, w)$, where V is the set of vertices, E is the set of edges and $w : V \times V \rightarrow \mathbb{R}^+$ is the *weighted* function that assigns a positive cost to each edge of the graph. The weight indicates how difficult is crossing a particular edge. The starting point is a node randomly chosen in one side of the graph (e.g. left side), whilst the exit point is another node randomly chosen in the opposite side to the starting one (e.g. right side). Every link is crossable in both directions. The colony is composed of two kinds of ants:

- *Low Performing Ants* (LPAs): they are always low performing in the sense that they do not work properly and so they can destroy, with a certain probability $0 \leq \rho_e \leq 1$, some edges of the network or, with a probability

$0 \leq \rho_v \leq 1$ some nodes of the network. They do not leave any amount of pheromone after crossing an edge (i, j) of their path;

- *High Performing Ants* (HPAs): they always are high performing, in fact, if they find they find a destroyed node they can repair it with a probability $0 \leq \rho_v \leq 1$ and, if they find a destroyed edge they can repair it with a probability $0 \leq \rho_e \leq 1$. Moreover, they release two different kinds of information about the path: the classic pheromone information after they have crossed ad edge (i, j), and a more sophisticate information named $\eta_{ij}(t) = 1/w_{ij}(t)$, where $w_{ij}(t)$ is the weight of the edge (i, j) at a time t and so $\eta_{ij}(t)$ indicate to the rest of the colony how difficult is that path.

It is important to highlight that the action of destroy an edge or a node means that this becomes impracticable, i.e. uncrossable. Instead, repair an edge or a node means that it is practicable again. Both actions, therefore, make the network dynamic. The number of HPAs in the colony is determined by the *performing factor* $p_f \in [0, 1]$, and therefore, once it is set, the remaining ants (i.e. $1 - p_f$) will be LPAs. Note that when $p_f = 1$, i.e. all ants are HPA, the ACO classical version is obtained.

Let be $A_i = \{j \in V : (i, j) \in E\}$ the set of vertices adjacent to vertex i and $\pi^k(t) = (\pi_1, \pi_2, \ldots, \pi_t)$ the set of vertices visited by an ant k at a certain time t, where $(\pi_i, \pi_{i+1}) \in E$ for $i = 1, \ldots, t - 1$. Due to the action of the HPAs that can repair damaged nodes and/or links, the path $\pi^k(t)$ is not just a simple path, because an ant can visit again a vertex due to a back-tracking operation. The probability $p_{ij}^k(t)$ with which an ant k placed on a vertex i chooses as destination one of its neighbor vertices j at the time t is defined according to the Ant Colony

Optimization *proportional transition rule*:

$$p_{ij}^{k}(t) = \begin{cases} \frac{\tau_{ij}(t)^{\alpha} \cdot \eta_{ij}^{\beta}}{\sum_{l \in J_i^k} \tau_{il}(t)^{\alpha} \cdot \eta_{il}^{\beta}} & \text{if } j \in J_i^k \\ 0 & \text{otherwise,} \end{cases} \tag{10.1}$$

where $J_i^k = A_i \setminus \{\pi_t^k\}$ are all the possible displacements of the ant k from vertex i, $\tau_{ij}(t)$ is the pheromone intensity on the edge (i, j) and $\eta_{ij}(t)$ is the desirability of the edge (i, j) at a given time t, while α and β are two parameters that determine the importance of pheromone intensity with respect to the desirability of an edge. For contextualization reasons with the environment/scenario tackled, from now on the term pheromone will be replaced with the term *trace*. The amount of trace released by the k ant after crossing an edge (i, j) at a time t is constant and it is defined as:

$$\Delta\tau_{ij}^{k}(t) = K. \tag{10.2}$$

The desirability $\eta_{ij}(t)$ at a given time t, establish how much an edge (i, j) is promising. In particular and it is defined as $\eta_{ji}(t)) = \frac{1}{w_{ij}(t)}$. This information is released by each ant as the trace, however it does not depend on the ant itself, but only on the edge (i, j). Each link is updated asynchronously with two kinds of updating rules based on the ticks T of the software used for the simulations[1]. A *local updating rule* that updates the trace levels at the end of each tour of the winning ant, according to the follow rule:

$$\tau_{ij}(t + 1) = \tau_{ij}(t) + K, \tag{10.3}$$

where K represents the trace that every ant leave after crossing an edge (i, j) and $\tau_{ij}(t)$ is the amount of trace on the link at time t. A *global updating rule* that

[1]Each tick correspond to an ant displacement and movement.

update the amount of trace on all the links of the network every T ticks:

$$\tau_{ij}(t+1) = (1-\rho) \cdot \tau_{ij}(t), \tag{10.4}$$

where $\tau_{ij}(t)$ is the amount of trace on the edge (i, j) at a time t and ρ is the evaporation decay parameter. The aim of the ants is to explore the graph and find in the shortest time, the cheapest path from the starting point to the end point, orienting themselves using the amount of trace on the paths and the information exchanged about their desirability. At the same time, they must maximize their number at the end point, that is the exit. Mathematically, this means the one have to optimize three different objective functions: minimize the *path cost function* and the *time cost function*, and maximize the *exit function* that represent how many ants have reached the end point. Since the path cost function and the time cost function must both be minimized, they have been put together into the following unified objective function:

$$\min \sum_{i=1}^{t-1} w(\pi_i^k, \pi_{i+1}^k) + |\pi^k|. \tag{10.5}$$

It represents both the minimization of the cost of the path and the resolution time, where the first term represents the path made by an ant k, while the second term represents the number of steps made by the same ant k. It can be used as a time term because each unit of time corresponds to an ant displacement, i.e. the number of the nodes visited by an ant corresponds to the resolution time.

Finally, the exit function is defined as:

$$\max \sum_{g \in G} \sum_{k \in N} k_g. \tag{10.6}$$

It represents the maximization of the number of ants that must reach the exit, where G is the total number of groups, g is the index of the group to which the ant k belongs, k_g is the ant k that belongs to g group and N is the set of ants.

10.3 Experiments and results

The simulations have been realized using two different kinds of scenarios, that correspond to different networks with increasing complexity. Within each scenario, two parameters of the model have been varied. In particular, the amount K of trace deposited by each ant on the links and the value of the parameter β that measures the importance of the information with respect to the amount of trace itself. This choice was meant to study and understand if and how the values of the model affect the performances of the colony when it is composed of two different kinds of ants. The two scenarios are:

- *Scenario B1*: a network with $|V| = 225$ nodes and $|E| = 348$ links.
- *Scenario B2*: a network with $|V| = 225$ nodes but $|E| = 495$ links.

The general experimental setup is the following. For each scenario, $N = 1000$ ants divided into $G = 10$ groups have been considered. This means that each group is composed of $N_g = 100$ ants that start their journey from the starting point at regular intervals computed multiplying the values of rows and columns, so $T_l = 225$ ticks. As said previously, the colony is composed of two different kinds of ants: high performing ants (HPAs) that always work at their best, and low performing ants (LPAs) that may destroy some nodes or links of their path. The number of HPAs and LPAs is regulated by a performing factor p_f that establishes the fraction of the first respect to the second. It goes from $p_f = 0.0$ (that defines a colony of just LPAs) to $p_f = 1.0$ (that defines a colony of just HPAs and correspond to the ACO classic version) with steps of $p_f = 0.10$. For instance, in a colony of 100 ants a value of $p_f = 0.30$ means that 30 ants are HPAs while the other 70 are LPAs.

Due to limited time resources, the ants must find the exit in a maximum time, which depends on the number of groups and the complexity of the network. This time is set to $T_{max} = 2 \times G \times T_l$, where G is the number of groups, T_l is the launch interval and 2 is just a corrective factor. The initial trace intensity on the links is set to 1.0 and it decreases over time according to the trace evaporation interval, $T_d = 50$ (i.e. every 50 ticks the amount of trace evaporate with the evaporation rate $\rho = 0.10$). For the scenarios defined as High Trace, the parameters α and β are both set to 1 and the amount of trace deposited by each ant on the links of its path is set to $K = 0.1$. For the scenarios defined as Low Trace, the parameter α is set to 1, the parameter β is set to 0.5 and the amount of trace deposited by each ant on the links of its path is set to $K = 0.001$. Since the parameter β regulates the influence of the information with respect to the amount of trace, one can expects that decreasing both β and K the colony will act taking more into account the information acquired about the path and less the information released with the trace. Finally, the edge destruction-repair probability and vertex destruction-repair probability are for both configurations $\rho_e = 0.02$ and $\rho_v = 0.02$. With these configurations of the parameters, 10 independent simulations have been performed, starting from the value $p_f = 0.0$ of the performing factor to $f = 1.0$, with steps of 0.1. Two different kinds of analysis have been done: (*i*) a *group analysis* to understand how many ants have reached the exit, considering both the value of the performing factor and the number of groups; and (*ii*) an *overall analysis* considering the (1) path cost found by the colony, (2) how much time the ants have used to find it, and (3) how many of them have reached the exit in time. In the following results, the label *High Trace* refers to a value of $K = 0.1$ and a value of $\beta = 1.0$, while the label *Low Trace* refers to a value of $K = 0.001$ and a

value of $\beta = 0.5$. It is worth emphasizing once again that, due to the dynamism of the network produced by the actions of the two types of ants, it is not possible to consider the shortest path as evaluation metric, and therefore the number of ants that reach the exit (to be maximized), the cost of the paths and the resolution time (both to be minimized) were considered as the investigation measure.

10.3.1 Group analysis

As said, in this first kind of analysis both the performing factor and the number of groups have been considered to evaluate the number of ants that have reached the exit. A heat map has been used to plot the results and by looking at the legend on the right of each plot one can easily understand that the lighter the blue is, the higher the value of the number of ants is. On the contrary, the darker the blue is, the lower the same number is. The absence of color implies that no ants have reached the exit for that value of the performing factor or for that value of the group. In Fig. 10.1 are shown the results obtained for the simulation performed in scenario B1 and in particular in Fig. 10.1a are plotted the number of ants that have reached the exit per ticks when there is a high-level trace. In Fig. 10.1b is plotted the same quantity but when there is a low-level trace.

Comparing Fig. 10.1a and Fig. 10.1b one can easily see that the best results, that is the maximum number of ants that reach the exit, are obtained not only for different values of the performing factor, but also for different values of the groups. In particular, when there is a high-level trace the best performances of the colony are obtained by the last groups and when the performing factor is round $p_f = 0.9$. On the contrary, comparing these results with the ones obtained in the same scenario with a low-level trace, one can see that in this case, the best results are obtained

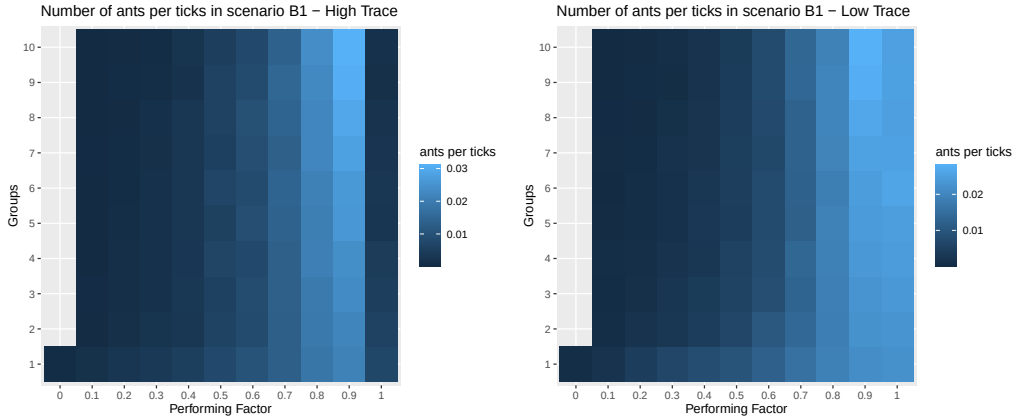

(a) (b)

Figure 10.1: Heat map representing the number of ants that have reached the exit per ticks in scenario B1. The performances of the colony change depending on the amount of the trace released by the ants: in (a) one can see that they reach their best for the last group $g = 10$ and when the performing factor is equal to $p_f = 0.9$, if there is a high level trace. The trend is similar in (b), that is when there is a low level trace released by the ants even if in this case the good performances continue to the value of the performing factor $p_f = 1.0$

from the last groups not only when the performing factor in equal to $p_f = 0.9$ but also when it is equal to $p_f = 1.0$. This indicates that the presence of LPAs is much more important when the trace level is high. In fact, it is noted that the number of ants per ticks exiting is greater for values of the performing factor equal to $f = 0.9$ or, a little bit lower, at $f = 0.8$. This behavior is similar for all the groups as the performing factor varies. These results are justified by the fact that when the trace is high, the ants are mistakenly affected and tend to follow incorrect paths. Furthermore, from the plots in Fig. 10.1 it is observed that in the case in which there is a high-level trace, the number of ants that reach the exit is higher respect

to the one obtained when there is a low-level trace. This indicates that the action of the LPAs is crucial to maximize the ants when there is a high-level trace, since for $p_f = 1.0$ the performances of the colony are worst. Fig. 10.2 shows the same

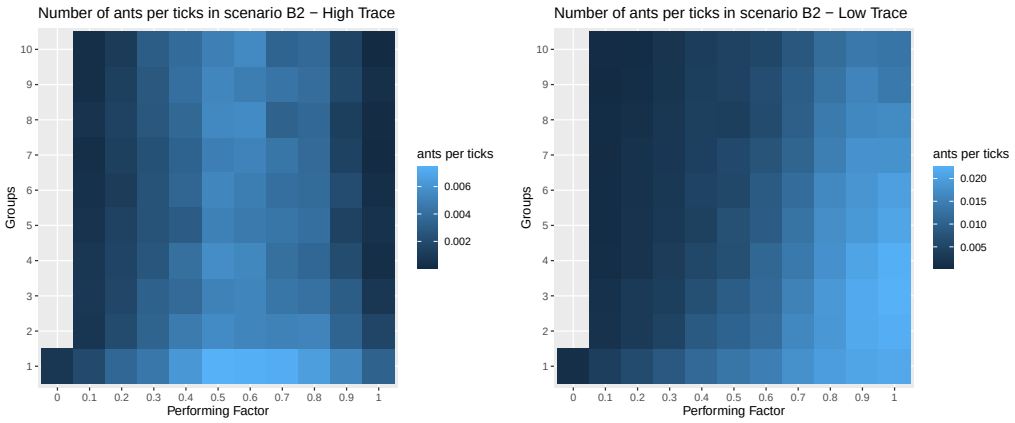

(a) (b)

Figure 10.2: Heat map representing the number of ants that have reached the exit per ticks in scenario B2. In (a) one can see that the colony reaches its best for the first groups and when the performing factor is round $p_f = 0.5$, if there is a high level trace. On the contrary, when there is a low level trace released, as in (b), the best performances are obtained for higher values of the performing factor, grater then $p_f > 0.7$ and for more groups following the firsts.

analysis carried out for scenario B2. The trend is similar to the one presented in the previous heat maps for scenario B1, but with some differences. In this case, when there is a high-level trace, as presented in Fig. 10.2a, in general the number of ants that reach the exit is lower than the one obtained for the same configuration but in scenario B1. Moreover, the best results are achieved by the first groups of the colony when the performing factor is round $p_f = 0.5$ that is, when it is composed of some LPAs. On the contrary, when there is a low-level trace, as in Fig. 10.2b,

the optimum is achieved by the first group and when the colony is composed by mainly HPAs, that is when the performing factor is equal to $p_f = 1.0$. This makes stronger the thesis of this work, for which a high trace confuses the colony and so, at the same time, a small percentage of LPAs stimulates the rest of the group to change its behavior.

10.3.2 Overall analysis

This second kind of analysis evaluates the performances of the whole colony considering only how they vary with respect to the performing factor, not considering the number of groups in which are divided the ants. The analysis is carried out considering, as in the Section 10.3.1, the different performances of the colony when there is a high-level trace and a low-level trace. The quantities analyzed are the number of ants that have reached the exit, the path cost, and the resolution time. The aim of the experiments was to maximize the number of ants and minimize the path cost and the resolution time. Fig. 10.3 shows how many ants have reached the exit in scenario B1. In particular, Fig. 10.3a represents the results obtained for high-level trace, while Fig. 10.3b represents the ones obtained for low-level trace. As one can see, the actions of the LPAs are more powerful and useful when there is an excess of trace released by all the ants, since the colony reaches better results when there is a small percentage of LPAs within it, as is clear from Fig. 10.3a for which the best value is obtained when the performing factor $p_f = 0.9$. On the other hand, the presence of LPAs seems to not boost the performances of the colony when there is a low-level trace. Fig. 10.3b shows that the number of ants that reached the exit is approximately the same for $p_f = 0.9$ and $p_f = 1.0$, indicating that the presence of LPAs does not affect positively the colony.

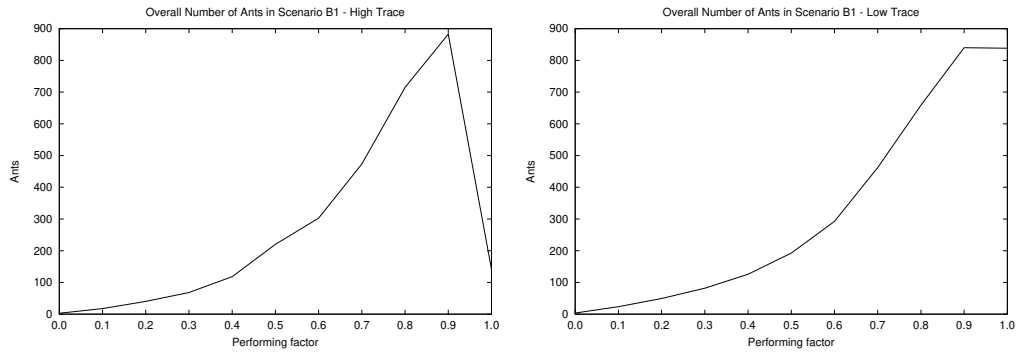

(a) (b)

Figure 10.3: Overall number of ants that have reached the exit in scenario B1. In (a) the values obtained for a high level trace; in (b) the ones obtained for a low level trace. The presence of LPAs is much more important and useful when there is a high-level trace, leading the colony to better performances. The best values are obtained for $p_f = 0.9$ when there is a high-level trace and for $p_f = 1.0$ when there is a low-level trace.

The same considerations can be done for scenario B2, whose results are shown in Fig. 10.4. In particular, Fig. 10.4a shows how many ants have reached the exit when there is a high-level trace. In this case, the maximum number of ants is obtained when the performing factor is $p_f = 0.5$. Fig. 10.4b, on the other hand, shows the same quantity when there is a low-level trace, and here the best performances of the colony are obtained when the performing factor is $p_f = 1.0$. As in the previous case, the presence of LPAs seems to be more important and helpful when there is an excess of trace release along the path since in this case, the colony has better performances when it is not composed of just HPAs. A note of interest is that scenario B2 has been obtained lower average values of the number of ants with respect to the ones obtained for scenario B1. This may depend on

the complexity of the network: the higher it is the worst the performances of the colony will be.

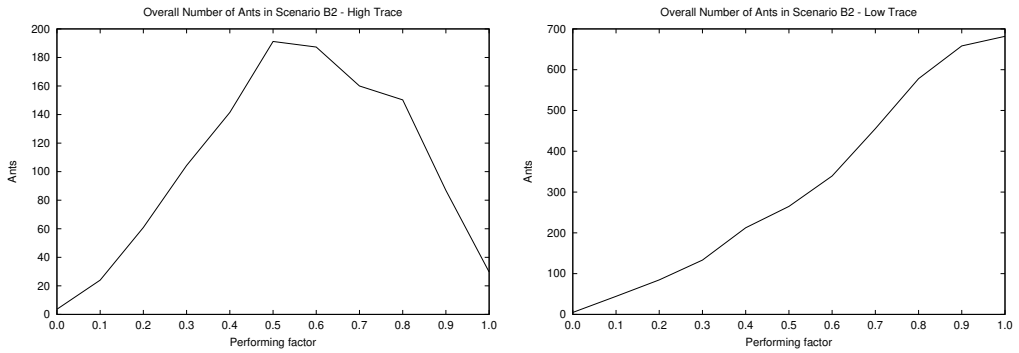

(a) (b)

Figure 10.4: Overall number of ants that have reached the exit in scenario B1. In (a) the values obtained for a high level trace; in (b) the ones obtained for a low level trace. As in Fig. 10.3, the presence of LPAs is much more helpful when there is a high-level trace. The best values are obtained for $p_f = 0.5$ when there is a high-level trace and for $p_f = 1.0$ when there is a low-level trace.

The path cost and the resolution time are both quantities to be minimized so they have been put together in the same plot. In particular, the principal plot represents the resolution time, the inset one the path cost. This has been done both for scenario B1, in Fig. 10.5, and for scenario B2, in Fig. 10.6. In particular, Fig. 10.5a represents how the resolution time and path cost vary with respect to the performing factor in scenario B1 with high-level trace; Fig. 10.5b shows the same quantities in the same scenario with a high-level trace. In this case, the best values are the lowest ones because they correspond to the best performances of the colony. Comparing these results with the ones regarding the number of ants in Fig. 10.3a, one can realize that in scenario B1, when there is a high-level trace,

the colony has better performances when it is composed of a small fraction of LPAs because the maximum number of ants that reaches the exit, the minimum value of the resolution time and the minimum of the path cost is obtained for a value of the performing factor equal to $p_f = 0.9$. Doing the same with Fig. 10.5b and Fig. 10.3b, one can see that when there is a low-level trace the presence of LPAs not only does not affect positively the number of ants that reach the exit but neither on the resolution time and on the path cost find by the colony. In this case, indeed, the best values are obtained when the colony is composed of just HPAs, reinforcing the hypothesis for which the presence of LPAs is useful to regulate the actions when there is an excess of trace.

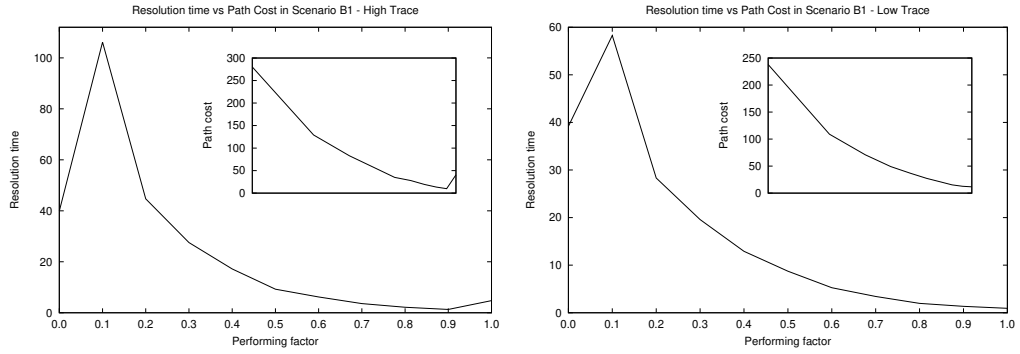

(a) (b)

Figure 10.5: Overall resolution time (principal plot) and path cost (inset plot) of the colony for scenario B1. In (a) the values obtained for a high-level trace; in (b) the ones obtained for a low level trace. As in Fig. 10.3, the presence of LPAs is much more helpful when there is a high-level trace. The best values are obtained for $p_f = 0.9$ when there is a high-level trace and for $p_f = 1.0$ when there is a low-level trace.

It is not surprising that the same results have been obtained also for scenario B2,

as represented in Fig. 10.6. In this case, the importance of the presence of LPAs is clear especially looking at the values obtained when there is a high-level trace. Indeed, there is a lot of difference between the path cost found by the colony (in the inset plot) when the performing factor is equal to $p_f = 1.0$ and the one obtained when the performing factor is equal to $p_f = 0.9$. The second value is much better than the first and it is obvious that the same worst performances are present also considering the resolution time in the principal plot, and the number of ants, as shown in Fig. 10.4a. On the contrary, but as previously shown, when there is a low-level trace, the presence of LPAs does not help the colony to boost its performances, which are better when it is composed of just HPAs. Fig. 10.6, indeed shows that the best values of the resolution time and the path cost are obtained when the performing factor is equal to $p_f = 1.0$.

10.4 Conclusions

This Chapter aims to investigate how different behaviors of the ants in the Ant Colony Optimization algorithm affect the global performances of the colony. To do this, two different kinds of ants have been considered: (1) *low performing ants* (LPAs), which can damage with certain probability nodes and links of their paths, and which do not help the rest of the colony sharing their information about the cost of each link; and (2) *high performing ants* (HPAs) which, on the contrary, may repair with a certain probability the damaged nodes and links and share their information about the cost of the links. The model has been tested on two networks with increasing complexity and has been investigated if and how the presence of LPA affects the performances of the group when different levels of information are present. Two different kinds of analysis have been carried out: (*i*) a *group analysis*,

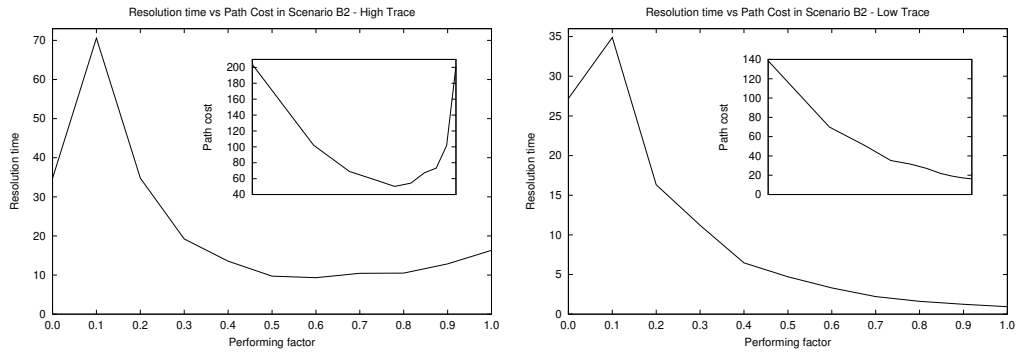

(a) (b)

Figure 10.6: Overall resolution time (principal plot) and path cost (inset plot) of the colony for scenario B1. In (a) the values obtained for a high-level trace; in (b) the ones obtained for a low level trace. As in Fig. 10.4, the presence of LPAs is much more helpful when there is a high-level trace. When there is a high-level trace, the best value of the resolution time is for $p_f = 0.6$ and the one for the path cost is for $p_f = 0.5$. When there is a low-level trace the same bests are obtained for $p_f = 1.0$.

to analyze how the number of ants that reach the endpoint of the network varies with respect to the performing factor and the group of the colony considered; and (*ii*) an *overall analysis* to analyze how the number of ants of the colony, the path cost find by it and its resolution time of the network vary taking into account only the performing factor. Both kinds of analysis have been realized naming High Trace the configuration for which the amount of pheromone released by the ants is $K = 0.1$ and the parameter $\beta = 1.0$ (i.e. more information available), and Low Trace the configuration for which the amount of pheromone release by the ants is $K = 0.001$ and the parameter $\beta = 0.5$ (i.e. less information available). From the group analysis, emerges that the presence of LPA helps the rest of the colony

especially when there is a condition of high-level trace because the disturbing actions performed by the LPAs stimulate the others to search for other paths and to share their information among the other groups of the colony. This seems to be true even for the overall analysis which considers the objective functions. The presence of LPAs is crucial when the amount of trace shared by the ants, and so present in the environment, is too high. An excess of information is self-defeating for the group because, since their actions are calibrated according to this quantity, it does not allow the ants to explore the rest of the network, letting them choose the same path over and over. In this sense, the presence of LPAs is helpful for the rest of the group because their actions force the rest of the colony to change its behavior in order to search for more fruitful paths.

Chapter 11

Optimization Algorithms for Detection of Social Interactions

11.1 Introduction

In last few years, many approaches have been proposed to detect communities in social networks using diverse ways. Community detection is one of the most important research topics in network science and graph analysis. Informally, a community is defined as a set of network's elements that are highly linked within the group and weakly linked to the outside. Modeling and examining complex systems that contain biological, ecological, economic, social, technological, and other information is a very difficult process because the systems used for the real-world data representation contain highly important information, such as social relationships among people or information exchange interactions between molecular structures in a body. For this reason, the study of community structures inspires intense research activities to visualize and understand the dynamics of a network at different scales [97, 104, 65]. In order to evaluate the quality of node

partitions of a network, the *modularity* is certainly the most used quality index [170].

Taking the modularity (Q) into account as an evaluation measure, community detection can easily be seen as a combinatorial optimization problem, since the problem aims to find a clustering that maximizes Q. It is also a hard optimization problem since Community Detection has been proven to be an $\mathcal{NP}$-complete problem [27]. Therefore, several search algorithms (both exact and approximate) for clustering problems have been proposed, and, generally, they have been proven to be robust in finding as cohesive as possible communities in large and complex networks [168, 169]. It is well known in the literature that metaheuristics work better than exact methods in large, complex, and uncertainty environments. Indeed, they are approximation methods successfully applied on many hard and complex problems able to find good solutions within reasonable computing times [213]. In this work, I propose two Immunological Algorithms for the community detection problem, called Opt-IA and Hybrid-IA, respectively. The first is based on a random and blind search, and employs specifically designed stochastic operators to carefully explore the search space, while Hybrid-IA uses a Local Search (LS) technique that deterministically tries to refine the solutions found so far. The main goal in this work is to prove the efficiency, robustness, and reliability of the two immune-inspired algorithms in community detection problem, as they have been successfully applied to several other areas and optimization tasks on networks. The efficiency and robustness of both algorithms were tested on several social networks (with different sizes), and, further, a comparison with seven other metaheuristic methods has also been performed in order to assess the reliability of Opt-IA and Hybrid-IA with respect to the state-to-the-art on community detection. In view

of such comparisons, I am able to assert that both immunological algorithms outperforms all other methods used for comparison, and find the best modularity in all tested networks. By reducing the comparison to only Opt-IA and Hybrid-IA, it is possible to assert overall that the algorithms are comparable, although the first one, as expected, needs a higher number of generations due to its random and blind search. Finally, it is important to underline the fact that, differently than all other algorithms used for comparison, which have been tested and refined over the years, Opt-IA and Hybrid-IA are already very competitive and successful, even though they are at a first stage of development in community detection tasks, and still need a deep study of their key parameters and operators. The rest of the chapter is organized as follows. In Section 11.2, the problem of community detection is introduced and the definition of the modularity measure are formulated. In Section 11.3, the two immunological algorithms are introduced and I focus the description primarily on their common concepts, whilst the detailed descriptions on their features and operators developed are presented, respectively, in Sections 11.3.1 (Opt-IA) and Section 11.3.2 (Hybrid-IA). In Section 11.4, all experiments performed and comparisons done are described in detail, including the used dataset and experimental protocol, and an analysis on the convergence behavior of the two proposed immunological algorithms (Opt-IA and Hybrid-IA). Finally, conclusions and some future research directions are presented in Section 11.5.

11.2 Mathematical Definition of Modularity in Networks

The main aims in community detection are to uncover the inherent community structure of a network, that is to say, those groups of nodes sharing common and similar properties. This means, then, to detect groups (*communities* or *modules*) internally strongly connected, and externally weakly connected. Being able to detect community structures is a key and relevant task in many areas (biology, computer science, engineering, economics, and politics) because they allow for uncovering and understanding important information about the function of the network itself and how its elements affect and interact with each other. For instance, in World Wide Web networks, the communities can identify those pages dealing with topics which are related; in biological networks, instead, they correspond to proteins having the same specific function; in social sciences, they can identify circles of friends or people who have the same hobby, or those people who live in the same neighborhood.

In order to evaluate the quality of the uncovered groups in a network, *modularity* is certainly the most used quality index [170]. It is based on the idea that a random graph is not expected to have a community structure; therefore, the possible existence of communities can be revealed by the difference of density between vertices of the graph and vertices of a random graph with the same size and degree distribution. Formally, it can be defined as follows: given an undirected graph $G = (V, E)$, with V the set of vertices ($|V| = N$), and E the set of edges ($|E| = M$),

the modularity of a community is defined as:

$$Q = \frac{1}{2M}\left[\sum_{i=1}^{N}\sum_{j=1}^{N}\left(A_{ij} - \frac{d_i d_j}{2M}\right)\delta(i,j)\right], \tag{11.1}$$

where A_{ij} is the adjacency matrix of G, d_i and d_j are the degrees of nodes i and j respectively, and $\delta(i,j) = 1$ if i, j belong to the same community, 0 otherwise. As asserted by Brandes et al. in [27], the modularity value for unweighted and undirected graphs lies in the range $[-0.5, 1]$. Then, a low Q value, i.e., close to the lower bound, reflects a bad clustering, and implies the absence of real communities, whilst good groups are identified by a high modularity value that implies the presence of highly cohesive communities. For a trivial clustering, with a single cluster, the modularity value is 0. However, the modularity has the tendency to produce large communities and, therefore, fails to detect communities which are comparatively small with respect to the network [95].

11.3 Immunological Algorithms

Immunological Algorithms (IA) are among the most used population-based metaheuristics, successfully applied in search and optimization tasks. They take inspiration from the dynamics of the immune system in performing its job of protecting living organisms. One of the features of the immune system that makes it a very good source of inspiration is its ability to detect, distinguish, learn, and remember all foreign entities discovered [96]. Both proposed algorithms, Opt-IA and Hybrid-IA, belong to the special class *Clonal Selection Algorithms* (CSA) [178, 49], whose efficiency is due to the three main immune operators: (i) cloning, (ii) hypermutation, and (iii) aging. Furthermore, both are based on two main concepts: antigen (Ag), which represents the problem to tackle, and B cell, or antibody (Ab)

that represents a candidate solution, i.e., a point in the solution space. At each time step t, both algorithms maintain a population of d candidate solutions: each solution is a subdivision of the vertices of the graph $G = (V, E)$ in communities. Let $N =\mid V \mid$, then a B cell $\vec{x}$ is a sequence of N integers belonging to the range $[1, N]$, where $x_i = j$ indicates that the vertex i has been added to the cluster j. The population, for both algorithms, is initialized at the time step $t = 0$ randomly assigning each vertex i to a group j, with $j \in [1, N]$. Then, just after the initialization step, the fitness function (Equation (11.1)) is evaluated for each randomly generated element ($\vec{x} \in P^{(t)}$) by using the function ComputeFitness($P^{(t)}$). The two algorithms end their evolutionary cycle when the halting criterion is reached. For this work, it was fixed to a maximum number of generations ($MaxGen$).

Among all immunological operators, *cloning* is the only one that is roughly the same between Opt-IA and Hybrid-IA ($6th$ line in Algorithms 2 and 3). This operator simply copies dup times each B cell producing an intermediate population $P^{(clo)}$ of size $d \times dup$. I used a static cloning for both algorithms in order to avoid premature convergences. Indeed, if a number of clones proportional to to the fitness value is produced instead, I could have a population of B cells very similar to each other, and I would, consequently, be unable to perform a proper exploration of the search space getting easily trapped in local optima. Hybrid-IA, more in detail, assigns an age to each cloned B cell, which determines how long it can live in the population, from the assigned age until it reaches the maximum age allowed τ_B, a user-defined parameter). Specifically, a random age chosen in the range $[0 : \frac{2}{3}\tau_B]isassignedtoeachclone$. In this way, each clone is guaranteed to stay in the population for at least a fixed number of generations ($\frac{1}{3}\tau_B$ in the worst case). The age assignment and the aging operator (see Section 11.3.2) play a crucial role

on HYBRID-IA performances, and any evolutionary algorithm in general because they are able to keep a right amount of diversity among the solutions, thus avoiding premature convergences [64].

11.3.1 OPT-IA

OPT-IA [208] is a totally blind stochastic algorithm, a particular type of optimization method that generates a set of random solutions for the community detection problem. It is based on

(i) the *hypermutation operator*, which acts on each clone in order to explore its neighborhood;

(ii) the *precompetition operator*, which makes it possible to maintain a more heterogeneous population during the evolutionary cycle;

(iii) the *stochastic aging operator* whose aim is keep high diversity into the population and consequently help the algorithm in escaping from local optima; and, finally,

(iv) the *selection operator* which identifies the best d elements without repetition of fitness, ensuring heterogeneity into the population.

In Algorithm 2, the pseudocode of OPT-IA, and its key parameters, are described: The purpose of the hypermutation operator is to carefully explore the neighborhood of each solution in order to generate better solutions from iteration to iteration. It basically performs at most m mutations on each B cell, where m is a user-defined constant parameter. Unlike the other clonal selection algorithms, including HYBRID-IA, the m mutation rate of each element is not determined by a law

Algorithm 2 Pseudo-code of OPT-IA

```
1: procedure OPT-IA(d, dup, m, P_die)
2:     t ← 0
3:     P^(t) ← InitializePopulation(d);
4:     ComputeFitness(P^(t))
5:     while ¬StopCriterion do
6:         P^(clo) ← Cloning(P^(t), dup)
7:         P^(hyp) ← Hypermutation(P^(clo), m)
8:         ComputeFitness(P^(hyp))
9:         P^(pre) ← Precompetition(P^(t))
10:        P_a^(pre) ← StochasticAging(P^(pre), P_die)
11:        P^(t+1) ← Selection(P_a^(pre), P^(hyp))
12:        t ← t + 1;
13:    end while
14: end procedure
```

inversely proportional to the fitness function, but it will be the same for anyone. In this way, possible premature convergences are avoided. In this algorithm, three different types of mutation have been designed, which can act on a single node (local operators) or a set of nodes (global operators):

1. *equiprobability*: randomly select a vertex from the solution and reassign it to a cluster among those existing at that time. Each cluster has the same probability of being selected;

2. *destroy*: randomly select a cluster c_i from the solution $\vec{x}$, a percentage P in the range $[1\%, 50\%]$, and a cluster c_j in the range $[1, N]$. All vertices in c_i are then moved to the cluster c_j with P probability. Note that, if the cluster c_j does not exist, then a new community is created;

3. *fuse*: randomly select a cluster and assign all its nodes to a randomly selected cluster among those existing.

After the hypermutation operator, the fitness values for all mutated B cell are computed. Three operators act on the population at this point.

Precompetition operator: the primary aim of this operator is to obtain a more heterogeneous population by trying to maintain solutions which have different community numbers in order to better explore the search space. Basically, this operator randomly selects two different B cells from $P^{(t)}$, and, if they have same community number, the one with a lower fitness value will be deleted with a 50% probability.

StochasticAging operator: this operator helps the algorithm to escape from local optima by introducing diversity in the population. At each iteration, each B cell in $P^{(pre)}$ will be removed with probability P_{die} (a user-defined parameter). Using this type of aging operator, Opt-IA is able to, on one hand, to introduce diversity in the population, which is crucial for jumping out from local optima, and, on the other hand, to have an accurate exploration and exploitation of the neighborhoods.

Selection operator: finally, the selection operator has the task to generate the new population for the next generation made up of the best B cells discovered so far. Therefore, the new population $P^{(t+1)}$ is created by selecting the best d B cells among the survivors in $P_a^{(pre)}$ and hypermutated B cells in $P^{(hyp)}$. It is important to highlight that no redundancy is allowed during the selection: if a hypermutated B cell is candidate to be selected for the new population $P^{(t+1)}$, but it has the same fitness value with someone in $P_a^{(pre)}$, then it will be discarded. This ensures monotonicity in the evolution dynamic.

11.3.2 HYBRID-IA

A fundamental difference between OPT-IA and HYBRID-IA is that the former, as described above, is a stochastic IA that finds solutions by random methods. The latter, instead, uses a deterministic local search, based on rational choices that refine and improve the solutions found so far. The pseudocode of HYBRID-IA is described in Algorithm 3.

Algorithm 3 Pseudo-code of HYBRID-IA.

1: **procedure** HYBRID-IA(d, dup, ρ, τ_B)
2: $t \leftarrow 0$
3: $P^{(t)} \leftarrow$ InitializePopulation(d)
4: ComputeFitness($P^{(t)}$)
5: **while** ¬StopCriterion **do**
6: $P^{(clo)} \leftarrow$ Cloning($P^{(t)}, dup$)
7: $P^{(hyp)} \leftarrow$ Hypermutation($P^{(clo)}, \rho$)
8: ComputeFitness($P^{(hyp)}$)
9: $(P_a^{(t)}, P_a^{(hyp)}) \leftarrow$ Aging($P^{(t)}, P^{(hyp)}, \tau_B$)
10: $P^{(select)} \leftarrow (\mu + \lambda)-$Selection($P_a^{(t)}, P_a^{(hyp)}$)
11: $P^{(t+1)} \leftarrow$ LocalSearch($P^{(select)}$)
12: ComputeFitness($P^{(t+1)}$)
13: $t \leftarrow t + 1$;
14: **end while**
15: **end procedure**

The hypermutation operator developed in HYBRID-IA has the main goal of exploring the neighborhoods of solutions by evaluating how good each clone is. Unlike OPT-IA, the mutation rate is determined through an *inversely proportional* law to the fitness function value of the B cell considered, that is, the better the fitness

value of the element is, the smaller the mutation rate will be. In particular, let $\vec{x}$ be a cloned B cell, the *mutation rate* $\alpha = e^{-\rho \hat{f}(\vec{x})}$ is defined as the probability to move a node from one community to another one, where ρ, a user-defined parameter that determines the shape of the mutation rate, and $\hat{f}(\vec{x})$ is the fitness function normalized in the range $[0, 1]$. Formally, the designed hypermutation works as follows: for each B cell, two communities c_i and c_j are randomly chosen ($c_i \neq c_j$): the first is chosen among all existing ones , and the second in the range $[1, N]$. Then, all vertices in c_i are moved to c_j with probability given by α. If a value that does not correspond to any currently existing community is assigned to c_j, a new community c_j is created and added to the existing ones. The idea behind this approach is to better explore the search space and create and discover new communities by moving a variable percentage of nodes from existing communities. This search method balances the effects of local search (as described below), by allowing the algorithm to avoid premature convergences towards local optima.

The static aging operator in Hybrid-IA acts on each mutated B cells by removing older ones from the two populations $P^{(t)}$ and $P^{(hyp)}$. Basically, let τ_B be the maximum number of generations allowed for every B cell to stay in its population; then, once the age of a B cell exceeds τ_B (i.e., age=τ_B+1), it will be removed independently from its fitness value. However, an exception may be done for the best current solution, which is kept into the population even if its age is older than τ_B. Such a variant of the aging operator is called *elitist aging operator*. In the overall, the main goal of this operator is to allow the algorithm to escape and jump out from local optima, assuring a proper turnover between the B cells in the population, and producing, consequently, high diversity among them.

After the aging operator, the best d survivors from both populations $P_a^{(t)}$ and

$P_a^{(hyp)}$ are selected, in order to generate the temporary population $P^{(select)}$, on the local search will be performed. Such a selection is performed by the $(\mu + \lambda)$-*Selection operator*, where $\mu = d$ and $\lambda = (d \times dup)$. The operator identifies the d best elements among the set of offsprings and the old parent B cells, ensuring consequently monotonicity in the evolution dynamics.

The Local Search designed and introduced in HYBRID-IA is the key operator to properly speed up the convergence of the algorithm, and, in a way, drive it towards more promising regions. Furthermore, it intensifies the search and explore the neighborhood of each solution using the well-known *Move Vertex* approach (MV) [124]. The basic idea of the proposed LS is to assess deterministically if it is possible to move a node from its community to another one within its neighbors. The MV approach takes into account the *move gain* that can be defined as the variation in modularity produced when a node is moved from a community to another. Before formally defining the move gain, it is important to point out that the modularity Q, defined in Equation (11.1), can be rewritten as:

$$Q(c) = \sum_{i=1}^{k} \left[\frac{\ell_i}{M} - \left(\frac{d_i}{2M} \right)^2 \right], \tag{11.2}$$

where k is the number of the found communities; $c = \{c_1, \ldots, c_i, \ldots c_k\}$ is the set of communities that is the partitioning of the set of vertice V; l_i and d_i are, respectively, the number of links inside the community i, and the sum of the degrees of vertices belonging to the i community. The *move gain* of a vertex $u \in c_i$ is, then, the modularity variation produced by moving u from c_i to c_j, that is:

$$\Delta Q_u(c_i, c_j) = \frac{l_{c_j}(u) - l_{c_i}(u)}{M} + d_V(u) \left[\frac{d_{c_i} - d_V(u) - d_{c_j}}{2M^2} \right], \tag{11.3}$$

where $l_{c_i}(u)$ and $l_{c_j}(u)$ are the number of links from u to nodes in c_i and c_j

respectively, and $d_V(u)$ is the degree of u when considering all the vertices V. If $\Delta Q_u(c_i, c_j) > 0$, then moving node u from c_i to c_j produces an increment in modularity, and then a possible improvement. Consequently, the goal of MV is to find a node u to move to an adjacent community in order to maximize ΔQ_u:

$$\underset{v \in Adj(u)}{\operatorname{argmax}} \Delta Q_u(i, j), \tag{11.4}$$

where $u \in C_i$, $v \in C_j$ and $Adj(u)$ is the adjacency list of node u.

For each solution in $P^{(select)}$, the Local Search begins by sorting the communities in increasing order with respect to the ratio between the sum of inside links and the sum of the node degrees in the community. In this way, poorly formed communities are identified. After that, MV acts on each community of the solution, starting from nodes that lie on the border of the community, that is, those that have at least an outgoing link. In addition, for communities, the nodes are sorted with respect to the ratio between the links inside and node degree. The key idea behind LS is to deterministically repair the solutions which were produced by the hypermutation operator, by discovering then new partitions with higher modularity value. Equation (11.3) can be calculated efficiently because M and $d_V(u)$ are constants, the terms l_{c_i} and d_{c_i} can be stored and updated using appropriate data structures, while the terms $l_{c_i}(u)$ can be calculated during the exploration of all adjacent nodes of u. Therefore, the complexity of the move vertex operator is linear on the dimension of the neighborhood of node u.

11.4 Results

In this section, all the experiments and comparisons performed on the two proposed algorithms, Opt-IA and Hybrid-IA, are presented, in order to assess their

efficiency and robustness in detecting highly linked communities. Different social networks have been taken into account for the experimental analyses conducted on the two algorithms, and for their comparison with other efficient metaheuristics which are present in literature.

The instances are well-known networks used for the community detection problem and their characteristics are summarized and reported in Table 11.1. *Gravy's Zebra* [212] is a network created by Sundaresan et al. in which a link between to nodes indicates that a pair of zebras appeared together at least once during the study. In *Zachary's Karate Club* [231] network, collected by Zachary in 1977, a node represents a member of the club and an edge represents a tie between two members of the club. *Bottlenose Dolphins* [143] is an undirected social network of dolphins where an edge represents a frequent association. *Books about US Politics* [130] is a network of books sold, compiled by Krebs, where edges represent frequent co-purchasing of books by the same buyers. Another network considered is *American College Football* [97], a network of football games between colleges. *Jazz Musicians* [98] is the collaboration network between Jazz musicians. Each node is a Jazz musician and an edge denotes that two musicians have played together in a band. These specific networks have been chosen because they are the most used as test benches and, consequently, allowed us to compare my algorithms with several others and, in particular, with different metaheuristics. Although there exist bigger networks in literature, large and meaningful comparisons are more difficult to develop.

For all experiments carried out and presented in this section, both Opt-IA and Hybrid-IA maintain a population of B cells of size $d = 100$, whereas the number of generated clones depends upon the approach used. Since Opt-IA needs high

variability, $dup = 10$ has been set for larger networks ($|V| \geq 100$), and $dup = 4$ for smaller ones ($|V| < 100$); $dup = 2$, has been, instead, set in HYBRID-IA for all tested network types.

Table 11.1: The social networks used in the experiments.

Name	$\boldsymbol{\|V\|}$	$\boldsymbol{\|E\|}$
Grevy's Zebras [212]	28	111
Zachary's Karate Club [231]	34	78
Bottlenose Dolphins [143]	62	159
Books about US Politics [130]	105	441
American College Football [97]	115	613
Jazz Musicians Collaborations [98]	198	2742

Moreover, the m and P_{die} parameters in OPT-IA have been set to 1 and 0.02, respectively; however, for HYBRID-IA, ρ and τ_B have been set to 1.0 and 5. Note that all parameters of OPT-IA have been determined through careful tuning experiments, whilst those of HYBRID-IA have been identified both from the knowledge learned by previous works [178, 49], and from a preliminary and not in-depth experiments. As described above, the maximum number of generations has been taken into account as stopping criterion. For all experiments performed in this research work, it was fixed $MaxGen = 1000$ for OPT-IA, and $MaxGen = 100$ for HYBRID-IA. Note that a higher iterations number has been considered for OPT-IA due to its blind search, which, for obvious reasons, requires larger time steps to reach acceptable solutions.

Initially, the experimental analysis has been focused on the inspection of the efficiency of both algorithms, OPT-IA and HYBRID-IA, in terms of convergence

and solution quality found. In Figure 11.1, the convergence behavior of both OPT-IA and HYBRID-IA on the *Books about US Politics* network is showed. In this plot, the curves represent the evolution of the best and average fitness of the population; the standard deviation of the fitness values of the population is superimposed onto the average fitness and gives an idea about how heterogeneous the elements in the population are.

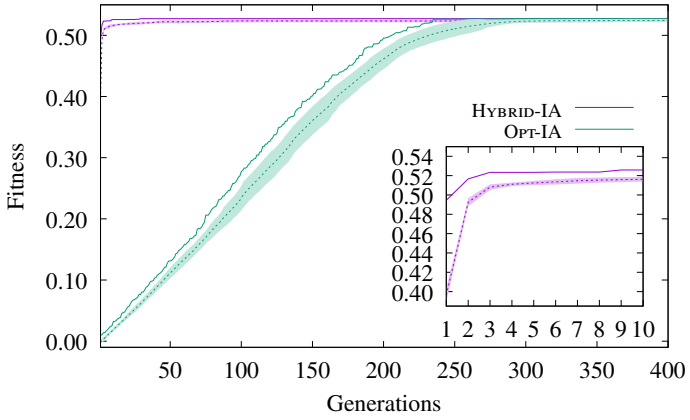

Figure 11.1: Convergence behavior of OPT-IA and HYBRID-IA on the *Books about US Politics* network.

From Figure 11.1, one can note how OPT-IA converges more slowly towards the best solution, as expected, always keeping a certain variability within the population. This allows the algorithm to better explore the search space. When the population is composed of very different elements, i.e., when the standard deviation is high, the algorithm discovers new solutions, significantly improving the current best solution. However, after about 250 generations, OPT-IA reaches the optimal solution and the curves (best and average fitness) tend to overlap. Moreover, the achievement of the optimal solution helps the creation of better clones,

reducing the variability of the population. Unlike OPT-IA, HYBRID-IA converges easily thanks to the local search applied to the elements after the selection phase. As can be noted from the inset plot in Figure 11.1, HYBRID-IA reaches the optimal solution after a few generations. Even in this case, once the best solution is reached, the population follows the same trend of the curve of the best fitness, and both curves continue (almost) as a single line. If on one hand the local search helps to quickly discover good solutions, on the other, it reduces the diversity inside the population, reducing then the exploration of the search space. In particular, as demonstrated by the worst value found in the *Jazz Musicians* network, reported in Table 11.2, HYBRID-IA prematurely converges towards local optima, from which it will hardly be able to get out. At the end of the analysis of Figure 11.1, it is possible to conclude that the stochastic operators designed in OPT-IA guarantee an excellent and large exploration of the search space, but with the disadvantage of requiring a longer evolution time; however, the local search developed in HYBRID-IA, and relative sorting criteria, allow for quickly discovering good solutions to exploit during the evolutionary process.

In order to evaluate the performances and reliability of both immunological algorithms with respect the state-of-the-art, a wide comparison has been performed with several metaheuristics, and a well-known deterministic algorithm, on the all dataset reported in Table 11.1. In particular, OPT-IA and HYBRID-IA have been compared with: LOUVAIN [25], a greedy optimization method; HDSA, a Hyper-Heuristics Differential Search Algorithm based on the migration of artificial superorganisms [39]; BADE, an improved Bat Algorithm based on Differential Evolution algorithm [211, 210]; SSGA, a Scatter Search [99, 146] based on Genetic Algorithm; BB-BC, a modified Big Bang–Big Crunch algorithm [74];

BA, an adapted Bat Algorithm for community detection [227]; GSA, a Gravitational Search Algorithm re-designed for solving the community detection problem [185]; and MA-NET, a Memetic Algorithm [154]. For all algorithms, I considered $MaxGen = 100$, except for OPT-IA, as described above, and MA-NET whose stopping criterion has been set to 30 generations without improvement (see [154] for details). All results of the above methods, as well as the experimental protocol, have been taken from Atay et al. [9], except for LOUVAIN (I have considered the LOUVAIN algorithm included in *igraph R package*) and MA-NET.

The comparison performed on all dataset is reported in Table 11.2, where I show for each algorithm (where possible) the *best*, *mean*, and *worst* values of the Q modularity; standard deviation (σ), and, finally, the created communities number (k). Furthermore, whilst the experiments for OPT-IA and HYBRID-IA were performed on 100 independent runs, for all other compared algorithms, only 30 independent runs have been considered, excepts for MA-NET with 50 runs. It is important to note that, for the MA-NET outcomes, the values reported, and taken from [154], have been rounded to third decimal places unlike the others that are instead based on four decimals. Obviously, all 10 algorithms optimize the same fitness function reported in Equation (11.1) and rewritten in a simpler way in Equation (11.2).

From Table 11.2, it is possible to note that all algorithms reach the optimal solution in the first two networks *Zebra* and *Karate Club*, except LOUVAIN, which fails on the second; on all the other network instances, both OPT-IA and HYBRID-IA outperform all other compared algorithms, matching their best values only with HDSA and MA-NET ones. It is important to point out, which proves even more the efficiency of the two proposed immunological algorithms, how the *mean* values obtained by OPT-IA and HYBRID-IA, on all tested networks, are better than the best

modularity found by the other algorithms, such as: BADE, SSGA, BB-BC, BA, and GSA; even on the *Dolphins* and *Football* networks, the worst modularity value obtained by OPT-IA is equal to or greater than the best one obtained by the same algorithms. On the *Dolphins* network, OPT-IA reaches a better mean value than HYBRID-IA, HDSA, and MA-NET, since, because of its random/blind exploration of the search space, it jumps out from local optima more easily than the other three. The opposite behavior of OPT-IA occurs when the size and complexity of the networks increase. In such a case, it obviously needs more generations to converge towards the optimal solutions and this is highlighted by the mean value and the standard deviation obtained for *Political Books* and *Football*. Note that, with longer generations, OPT-IA finds roughly the same mean values as HYBRID-IA. HYBRID-IA shows more stable results on all tested networks than OPT-IA, obtaining lower standard deviation values on all instances. On *Dolphins* network, HYBRID-IA has a mean value slightly lower than OPT-IA and HDSA, while in *Political Books* lower only than HDSA. As described above, this is due to the local search that leads the algorithm to a premature convergence towards local optima, obtaining the lowest worst value. Furthermore, HDSA is a hyper-heuristic which uses a genetic algorithm and scatter search to create the initial population for the differential search algorithm, speeding up the convergence of the algorithm, and reducing the spread of results. In *Jazz Musicians* network, both OPT-IA and HYBRID-IA algorithms obtain similar results, comparable to those obtained by MA-NET. Finally, if I focus on the comparison with only the deterministic LOUVAIN algorithm, both immunological algorithms outperform it in almost all networks (3 out of 6). In conclusion, from the experimental analysis, it is possible to assert that both OPT-IA and HYBRID-IA perform very well on networks (large and

small) considered for the experiments and are competitive with the state-of-the-art in terms of efficiency and robustness. Furthermore, inspecting the found mean values, I can see that both algorithms show themselves to be reliable optimization methods in detecting highly linked communities.

11.4.1 Large Synthetic Networks

In order to assess the scalability of HYBRID-IA, as last step of this research work, I considered larger synthetic networks with 1000 and 5000 vertices. The clear advantages of using them are given by the knowledge of the communities and consequently by the possibility of evaluating the goodness of the detected communities, as well as the possibility of testing the algorithm on different scenarios and complexities. The validity of this benchmark is given by faithfully reproducing the keys features of real graphs communities. The new benchmark was produced using the LFR algorithm proposed by Lancichinetti and Fortunato in [134]. Two different network instances were considered with $|V| = 1000$ and $|V| = 5000$, respectively, considering $k = 20$ as average degree and $k_{max} = 50$ as maximum degree. For both values of $|V|$, I considered $\tau_1 = 2$ as exponent of the degrees distribution and $\tau_2 = 1$ for the one of the communities' sizes. Moreover, about the community dimension, I fixed $min_c = 10$ and $max_c = 50$, respectively, minimum and maximum sizes. Finally, the mixing parameter μ_t was varied from 0.1 to 0.7, which identifies the relationships percentage of a node with those belonging to different communities. Therefore, the larger the value of μ_t, the larger are the relationships that a vertex has with other nodes outside its community. More details on the LFR algorithm, the key parameters, and the generated benchmark can be found in [135, 134].

Thanks to the advantages offered by the synthetic networks, I took into account a new evaluation metric in order to confirm the efficiency of the proposed HYBRID-IA in detecting strong communities. In particular, I considered the *Normalized Mutual Information* (NMI) [61], which is a widely used measure to compare community detection methods since it discloses the similarity between the true community and the detected community structures. Thus, while the modularity allows for assessing how cohesive the detected communities are, the NMI allows for evaluating how similar they are with respect to the real ones. In Table 11.3, the outcomes of HYBRID-IA on these new synthetic datasets are then reported and compared to the ones obtained by LOUVAIN. Modularity (Q) and NMI values are presented and considered for the comparisons. In the first column of the table, the features of each instance tackled are also shown. Analyzing the comparison, it is possible to see how HYBRID-IA outperforms LOUVAIN in all networks with 1000 vertices with respect to the Q modularity metric, whilst the opposite happens for those instances with 5000 vertices, where instead LOUVAIN outperforms HYBRID-IA. This gap is due to the combination between the random search and local search that, together with the diversity produced by the immune operators, requires a longer convergence time than the LOUVAIN one. It is important to point out that very likely, with a larger number of generations, HYBRID-IA would reach comparable results to LOUVAIN in terms of Q modularity also on these larger networks. Different instead is the assessment of the comparison if it is analyzed with respect the NMI metric [61]: HYBRID-IA outperforms LOUVAIN in all networks, and this proves a better ability of the hybrid immune algorithm proposed in detecting communities closer to the true ones than the greedy optimization algorithm. Note that, although modularity assesses the cohesion of the communities detected, maximizin Q might

not correspond to detect the true communities.

11.4.2 On the Computational Complexity of Opt-IA and Hybrid-IA

Both algorithms are population based algorithms; therefore, any analysis of their computational complexity must deal not only with the size of the input problems and its implementation, which in turn implies the analysis of the computational cost of computing the fitness of any individual, but also with the choice of the key parameters, such as the number of elements in the population d, the total number of iterations $MaxGen$,, etc. I will discuss these issues properly in what follows. When I look at the code for Opt-IA, I have the following:

- Any element of the population, i.e., a tentative solution, is an array of length N, where N is the number of vertices of the input graph.
- The operator InitializePopulation(d) randomly creates a population of d tentative solutions. Thus, total cost is $O(dN)$. However, I stress here the fact that d, which is set experimentally, is actually constant, i.e., it does not depend on the size of the input. In my case, I fixed to the value 100 for all of the experiments. This allows us to say that the cost of the procedure is actually $O(N)$.
- The operator ComputeFitness() computes the fitness for all the $d = 100$ elements of the population. A bound on the cost of the procedure can easily be computed using Equation (11.1), and it clearly is $O(N^2)$.
- The operator Cloning() creates dup copies of each of the elements of the population. As you can see from my settings, dup is a parameter which

does not depend on the size of the input graph, but just on the nature of the algorithm. This allows us to say that the cost of Cloning() is $O(N)$.

- The operator Hypermutation() mutates each element of the population with constant probability m. As I described earlier, I have three different implementations. In all three cases, I have either the random selection of a vertex or the random selection of a cluster. In the two most time-consuming implementations, namely *destroy* and *fuse*, I might have the reallocation of several vertices. Thus, all in all, Hypermutation() has an upper bound $O(N)$.

- The operator Precompetition() randomly selects two vertices, checks their community numbers, and, if they are the same, it deletes with probability $1/2$ the one with lower fitness. Since the fitness value was already computed, the overall cost of the operator is clearly $O(1)$.

- The operator StochasticAging() goes through all the elements of the population and removes an element with the user defined probability P_{die}. Thus, its overall cost is $O(N)$.

- Finally, the operator Selection() chooses, without repetition of fitness values, the best d B cells among $P_a^{(pre)}$ and $P^{(hyp)}$. As I underlined before, the number of elements in these two populations is constant with respect to the size of the input, so I can simply say that the cost of the operator is $O(1)$.

In summary, the cost of one iteration of Opt-IA has a computational upper bound $O(N^2 + N) = O(N^2)$. Finally, let us take into consideration the number of iterations. I mentioned that for all the experiments concerning Opt-IA the number of generations was fixed to 1000. For the bigger graphs, it is a number smaller than the number of edges and about five times the number of vertices. It is clear,

though, that, contrary to the other parameters, the number of generations cannot be considered independent from the size of the input. The bigger the input, the bigger is the number of generations that I expect to need. However, how does it grow with respect to N? The possibility of keeping it constant for large graphs, and the results of my experiments tell us that such a growth is at worst linear with respect to N. Thus, if I want to be very cautious in estimating the overall complexity of Opt-IA, I can say that I need at most $c \cdot N$ generations to obtain good results. If I check again Figure 11.1, I see that. after about $250 \sim 2.5|V|$ generations, Opt-IA reaches the optimal solution. In general, I estimate that the number of generations is at most $5 \cdot |N|$. If I add such a bound on the overall computational analysis of Opt-IA , I can certainly claim that the upper bound for its running time is $O(N^3)$. If I study the computational cost of Hybrid-IA, I find very few differences with what I saw for Opt-IA. Namely,

- The operator Hypermutation() in the worst case moves all the vertices from one community to another, but it is still obviously $O(N)$.
- The operator Aging() goes through all the elements of the populations which I consider a constant number, again independent from the size of the input graph, so, all in all, it is $O(1)$.
- The operator LocalSearch() acts on every vertex of the given graph and explores its vicinity. Therefore, I can estimate that its work has an upper bound $O(N^2)$.

In summary, the cost of one iteration of Hybrid-IA has a computational upper bound $O(N^2)$, just like Opt-IA, though clearly higher internal constant factors. Such a constant factor is balanced by the number of generations. I fixed it to

100 for all the experiments, including the very large synthetic graphs, where I noted I should have probably had a larger number of generations. Once again, the number of generations cannot be considered independent from the size of the input. However, certainly for HYBRID-IA, it is asymptotically not larger than what I estimated for OPT-IA. Moreover, even assuming that its growth is linear with respect to $|V|$, the constant factor is definitively smaller. In any case, I can conclude that, also for HYBRID-IA, I have a computational upper bound $O(N^3)$.

11.5 Conclusions

Two novel immunological algorithms have been developed for the community detection, one of the most challenging problems in network science, with an important impact on many research areas. The two algorithms, respectively OPT-IA and HYBRID-IA, are inspired by the clonal selection principle, and take advantage of the three main immune operators of cloning, hypermutation, and aging. The main difference between the two algorithms is the designed search strategy: OPT-IA performs a random and blind search in the search space, and it is coupled with pure stochastic operators, whilst HYBRID-IA is based on a refinement of the current best solutions through a deterministic local search. The efficiency and efficacy of both algorithms have been tested on several real social networks, different both in complexity and size. From the experimental analysis, it emerges that OPT-IA, thanks to its structure, carries out a careful exploration of the solutions space, but it needs a larger number of iterations, whilst HYBRID-IA quickly discovers good solutions, and exploits them during the evolutionary cycle. OPT-IA and HYBRID-IA have also been compared with seven efficient metaheuristics (included one Hyper-Heuristic), and one greedy optimization method. The obtained outcomes

prove the reliability of both algorithms, showing competitiveness, and efficiency with respect to all other algorithms to which they are compared.

In particular, they prove that, under the same conditions, both OPT-IA and HYBRID-IA reach better solutions (i.e., higher modularity) than the other algorithms, including LOUVAIN. Moreover, these results, along with previous successful applications in several optimization tasks on networks, prove once again that my proposed immunological approach and algorithm is one of the best metaheuristics methods in literature.

Several points need to be carefully analyzed as future work, such as an appropriate parameters tuning, an improvement of effectiveness of the hypermutation operator, and local search method in order to build more efficiently the clusters, better guide the move of the nodes between the clusters, and speed up the convergence. Finally, an obvious future research direction is to tackle larger networks, especially biological ones, which are harder and of high relevance.

Table 11.2: Comparison of Opt-IA and Hybrid-IA on social networks with reference algorithms. For HDSA, BADE, SSGA, BB-BC, BA, and GSA the results are calculated over 30 independent runs, while for MA-Net over 50 independent runs.

		Algorithms									
Networks		**Louvain**	**Opt-IA**	**Hybrid-IA**	**HDSA**	**BADE**	**SSGA**	**BB-BC**	**BA**	**GSA**	**MA-Net**
	Best	**0.2768**	**0.2768**	**0.2768**	**0.2768**	**0.2768**	**0.2768**	**0.2768**	**0.2768**	**0.2768**	-
	Mean	-	0.2768	0.2768	0.2768	0.2768	0.2768	0.2766	0.2768	0.2768	-
Zebra	*Worst*	-	0.2768	0.2768	0.2768	0.2768	0.2768	0.2761	0.2768	0.2768	-
	σ	-	0.0000	0.0000	0.0000	0.0000	0.0000	0.0003	0.0000	0.0000	-
	k	4	4	4	4	4	4	4	4	4	-
	Best	0.4188	**0.4198**	**0.4198**	**0.4198**	**0.4198**	**0.4198**	**0.4198**	**0.4198**	**0.4198**	0.420
	Mean	-	0.4198	0.4198	0.4198	0.4188	0.4198	0.4196	0.4133	0.4170	0.419
Karate Club	*Worst*	-	0.4198	0.4198	0.4198	0.4156	0.4198	0.4188	0.3946	0.4107	-
	σ	-	0.0000	0.0000	0.0000	0.0018	0.0000	0.0004	0.0105	0.0037	0.002
	k	4	4	4	4	4	4	4	4	4	4
	Best	0.5185	**0.5285**	**0.5285**	**0.5285**	0.5268	0.5257	0.5220	0.5157	0.4891	0.529
	Mean	-	**0.5285**	0.5273	0.5282	0.5129	0.5200	0.5141	0.4919	0.4677	0.523
Dolphins	*Worst*	-	0.5268	0.5220	0.5276	0.4940	0.5156	0.5049	0.4427	0.4517	-
	σ	-	0.0003	0.0009	0.0005	0.0120	0.0040	0.0068	0.0289	0.0155	0.004
	k	5	5	5	5	4	5	5	4	6	5
	Best	0.5205	**0.5272**	**0.5272**	**0.5272**	0.5239	0.5221	0.4992	0.5211	0.4775	0.527
	Mean	-	0.5267	0.5270	**0.5272**	0.5178	0.5203	0.4914	0.5020	0.4661	0.526
Political Books	*Worst*	-	0.5063	0.5246	0.5272	0.5137	0.5167	0.4799	0.4815	0.4558	-
	σ	-	0.0028	0.0005	0.0000	0.0042	0.0024	0.0084	0.0149	0.0079	0.002
	k	4	5	5	5	4	5	9	3	5	5
	Best	**0.6046**	**0.6046**	**0.6046**	**0.6046**	0.5646	0.5330	0.5171	0.5523	0.4175	0.605
	Mean	-	0.5989	**0.6039**	0.6033	0.5513	0.5277	0.5061	0.5272	0.4032	0.601
Football	*Worst*	-	0.5736	0.6031	0.6019	0.5430	0.5189	0.4986	0.4742	0.3905	-
	σ	-	0.0078	0.0007	0.0009	0.0085	0.0057	0.0069	0.0325	0.0109	0.003
	k	10	10	10	10	11	6	10	7	5	10
	Best	**0.4451**	**0.4451**	**0.4451**	-	-	-	-	-	-	**0.445**
	Mean	-	0.4449	**0.4450**	-	-	-	-	-	-	0.445
Jazz Musicians	*Worst*	-	0.4449	0.4446	-	-	-	-	-	-	-
	σ	-	0.0001	0.0002	-	-	-	-	-	-	0.000
	k	4	4	4	-	-	-	-	-	-	4

Table 11.3: Comparison between HYBRID-IA and LOUVAIN on Synthetic Networks with 1000 and 5000 vertices, with respect to modularity (Q) and NMI evaluation metrics.

	HYBRID-IA		**LOUVAIN**		**DIFFERENCE**	
$(\|V\|, k, \mu_t)$	Q	NMI	Q	NMI	Q	NMI
(1000, 20, 0.1)	0.8606	**0.9980**	0.8607	0.9931	−0.0001	+0.0049
(1000, 20, 0.2)	0.7622	**0.9970**	0.7622	0.9909	0.0	+0.0061
(1000, 20, 0.3)	0.6655	**0.9927**	0.6642	0.9790	+0.0013	+0.0137
(1000, 20, 0.4)	0.5668	**0.9905**	0.5656	0.9588	+0.0012	+0.0317
(1000, 20, 0.5)	0.4685	**0.9857**	0.4685	0.9393	0.0	+0.0464
(1000, 20, 0.6)	0.3687	**0.9767**	0.3658	0.9084	+0.0029	+0.0683
(1000, 20, 0.7)	0.2707	**0.9127**	0.2635	0.6969	+0.0072	+0.2158
(5000, 20, 0.1)	0.8923	**0.9991**	0.8934	0.9589	−0.0011	+0.0402
(5000, 20, 0.2)	0.7927	**0.9966**	0.7948	0.9399	−0.0021	+0.0567
(5000, 20, 0.3)	0.6929	**0.9967**	0.6959	0.9282	−0.0030	+0.0685
(5000, 20, 0.4)	0.5931	**0.9945**	0.5975	0.9076	−0.0044	+0.0869
(5000, 20, 0.5)	0.4936	**0.9953**	0.5001	0.8789	−0.0065	+0.1164
(5000, 20, 0.6)	0.3939	**0.9976**	0.4027	0.8518	−0.0088	+0.1458
(5000, 20, 0.7)	0.2929	**0.9942**	0.3033	0.8064	−0.0104	+0.1878
(5000, 20, 0.7)	0.2929	**0.9942**	0.3033	0.8064	−0.0104	+0.1878

Chapter 12

Discovering Entities Similarities in Biological Networks Using a Hybrid Immune Algorithm

12.1 Introduction

In the last few years, significant advances in biological technology and the rapid adoption of high-throughput approaches [218] have made possible to measurement of tens of thousands of ”omic” data points across multiple levels (DNA, RNA, protein, metabolite, etc.) from a biological sample. The availability of a large amount of data has changed and revised the approach to the biology leading to the development of new methods based on the integration analysis of molecular data with mathematical models, and the consequently establishment and consolidation of the Systems Biology, an interdisciplinary research area that uses a holistic approach to the research biological by crossing the field of systems theory and applied mathematical methods with the aim to derive global models of cellular

processes in physiology and disease. The challenge from the systems biology perspective is how to convert the data into information and knowledge that improve patient personalized therapy. Becomes therefore necessary to carry out a high-level analysis from a representation of a biological system.

Networks are probably the most suitable tool for this type of investigation. They allow a representation of the binary relationships between biological entities and are for this reason the most used tool in systems biology [13, 15]. They also provide a mathematical representation of biological systems, within which nodes represent proteins, as in the case of protein-protein iteration networks, or genes and transcription factors, as in the case of regulation networks gene and gene co-expression networks, or representatives of metabolites, in the case of metabolic networks. These interactions determine the molecular and cellular mechanisms responsible for healthy and diseased states in organisms and can be physical or functional. In this second case the nodes of the network are associated with each other in modules, where a tightly connected group of nodes share a common function to perform a certain task. The modules detected by biological networks are generally responsible for a common phenotype and are useful in providing insights related to biological functionality. Disease phenotypes are generally caused by the failure of groups of genes that are referred to as the disease form. Since the genes responsible for a phenotype often have common functions, there is a strong association between pathological and functional modules [100, 10, 15]. The detection of modules within biological networks, generally responsible for a common phenotype, is useful and crucial in providing insights into the biological functionality of these genes. The techniques that allow the identification of modules, known as *community detection* techniques, are methods that play a

key role in obtaining the functional modules which appear to be closely related to pathological forms, the recognition of which would be useful for the molecular understanding and etiology of the disease. From this would arise the development of specific drugs whose targets would be the genes belonging to these modules.

In this research work, a hybrid immune algorithm for the community detection is proposed, which takes inspiration from the immune system dynamics, and it is based on carrying out an effective exploration of large search spaces, combining a random search process with a deterministic one, and in an efficient exploitation of the learning gained. Albeit the algorithm has been successful applied on several research areas, included also community detection [208, 50], the main goal of this work is to consolidate the goodness and reliability of the proposed algorithm in detecting community structures on large size biological networks. Furthermore, to pursue this aim, an investigation has been also conducted on how similar the detected communities to real ones are.

The rest of the paper is organized as follows. In section 12.2 is introduced and described the community detection problem and its relevance in biological context. The detection has been performed on the basis of modularity optimization, which is described, and formally defined in Sect. 12.2.1. The proposed and developed HYBRID-IA is explained in detail in Sect. 12.3. In Sect. 12.4 is presented a summary of the biological networks used as data set, whilst outcomes and comparisons are displayed and discussed in Sect. 12.5. In particular, in Sect. 12.5.1 is presented the convergence and learning analysis performed, while in Sect. 12.5.2 are discussed in detail all results obtained and all comparisons conducted. In Sect. 12.5.3, instead, are presented the investigation performed on Hybrid-IA with respect the NMI metric evaluation. Finally in Sect. 12.6 are given

and discussed the conclusions on this work.

12.2 Community Detection

Community detection is one of the most important research topics in network science and graph analysis, as it allows to understand the dynamics of a complex network at different scales [97, 104, 65], such as for instance connections and interactions between underlying entities, and, consequently, uncover many important information that become useful and crucial in many application areas: biology; medicine; economic; social sciences; and many others. However, modeling and examining complex systems is a very difficult process because the systems used for the real-world data representation contain highly important information: social relationships among people or information exchange and interactions between molecular structures. It follows, then, that the study of community structures in a network is central issue in better understanding such dynamics, and, for this, it has inspired intense research activities. Indeed, detecting highly linked communities can lead to many benefits, such as understanding how the elements of a network (biological genes, for instance) interact and affect each other. Informally, a community in a network is defined as a set of elements that are highly linked within the group and weakly linked to the outside.

The modularity (Q) is an evaluation measure commonly used for assessing the quality of node partitions detected in a network [170]. Hence, the community detection problem can be easily summed up in finding clustering that maximized Q, whose decision version has been proved to be a $\mathcal{NP}$-complete problem [27]. Several search algorithms for clustering problems have been developed and proved to be robust in finding as good communities as possible in complex networks

[168, 169]. However, from the literature is possible to note that metaheuristics approaches are more suitable on this optimization problem than exact methods, being able to find good solutions within reasonable computing times. This is due to the ability of the former to effectively tackle problems in complex, large and uncertain environments [213].

In this research paper a *Hybrid Immunological Algorithm* for the community detection problem, called HYBRID-IA, is proposed, which, in addition to the immune operators, makes use of a Local Search (LS) technique that deterministically tries to refine the solutions found. The goal of this paper is to prove the efficiency, robustness, and primarily reliability of HYBRID-IA in community detection, with main reference to the biological networks.

12.2.1 Modularity Optimization in Networks

Community detection is then a powerful tool to understanding the structure of complex networks, and ultimately extracting useful information from them. Note that a closely connection imply a faster rate of information transmission, instead of a loosely connected community. On the one hand, a network is represented by a number of individual nodes connected by edges, with a certain degree of interaction between some nodes; on the other hand, communities are defined as groups of nodes, densely interconnected, but in sparse order with the rest of the network. The modularity is based on the idea that a random graph is not expected to have a community structure, therefore, the possible existence of communities can be revealed by the difference of density between vertices of the graph and vertices of a random graph with the same size and same degree distribution.

Formally modularity is defined as follow: given an undirected graph $G = (V, E)$,

with V the set of vertices ($|V| = N$), and E the set of edges ($|E| = M$), the modularity of a community is defined by:

$$Q = \frac{1}{2M}\left[\sum_{i=1}^{N}\sum_{j=1}^{N}\left(A_{ij} - \frac{d_i d_j}{2M}\right)\delta(i,j)\right], \tag{12.1}$$

where A_{ij} is the adjacency matrix of G, d_i and d_j are the degrees of nodes i and j respectively; $\delta(i,j) = 1$ if i, j belong to the same community, 0 otherwise.

As asserted in [27], the modularity value for unweighted and undirected graphs lies in the range $[-0.5, 1]$, therefore, a low Q value (close to the lower bound) reflects a bad graph partitioning, and implies the absence of real communities; good partitions are instead identified by a higher modularity value that implies the presence of highly cohesive communities. For a trivial clustering, with a single cluster, the modularity value is 0. Interestingly, the modularity has the tendency to produce large communities and, therefore, fails in detecting communities that are comparatively small with respect to the network [95]. Taking into account the Q modularity as an evaluation measure, the community detection can easily be seen as a combinatorial optimization problem as the problem aims to find a clustering that maximize Q.

12.3 Hybrid-IA: the Hybrid Immune Algorithm

Immunological Algorithms (IA) are among the most used population-based meta-heuristics, successfully applied in search and optimization tasks. They take inspiration from the dynamics of the immune system in performing its job of protecting living organisms. One of the features of the immune system that makes it a very good source of inspiration is its ability to detect, distinguish, learn, and remember all foreign entities discovered [96]. Hybrid-IA [50] uses a deterministic local

search, based on rational choices that refine and improve the solutions found so far and belongs to the special class *Clonal Selection Algorithms* (CSA) [178, 49], whose efficiency is due to the three main immune operators: (i) cloning, (ii) hypermutation, and (iii) aging. Furthermore, this algorithm is based on two main concepts: antigen (Ag), which represents the problem to tackle, and B cell, or antibody (Ab) that represents a candidate solution, i.e. a point in the solution space. At each time step t, the algorithm maintains a population of d candidate solutions: each solution is a subdivision of the vertices of the graph $G = (V, E)$ in communities. Let $N = |V|$, a B cell $\vec{x}$ is a sequence of N integers belonging to the range $[1, N]$, where $x_i = j$ indicates that the vertex i has been added to the cluster j. The population is initialized at the time step $t = 0$ randomly assigning each vertex i to a group j, with $j \in [1, N]$. Just after the initialization step, the algorithm evaluate the fitness function of each generated element ($\vec{x} \in P^{(t)}$), i.e. Equation 12.1, using the procedure ComputeFitness($P^{(t)}$) HYBRID-IA ends its evolution once the halting criterion is reached, which was fixed to a maximum number of generations (T_{max}). The pseudocode of HYBRID-IA is described in Algorithm 4.

Cloning is the first immune operator to be carried out, which simply copies dup times each B cell producing an intermediate population $P^{(clo)}$ of size $d \times dup$. A static version was considered for avoiding premature convergences, which can instead occur using the proportional one. Indeed, if a number of clones proportional to the fitness value is produced, preferring the cloning of the best through a higher number of clones, already in the first iterations is very likely that a population of B cells very similar to each other is obtained, with the outcome to cannot perform a proper exploration of the search space, and thus getting easily trapped in local optima. Once a clone is created, HYBRID-IA assigns an age to it that determines

Algorithm 4 Pseudo-code of HYBRID-IA.

1: **procedure** HYBRID-IA(d, dup, ρ, τ_B)
2: $t \leftarrow 0$
3: $P^{(t)} \leftarrow$ InitializePopulation(d)
4: ComputeFitness($P^{(t)}$)
5: **while** ¬StopCriterion **do**
6: $P^{(clo)} \leftarrow$ Cloning($P^{(t)}, dup$)
7: $P^{(hyp)} \leftarrow$ Hypermutation($P^{(clo)}, \rho$)
8: ComputeFitness($P^{(hyp)}$)
9: $(P_a^{(t)}, P_a^{(hyp)}) \leftarrow$ Aging($P^{(t)}, P^{(hyp)}, \tau_B$)
10: $P^{(select)} \leftarrow (\mu + \lambda)-$Selection($P_a^{(t)}, P_a^{(hyp)}$)
11: $P^{(t+1)} \leftarrow$ LocalSearch($P^{(select)}$)
12: ComputeFitness($P^{(t+1)}$)
13: $t \leftarrow t + 1$;
14: **end while**
15: **end procedure**

how long the clone/solution can live inside the population: from such assigned age until it reaches the maximum age allowed τ_B (user-defined parameter). Specifically, a random age chosen in the range $[0 : \frac{2}{3}\tau_B]$ is assigned to each clone. In this way, each clone is guaranteed to stay in the population for at least a fixed number of generations ($\frac{1}{3}\tau_B$ in the worst case). The age assignment and the aging operator (described below) play a crucial role on HYBRID-IA performances, and any evolutionary algorithm in general, because they are able to keep a right amount of diversity among the solutions, helping thus the algorithm to avoid premature convergences [64].

The aims of the *hypermutation* operator is to generate new elements, acting on each clone in $P^{(clo)}$, with the main purpose to efficiently and carefully explore the search space. Just as happens in the natural immune system, the number of changes on each clone, called *mutation rate*, is determined through an *inversely proportional* law to the fitness function value of the B cell considered: better the fitness value of the solution, smaller the relative mutation rate will be. In particular, let $\vec{x}$ be a cloned B cell, the mutation rate $\alpha = e^{-\rho \hat{f}(\vec{x})}$ is defined as the probability to move a node from one community to another one, where ρ is a user-defined parameter that determines the shape of the mutation rate, and $\hat{f}(\vec{x})$ is the fitness function normalized in the range $[0, 1]$. In Figure 12.1 is shown how the mutation shape ρ affects the probability α for different values of fitness function.

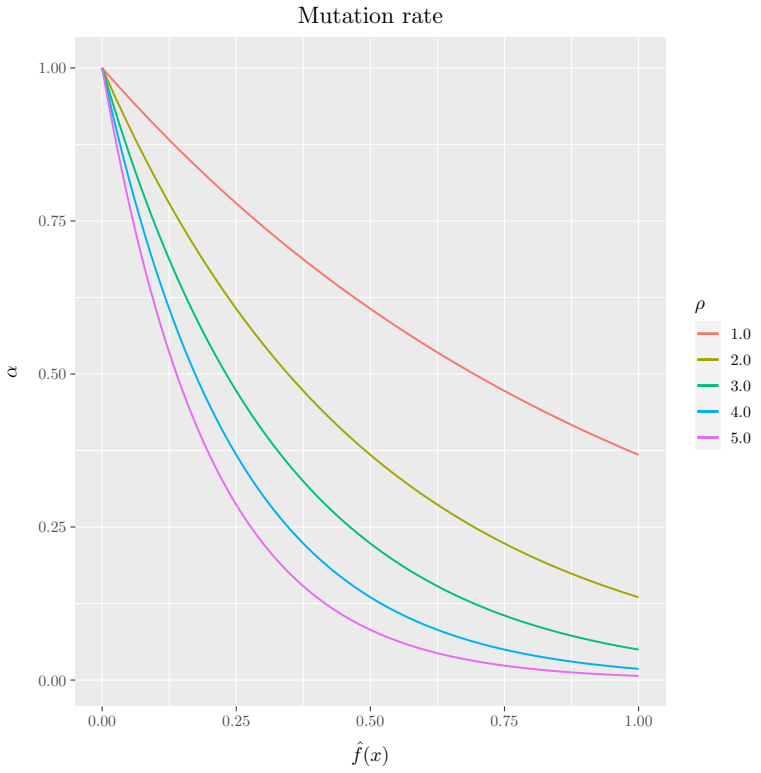

Figure 12.1: The mutation rate α for different values of the mutations shape ρ.

Formally, it works as follows: for each B cell, two communities c_i and c_j are randomly chosen ($c_i \neq c_j$): the first one is chosen among all existing ones, while the second one in the range $[1, N]$. Then, all vertices in c_i are moved to c_j with probability given by α. If a value that does not correspond to any currently existing community is assigned to c_j, a new community c_j is created and added to the existing ones. Depending on c_j, I can have a merging operator (Figure 12.2), where a subset of vertices will be moved to another community, or splitting operator (Figure 12.2), where a same subset of nodes will create a new community. The idea behind this approach is create and discover new communities by moving a variable percentage of nodes from existing communities. This search method balances the effects of local search (as described below), by allowing the algorithm to avoid premature convergences towards local optima.

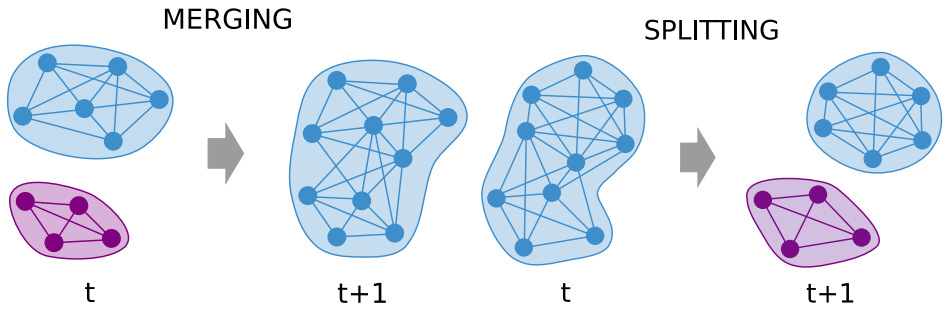

Figure 12.2: Hypermutation operator. A subset of nodes from community c_i will be merged to an existing community c_j. A subset of nodes from community c_i will be splitted to create a new community c_j.

The *static aging operator* is the one that plays in the overall the central role on the efficiency and reliability of Hybrid-IA, particularly when it is applied on complex and large problems. It simply acts on each mutated B cells by removing older ones from the two populations $P^{(t)}$ and $P^{(hyp)}$. Let τ_B be the maximum number

of generations allowed for every B cell to stay in the population; once the age of a B cell exceeds τ_B (age = τ_B+1), it will be removed from the relative population, independently from its fitness value. However, an exception may be done for the best current solution, which is kept alive even if its age is older than τ_B. Such variant is called *elitist aging operator*. The purpose of this operator is, then, allow the algorithm to escape and jump out from local optima, assuring a proper turnover between the B cells in the population, and producing, consequently, high diversity among them.

The last operator to be performed within the evolutionary cycle is the $(\mu + \lambda)$-*Selection operator*, with $\mu = d$ and $\lambda = (d \times dup)$, which has the aim to select the best d survivors from both populations $P_a^{(t)}$ and $P_a^{(hyp)}$, producing a temporary population $P^{(select)}$, on which the local search will be performed later. Basically it identifies the best d elements among the set of offsprings and the parent B cells (those survived to the aging step), ensuring monotonicity in the evolution dynamics.

The local search designed and introduced is the key operator to properly speed up the convergence of the algorithm, and, in a way, drive it towards more promising regions. Furthermore, it intensifies the search and explore the neighborhood of each solution using the well-known *Move Vertex* approach (MV) [124]. The basic idea of the proposed LS is to assess deterministically if it is possible to move a node from its community to another one within its neighbors. The MV approach takes into account the *move gain* that can be defined as the variation in modularity produced when a node is moved from a community to another. Before formally defining the move gain, it is important to point out that the modularity Q, defined

in Equation (12.1), can be rewritten as:

$$Q(c) = \sum_{i=1}^{k} \left[\frac{\ell_i}{M} - \left(\frac{d_i}{2M} \right)^2 \right], \tag{12.2}$$

where k is the number of the found communities; $c = \{c_1, \ldots, c_i, \ldots c_k\}$ is the set of communities that is the partitioning of the set of vertices V; l_i and d_i are, respectively, the number of links inside the community i, and the sum of the degrees of vertices belonging to the i community. Thus, the *move gain* of a vertex $u \in c_i$ is the modularity variation produced by moving u from c_i to c_j, that is:

$$\Delta Q_u(c_i, c_j) = \frac{l_{c_j}(u) - l_{c_i}(u)}{M} + d_V(u) \left[\frac{d_{c_i} - d_V(u) - d_{c_j}}{2M^2} \right], \tag{12.3}$$

where $l_{c_i}(u)$ and $l_{c_j}(u)$ are the number of links from u to nodes in c_i and c_j respectively, and $d_V(u)$ is the degree of u when considering all the vertices V. If $\Delta Q_u(c_i, c_j) > 0$, then moving node u from c_i to c_j produces an increment in modularity, and therefore a possible improvement. Consequently, the goal of MV is to find a node u to move to an adjacent community in order to maximize ΔQ_u:

$$arg \max_{v \in Adj(u)} \Delta Q_u(i, j), \tag{12.4}$$

where $u \in C_i$, $v \in C_j$ and $Adj(u)$ is the adjacency list of node u.

For each solution in $P^{(select)}$, the Local Search begins by sorting the communities in increasing order with respect to the ratio between the sum of inside links and the sum of the node degrees in the community. In this way, poorly formed communities are identified. After that, MV acts on each community of the solution, starting from nodes that lie on the border of the community, that is, those that have at least an outgoing link. In addition, for communities, the nodes are sorted with respect to the ratio between the links inside and node degree. The key idea behind LS is to deterministically repair the solutions which were produced by the

hypermutation operator, by discovering then new partitions with higher modularity value. Equation (12.3) can be calculated efficiently because M and $d_V(u)$ are constants, the terms l_{c_i} and d_{c_i} can be stored and updated using appropriate data structures, while the terms $l_{c_i}(u)$ can be calculated during the exploration of all adjacent nodes of u. Therefore, the complexity of the move vertex operator is linear on the dimension of the neighborhood of node u.

12.4 Biological Networks Data Set

In this section, the eight different biological networks used during the tests are summarized, and for which the communities were identified. They are grouped into the three types described below and refer to biological interactions and main molecular networks.

12.4.1 Protein-Protein Interaction Networks

The physical interaction between the proteins have always been an important consideration for the gene function. Proteins are the main participants in a variety of biological processes inside cells, including signal transduction, homeostasis control, maintenance of internal balance and developmental processes [237]. They rarely function independently but form protein complexes [102]. The mathematical representation of the physical contacts between proteins inside the cell can be obtained through a non-direct binary physical PPI network [140], in which nodes represent proteins and whose edges connect pairs of interacting proteins. By considering the spatial and temporal aspects of interactions, networks can help understand the general organization of protein-protein connections and discover

the principles of their organization within the cell. These have a fundamental role in all biological processes and in all organisms [218], therefore a complete knowledge of PPIs and their protein interconnections, would allow the understanding of cell physiology in pathogenic (and normal) states. This would have a great impact for disease diagnosis, disease genes often interact with other disease genes [100], as well as for drug discovery and disease treatment [152, 215, 66]. In this work, two small *Cattle PPI* and *Helicobacter pylori PPI* Protein-Protein interactions [33, 226, 183] and two large networks (with a number of vertices > 2000), related to Yeast PPI instances [229, 28] have been considered. All networks in question are related to the data of interactions between proteins in the three different organisms mentioned before (cattle, helicobacter pylori and yeast) where each node represents a protein and they are linked if they interact physically within the cell.

12.4.2 Metabolic Networks

With the technological advancement and the sequencing of whole genomes, as well as it has been possible to reconstruct the protein-protein interaction networks described above, it has also been possible to obtain the networks of biochemical reactions in many organisms. Metabolic networks are powerful tools to represent and study a complete set of relationships between metabolites, a small chemical compound, and proteins/enzymes. They describe the set of processes and reactions that determine the biochemical and physiological properties of a cell, including the chemical reactions of metabolism, the metabolic pathways and regulatory interactions that drive these reactions. Metabolic networks make it possible to detect diseases given an enzymatic defect in a reaction that can affect flows in subsequent reactions. These defects often cause cascading effects responsible for

associated metabolic diseases [136]. Therefore, this type of networks can be used to understand if metabolic disorders are linked due to their related reactions [195]. In order to investigate this functional information, it's necessary to identify the functional modules in it [228]. Identify the communities in the metabolic networks will help in understanding the pathways and cycles in metabolic networks [94]. In the two considered real networks, the metabolic network of *Caenorhabditis elegans* and *E. Coli bacteria* [71, 198], each vertex represents a metabolite, and each direct link a reaction between them that binds the metabolite with the reaction product.

12.4.3 Transcriptional Regulatory Networks

Understanding the mechanisms underlying the regulation of gene expression is the main goal of contemporary biology. Important cellular processes, such as cell differentiation, cell cycle and metabolism are controlled by the complex biological mechanism of gene regulation. However, the relationship between structure and regulatory function is not easy to observe experimentally. Therefore, a Systems Biology-based approach is needed. In this regard, network theory is useful for understanding the activity behind these complex transcriptional regulatory mechanisms [14]. The transcriptional network can be represented as a direct graph, composed of transcription factors (TFs) and target genes (TGs) which are regulated in a tightly coordinated way. Within the network each node represents a gene (or operon, in the case of prokaryotic organisms) and the edges represent direct transcriptional regulation. Each edge is directed from a gene (or operon) that encodes a transcription factor to a gene (or operon) that is regulated by that transcription factor. Transcription factors are modular proteins that regulate the

gene expression of other proteins by binding to specific sites in the DNA (promoter sites) and allowing (or preventing) the synthesis of mRNA. The relationships between TFs and their targets (TGs) determines a given phenotype [186]. Moreover, in transcription regulatory networks, modules (or communities) correspond to sets of co-regulated genes [32, 145, 223, 240]. For this reason, the problem of community detection, plays a relevant role [214]. Escherichia coli and Saccharomyces cerevisiae are two well-known organisms often used as a model for studying gene regulation. In this work, two transcriptional regulatory network, *E. Coli TRN* and *Yeast TRN* [204, 150] have been considered, constituted by transcription factors and target genes, where each edge in network is directed from an operon that encodes a TF to an operon that it directly regulates.

12.4.4 Synthetic Networks

In addition to real biological networks, artificial instances were also taken into account in the experimental phase. These synthetic networks can be generated with different characteristics and with a known community structure. Using these kind of networks, allows to test the algorithms on different scenarios and gives the possibility of evaluating the goodness of the detected communities. The algorithm used to generate these synthetic networks is the *LFR benchmarks*, proposed in [135, 134]. The algorithm assumes that both the distributions of degree and community size are power laws, with exponents τ_1 and τ_2, respectively. The mixing parameter μ_t, identifies the relationship between the node's external and internal degree. In particular, each vertex of the networks shares a fraction $1 - \mu_t$ of its edges with the other vertices of its community and a fraction μ_t with other vertices outside of its community. Also, the LFR benchmarks can be used to generate directed

and weighted synthetic networks with overlapping communities. More details on the LFR algorithm about key parameters and how to generate benchmark can be found in [135, 134].

12.5 Experimental results

For evaluating the efficiency and reliability of HYBRID-IA, many experiments have been performed on all biological networks described above. In each experiment HYBRID-IA maintains a population of $d = 100$ B cells; uses a duplication parameter $dup = 2$; keeps a solution for at most $\tau_B = 5$ generations within the population; and uses $\rho = 1.0$ as mutation shape.

12.5.1 Convergence and Learning Analysis

In the initial part of the experimental phase, the analysis has been focused on the convergence behavior and learning rate in order to inspect the efficiency of HYBRID-IA. For this study, artificial networks have been taken into account as benchmark instances, which have been generated by the LFR algorithm [135, 134] and described in Section 12.4.4. In particular, networks with 1000 nodes and average degree 15 and 20, and networks with $|V| = 5000$ and average degree 20 and 25 have been generated. For each of these networks generated, the maximum degree was set to 50, while the exponents of the power laws, which control the degree and community sizes distribution (τ_1 and τ_2), have been set to 2 and 1, respectively. A minimum of 10 nodes to a maximum of 50 have been set as sizes of the communities. The mixing parameter μ_t was fixed to 0.5. Finally, for these experiments, a maximum number of generations $T_{max} = 100$ was set, and 5 random

instances were generated for each network parameters configuration.

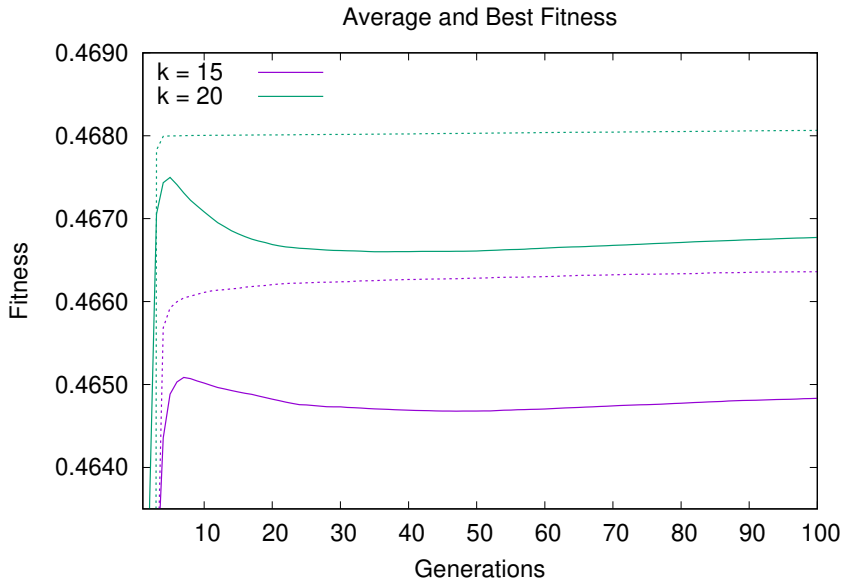

Figure 12.3: Convergence behavior of HYBRID-IA: average and best fitness value versus generations on `LFR(1000,15,0.5)` and `LFR(1000,20,0.5)`.

In Figure 12.3 is shown the convergence plot on the LFR instances with 1000 nodes and average degree k of 15 and 20. The two curves represent the best and average fitness of the population and both are averaged over 100 independent runs. From this plot can be noted how the two curves of the best fitness have the same trend for both values of k: reach a high value of modularity in the early generations and then improves slowly. The improvement for $k = 20$ compared to the first generations is minimal, while for $k = 15$ the increase in modularity is slightly more significant. Instead, the average fitness curves have a similar trend in the first generations, but subsequently decrease and then gradually increase. From these two curves can be seen how the population maintains a good degree of diversity within the population, favoring thus a better exploration of the search space.

A similar situation can be also observed on the LFR instances with 5000 nodes.

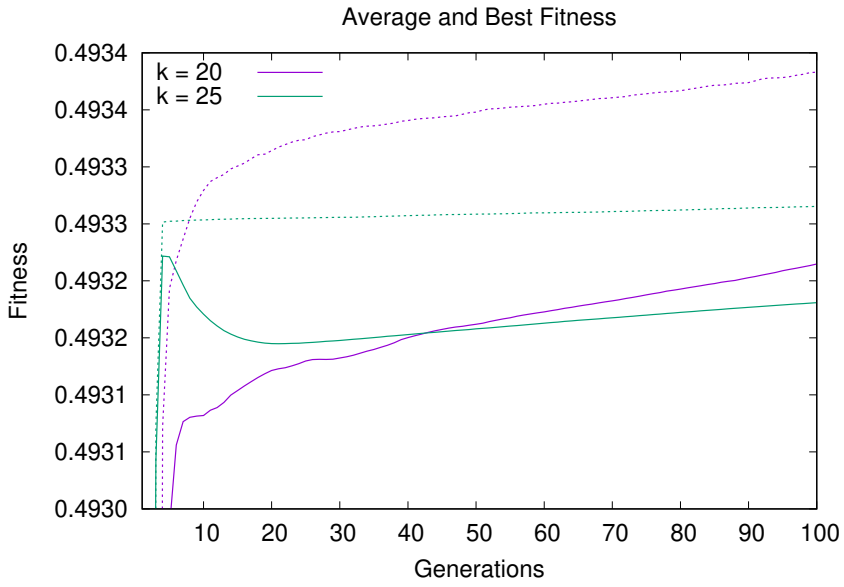

Figure 12.4: Convergence behavior of Hybrid-IA: average and best fitness value versus generations on `LFR(5000,20,0.5)` and `LFR(5000,25,0.5)`.

The plots in Figure 12.4 shows the best and average fitness of the population for $k = 20$ and $k = 25$. For $k = 25$, Hybrid-IA obtains a high value of modularity in a few generations, and after that it stays in a steady-state for the rest of the execution, reaching a high-modularity plateau [101]. On the other hand, for $k = 20$ the algorithm has a growth much more constant and linear, both in terms of the best solution and average of the population. Also in this case, the two curves of best and average fitness are well separated, indicating that the algorithm maintains a good diversity of solutions within the population.

Once analyzed the convergence behavior, an investigation on the learning ability of Hybrid-IA has been performed as well, using the information gain that measure the quantity of information the algorithm gains during the evolutionary process

[132, 52], that is the amount of information learned compared to the randomly generated initial population. At each generations t, let B_m^t be the number of the B cells that have the fitness function value to m; the candidate solutions distribution function $f_m^{(t)}$ can be defined as the ratio between the number B_m^t and the total number of candidate solutions:

$$f_m^{(t)} = \frac{B_m^t}{\sum_{m=0}^{h} B_m^t} = \frac{B_m^t}{d}. \tag{12.5}$$

It follows that the information gain $K(t, t_0)$ can be calculated as:

$$K(t, t_0) = \sum_m f_m^{(t)} \log(f_m^{(t)} / f_m^{(t_0)}). \tag{12.6}$$

The plots in Figures 12.5 and 12.6 show the information gain obtained by the algorithm during its running in different scenarios. For both values of $|V|$, HYBRID-IA is able to learn information step by step, showing thus an increasing curve until to reach a steady-state, which is exactly when the modularity of all solutions begins to become similar. The monotonically increasing of the information gain curve until reaching a steady-state is consistent with the *maximum information-gain principle*: $\frac{dK}{dt} \geq 0$.

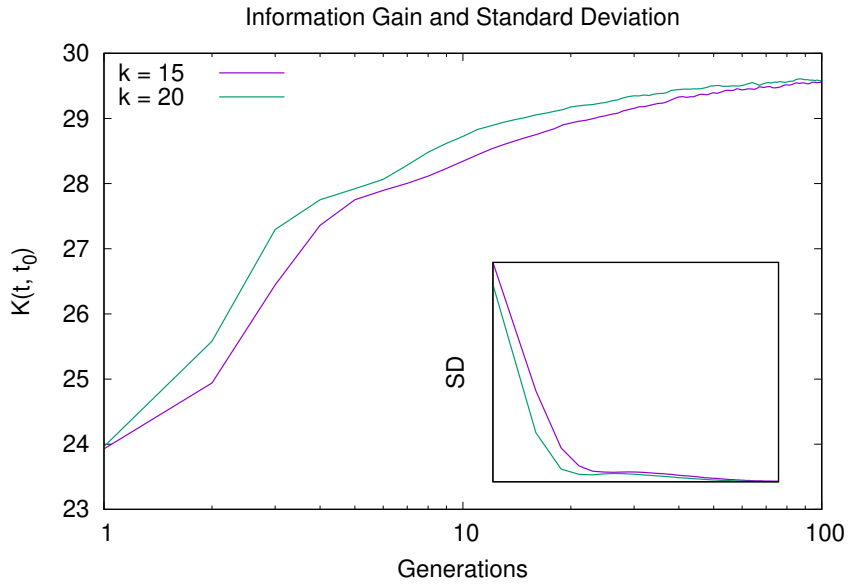

Figure 12.5: Learning ability of HYBRID-IA: information gain and standard deviation versus generations on `LFR(1000,15,0.5)` and `LFR(1000,20,0.5)`,

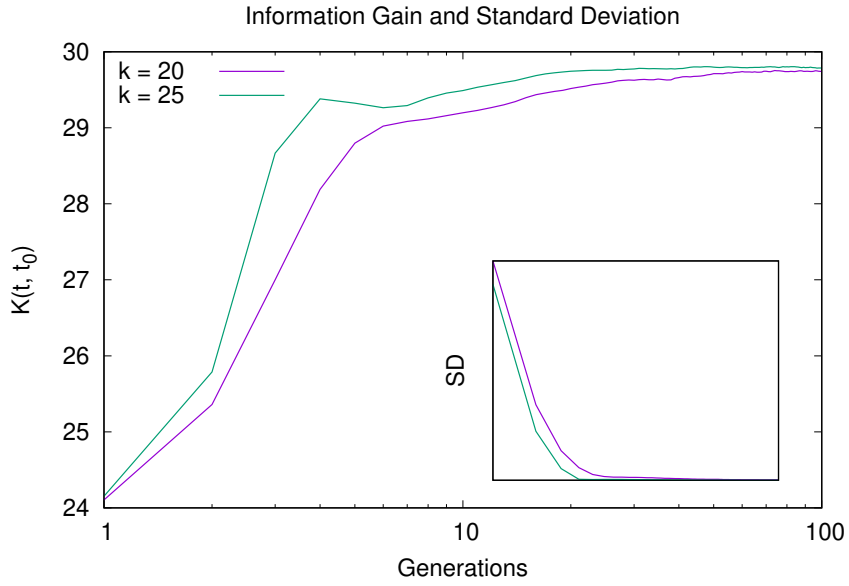

Figure 12.6: Learning ability of HYBRID-IA: information gain and standard deviation versus generations on `LFR(5000,20,0.5)` and `LFR(5000,25,0.5)`.

In the overall, the convergence behavior and learning process analyzed (Figs. 12.3, 12.4 and 12.5, 12.6), suggest that HYBRID-IA finds very quickly good solutions in networks with medium/high density (i.e. $k = 20$ for 1000 nodes and $k = 25$ for 5000), as the community structure is well-defined. On the other hand, on sparse networks, with an unclear community structure, the algorithm converges more slowly. In addition, a convergence analysis on the network *E.coli MRN* [198] was carried out, which presents a very low density (less than 1%). In Figures 12.7 and 12.8 are shown the plots relative to the run in which Hybrid-IA has reached its best solution. Again, after the initial climb, the algorithm begins its exploration around the solutions found, gradually improving. In some places (inset plot of Figure 12.7) the algorithm seems to stagnate in some local optima but, thanks to the *aging* operator, manages to escape, finding better solutions. During these phases, the population tends to reduce its diversity, being almost entirely composed of solutions of equal quality.

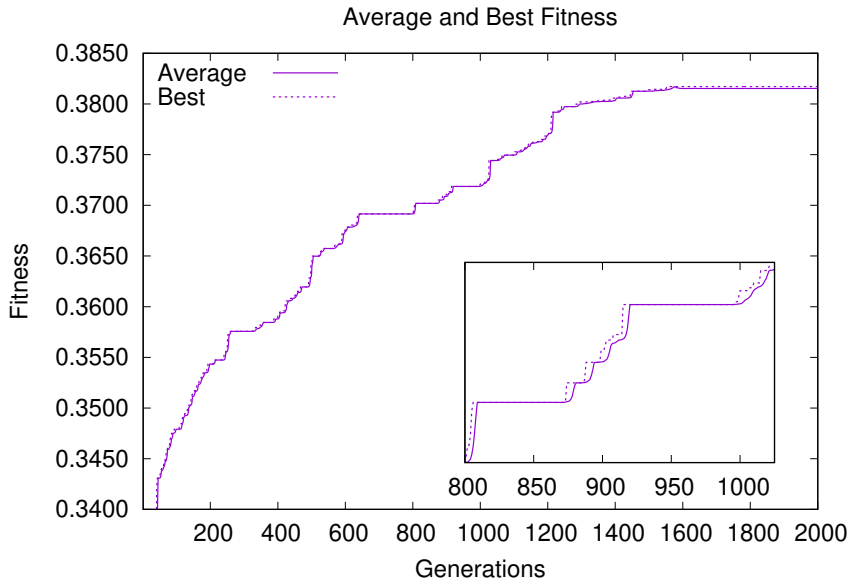

Figure 12.7: Convergence behaviour of HYBRID-IA on *E.coli MRN* network. Average and best fitness value of the population versus generations.

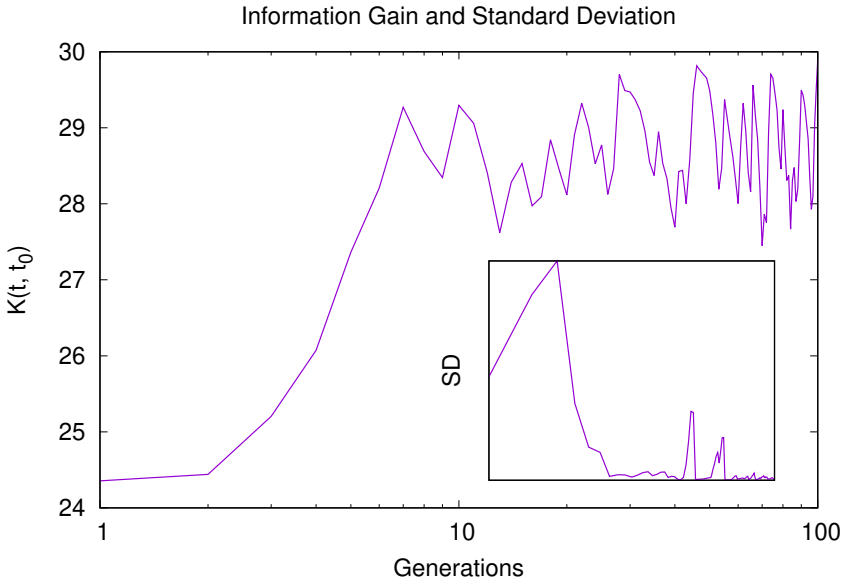

Figure 12.8: Convergence behaviour of HYBRID-IA on *E.coli MRN* network Information gain and standard deviation versus generations.

12.5.2 The Biological Networks

In this section, the outcomes obtained by HYBRID-IA on the biological networks, described above and summarize in Table 12.1, are presented and analyzed. For proving the competitiveness and reliability of HYBRID-IA with respect to the state of the art and assessing its performance in general, the algorithm was compared to other well-known metaheuristics, each based on a modularity optimization approach [9]. In particular, it was compared with an effective Hyper-Heuristics

Table 12.1: The biological networks used in the experiments.

Name	*Ref*	$\|V\|$	$\|E\|$
Cattle PPI	[33]	268	303
E.coli TRN	[204]	418	519
C.elegans MRN	[71]	453	2025
Yeast TRN	[150]	688	1078
Helicobacter pylori PPI	[226],[183]	724	1403
E.coli MNR	[198]	1039	4741
Yeast PPI (1)	[229]	2018	2705
Yeast PPI (2)	[28]	2284	6646

Differential Search Algorithm based on the migration of artificial superorganisms (HDSA) [39]; an improved Bat Algorithm based on Differential Evolution algorithm (BADE) [210]; a Scatter Search algorithm based on the Genetic Algorithm (SSGA) [99, 146]; a modified Big Bang–Big Crunch algorithm (BB-BC) [74], the original Bat Algorithm based on echolocation behavior of bats adapted for community detection (BA) [227]; and the original Gravitational Search Algorithm,

re-designed for solving the community detection problem (GSA) [185]. Further, the LOUVAIN algorithm [25], a greedy optimization method that attempts to optimize the modularity, was also considered for the comparison. The parameter configuration used by HYBRID-IA is the same described above, whilst the number of generations (T_{max}) considered depends on the size of the biological network tested: for instances with less than 1000 nodes, T_{max} was set to 1000, while for the ones with more than 1000 nodes, T_{max} is 2000.

Table 12.2 displays the detailed results of HYBRID-IA in comparisons to the others, and presents, for each algorithm, the best values of the Q modularity ($Best$) found, the average of the values ($Mean$), the worst modularity ($Worst$), the standard deviation (StD) and the number of community structures (k) detected by the best solution. Noticeably, proposed HYBRID-IA algorithm outperformed all metaheuristics in terms of both the value of modularity obtained and mean value, except HDSA in the *E.coli TRN* biological network, although it still provides an upper limit very close to that obtained. It is important to highlight that HYBRID-IA results underline the efficiency of the proposed algorithm, also proved by the fact that the average values obtained on *Cattle PPI*, *E. Coli TRN*, *C. elegans MRN* and *Helicobacter pylory PPI networks* are better than the $Best$ modularity values obtained by the other algorithms, with the exception of the Hyper-heuristic Differential Search Algorithm (HDSA). Furthermore, from the analysis of the results obtained by the LOUVAIN algorithm, the only deterministic algorithm included in the comparison, it is clear how HYBRID-IA performs well equating the modularity value in the *Cattle PPI* dataset, and exceeding it in the *C. Elegans MRN* and *E. Coli MRN* networks. For these datasets, the Figures 12.9, 12.12, 12.13 show the detected community structures by HYBRID-IA. Figure 12.10 shows the commu-

Table 12.2: Comparisons of the results of HYBRID-IA obtained on biological networks with other algorithms. The results are calculated over 100 independent runs for HYBRID-IA and LOUVAIN, while over 30 runs for the rest.

Name		HYBRID-IA	LOUVAIN	HDSA	BADE	SSGA	BB-BC	BA	GSA
	k	40	40	40	41	40	48	42	43
	Best	0.7195	0.7195	0.7195	0.7183	0.7118	0.7095	0.7143	0.7053
Cattle PPI	Worst	0.7011	0.7181	0.7194	0.7059	0.7052	0.7079	0.7063	0.6949
	Mean	0.7154	0.7193	0.7195	0.7138	0.7079	0.7084	0.7100	0.6983
	StD	0.0037	0.0005	0.0001	0.0051	0.0025	0.0007	0.0035	0.0041
	k	43	41	47	58	61	71	56	61
	Best	0.7785	0.7793	0.7822	0.7680	0.7507	0.7520	0.7629	0.7416
E.coli TRN	Worst	0.7563	0.7747	0.7808	0.7560	0.7412	0.7452	0.7542	0.7328
	Mean	0.7701	0.7779	0.7815	0.7621	0.7457	0.7485	0.7599	0.7375
	StD	0.0049	0.0011	0.0006	0.0043	0.0035	0.0026	0.0034	0.0034
	k	10	10	13	25	22	21	22	24
	Best	0.4506	0.4490	0.4185	0.3473	0.3336	0.3374	0.3514	0.3063
C.elegans MRN	Worst	0.4321	0.4216	0.3962	0.3335	0.3124	0.3194	0.3356	0.2974
	Mean	0.4437	0.4365	0.4074	0.3385	0.3220	0.3266	0.3438	0.3039
	StD	0.0040	0.0049	0.0010	0.0054	0.0077	0.0074	0.0073	0.0037
	k	33	26	-	-	-	-	-	-
	Best	0.7668	0.7683	-	-	-	-	-	-
Yeast TRN	Worst	0.7363	0.7489	-	-	-	-	-	-
	Mean	0.7569	0.7607	-	-	-	-	-	-
	StD	0.0050	0.0033	-	-	-	-	-	-
	k	51	24	52	69	70	75	62	77
	Best	0.5359	0.5462	0.5086	0.4926	0.4726	0.4681	0.4900	0.4600
Helicobacter pylori PPI	Worst	0.5104	0.5356	0.5048	0.4809	0.4659	0.4642	0.4738	0.4549
	Mean	0.5240	0.5410	0.5078	0.4854	0.4695	0.4660	0.4814	0.4567
	StD	0.0056	0.0025	0.0017	0.0047	0.0021	0.0018	0.0073	0.0020
	k	13	8	-	-	-	-	-	-
	Best	0.3817	0.3734	-	-	-	-	-	-
E.coli MRN	Worst	0.3598	0.3450	-	-	-	-	-	-
	Mean	0.3695	0.3583	-	-	-	-	-	-
	StD	0.0042	0.0058	-	-	-	-	-	-
	k	159	46	-	-	-	-	-	-
	Best	0.5796	0.5961	-	-	-	-	-	-
Yeast PPI (2)	Worst	0.5524	0.5870	-	-	-	-	-	-
	Mean	0.5652	0.5925	-	-	-	-	-	-
	StD	0.0052	0.0019	-	-	-	-	-	-
	k	353	213	-	-	-	-	-	-
	Best	0.7002	0.7648	-	-	-	-	-	-
Yeast PPI (1)	Worst	0.6602	0.7519	-	-	-	-	-	-
	Mean	0.6798	0.7609	-	-	-	-	-	-
	StD	0.0078	0.0022	-	-	-	-	-	-

nities generated for *E.coli TRN* network. For the other instances considered, the modularity is however close to the optimal one. Finally, as will be explained in detail in the next section, although LOUVAIN manages to achieve a better maximization of the modularity value than the ones achieved by HYBRID-IA, the latter reveals a higher number of communities. This is due to the different nature of two algorithms, where LOUVAIN algorithm tends to aggregate communities.

12.5.3 Normalized Mutual Information

In order to uphold the efficiency and reliability of HYBRID-IA in detecting strong communities, a new evaluation metric has been considered. Thanks to the advantages offered by the synthetic networks (see Section 12.4.4), the *Normalized Mutual Information* (NMI) [61] has been taken into account, which is a widely used measure to compare community detection methods as it discloses the similarity between the genuine community (target) and the detected community structures. While the modularity allows for getting the measure of how cohesive the detected communities are, the NMI allows for assessing how similar they are concerning the real ones. For this analysis a new dataset of LFR instances has been generated, with the mixing parameter μ_t that ranges from 0.1 to 0.8.

In Table 12.3, the HYBRID-IA outcomes on these new synthetic datasets are reported and compared to the ones obtained by LOUVAIN. The features of the LFR networks tested are shown in the first column; for each of these parameters, 5 random instances have been generated. The values of modularity Q and NMI have been computed over 100 independent runs for both algorithms. Analysing the comparison, it is possible to see how LOUVAIN outperforms HYBRID-IA in almost all networks with 1000 vertices with respect to the Q modularity metric,

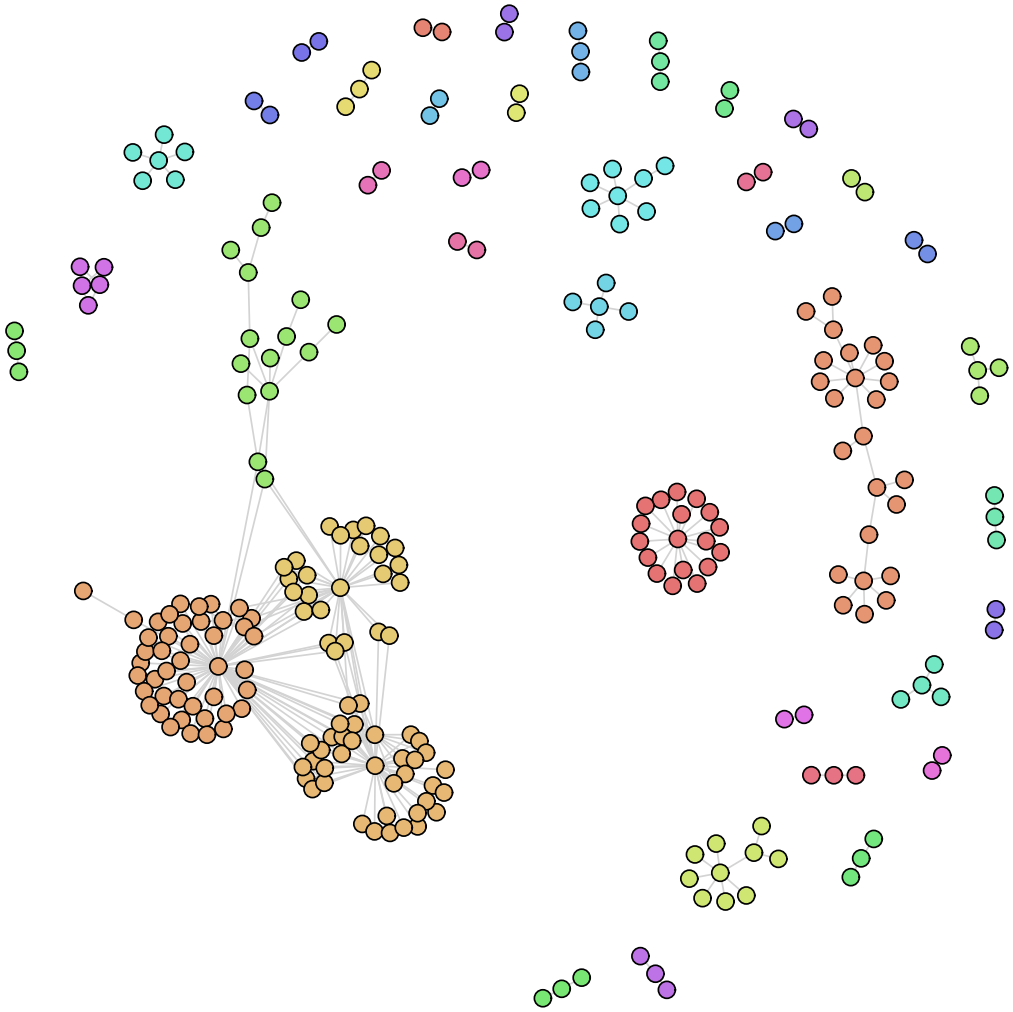

Figure 12.9: Community structure identified by HYBRID-IA on 12.9 *Cattle PPI*.

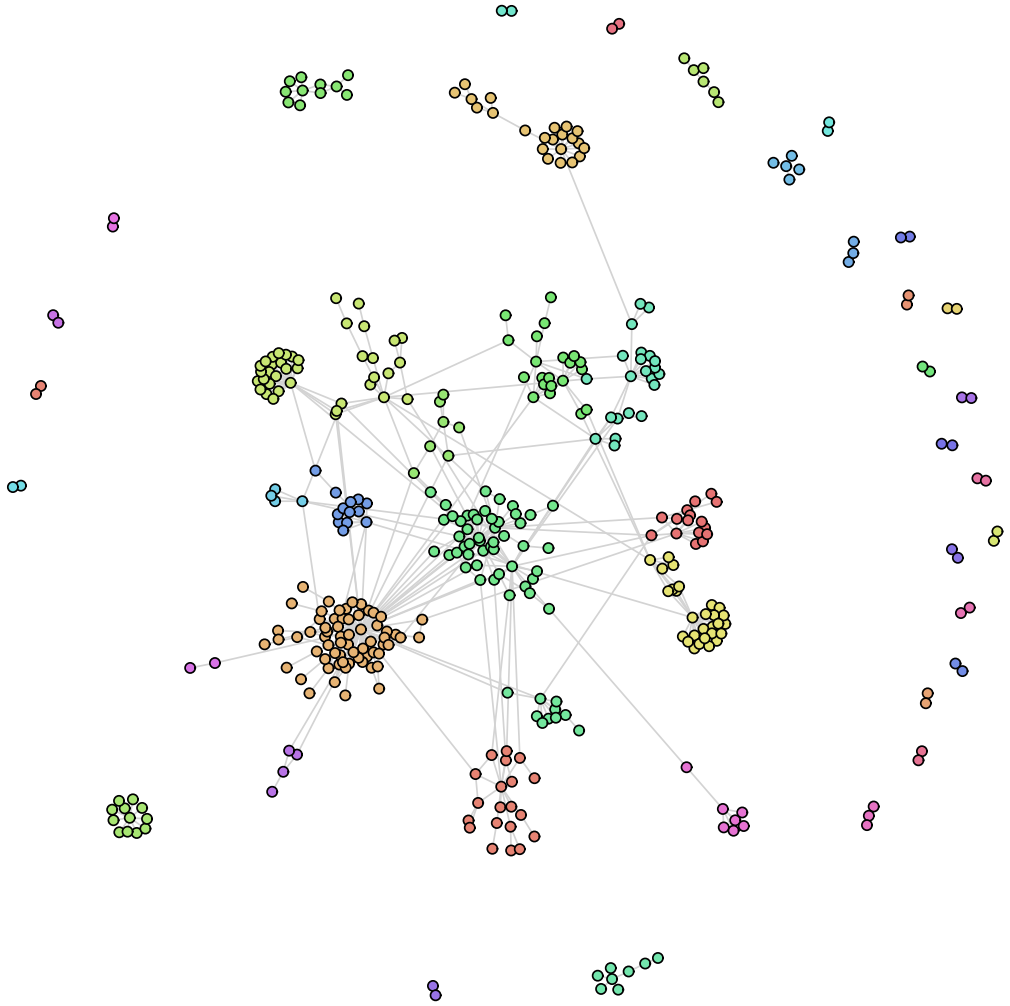

Figure 12.10

Figure 12.11: Community structure identified by HYBRID-IA on 12.10 *E.coli TRN* networks.

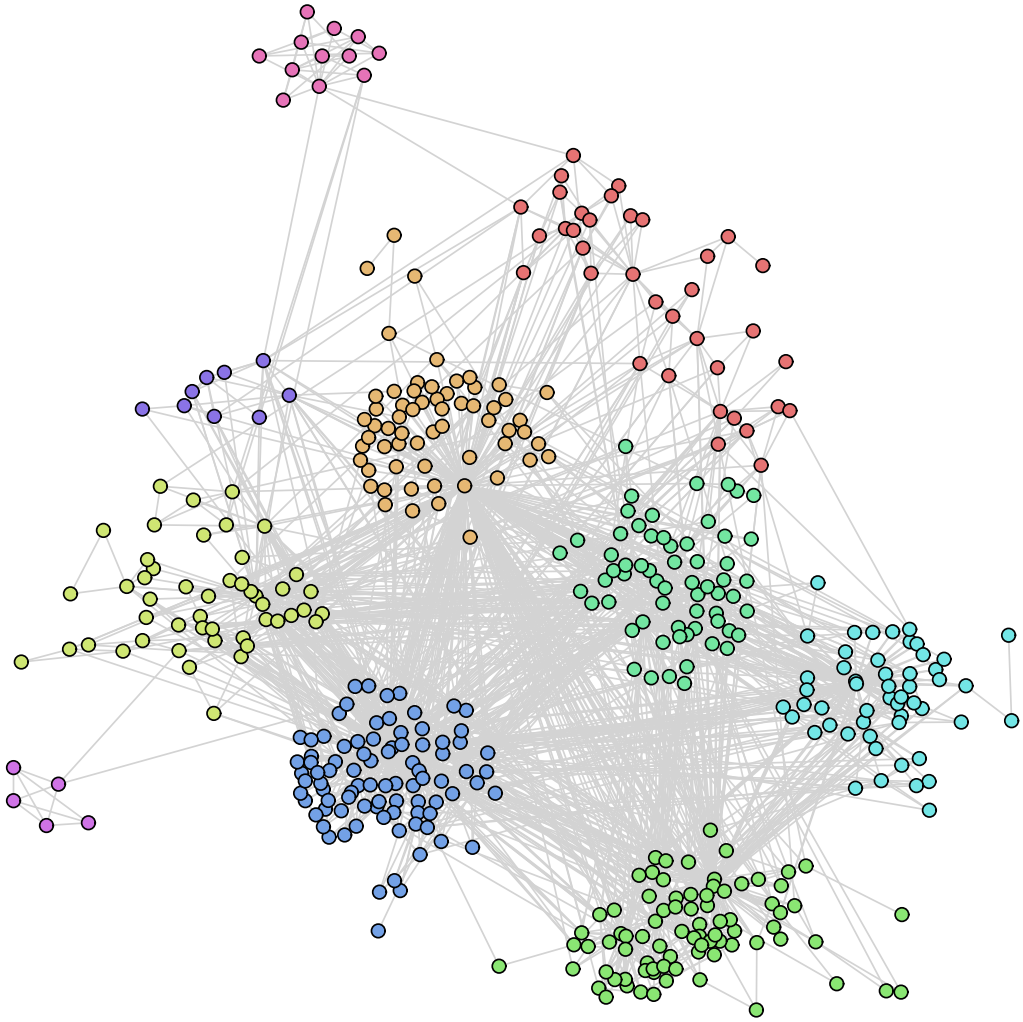

Figure 12.12: Community structure identified by HYBRID-IA on 12.12 *C.elegans MRN*.

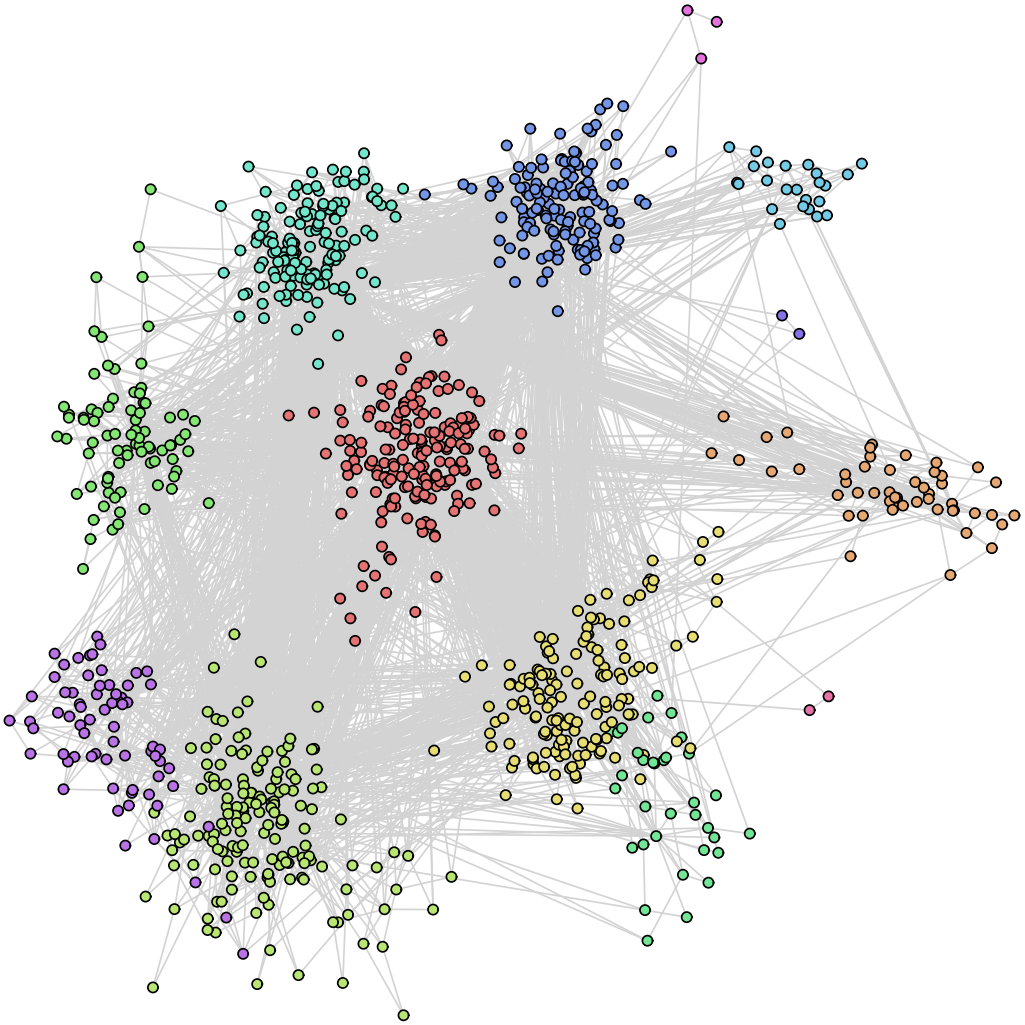

Figure 12.13

Figure 12.14: Community structure identified by HYBRID-IA on 12.13 *E.coli MRN* networks.

Table 12.3: Comparison between HYBRID-IA and LOUVAIN on synthetic networks with 1000 and 5000 vertices, with respect to modularity (Q) and NMI evaluation metrics.

	HYBRID-IA		LOUVAIN	
$(\|V\|, k, \mu_t)$	Q	NMI	Q	NMI
(1000, 15, 0.1)	0.8608	**0.9951**	0.8608	0.9918
(1000, 15, 0.2)	0.7621	**0.9894**	0.7623	0.9807
(1000, 15, 0.3)	0.6646	**0.9862**	0.6651	0.9716
(1000, 15, 0.4)	0.5654	**0.9836**	0.5660	0.9691
(1000, 15, 0.5)	0.4670	**0.9847**	0.4688	0.9462
(1000, 15, 0.6)	0.3688	**0.9612**	0.3718	0.9113
(1000, 15, 0.7)	0.2712	**0.5467**	0.2675	0.4977
(1000, 15, 0.8)	0.2415	**0.1600**	0.2354	0.1536
(1000, 20, 0.1)	0.8606	**0.9980**	0.8607	0.9931
(1000, 20, 0.2)	0.7622	**0.9964**	0.7622	0.9914
(1000, 20, 0.3)	0.6656	**0.9921**	0.6658	0.9830
(1000, 20, 0.4)	0.5668	**0.9910**	0.5676	0.9656
(1000, 20, 0.5)	0.4685	**0.9829**	0.4700	0.9491
(1000, 20, 0.6)	0.3688	**0.9748**	0.3712	0.9263
(1000, 20, 0.7)	0.2714	**0.9244**	0.2737	0.8230
(1000, 20, 0.8)	0.2169	0.1708	0.2069	**0.1793**
(5000, 20, 0.1)	0.8923	**0.9988**	0.8934	0.9586
(5000, 20, 0.2)	0.7927	**0.9965**	0.7949	0.9394
(5000, 20, 0.3)	0.6929	**0.9965**	0.6960	0.9252
(5000, 20, 0.4)	0.5931	**0.9948**	0.5976	0.9065
(5000, 20, 0.5)	0.4936	**0.9951**	0.5003	0.8779
(5000, 20, 0.6)	0.3939	**0.9966**	0.4030	0.8474
(5000, 20, 0.7)	0.2932	**0.9927**	0.3056	0.8145
(5000, 20, 0.8)	0.2084	**0.3285**	0.2102	0.2634
(5000, 25, 0.1)	0.8922	**0.9993**	0.8925	0.9770
(5000, 25, 0.2)	0.7925	**0.9988**	0.7936	0.9527
(5000, 25, 0.3)	0.6929	**0.9986**	0.6948	0.9348
(5000, 25, 0.4)	0.5931	**0.9987**	0.5966	0.9125
(5000, 25, 0.5)	0.4934	**0.9955**	0.4983	0.8907
(5000, 25, 0.6)	0.3939	**0.9950**	0.4008	0.8621
(5000, 25, 0.7)	0.2940	**0.9951**	0.3037	0.8285
(5000, 25, 0.8)	0.1872	**0.6067**	0.1942	0.5654

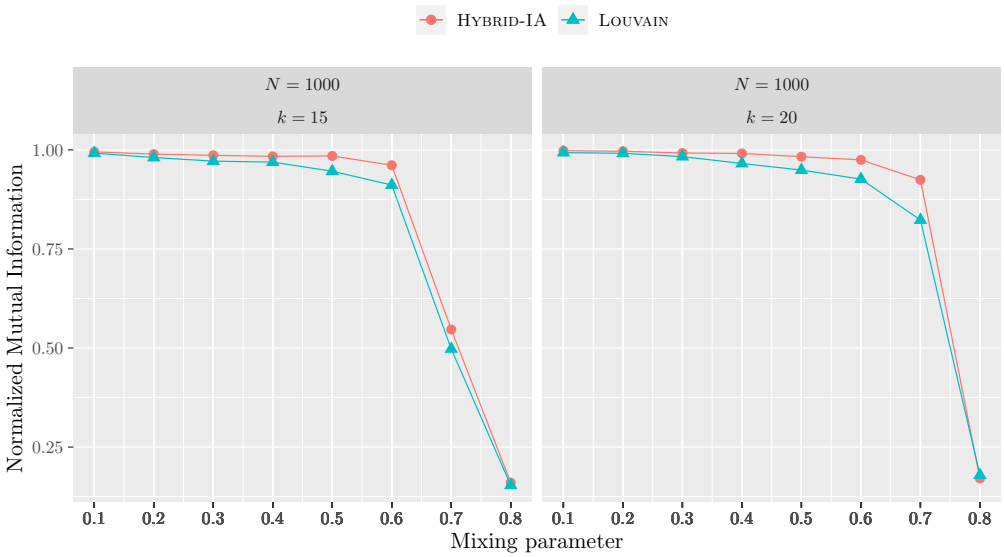

Figure 12.15: Performances of HYBRID-IA and LOUVAIN on the LFR instances with 1000 nodes and average degree 15 and 20. The plots show the normalized mutual information as function of the mixing parameter. Each point corresponds to an average over 5 graph realizations and 100 runs.

and in all instances with 5000 vertices. On the other hands, though, HYBRID-IA outperforms LOUVAIN in all networks with respect to the NMI index, except just for one $(1000, 20, 0.8)$. This gap is due to the combination between the random search and local search that, together with the diversity produced by the immune operators, requires a longer convergence time than LOUVAIN. Indeed, LOUVAIN is a multilevel algorithm that which obtain a good modularity, but it aggregates too much the communities, bypassing the real community structure of the networks. This proves a better ability of the hybrid immune algorithm proposed in detecting communities closer to the true ones than the greedy optimization algorithm. Importantly, although modularity assesses the cohesion of the communities detected, maximizing Q might not correspond to detecting true communities.

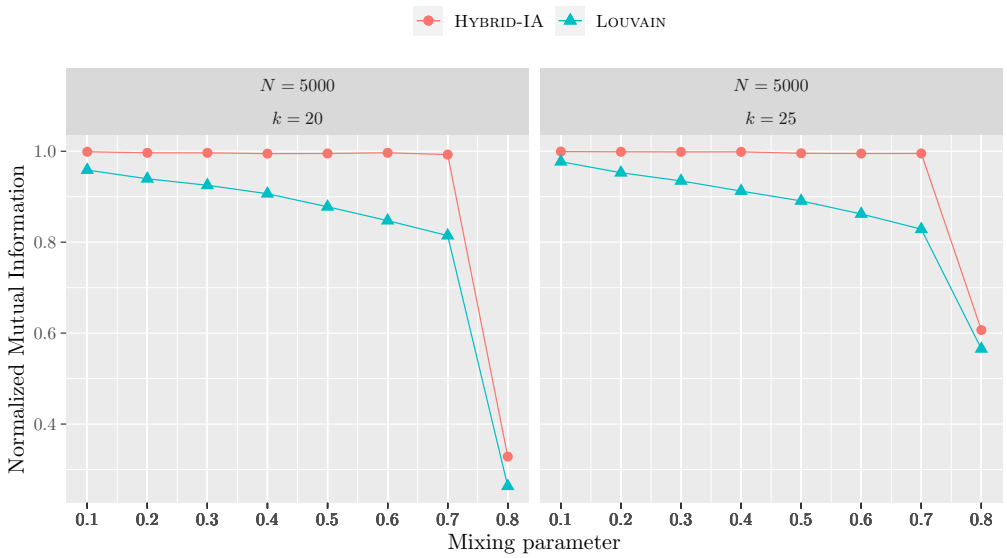

Figure 12.16: Performances of Hybrid-IA and Louvain on the LFR instances with 5000 nodes and average degree 20 and 25. The plots show the normalized mutual information as function of the mixing parameter. Each point corresponds to an average over 5 graph realizations and 100 runs.

In Figure 12.15 are shown the curves of the NMI index for all LFR benchmarks with 1000 vertices. From these plots can be observed that the two curves have the same trend: for low values of μ_t ($\leq$ 0.3), both algorithms obtain similar results, and the NMI curves growth as a common line, while as the μ_t parameter increases, the gap between HYBRID-IA and LOUVAIN begins to be more consistent. Moreover, when the mixing parameter increases, the generated LFR networks have a community structure not well-defined, resulting in low values of NMI for both algorithms. In Figure 12.16 are shown the curves of the NMI for the LFR networks with 5000 nodes. For these instances, instead, the difference between LOUVAIN and HYBRID-IA is much more substantial, and it is evident even at low values of μ_t.

12.6 Conclusions

Being able to efficiently analyze complex networks is one of the most crucial and central issue in many areas, included systems biology, since through them is possible to understand and identify dynamics and structures of molecular interactions. In general, disease phenotypes are generally caused by the failure of modules of genes that often have similar biological roles. In light of this, being able to detect elements of a network that have characteristic in common, or similar functions, plays a key and useful role in providing insights into the biological functionality of these elements. Therefore, developing efficient and robust algorithmic methods able to uncover such elements in biological networks may help in detecting those groups of genes that are cause of disease, and, consequently, useful in the development of specific and targeted drugs. The problem to identify modules in a network is known as *community detection*.

A *Hybrid Immune Algorithm*, called HYBRID-IA, was designed for the community detection problem and was tested on several large biological networks. The strength of HYBRID-IA is given not only by the immune operators (cloning, hypermutation and aging) but also by a specially designed Local Search, which aims to speed up the convergence of HYBRID-IA towards promising regions. Basically, it attempt deterministically to move a node from the belonging community to an other within its neighbors with the purpose to refine and improve the solutions discovered.
For assessing the robustness of HYBRID-IA, a comparison with other metaheuristics, hyper-heuristic and the well-known greedy algorithm LOUVAIN has been performed. Such comparison has been conducted based on the *modularity function maximization*. However, due the limitation of the modularity optimization in detecting communities that are comparatively small, the HYBRID-IA performances have been also evaluated with respect the *Normalized Mutual Information* (NMI) that is a commonly evaluation metric used in community detection, which simply assesses how similar the communities discovered are with respect to the real ones. Inspecting, in the overall, all outcomes obtained and all comparisons performed clearly emerges how HYBRID-IA outperforms all metaheuristics and hyper-heuristics compared in term of best and mean modularity values. Focusing only on the comparison with LOUVAIN, is possible to assert that although HYBRID-IA finds slightly lower modularity values, it is still able to detect more similar communities to the real ones with respect those discovered by LOUVAIN.

Chapter 13

Final Conclusions

In this thesis, I presented my research papers in which I had spent the last three years. The aim of my research topic is to investigate, with different techniques and approaches the behaviour, the strategies and the interactions between agents. Firstly, I presented the part of my study on game theoretical approach using variational inequalities and multi-stage integer programming models, both static and dynamic, i.e. models in which no randomness is involved in the development of future states of the system. The approach used to solve the different models, with continuous variables, is finding a solution of variational inequality problem. Otherwise, the model proposed in Chapter 4, is solved as a integer linear problem and using a genetic algorithm. Secondly, I presented the part of my study on stochastic models, under uncertainly, during emergencies situations. Each model presented in Chapter 5,6 and 7 is based on two-stage stochastic variational inequality approach. Finally, I presented my study on Metaheuristics focusing on two main aspects: the Swarm Intelligence, in detail on Ant Colony Optimization, and the Immunological Algorithms to solve the problem of the Community Detection.

In my personal opinion, the most important thesis results are inside the opportunity

to study in depth the problems of two-stage stochastic variational inequalities models, covered in Chapters 5,6 and 7, topics that had not yet been thoroughly investigated before 2020. On the other hand, the most novel elements fit into the up-to-date research areas are the study of YouTube and eBay social networks dynamics solved using a variational inequality approach (see 1, 2 and 3). Furthermore, the possibility of having two supervisors has given me ample space for study and research in different fields, as can be seen from the thesis. As a consequence, we investigate a correlation between Ant Colony Optimization (which is a metaheurstic approach) and the game theoretical approach. This kind of analysis it does not appear to have precedent in the literature (see 8).

Some next steps on following-up some of the investigations presented in the thesis are, for instance, the model presented in the Chapter 3 that has been extended from variational inequality to evolutionary variational inequality problem and submitted for review. Furthermore, a numerical example has been included; in this example the importance and relevance of the model created and solved is highlighted. In the near future, as regards the two-stage stochastic problems, such as Chapters 5, 6 and 7, I would like to investigate and extend my works to three-stage stochastic variational inequality problems by considering no longer a single stochastic phase but two. This concerns both the evacuation problem and the model of shipments of medical items. Furthermore, an other future project, in collaboration with both of mine supervisors, is to produce a genetic algorithm to solve the supply chains. In particular, the idea is to solve the evacuation model present in Chapter 7, through a genetic algorithm. Starting by the ideas developed in Chapters 8, 9 and 10, I would like to insert a dynamism within each group and the respective strategies of the agents, using more dynamic parameters to realize the graph. Finally, regarding

the last chapters, as soon as we have the response from the article of Chapter 11, we will try to test the algorithm on even bigger instances.

In conclusion, the work done during this Ph.D course gave me a lot of satisfaction both from the point of view of personal results obtained and achievements at European level. In fact, at the beginning of the academic year 2021-2022, the works presented in the thesis has been evaluated in an excellent way, so as to receive the YoungWomen4OR Award as one of the best twelve Young Operational Research researchers in all of Europe. This Award was personally given, by the President Prof. Marc Sevaux of the Association of European Operational Research Societies (EURO), during the last conference EURO2022 held in Espoo, Finland, in July 2022. Surely, this was a fully rewarding and challenging result, the result of intense and demanding years.

Appendix A

Literature Review/Preliminaries

A.1 Game Theory

Some game-theoretic ideas can be traced to the 18th century, but the major development of the theory began in the 1920s with the work of the mathematician Emile Borel (1871–1956) and the polymath John Von Neumann (1903–57). A decisive event in the development of the theory was the publication in 1944 of the book Theory of games and economic behavior by Von Neumann and Oskar Morgenstern. In the 1950s game-theoretic models began to be used in economic theory and political science, and psychologists began studying how human subjects behave in experimental games. In the 1970s game theory was first used as a tool in evolutionary biology. Subsequently, game theoretic methods have come to dominate microeconomic theory and are used also in many other fields of economics and a wide range of other social and behavioral sciences. The 1994 Nobel prize in economics was awarded to the game theorists John C. Harsanyi (1920–2000), John F. Nash (1928–2015), and Reinhard Selten (1930–2016). The computation of economic and game theoretic equilibria has been of great interest in the academic

and professional communities ever since the path-breaking paper by Lemke and Howson [150] and the seminal work by Herbert Scarf [236] in the mid-1960's and early 1970's. The initial impetus for research on computing equilibria came from the need to empirically analyze general equilibrium theory and to apply this theory to study problems of taxation, unemployment, etc. In recent years, the growth of experimental economics and the use of sophisticated strategic planning models by industry has revitalized the need for efficient methods to analyze and numerically solve models of economic and game theoretic equilibria.

A.2 Nash equilibrium problem

A Nash equilibrium is an action profile a^* with the property that no player i can do better by choosing an action different from a_i^* , given that every other player j adheres to a_j^* . In the idealized setting in which the players in any given play of the game are drawn randomly from a collection of populations, a Nash equilibrium corresponds to a steady state. If, whenever the game is played, the action profile is the same Nash equilibrium a^*, then no player has a reason to choose any action different from her component of a^*; there is no pressure on the action profile to change. Expressed differently, a Nash equilibrium embodies a stable "social norm": if everyone else adheres to it, no individual wishes to deviate from it. The second component of the theory of Nash equilibrium is that the players' beliefs about each other's actions are correct implies, in particular, two players' beliefs about a third player's action are the same. For this reason, the condition is sometimes said to be that the players' "expectations are coordinated". The situations to which I wish to apply the theory of Nash equilibrium do not in general correspond exactly to the idealized setting described above. For example, in some

cases the players do not have much experience with the game; in others they do not view each play of the game in isolation. Whether or not the notion of Nash equilibrium is appropriate in any given situation is a matter of judgment. In some cases, a poor fit with the idealized setting may be mitigated by other considerations. For example, inexperienced players may be able to draw conclusions about their opponents' likely actions from their experience in other situations, or from other sources. Ultimately, the test of the appropriateness of the notion of Nash equilibrium is whether it gives us insights into the problem at hand. With the aid of an additional piece of notation, I can state the definition of a Nash equilibrium precisely. Let a be an action profile, in which the action of each player i is a_i. Let a_i' be any action of player i (either equal to a_i, or different from it). Then (a_i', a_{-i}) denotes the action profile in which every player j except i chooses her action a_j as specified by a, whereas player i chooses a_i'. (The $-i$ subscript on a stands for "except i".) That is, (a_i', a_{-i}) is the action profile in which all the players other than i adhere to a while i "deviates" to a_i'. (If $a_i' = a_i$ then of course $(a_i', a_{-i}) = (a_i, a_{-i}) = a$. Using this notation, I can restate the condition for an action profile a^* to be a Nash equilibrium: no player i has any action a_i for which she prefers (a_i, a^*) to a^*. Equivalently, for every player i and every action a_i of player i, the action profile a^* is at least as good for player i as the action profile (a_i, a^*_{-i}).

Definition A.2.1 (Nash equilibrium of strategic game with ordinal preferences)**.** *The action profile a^* in a strategic game with ordinal preferences is a Nash equilibrium if, for every player i and every action a_i of player i, a^* is at least as good according to player i's preferences as the action profile (a_i, a^*_{-i}) in which player i chooses a_i while every other player j chooses a^*_j . Equivalently, for every*

player i,

$$u_i(a^*) \geq u_i(a_i, a^*_{-i}) \tag{A.1}$$

for every action ai of player i, where u_i is a payoff function that represents player i's preferences.

This definition implies neither that a strategic game necessarily has a Nash equilibrium, nor that it has at most one. Examples in the next section show that some games have a single Nash equilibrium, some possess no Nash equilibrium, and others have many Nash equilibria. The definition of a Nash equilibrium is designed to model a steady state among experienced players. An alternative approach to understanding players' actions in strategic games assumes that the players know each others' preferences, and considers what each player can deduce about the other players' actions from their rationality and their knowledge of each other's rationality.

A.2.1 Generalized Nash equilibrium problem

The Generalized Nash equilibrium problem **(GNEP for short)** is an important model that has its roots in the economic sciences but is being fruitfully used in many different fields. Although the GNEP is a model that has been used actively in many fields in the past 50 years, it is only since the mid 1990s that research on this topic gained momentum. The GNEP lies at the intersection of many different disciplines (e.g. economics, engineering, mathematics, computer science, and sometimes researchers in different fields worked independently and unaware of existing results. As I already mentioned, many researchers from different fields worked on the GNEP, and this explains why this problem has a number of different names in the literature including pseudo-game, social equilibrium problem, equilibrium

programming, coupled constraint equilibrium problem, and abstract economy. I will stick to the term generalized Nash equilibrium problem that seems the favorite one by researchers in recent years.

Formally, the GNEP consists of N *players*, each player ν controlling the variables $x^\nu \in \mathbb{R}^{n_\nu}$. I denote by x the vector formed by all these decision variables:

$$\boldsymbol{x} = \begin{pmatrix} x^1 \\ \vdots \\ x^N \end{pmatrix} \tag{A.2}$$

which has dimension $n := \sum_{\nu=1}^{N} n_\nu$, and by $\mathbf{x}^{-\nu}$ the vector formed by all the players' decision variables except those of player $\nu = 1$. To emphasize the νth player's variables within $\mathbf{x}$, I sometimes write $(x^\nu, \mathbf{x}^{-\nu})$ instead of $\mathbf{x}$. Note that this is still the vector $x = (x^1, \ldots, x^\nu, \ldots x^N)$ and that, in particular, the notation $(x^\nu, \mathbf{x}^{-\nu})$ does not mean that the block components of $\mathbf{x}$ are reordered in such a way that x^ν becomes the first block. Each player has an objective function $\theta_\nu : \mathbb{R}^n \to \mathbb{R}$ that depends on both his own variables x^ν as well as on the variables $\mathbf{x}^{-\nu}$ of all other players. This mapping θ_ν is often called the utility function of player ν, sometimes also the payoff function or loss function, depending on the particular application in which the GNEP arises.

Furthermore, each player's strategy must belong to a set $X_\nu(\mathbf{x}^{-\nu}) \subseteq \mathbb{R}^{n_\nu}$ that depends on the rival players' strategies and that I call the feasible set or strategy space of player ν.

The aim of player ν, given the other players' strategies $\mathbf{x}^{-\nu}$, is to choose a strategy x^ν that solves the minimization problem

$$\text{minimize}_{x^\nu} \quad \theta_\nu(x^\nu, \mathbf{x}^{-\nu}) \quad \text{subject to } x^\nu \in X_\nu(\mathbf{x}^{-\nu}). \tag{A.3}$$

For any $\mathbf{x}^{-\nu}$, the solution set of problem (A.2.1) is denoted by $S_\nu(\mathbf{x}^{-\nu})$

Definition A.2.2. *The GNE is the problem of finding a vector $\bar{x}$ such that*

$$\bar{x}^\nu \in S_\nu(\boldsymbol{x}^{-\nu}) \qquad \forall \nu = 1, \ldots, N,$$

or equivalently,

$$\theta_\nu(\bar{x}^\nu, \bar{\boldsymbol{x}}^{-\nu}) \leq \theta_\nu(x^\nu, \bar{\boldsymbol{x}}^{-\nu}). \tag{A.4}$$

Such a point $\bar{x}$ is called a *(generalized Nash) equilibrium* or, more simply, a *solution* of the GNE.

A point $\bar{x}$ is therefore an equilibrium if no player can decrease his objective function by changing unilaterally $\bar{x}^\nu$ to any other feasible point. If I denote by $S(\mathbf{x})$ the set $S(\mathbf{x}) := \prod_{\nu=1}^{N} S_\nu(\mathbf{x}^{-\nu})$,I see that I can say that $\bar{x}$ is a solution if $\bar{x} \in S(\bar{x})$, i.e. if $\bar{x}$ is a fixed point of the point-to-set mapping S. If the feasible sets $X_\nu(\mathbf{x}^{-\nu})$ do not depend on the rival players' strategies, so I have $X_\nu(\mathbf{x}^{-\nu}) = X_\nu$ for some set $X_\nu \subseteq \mathbb{R}^{n_\nu} \quad \forall \nu = 1, \ldots, N$, the GNE reduces to the standard Nash equilibrium problem *(NEP for short)*, cf. definition A.2.1

A.3 The Variational Inequality Problem

Definition A.3.1. *The finite - dimensional variational inequality problem, $VI(F, \mathbb{K})$, is to determine a vector $x^* \in \mathbb{K} \subseteq \mathbb{R}^n$, such that*

$$F(x^*)^T \cdot (x - x^*) \geq 0$$

or, equivalently,

$$\langle F(x^*)^T, x - x^* \rangle \geq 0, \forall x \in \mathbb{K} \tag{A.5}$$

where F is a given continuous function from $\mathbb{K}$ to $\mathbb{R}^n$, $\mathbb{K}$ is a given closed convex set, and $\langle \cdot, \cdot \rangle$ denotes the inner product in n dimensional Euclidean space.

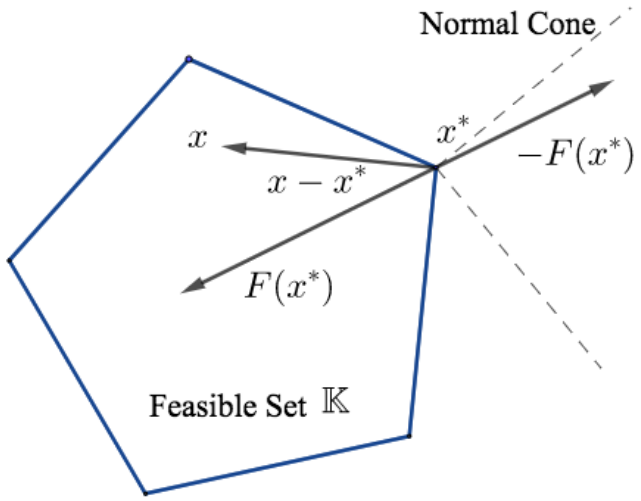

Figure A.1: Geometric interpretation of variational inequality problem

In geometric terms, the variational inequality (A.5) states that $F(x^*)^T$ is "orthogonal" to the feasible set $\mathbb{K}$ at the point x^*. This formulation, as shall be demonstrated, is particularly convenient because it allows for a unified treatment of equilibrium problems and optimization problems.

Indeed, many mathematical problems can be formulated as variational inequality problems, and several examples applicable to equilibrium analysis follow.

A.3.1 Systems of Equations

Many classical economic equilibrium problems have been formulated as systems of equations, since market clearing conditions necessarily equate the total supply with the total demand. In terms of a variational inequality problem, the formulation of a system of equations is as follows.

Proposition A.3.1. *Let $\mathbb{K} = \mathbb{R}^n$ and let $F : \mathbb{R}^n \to \mathbb{R}^n$ be a given function. A vector $x^* \in \mathbb{R}^n$ solves $VI(F, \mathbb{R}^n)$ if and only if $F(x^*) = 0$.*

Proof. If $F(x^*) = 0$, then inequality (A.5) holds with equality. Conversely, if x^* satisfies (A.5), let $x = x^* - F(x^*)$, which implies that $F(x^*)^T \cdot (-F(x^*)) \geq 0$, or $-||F(x^*)||^2 \geq 0$ and, therefore, $F(x^*) = 0$. □

Note that systems of equations, however, preclude the introduction of inequalities, which may be needed, for example, in the case of nonnegativity assumptions on certain variables such as prices.

A.3.2 Optimization Problems

An optimization problem is characterized by its specific objective function that is to be maximized or minimized, depending upon the problem and, in the case of a constrained problem, a given set of constraints. Possible objective functions include expressions representing profits, costs, market share, portfolio risk, etc. Possible constraints include those that represent limited budgets or resources, nonnegativity constraints on the variables, conservation equations, etc. Typically, an optimization problem consists of a single objective function. Both unconstrained and constrained optimization problems can be formulated as variational inequality problems. The subsequent two propositions and theorem identify the relationship between an optimization problem and a variational inequality problem.

Proposition A.3.2. *Let x^* be a solution to the optimization problem:*

$$\textit{Minimize } f(x) \tag{A.6}$$

$$\textit{subject to: } x \in \mathbb{K},$$

where f is continuously differentiable and $\mathbb{K}$ is closed and convex. Then x^* is a solution of the variational inequality problem:

$$\nabla f(x^*)^T \cdot (x - x^*) \geq 0, \forall x \in \mathbb{K} \tag{A.7}$$

Proof. Let $\phi(t) = f(x^* + t(x - x^*))$, $\forall t \in [0, 1]$. Since $\phi(t)$ achieves its minimum at $t = 0$, $0 \leq \phi'(0) = \nabla f(x^*)^T \cdot (x - x^*)$, that is, x^* is a solution of (7.4). □

Proposition A.3.3. *If $f(x)$ is a convex function and x^* is a solution to $VI(\nabla f, \mathbb{K})$, then x^* is a solution to the optimization problem* (A.6).

Proof. Since $f(x)$ is convex,

$$f(x) \geq f(x^*) + \nabla f(x^*)^T \cdot (x - x^*), \forall x \in \mathbb{K}. \tag{A.8}$$

But $\nabla f(x^*)^T \cdot (x - x^*) \geq 0$, since x^* is a solution to $VI(\nabla f, \mathbb{K})$. Therefore, from (7.5) one concludes that $f(x) \geq f(x^*), \forall x \in \mathbb{K}$, that is, x^* is a minimum point of the mathematical programming problem (A.6). □

If the feasible set $\mathbb{K} = \mathbb{R}^n$, then the unconstrained optimization problem is also a variational inequality problem. On the other hand, in the case where a certain symmetry condition holds, the variational inequality problem can be reformulated as an optimization problem. In other words, in the case that the variational inequality formulation of the equilibrium conditions underlying a specific problem is characterized by a function with a symmetric Jacobian, then the solution of the equilibrium conditions and the solution of a particular optimization problem are one and the same. I first introduce the following definition and then fix this relationship in a theorem.

Definition A.3.2. *An $n \times n$ matrix $M(x)$, whose elements $m_{ij}(x); i = 1, \ldots, n; j = 1, \ldots, n$, are functions defined on the set $S \subset \mathbb{R}^n$, is said to be positive semidefinite on S if $v^T M(x) v \geq 0, \forall v \in \mathbb{R}^n, x \in S$. It is said to be positive definite on S if $v^T M(x) v > 0, \forall v \neq 0, v \in \mathbb{R}^n, x \in S$. It is said to be strongly positive definite on S if $v^T M(x) v \geq \alpha ||v||^2$, for some $\alpha > 0, \forall v \in \mathbb{R}^n, x \in S$.*

Note that if $\gamma(x)$ is the smallest eigenvalue, which is necessarily real, of the symmetric part of $M(x)$, that is, $\frac{1}{2}[M(x) + M(x)^T]$, then it follows that

- $M(x)$ is positive semidefinite on S if and only if $\gamma(x) \geq 0, \forall x \in S$;
- $M(x)$ is positive definite on S if and only if $\gamma(x) > 0, \forall x \in S$;
- $M(x)$ is strongly positive definite on S if and only if $\gamma(x) \geq \alpha > 0, \forall x \in S$.

Theorem A.3.1. *Assume that $F(x)$ is continuously differentiable on $\mathbb{K}$ and that the Jacobian matrix:*

$$\nabla F(x) = \begin{bmatrix} \frac{\partial F_1}{\partial x_1} & \cdots & \frac{\partial F_1}{\partial x_n} \\ \vdots & \ddots & \vdots \\ \frac{\partial F_n}{\partial x_1} & \cdots & \frac{\partial F_n}{\partial x_n} \end{bmatrix}$$

is symmetric and positive semidefinite. Then there is a real-valued convex function $f : \mathbb{K} \rightarrow \mathbb{R}$ satisfying $\nabla f(x) = F(x)$ with x^* the solution of $VI(F, \mathbb{K})$ also being the solution of the mathematical programming problem:

$$\textit{Minimize } f(x)$$

$$\textit{subject to: } x \in \mathbb{K},$$

Proof. Under the symmetry assumption it follows from Green's Theorem that

$$f(x) = \int F(x)^T dx,$$

where $\int$ is a line integral. The conclusion follows from Proposition A.3.3. □

Hence, although the variational inequality problem encompasses the optimization problem, a variational inequality problem can be reformulated as a convex optimization problem, only when the symmetry condition and the positive semidefiniteness condition hold. The variational inequality, therefore, is the more general problem in that it can also handle a function $F(x)$ with an asymmetric Jacobian.

A.3.3 Complementarity Problems

The variational inequality problem also contains the complementarity problem as a special case. Complementarity problems are defined on the nonnegative orthant. Let $\mathbb{R}^n_+$ denote the nonnegative orthant in $\mathbb{R}^n$, and let $F : \mathbb{R}^n \to \mathbb{R}^n$. The nonlinear complementarity problem over $\mathbb{R}^n_+$ is a system of equations and inequalities stated as: Find $x^* \geq 0$ such that

$$F(x^*) \geq 0 \text{ and } F(x^*)^T \cdot x^* = 0. \tag{A.9}$$

Whenever the mapping F is affine, that is, whenever $F(x) = Mx + b$, where M is an $n \times n$ matrix and b an $n \times 1$ vector, problem (A.9) is then known as the linear complementarity problem.

The relationship between the complementarity problem and the variational inequality problem is as follows.

Proposition A.3.4. *$VI(F, \mathbb{R}^n_+)$ and $F(x^*) \geq 0, F(x^*)^T \cdot x^* = 0$ have precisely the same solutions, if any.*

Proof. First, it is established that if x^* satisfies $VI(F, \mathbb{R}^n_+)$, then it also satisfies the complementarity problem (A.9). Substituting $x = x^* + e_i$ into $VI(F, \mathbb{R}^n_+)$, where e_i denotes the n-dimensional vector with 1 in the i-th location and 0, elsewhere, one concludes that $F_i(x^*) \geq 0,$ and $F(x^*) \geq 0$.

Substituting now $x = 2x^*$ into the variational inequality, one obtains

$$F(x^*)^T \cdot (x^*) \geq 0. \tag{A.10}$$

Substituting then $x = 0$ into the variational inequality, one obtains

$$F(x^*)^T \cdot (-x^*) \geq 0 \tag{A.11}$$

and together imply that

$$F(x^*)^T \cdot x^* = 0.$$

Conversely, if x^* satisfies the complementarity problem, then

$$F(x^*)^T \cdot (x - x^*) \geq 0$$

since $x \in \mathbb{R}^n_+$ and $F(x^*) \geq 0$. □

A.3.4 Fixed Point Problems

Fixed point theory has been used to formulate, analyze, and compute solutions to economic equilibrium problems. The relationship between the variational inequality problem and a fixed point problem can be made through the use of a projection operator. First, the projection operator is defined.

Lemma A.3.1. *Let $\mathbb{K}$ be a closed convex set in $\mathbb{R}^n$. Then for each $x \in \mathbb{R}^n$, there is a unique point $y \in \mathbb{K}$, such that*

$$||x - y|| \leq ||x - z||, \forall z \in \mathbb{K}, \tag{A.12}$$

and y is known as the orthogonal projection of x on the set $\mathbb{K}$ with respect to the Euclidean norm, that is,

$$y = \mathbb{P}_{\mathbb{K}} x = argmin||x - z||, \quad z \in \mathbb{K}. \tag{A.13}$$

Proof. Let x be fixed and let $w \in \mathbb{K}$. Minimizing $||x-z||$ over all $z \in \mathbb{K}$ is equivalent to minimizing the same function over all $z \in \mathbb{K}$ such that $||x - z|| \leq ||x - w||$, which is a compact set. The function g defined by $g(z) = ||x - z||^2$ is continuous. Existence of a minimizing y follows because a continuous function on a compact set always attains its minimum. To prove that y is unique, observe that the square

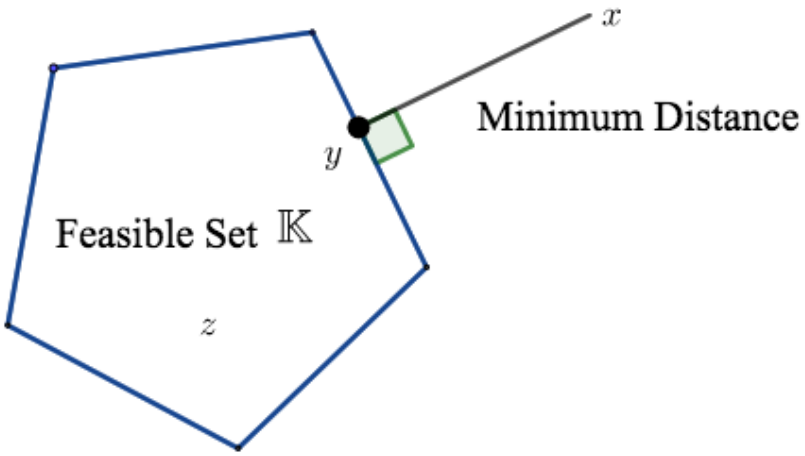

Figure A.2: The projection y of x on the set $\mathbb{K}$

of the Euclidean norm is a strictly convex function. Hence, g is strictly convex and its minimum is unique. □

Theorem A.3.2. *Let $\mathbb{K}$ be a closed convex set. Then $y = \mathbb{P}_{\mathbb{K}}x$ if and only if*

$$y^T \cdot (z - y) \geq x^T \cdot (z - y), \forall z \in \mathbb{K},$$

or

$$(y - x)^T \cdot (z - y) \geq 0, \forall z \in \mathbb{K}. \tag{A.14}$$

Proof. Note that $y = \mathbb{P}_{\mathbb{K}}x$ is the minimizer of $g(z)$ over all $z \in \mathbb{K}$. Since $\nabla g(z) = 2(z - x)$, the result follows from the optimality conditions for constrained optimization problems. □

A property of the projection operator which is useful both in qualitative analysis of equilibria and their computation is now presented.

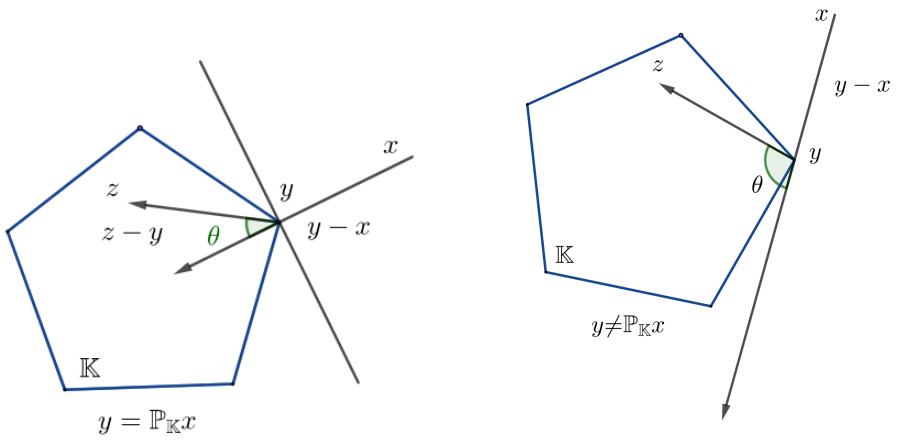

(a) (b)

Figure A.3: Geometric interpretation of $\langle (y-x)^T, z-y \rangle \geq 0$, for $y = \mathbb{P}_{\mathbb{K}}x,\ y \neq \mathbb{P}_{\mathbb{K}}x$

Corollary A.3.1. *Let $\mathbb{K}$ be a closed convex set. Then the projection operator $\mathbb{P}_{\mathbb{K}}$ is nonexpansive, that is*

$$||\mathbb{P}_{\mathbb{K}}x - \mathbb{P}_{\mathbb{K}}x'|| \leq ||x - x'||, \forall x, x' \in \mathbb{R}^n. \tag{A.15}$$

Proof. Given $x, x' \in \mathbb{R}^n$, let $y = \mathbb{P}_{\mathbb{K}}x$ and $y' = \mathbb{P}_{\mathbb{K}}x'$. Then from Theorem 2.4.1 note that for

$$y \in \mathbb{K} : y^T \cdot (z - y) \geq x^T \cdot (z - y), \forall z \in \mathbb{K} \tag{A.16}$$

$$y' \in \mathbb{K} : y'^T \cdot (z - y) \geq x^T \cdot (z - y'), \forall z \in \mathbb{K}, \tag{A.17}$$

Setting $z = y'$ in (A.16) and $z = y$ in (A.17) and adding the resultant inequalities, one obtains:

$$||y - y'||^2 = (y - y')^T \cdot (y - y') \leq (x - x')^T \cdot (y - y') \leq ||x - x'|| \cdot ||y - y'||$$

by an application of the Schwarz inequality. Hence,

$$||y - y'|| \leq ||x - x'||.$$

□

The relationship between a variational inequality and a fixed point problem is as follows.

Theorem A.3.3. *Assume that $\mathbb{K}$ is closed and convex. Then $x^* \in \mathbb{K}$ is a solution of the variational inequality problem $VI(F, \mathbb{K})$ if and only if for any $\gamma > 0, x^*$ is a fixed point of the map*

$$\mathbb{P}_{\mathbb{K}}x(I - \gamma F) : \mathbb{K} \to \mathbb{K},$$

that is,

$$x^* = \mathbb{P}_{\mathbb{K}}x(x^* - \gamma F(x^*)). \tag{A.18}$$

Proof. Suppose that x^* is a solution of the variational inequality, i.e.,

$$F(x^*)^T \cdot (x - x^*) \geq 0, \forall x \in \mathbb{K}.$$

Multiplying the above inequality by $-\gamma < 0$, and adding $x^{*T} \cdot (x - x^*)$ to both sides of the resulting inequality, one obtains

$$x^{*T} \cdot (x - x^*) \geq [x^* - \gamma + F(x^*)]^T \cdot (x - x^*), \forall x \in \mathbb{K}.$$

From Theorem A.3.2 one concludes that

$$x^* = \mathbb{P}_{\mathbb{K}}(x^* - \gamma F(x^*)).$$

Conversely, if $x^* = \mathbb{P}_{\mathbb{K}}(x^* - \gamma F(x^*))$, for $\gamma > 0$, then

$$x^{*T} \cdot (x - x^*) \geq (x^* - \gamma F(x^*))^T \cdot (x - x^*), \forall x \in \mathbb{K},$$

and, therefore,

$$F(x^*)^T \cdot (y - x^*) \geq 0, \forall y \in \mathbb{K}.$$

□

A.3.5 Basic Existence and Uniqueness Results

Variational inequality theory is also a powerful tool in the qualitative analysis of equilibria. I now provide conditions for existence and uniqueness of solutions to $VI(F, \mathbb{K})$ are provided. Existence of a solution to a variational inequality problem follows from continuity of the function F entering the variational inequality, provided that the feasible set $\mathbb{K}$ is compact. Indeed, I have the following:

Theorem A.3.4. ***(Existence Under Compactness and Continuity)***
If $\mathbb{K}$ is a compact convex set and $F(x)$ is continuous on $\mathbb{K}$, then the variational inequality problem admits at least one solution x^*.

Proof. According to Brouwer's Fixed Point Theorem, given a map $\mathbb{P} : \mathbb{K} \rightarrow \mathbb{K}$, with $\mathbb{P}$ continuous, there is at least one $x^* \in \mathbb{K}$, such that $x^* = \mathbb{P}x^*$. Observe that since $\mathbb{P}_{\mathbb{K}}$ and $(I - \gamma F)$ are each continuous, $\mathbb{P}_{\mathbb{K}}(I - \gamma F)$ is also continuous. The conclusion follows from compactness of K and Theorem A.3.3. □

In the case of an unbounded feasible set $\mathbb{K}$, Brouwer's Fixed Point Theorem is no longer applicable; the existence of a solution to a variational inequality problem can, nevertheless, be established under the subsequent condition. Let $B_R(0)$ denote a closed ball with radius R centered at 0 and let $\mathbb{K}_R = \mathbb{K} \cap B_R(0)$. $\mathbb{K}_R$ is then bounded. Let VI_R denote the variational inequality problem:
Determine ${x_R}^* \in \mathbb{K}_R$, such that

$$F({x_R}^*)^T \cdot (y - {x_R}^*) \geq 0, \forall y \in \mathbb{K}_R.$$

I now state:

Theorem A.3.5. *$VI(F, \mathbb{K})$ admits a solution if and only if there exists an $R > 0$ and a solution of VI_R, ${x_R}^*$, such that $||{x_R}^*|| < R$.*

Although $||x_R{}^*|| < R$ may be difficult to check, one may be able to identify an appropriate R based on the particular application.

Existence of a solution to a variational inequality problem may also be established under the coercivity condition, as in the subsequent corollary.

Corollary A.3.2. ***(Existence Under Coercivity)***

Suppose that F(x) satisfies the coercivity condition

$$\frac{(F(x) - F(x_0))^T \cdot (x - x_0)}{||x - x_0||} \rightarrow \infty \tag{A.19}$$

as $||x|| \rightarrow \infty$ *for* $x \in \mathbb{K}$ *and for some* $x_0 \in \mathbb{K}$. *Then* $VI(F, \mathbb{K})$ *always has a solution.*

Corollary A.3.3. *Suppose that* x^* *is a solution of* $VI(F, \mathbb{K})$ *and* $x^* \in \mathbb{K}^0$, *the interior of* $\mathbb{K}$. *Then* $F(x^*) = 0$.

Qualitative properties of existence and uniqueness become easily obtainable under certain monotonicity conditions. First I outline the definitions and then present the results.

Definition A.3.3. ***(Monotonicity)***

$F(x)$ *is monotone on* $\mathbb{K}$ *if*

$$[F(x^1) - F(x^2)]^T \cdot (x^1 - x^2) \geq 0, \quad \forall x^1, x^2 \in \mathbb{K}.$$

Definition A.3.4. ***(Strict Monotonicity)***

$F(x)$ *is strictly monotone on* $\mathbb{K}$ *if*

$$[F(x^1) - F(x^2)]^T \cdot (x^1 - x^2) > 0, \quad \forall x^1, x^2 \in \mathbb{K}, x^1 \neq x^2.$$

Definition A.3.5. ***(Strong Monotonicity)***

$F(x)$ *is strongly monotone on* $\mathbb{K}$ *if for some* $\alpha > 0$

$$[F(x^1) - F(x^2)]^T \cdot (x^1 - x^2) \geq \alpha ||x^1 - x^2||^2, \quad \forall x^1, x^2 \in \mathbb{K}.$$

Definition A.3.6. ***(Lipschitz continuity)***

$F(x)$ is Lipschitz continous on $\mathbb{K}$ if there exists an $L > 0$ such that

$$||F(x^1) - F(x^2)|| \leq L||x^1 - x^2||, \quad \forall x^1, x^2 \in \mathbb{K}.$$

A uniqueness result is presented in the subsequent theorem.

Theorem A.3.6. ***(Uniqueness)***

Suppose that $F(x)$ is strictly monotone on $\mathbb{K}$. Then the solution is unique, if one exists.

Proof. Suppose that x^1 and x^* are both solutions and $x^1 \neq x^*$. Then since both x^1 and x^* are solutions, they must satisfy:

$$F(x^1)^T \cdot (x' - x^1) \geq 0, \forall x' \in \mathbb{K} \tag{A.20}$$

$$F(x^*)^T \cdot (x' - x^*) \geq 0, \forall x' \in \mathbb{K} \tag{A.21}$$

After substituting x^* for x' in (A.20) and x^1 for x' in (A.21) and adding the resulting inequalities, one obtains:

$$[F(x^1) - F(x^*)]^T \cdot (x^* - x^1) \geq 0. \tag{A.22}$$

But inequality (A.22) is in contradiction to the definition of strict monotonicity. Hence, $x^1 = x^*$. □

Monotonicity is closely related to positive definiteness.

Theorem A.3.7. *Suppose that $F(x)$ is continuously differentiable on $\mathbb{K}$ and the Jacobian matrix*

$$\nabla F(x) = \begin{bmatrix} \frac{\partial F_1}{\partial x_1} & \cdots & \frac{\partial F_1}{\partial x_n} \\ \vdots & \ddots & \vdots \\ \frac{\partial F_n}{\partial x_1} & \cdots & \frac{\partial F_n}{\partial x_n} \end{bmatrix}$$

which need not be symmetric, is positive semidefinite (positive definite). Then $F(x)$ is monotone (strictly monotone).

Proposition A.3.5. *Assume that $F(x)$ is continuously differentiable on $\mathbb{K}$ and that $\nabla F(x)$ is strongly positive definite. Then $F(x)$ is strongly monotone.*

One obtains a stronger result in the special case where $F(x)$ is linear.

Corollary A.3.4. *Suppose that $F(x) = Mx + b$, where M is an $n \times n$ matrix and b is a constant vector in $\mathbb{R}^n$. The function F is monotone if and only if M is positive semidefinite. F is strongly monotone if and only if M is positive definite.*

Proposition A.3.6. *Assume that $F : \mathbb{K} \to \mathbb{R}^n$ is continuously differentiable at $\bar{x}$. Then $F(x)$ is locally strictly (strongly) monotone at $\bar{x}$ if $\nabla F(\bar{x})$ is positive definite (strongly positive definite), that is,*

$$v^T F(\bar{x}) v > 0, \forall v \in \mathbb{R}^n, v \neq 0,$$

$$v^T \nabla F(\bar{x}) v \geq \alpha ||v||^2, \text{ for some } \alpha > 0, \forall v \in \mathbb{R}^n.$$

The following theorem provides a condition under which both existence and uniqueness of the solution to the variational inequality problem are guaranteed. Here no assumption on the compactness of the feasible set $\mathbb{K}$ is made.

Theorem A.3.8. *Assume that $F(x)$ is strongly monotone. Then there exists precisely one solution x^* to $VI(F, \mathbb{K})$.*

Proof. Existence follows from the fact that strong monotonicity implies coercivity, whereas uniqueness follows from the fact that strong monotonicity implies strict monotonicity. □

Hence, in the case of an unbounded feasible set $\mathbb{K}$, strong monotonicity of the function F guarantees both existence and uniqueness. If $\mathbb{K}$ is compact, then existence is guaranteed if F is continuous, and only the strict monotonicity condition needs to hold for uniqueness to be guaranteed.

Assume now that $F(x)$ is both strongly monotone and Lipschitz continuous. Then the projection $\mathbb{P}_{\mathbb{K}}[x - \gamma F(x)]$ is a contraction with respect to x, that is, I have the following:

Theorem A.3.9. *Fix* $0 < \gamma \leq \frac{\alpha}{L^2}$ *where* α *and* L *are the constants appearing, respectively, in the strong monotonicity and the Lipschitz continuity condition definitions. Then*

$$||\mathbb{P}_{\mathbb{K}}(x - \gamma F(x)) - \mathbb{P}_{\mathbb{K}}(y - \gamma F(y))|| \leq \beta ||x - y||$$

for all $x, y \in \mathbb{K}$*, where*

$$(1 - \gamma\alpha)^{\frac{1}{2}} \leq \beta < 1.$$

An immediate consequence of Theorem A.3.9 and the Banach Fixed Point Theorem is:

Corollary A.3.5. *The operator* $\mathbb{P}_{\mathbb{K}}(x - \gamma F(x))$ *has a unique fixed point* x^*.

A.3.6 Stability and Sensitivity Analysis

Important issues in the qualitative analysis of equilibrium patterns are the stability and sensitivity of solutions when the problem is subjected to perturbations in the data.

The following theorem establishes that a small change in the function F entering the variational inequality induces a small change in the resulting solution pattern. Denote the original function by F with solution x to $VI(F, \mathbb{K})$ and the perturbed

function by F^* with solution x^* to $VI(F^*, \mathbb{K})$.

Assume that the strong monotonicity condition on F holds. Then one has:

Theorem A.3.10. *Let α be the positive constant in the definition of strong monotonicity. Then*

$$||x^* - x|| \leq \frac{1}{\alpha}||F^*(x^*) - F(x^*)||. \tag{A.23}$$

Proof. The vectors x and x^* must satisfy the variational inequalities

$$F(x)^T \cdot (x' - x) \geq 0, \forall x' \in \mathbb{K} \tag{A.24}$$

$$F(x^*)^T \cdot (x' - x^*) \geq 0, \forall x' \in \mathbb{K} \tag{A.25}$$

Rewriting (A.24) for $x' = x^*$ and (A.25) for $x' = x$, and then adding the resulting inequalities, one obtains

$$[F^*(x^*) - F(x)]^T \cdot (x^* - x) \leq 0. \tag{A.26}$$

or

$$[F^*(x^*) - F(x) + F(x^*) - F(x^*)]^T \cdot (x^* - x) \leq 0. \tag{A.27}$$

Using then the monotonicity condition, (A.27) yields

$$[F^*(x^*) - F(x)^*]^T \cdot (x - x^*) \geq [F(x) - F(x^*)]^T \cdot (x - x^*) \geq \alpha||x - x^*||^2. \tag{A.28}$$

By virtue of the Schwartz inequality, (A.28) gives

$$\alpha||x^* - x||^2 \leq ||F^*(x^*) - F(x^*)|| \cdot ||x^* - x||,$$

from which A.23 follows. □

A.4 Projected Dynamical Systems

A plethora of equilibrium problems, including network equilibrium problems, can be uniformly formulated and studied as finite-dimensional variational inequality problems.

Indeed, it was precisely the traffic network equilibrium problem, as stated by Smith (1979), and identified by Dafermos (1980) to be a variational inequality problem, that gave birth to the ensuing research activity in variational inequality theory and applications in transportation science, regional science, operations research/management science, and, more recently, in economics.

Finite-dimensional variational inequality theory by itself, however, provides no framework for the study of the dynamics of competitive systems. Rather, it captures the system at its equilibrium state and, hence, the focus of this tool is static in nature.

Dupuis and Nagurney (1993) proved that, given a variational inequality problem, there is a naturally associated dynamical system, the stationary points of which correspond precisely to the solutions of the variational inequality problem. This association was first noted by Dupuis and Ishii (1991).

This dynamical system, first referred to as a projected dynamical system by Zhang and Nagurney (1995), is non-classical in that its right-hand side, which is a projection operator, is discontinuous. The discontinuities arise because of the constraints underlying the variational inequality problem modeling the application in question. Hence, classical dynamical systems theory is no longer applicable.

Nevertheless, as demonstrated rigorously in Dupuis and Nagurney (1993), a projected dynamical system may be studied through the use of the Skorokhod Problem

(1961), a tool originally introduced for the study of stochastic differential equations with a reflecting boundary condition. Existence and uniqueness of a solution path, which is essential for the dynamical system to provide a reasonable model, were also established therein. One of the notable features of this tool, whose rigorous theoretical foundations were laid in Dupuis and Nagurney (1993), is its relationship to the variational inequality problem.

Projected dynamical systems theory, however, goes further than finite-dimensional variational inequality theory in that it extends the static study of equilibrium states by introducing an additional time dimension in order to allow for the analysis of disequilibrium behavior that precedes the equilibrium.

In particular, I associate with a given variational inequality problem, a nonclassical dynamical system, called a projected dynamical system. The projected dynamical system is interesting both as a dynamical model for the system whose equilibrium behavior is described by the variational inequality, and, also, because its set of stationary points coincides with the set of solutions to a variational inequality problem. In this framework, the feasibility constraints in the variational inequality problem correspond to discontinuities in the right-hand side of the differential equation, which is a projection operator. Consequently, the projected dynamical system is not amenable to analysis via the classical theory of dynamical systems.

I present the definition of a projected dynamical system, which evolves within a constraint set $\mathbb{K}$. Its stationary points are identified with the solutions to the corresponding variational inequality problem with the same constraint set.

I then state in a theorem the fundamental properties of such a projected dynamical system in regards to the existence and uniqueness of solution paths to the governing ordinary differential equation. We, subsequently, provide an interpretation of the

ordinary differential equation that defines the projected dynamical system, along with a description of how the solutions may be expected to behave.
For additional qualitative results, in particular, stability analysis results, see Nagurney and Zhang (1996). For a discussion of the general iterative scheme and proof of convergence, see Dupuis and Nagurney (1993).

A.4.1 The Variational Inequality Problem and PDS

As I have shown, the variational inequality (A.5) has been used to formulate a plethora of equilibrium problems ranging from traffic network equilibrium problems to spatial oligopolistic market equilibrium problems.
Finite-dimensional variational inequality theory, however, provides no framework for studying the underlying dynamics of systems, since it considers only equilibrium solutions in its formulation. Hence, in a sense, it provides a static representation of a system at its *steady state.* One would, therefore, like a theoretical framework that permits one to study a system not only at its equilibrium point, but also in a dynamical setting.
The definition of a projected dynamical system **(PDS)** is given with respect to a closed convex set $\mathbb{K}$, which is usually the constraint set underlying a particular application, such as, for example, network equilibrium problems, and a vector field F whose domain contains $\mathbb{K}$.
As noted in Dupuis and Nagurney (1993), (see, [78]), it is expected that such projected dynamical systems will provide mathematically convenient approximations to more *realistic* dynamical models that might be used to describe non-static behavior.
The relationship between a projected dynamical system and its associated vari-

ational inequality problem with the same constraint set is then highlighted. For completeness, I also recall the fundamental properties of existence and uniqueness of the solution to the ordinary differential equation **(ODE)** that defines such a projected dynamical system.

A.4.2 Theoretical preliminaries of PDS

I recall some typical concepts of convex analysis (see, for instance, [120, 188]), and confine my attention to the Euclidean space. Let $\Omega \subseteq \mathbb{R}^n$ be a non-empty, closed and convex set, the tangent cone to Ω at x, $T_\Omega(x)$, is defined by

$$T_\Omega(x) = \overline{\cup_{h>0}(\Omega - x)/h},$$

and the normal cone to Ω at x, $N_\Omega(x)$, is defined by

$$N_\Omega(x) = \{v \in \mathbb{R}^n : \langle v, y - x\rangle \leq 0, \forall y \in \Omega\}.$$

If $\Omega \subseteq \mathbb{R}^n$ is a polyhedral set, namely,

$$\Omega = \{x : \langle a_i, x\rangle \leq \alpha_i, i = 1, \ldots, m\},$$

where $a_i \in \mathbb{R}^n$ and $\alpha_i \in \mathbb{R}$, $\forall i$, then it results

$$N_\Omega(x) = \{y_1 a_1 + \ldots, y_m a_m | y_i \geq 0, i \in I(x), y_i = 0, \forall i \notin I(x)\},$$
$$I(x) = \{i : \langle a_i, x\rangle = \alpha_i\}.$$

If $C = C_1 \times \cdots \times C_m$ for closed sets $C_i \in \mathbb{R}^{n_i}$, $n_i \in \mathbb{N}$ for all i, then at any $\bar{x} = (\bar{x}_1, \ldots, \bar{x}_m)$ with $\bar{x}_i \in C_i$, I have

$$N_C(\bar{x}) = N_{C_1}(\bar{x}_1) \times \cdots \times N_{C_m}(\bar{x}_m).$$

Let us introduce the projection operator $P_\Omega : \mathbb{R}^n \to \Omega$, where $P_\Omega(v)$ is such that

$$\|P_\Omega(z) - z\| = \inf_{y\in\Omega} \|y - z\|.$$

I also consider the operator

$$\Pi_\Omega : \Omega \times \mathbb{R}^n \to \mathbb{R}^n,$$

defined by the directional derivative

$$\Pi_\Omega(x, v) = \lim_{t\to 0} \frac{P_\Omega(x + tv) - x}{t}.$$

Thus, $\Pi_\Omega(x, v) = P_{T_\Omega(x)}v$, namely, $\Pi_\Omega(x, v)$ is the metric projection of v onto the tangent cone to Ω at x. In addition, as in [40] and references therein, there exists $n \in N_\Omega(x)$ such that

$$v = \Pi_\Omega(x, v) + n. \tag{A.29}$$

Following [72, 164], a projected dynamical system (PDS) is an ordinary differential equation of the form

$$\dot{x} = \Pi_\Omega(x, -\varphi(x)), \tag{A.30}$$

where $\varphi : \Omega \to \mathbb{R}^n$ is a given vector field. A solution to (A.30) is a function $x : [0, \infty) \to \Omega$ that is absolutely continuous and satisfies

$$\dot{x}(t) = \Pi_\Omega(x(t), -\varphi(x(t))),$$

except for a set of Lebesgue measure zero.

The problem is complemented by the initial condition $x(0) = x^0 \in \Omega$. Problem (A.30) is a non standard ordinary differential equation, where the right-hand side is related to the projection operator, and thus, is discontinuous on the boundary of

Ω. I also note that a solution of the dynamical system belongs to the constraint set Ω. A vector x^* is an equilibrium point or stationary point of the projected dynamical system if x^* satisfies

$$\Pi_\Omega(x^*, -\varphi(x^*)) = 0.$$

This means that once the projected dynamical system reaches x^* at some time $t \geq 0$, it will remain at x^* for all future times.

An important feature of projected dynamical systems is that the set of stationary points coincides with the set of solutions of the finite-dimensional and time-independent variational inequality (see, [78])

$$\langle \varphi(x^*), x - x^* \rangle \geq 0, \quad \forall x \in \Omega.$$

Moreover, problem (A.30) is equivalent to

$$\dot{x} = P_{T_\Omega(z)}\Big(- \varphi(x)\Big).$$

Due to (A.29), the initial value problem

$$\dot{x} = \Pi_\Omega(x, -\varphi(x)), \quad x(0) = x^0 \in \Omega \tag{A.31}$$

consists in finding the solution of minimal norm to the initial condition $x(0) = x^0 \in \Omega$ and the differential variational inequality

$$\dot{x}(t) \in -\Big(N_\Omega(x(t)) + \varphi(x(t))\Big). \tag{A.32}$$

The above problem is, in turn, equivalent to finding the solution of minimal norm to the initial condition $x(0) = x^0 \in \Omega$ and the projected variational inequality

$$\dot{x}(t) \in P_{T_\Omega(x(t))}\Big(- \varphi(x(t))\Big).$$

The following result gives the existence of PDS (see, [78]).

Theorem A.4.1. *Let $\Omega \subset \mathbb{R}^n$ be a polyhedron. Suppose that $x^0 \in \Omega$, and assume that $\varphi : \Omega \to \mathbb{R}^n$ is a vector field with linear growth, namely, there exists $M > 0$ so that for all $x \in \Omega$, $\|\varphi(x)\| \leq M(1 + \|x\|)$. Then, the initial value problem* (A.31) *has unique absolutely continuous solution on the interval* $[0, \infty[$.

I note that Lipschitz continuity implies the linear growth assumption and, hence, it is a sufficient condition for the existence of a unique solution to projected dynamical systems.

A.4.3 Stability of solutions

In this section, I focus my attention on the stability of solutions under perturbations; see [40, 164, 156]. In the theory of PDS, monotonicity concept and its extensions are connected to stability. In fact, monotonicity describes the behavior of perturbed equilibria and show the existence of periodic cycles.

I consider variational inequality (1.10) and the associated projected dynamical system

$$\dot{x} = \Pi_{\Omega}(x, -\varphi(x)), \quad x(0) = x^0 \in \Omega \tag{A.33}$$

In the following, $B(x^*, \delta)$ denotes the open ball centered at x^* with radius δ.

Definition A.4.1. *Let x^* be a critical point of (A.33).*

- *x^* is called monotone attractor if there exists $\delta > 0$ such that, for every solution $x(t)$ with $x(0) \in B(x^*, \delta) \cap \Omega$, $\|x(t) - x^*\|$ is a non increasing function of t.*

- *x^* is a strictly monotone attractor if $\|x(t) - x^*\|$ is decreasing to 0 in t.*

- *x^* is a strictly global monotone attractor if the above property holds for any solution $x(t)$ such that $x(0) \in \Omega$.*

- *x^* is exponentially stable if the solutions starting from points close to x^* are convergent to x^* with exponential rate, namely, if there is $\delta > 0$ and two constants $b > 0$ and $C > 0$ such that for every solution $x(t)$, with $x(0) \in B(x^*, \delta) \cap \Omega$, it results*

$$\|x(t) - x^*\| \leq C\|x(0) - x^*\|e^{-bt}, \quad \forall t \geq 0.$$

- *x^* is globally exponentially stable if the above property holds for all solutions $x(t)$ such that $x(0) \in \Omega$.*

Bibliography

[1] U. Aickelin, E. Burke, and J. Li. “An estimation of distribution algorithm with intelligent local search for rule-based nurse rostering”. In: *Journal of the Operational Research Society* 58 (2007), pp. 1574–1585.

[2] U. Aickelin and K. Dowsland. “An indirect genetic algorithm for a nurse scheduling problem”. In: *Computers & Operations Research* 31 (2004), pp. 761–778.

[3] K. Akka and F. Khaber. “Mobile robot path planning using an improved ant colony optimization”. In: *International Journal of Advanced Robotic Systems* 15.3 (2018). DOI: 10.1177/1729881418774673.

[4] R. Aldrighetti, I. Zennaro, S. Finco, and D. Battini. “Healthcare supply chain simulation with disruption considerations: A case study from Northern Italy”. In: *Global Journal of Flexible Systems Management* 20.1 (2019), pp. 81–102.

[5] E. Altman, F. De Pellegrini, R. El-Azouzi, D. Miorandi, and T. Jimenez. “Emergence of equilibria from individual strategies in online content diffusion”. In: *IEEE NetSciCom - 5th International Workshop on Network*

Science for Communication Networks. 2013 IEEE Conference on Computer Communications Workshops (INFOCOM WKSHPS). Turin, Italy, Apr. 2013, pp. 181–186. DOI: 10.1109/INFCOMW.2013.6562879. URL: https://hal.inria.fr/hal-00913225.

[6] E. Altman, A. Jain, N. Shimkin, and C. Touati. "Dynamic games for analyzing competition in the Internet and in on-line social networks". In: *International conference on network games, control, and optimization*. Springer. 2016, pp. 11–22.

[7] K. J. Arrow and G. Debreu. "Existence of an Equilibrium for a Competitive Economy". In: *Econometrica* 22.3 (1954), pp. 265–290. ISSN: 00129682, 14680262. URL: http://www.jstor.org/stable/1907353.

[8] S. Atakan and S. Sen. "A progressive hedging based branch-and-bound algorithm for mixed-integer stochastic programs". In: *Computational Management Science* 15.3 (2018), pp. 501–540.

[9] Y. Atay, I. Koc, I. Babaoglu, and H. Kodaz. "Community detection from biological and social networks: A comparative analysis of metaheuristic algorithms". In: *Applied Soft Computing* 50 (2017), pp. 194–211. DOI: 10.1016/j.asoc.2016.11.025.

[10] M. Aureli et al. "Activity of plasma membrane β-galactosidase and β-glucosidase". In: *FEBS Letters* 583.15 (2009), pp. 2469–2473. DOI: 10.1016/j.febslet.2009.06.048.

[11] D. Aussel and S. Sagratella. "Sufficient conditions to compute any solution of a quasivariational inequality via a variational inequality". In: *Mathe-*

matical Methods of Operations Research 85 (Feb. 2017). DOI: 10.1007/s00186-016-0565-x.

[12] D. Aussel, R. Gupta, and A. Mehra. "Evolutionary variational inequality formulation of the generalized Nash equilibrium problem". In: *Journal of Optimization Theory and Applications* 169.1 (2016), pp. 74–90.

[13] A.-L. Barabasi and Z. N. Oltvai. "Network biology: understanding the cell's functional organization". In: *Nature Reviews Genetics* 5.2 (2004), pp. 101–113. DOI: 10.1038/nrg1272.

[14] A.-L. Barabási, R. Albert, and H. Jeong. "Scale-free characteristics of random networks: the topology of the world-wide web". In: *Physica A: Statistical Mechanics and its Applications* 281.1-4 (2000), pp. 69–77. DOI: 10.1016/S0378-4371(00)00018-2.

[15] A.-L. Barabási, N. Gulbahce, and J. Loscalzo. "Network medicine: a network-based approach to human disease". In: *Nature Reviews Genetics* 12.1 (2011), pp. 56–68. DOI: 10.1038/nrg2918.

[16] A. Barbagallo, P. Daniele, and A. Maugeri. "Variational formulation for a general dynamic financial equilibrium problem: balance law and liability formula". In: *Nonlinear Analysis: Theory, Methods & Applications* 75.3 (2012), pp. 1104–1123.

[17] A. Barbagallo. "On the regularity of retarded equilibria in time-dependent traffic equilibrium problems". In: *Nonlinear Analysis: Theory, Methods & Applications* 71.12 (2009), e2406–e2417.

[18] G. Barbarosoğlu and Y. Arda. “A two-stage stochastic programming framework for transportation planning in disaster response”. In: *Journal of the operational research society* 55.1 (2004), pp. 43–53.

[19] E. Battegazzorre, A. Bottino, M. Domaneschi, and G. P. Cimellaro. “IdealCity: A hybrid approach to seismic evacuation modeling”. In: *Advances in Engineering Software* 153 (2021), p. 102956. DOI: 10.1016/j.advengsoft.2020.102956.

[20] V. Bayram and H. Yaman. “A stochastic programming approach for shelter location and evacuation planning”. In: *RAIRO-Operations Research* 52.3 (2018), pp. 779–805.

[21] T. Bektas. “The multiple traveling salesman problem: an overview of formulations and solution procedures”. In: *omega* 34.3 (2006), pp. 209–219.

[22] P. Beraldi, M. Bruni, and D. Conforti. “A solution approach for two-stage stochastic nonlinear mixed integer programs”. In: *Algorithmic Operations Research* 4.1 (2009), pp. 76–85.

[23] I. Berrada, J. Ferland, and P. Michelon. “A multi-objective approach to nurse scheduling with both hard and soft constraints”. In: *Socio-Economic Planning Sciences* 30 (1996), pp. 183–193.

[24] I. Blöchliger. “Modeling staff scheduling problems. A tutorial”. In: *European Journal of Operational Research* 158 (2004), pp. 533–542.

[25] V. D. Blondel, J.-L. Guillaume, R. Lambiotte, and E. Lefebvre. “Fast unfolding of communities in large networks”. In: *Journal of Statistical Mechanics: Theory and Experiment* 2008.10 (Oct. 2008), P10008. DOI: 10.1088/1742-5468/2008/10/P10008.

[26] M. Brand, M. Masuda, N. Wehner, and X. Yu. “Ant Colony Optimization algorithm for robot path planning”. In: *2010 International Conference On Computer Design and Applications*. Vol. 3. 2010, pp. V3-436–V3-440. DOI: 10.1109/ICCDA.2010.5541300.

[27] U. Brandes et al. “On Modularity Clustering”. In: *IEEE Transactions on Knowledge and Data Engineering* 20.2 (Feb. 2008), pp. 172–188. DOI: 10.1109/TKDE.2007.190689.

[28] D. Bu et al. “Topological structure analysis of the protein-–protein interaction network in budding yeast”. In: *Nucleic Acids Research* 31.9 (May 2003), pp. 2443–2450. DOI: 10.1093/nar/gkg340.

[29] E. Burke, T. Curtois, R. Qu, and G. Van den Berghe. “A scatter search method- ology for the nurse rostering problem”. In: *Journal of the Operational Research Society* 61 (2010), pp. 1667–1679.

[30] E. Burke, P. De Causmaecker, S. Petrovic, and G. Van den Berghe. “Metaheuristics for handling time interval coverage constraints in nurse scheduling”. In: *Applied Artificial Intelligence* 20 (2006), pp. 743–766.

[31] Z. Cai, W. Wang, S. Zhang, and Z. Jiang. “Ant colony optimization for component assignment problems in circular consecutive-k-out-of-n systems”. In: *2017 IEEE International Conference on Industrial Engineering and Engineering Management (IEEM)*. 2017, pp. 954–958.

[32] L. Cantini, E. Medico, S. Fortunato, and M. Caselle. “Detection of gene communities in multi-networks reveals cancer drivers”. In: *Scientific Reports* 5 (2015), p. 17386. DOI: 10.1038/srep17386.

[33] *Cattle Protein-protein Interactions*. https://biit.cs.ut.ee/graphweb/welcome.cgi?t=examples. 2009.

[34] M. Cha, H. Kwak, P. Rodriguez, Y.-Y. Ahn, and S. Moon. "Analyzing the Video Popularity Characteristics of Large-Scale User Generated Content Systems". In: 17.5 (2009). ISSN: 1063-6692. DOI: 10.1109/TNET.2008.2011358. URL: https://doi.org/10.1109/TNET.2008.2011358.

[35] M. Cha, H. Kwak, P. Rodriguez, Y.-Y. Ahn, and S. Moon. "I Tube, You Tube, Everybody Tubes: Analyzing the World's Largest User Generated Content Video System". In: *Proceedings of the 7th ACM SIGCOMM Conference on Internet Measurement*. IMC '07. San Diego, California, USA: Association for Computing Machinery, 2007, pp. 1–14. ISBN: 9781595939081. DOI: 10.1145/1298306.1298309. URL: https://doi.org/10.1145/1298306.1298309.

[36] C. K. Chan, Y. Zhou, and K. H. Wong. "A dynamic equilibrium model of the oligopolistic closed-loop supply chain network under uncertain and time-dependent demands". In: *Transportation Research Part E: Logistics and Transportation Review* 118 (2018), pp. 325–354.

[37] D. Chang, L. Cui, and Z. Huang. "A Cellular-Automaton Agent-Hybrid Model for Emergency Evacuation of People in Public Places". In: *IEEE Access* 8 (2020), pp. 79541–79551. DOI: 10.1109/ACCESS.2020.2986012.

[38] X. Chen, T. K. Pong, and R. J. Wets. "Two-stage stochastic variational inequalities: an ERM-solution procedure". In: *Mathematical Programming* 165.1 (2017), pp. 71–111.

[39] P. Civicioglu. “Transforming geocentric cartesian coordinates to geodetic coordinates by using differential search algorithm”. In: *Computers & Geosciences* 46 (2012), pp. 229–247. DOI: 10.1016/j.cageo.2011.12.011.

[40] M.-G. Cojocaru, C. T. Bauch, and M. D. Johnston. “Dynamics of vaccination strategies via projected dynamical systems”. In: *Bulletin of mathematical biology* 69.5 (2007), pp. 1453–1476.

[41] M.-G. Cojocaru, P. Daniele, and A. Nagurney. “Double-layered dynamics: a unified theory of projected dynamical systems and evolutionary variational inequalities”. In: *European Journal of Operational Research* 175.1 (2006), pp. 494–507.

[42] M.-G. Cojocaru, P. Daniele, and A. Nagurney. “Projected dynamical systems, evolutionary variational inequalities, applications, and a computational procedure”. In: *Pareto Optimality, Game Theory and Equilibria*. Springer, 2008, pp. 387–406.

[43] G. Colajanni, P. Daniele, S. Giuffrè, and A. Nagurney. “Cybersecurity investments with nonlinear budget constraints and conservation laws: variational equilibrium, marginal expected utilities, and Lagrange multipliers”. In: *International Transactions in Operational Research* 25.5 (2018), pp. 1443–1464.

[44] P. Consoli, A. Collerà, and M. Pavone. “Swarm Intelligence heuristics for Graph Coloring Problem”. In: *2013 IEEE Congress on Evolutionary Computation*. 2013, pp. 1909–1916. DOI: 10.1109/CEC.2013.6557792.

[45] C. Crespi, G. Fargetta, M. Pavone, and S. R. A. “How a Different Ant Behavior Affects on the Performances of the Whole Colony”. In: *Meta-*

heuristics International Conference (MIC2022, in press). Lecture Notes in Computer Science. Springer, 2022.

[46] C. Crespi, G. Fargetta, M. Pavone, and R. A. Scollo. "An Agent-Based Model to Investigate Different Behaviours in a Crowd Simulation". In: *International Conference on Bioinspired Optimization Methods and Their Applications*. Springer. 2022, pp. 1–14.

[47] C. Crespi, G. Fargetta, M. Pavone, R. A. Scollo, and L. Scrimali. "A Game Theory Approach for Crowd Evacuation Modelling". In: *Bioinspired Optimization Methods and Their Applications (BIOMA2020)*. Ed. by B. Filipič, E. Minisci, and M. Vasile. Vol. 12438. Lecture Notes in Computer Science. Cham: Springer, 2020, pp. 228–239. DOI: 10.1007/978-3-030-63710-1_18.

[48] C. Crespi, R. A. Scollo, and M. Pavone. "Effects of Different Dynamics in an Ant Colony Optimization Algorithm". In: *2020 7th International Conference on Soft Computing Machine Intelligence (ISCMI2020)*. IEEE, Nov. 2020, pp. 8–11. DOI: 10.1109/ISCMI51676.2020.9311553.

[49] V. Cutello, M. Oliva, M. Pavone, and R. A. Scollo. "An Immune Metaheuristics for Large Instances of the Weighted Feedback Vertex Set Problem". In: *2019 IEEE Symposium Series on Computational Intelligence (SSCI)*. Dec. 2019, pp. 1928–1936. DOI: 10.1109/SSCI44817.2019.9002988.

[50] V. Cutello, G. Fargetta, M. Pavone, and R. A. Scollo. "Optimization Algorithms for Detection of Social Interactions". In: *Algorithms* 13.6 (2020), p. 139. DOI: 10.3390/a13060139.

[51] V. Cutello, G. Fargetta, M. Pavone, R. A. Scollo, and A. G. Spampinato. "Discovering Entities Similarities in Biological Networks Using a Hybrid Immune Algorithm". In: *Swarm and Evolutionary Computation (under second revision)* ().

[52] V. Cutello, G. Nicosia, and M. Pavone. "An immune algorithm with stochastic aging and Kullback entropy for the chromatic number problem". In: *Journal of Combinatorial Optimization* 14.1 (2007), pp. 9–33. DOI: 10.1007/s10878-006-9036-2.

[53] P. Daniele and D. Sciacca. "A dynamic supply chain network for PPE during the Covid-19 pandemic". In: *J. Appl. Numeric. Opt* 3.2 (2021), pp. 403–424.

[54] P. Daniele. *Dynamic networks and evolutionary variational inequalities*. Edward Elgar Publishing, 2006.

[55] P. Daniele and S. Giuffrè. "General infinite dimensional duality and applications to evolutionary network equilibrium problems". In: *Optimization Letters* 1.3 (2007), pp. 227–243.

[56] P. Daniele and S. Giuffrè. "Random variational inequalities and the random traffic equilibrium problem". In: *Journal of Optimization Theory and Applications* 167.1 (2015), pp. 363–381.

[57] P. Daniele, S. Giuffrè, G. Idone, and A. Maugeri. "Infinite dimensional duality and applications". In: *Mathematische Annalen* 339.1 (2007), pp. 221–239.

[58] P. Daniele, S. Giuffré, and A. Maugeri. “Remarks on general infinite dimensional duality with cone and equality constraints”. In: *Commun. Appl. Anal* 13.4 (2009), pp. 567–578.

[59] P. Daniele, S. Giuffrè, and A. Maugeri. “General traffic equilibrium problem with uncertainty and random variational inequalities”. In: *Optimization in Science and Engineering*. Springer, 2014, pp. 89–96.

[60] P. Daniele and L. Scrimali. “Strong nash equilibria for cybersecurity investments with nonlinear budget constraints”. In: *New Trends in Emerging Complex Real Life Problems*. Springer, 2018, pp. 199–207.

[61] L. Danon, A. Díaz-Guilera, J. Duch, and A. Arenas. “Comparing community structure identification”. In: *Journal of Statistical Mechanics: Theory and Experiment* 2005.09 (Sept. 2005), P09008–P09008. DOI: 10.1088/1742-5468/2005/09/p09008.

[62] F. De Pellegrini, A. Reiffers, and E. Altman. “Differential games of competition in online content diffusion”. In: *2014 IFIP Networking Conference*. IEEE. 2014, pp. 1–9.

[63] W. Deng, J. Xu, and H. Zhao. “An Improved Ant Colony Optimization Algorithm Based on Hybrid Strategies for Scheduling Problem”. In: *IEEE Access* 7 (2019), pp. 20281–20292. DOI: 10.1109/ACCESS.2019.2897580.

[64] A. Di Stefano, A. Vitale, V. Cutello, and M. Pavone. “How long should offspring lifespan be in order to obtain a proper exploration?” In: *2016 IEEE Symposium Series on Computational Intelligence (SSCI)*. Dec. 2016, pp. 1–8. DOI: 10.1109/SSCI.2016.7850270.

[65] W. Didimo and F. Montecchiani. “Fast layout computation of clustered networks: Algorithmic advances and experimental analysis”. In: *Information Sciences* 260 (2014), pp. 185–199. DOI: 10.1016/j.ins.2013.09.048.

[66] G. Diss et al. “Integrative avenues for exploring the dynamics and evolution of protein interaction networks”. In: *Current Opinion in Biotechnology* 24.4 (2013), pp. 775–783. DOI: 10.1016/j.copbio.2013.02.023.

[67] C. Dogbe. “On the modelling of crowd dynamics by generalized kinetic models”. In: *Journal of Mathematical Analysis and Applications* 387.2 (2012), pp. 512–532. DOI: 10.1016/j.jmaa.2011.09.007.

[68] C. Dogbé. “Modeling crowd dynamics by the mean-field limit approach”. In: *Mathematical and Computer Modelling* 52.9-10 (2010), pp. 1506–1520. DOI: 10.1016/j.mcm.2010.06.012.

[69] M. Dorigo and L. Gambardella. “Ant colony system: a cooperative learning approach to the traveling salesman problem”. In: *IEEE Transactions on Evolutionary Computation* 1.1 (1997), pp. 53–66. DOI: 10.1109/4235.585892.

[70] M. Dorigo and T. Stützle. “Ant Colony Optimization: Overview and Recent Advances”. In: *Handbook of Metaheuristics*. Ed. by M. Gendreau and J.-Y. Potvin. Cham: Springer International Publishing, 2019, pp. 311–351. DOI: 10.1007/978-3-319-91086-4_10.

[71] J. Duch and A. Arenas. “Community detection in complex networks using extremal optimization”. In: *Physical Review E* 72 (2 Aug. 2005), p. 027104. DOI: 10.1103/PhysRevE.72.027104.

[72] P. Dupuis and A. Nagurney. “Dynamical systems and variational inequalities”. In: *Annals of Operations Research* 44.1 (1993), pp. 7–42.

[73] A. El Adoly, M. Gheith, and N. Fors. “A new formulation and solution for the nurse scheduling problem: A case study in Egypt”. In: *Alexandria Engineering Journal* 57 (2018), pp. 2289–2298.

[74] O. K. Erol and I. Eksin. “A new optimization method: Big Bang–Big Crunch”. In: *Advances in Engineering Software* 37.2 (2006), pp. 106–111. DOI: 10.1016/j.advengsoft.2005.04.005.

[75] J. Euchi, S. Zidi, and L. Laouamer. “A Hybrid Approach to Solve the Vehicle Routing Problem with Time Windows and Synchronized Visits In-Home Health Care”. In: *Arabian Journal for Science and Engineering* 45 (2020), pp. 10637–10652.

[76] F. Facchinei, A. Fischer, and V. Piccialli. “On generalized Nash games and variational inequalities”. In: *Operations Research Letters* 35.2 (2007), pp. 159–164.

[77] F. Facchinei and C. Kanzow. “Generalized Nash equilibrium problems”. In: *Annals of Operations Research* 175.1 (2010), pp. 177–211.

[78] F. Facchinei and J.-S. Pang. *Finite-dimensional variational inequalities and complementarity problems*. Springer, 2003.

[79] F. Facchinei, V. Piccialli, and M. Sciandrone. “Decomposition algorithms for generalized potential games”. In: *Computational Optimization and Applications* 50.2 (2011), pp. 237–262.

[80] F. Facchinei and S. Sagratella. “On the computation of all solutions of jointly convex generalized Nash equilibrium problems”. In: *Optimization Letters* 5.3 (2011), pp. 531–547.

[81] P. Falsaperla, F. Raciti, and L. Scrimali. “A variational inequality model of the spatial price network problem with uncertain data”. In: *Optimization and Engineering* 13.3 (2012), pp. 417–434.

[82] S. V. Fani and A. P. Subriadi. “Business continuity plan: examining of multi-usable framework”. In: *Procedia Computer Science* 161 (2019), pp. 275–282.

[83] F. Faraci and F. Raciti. “On generalized Nash equilibrium in infinite dimension: the Lagrange multipliers approach”. In: *Optimization* 64.2 (2015), pp. 321–338.

[84] G. Fargetta, A. Maugeri, and L. Scrimali. “A Stochastic Nash Equilibrium Problem for Medical Supply Competition”. In: *Journal of Optimization Theory and Applications* (2022), pp. 1–27.

[85] G. Fargetta and L. Scrimali. “A game theory model of online content competition”. In: *Advances in Optimization and Decision Science for Society, Services and Enterprises*. Springer, 2019, pp. 173–184.

[86] G. Fargetta and L. Scrimali. “A Multi-stage Integer Linear Programming Problem for Personnel and Patient Scheduling for a Therapy Centre.” In: *ICORES*. 2022, pp. 354–361.

[87] G. Fargetta and L. Scrimali. “A two-stage variational inequality for medical supply in emergency management”. In: *Optimization and Decision Science*. Springer, 2021, pp. 91–102.

[88] G. Fargetta and L. Scrimali. “Closed-Loop Supply Chain Network Equilibrium with Online Second-Hand Trading”. In: *Optimization in Artificial Intelligence and Data Sciences*. Springer, 2022, pp. 117–127.

[89] G. Fargetta and L. Scrimali. “Generalized Nash equilibrium and dynamics of popularity of online contents”. In: *Optimization Letters* (2020), pp. 1–19. DOI: 10.1007/s11590-019-01528-4.

[90] G. Fargetta and L. Scrimali. “Optimal emergency evacuation with uncertainty”. In: *Mathematical Analysis in Interdisciplinary Research*. Springer, 2021, pp. 261–279.

[91] G. Fargetta and L. Scrimali. “Time-Dependent Generalized Nash Equilibria in Social Media Platforms”. In: *International Conference on Optimization and Decision Science (ODS2022, in press)*. Springer, 2022.

[92] S. Fidanova and P. Pop. “An improved hybrid ant-local search algorithm for the partition graph coloring problem”. In: *Journal of Computational and Applied Mathematics* 293 (2016), pp. 55–61. DOI: https://doi.org/10.1016/j.cam.2015.04.030.

[93] E. Forcael et al. “Ant colony optimization model for tsunamis evacuation routes”. In: *Computer–Aided Civil and Infrastructure Engineering* 29.10 (2014), pp. 723–737. DOI: 10.1111/mice.12113.

[94] S. Fortunato. “Community detection in graphs”. In: *Physics Reports* 486.3-5 (2010), pp. 75–174. DOI: 10.1016/j.physrep.2009.11.002.

[95] S. Fortunato and M. Barthélemy. “Resolution limit in community detection”. In: *Proceedings of the National Academy of Sciences* 104.1 (2007), pp. 36–41. DOI: 10.1073/pnas.0605965104.

[96] S. Fouladvand, A. Osareh, B. Shadgar, M. Pavone, and S. Sharafi. "DENSA: An effective negative selection algorithm with flexible boundaries for self-space and dynamic number of detectors". In: *Engineering Applications of Artificial Intelligence* 62 (2017), pp. 359–372. DOI: 10.1016/j.engappai.2016.08.014.

[97] M. Girvan and M. E. J. Newman. "Community structure in social and biological networks". In: *Proceedings of the National Academy of Sciences* 99.12 (2002), pp. 7821–7826. DOI: 10.1073/pnas.122653799.

[98] P. M. Gleiser and L. Danon. "Community structure in Jazz". In: *Advances in Complex Systems* 06.04 (2003), pp. 565–573. DOI: 10.1142/S0219525903001067.

[99] F. Glover. "Heuristics for integer programming using surrogate constraints". In: *Decision Sciences* 8.1 (1977), pp. 156–166. DOI: 10.1111/j.1540-5915.1977.tb01074.x.

[100] K.-I. Goh et al. "The human disease network". In: *Proceedings of the National Academy of Sciences* 104.21 (2007), pp. 8685–8690. DOI: 10.1073/pnas.0701361104.

[101] B. H. Good, Y.-A. de Montjoye, and A. Clauset. "Performance of modularity maximization in practical contexts". In: *Physical Review E* 81 (4 Apr. 2010), p. 046106. DOI: 10.1103/PhysRevE.81.046106.

[102] H. Gu, P. Zhu, Y. Jiao, Y. Meng, and M. Chen. "PRIN: a predicted rice interactome network". In: *BMC Bioinformatics* 12.1 (2011), pp. 1–13. DOI: 10.1186/1471-2105-12-161.

[103] T. Gu, C. Wang, and G. He. “A VR-Based, Hybrid Modeling Approach to Fire Evacuation Simulation”. In: *Proceedings of the 16th ACM SIGGRAPH International Conference on Virtual-Reality Continuum and Its Applications in Industry*. VRCAI ’18. Tokyo, Japan: Association for Computing Machinery, 2018. DOI: 10.1145/3284398.3284409.

[104] N. Gulbahce and S. Lehmann. “The art of community detection”. In: *BioEssays* 30.10 (2008), pp. 934–938. DOI: 10.1002/bies.20820.

[105] J. Gwinner, B. Jadamba, A. A. Khan, and F. Raciti. *Uncertainty Quantification in Variational Inequalities: Theory, Numerics, and Applications*. Chapman and Hall/CRC, 2021.

[106] J. Gwinner and F. Raciti. “On a class of random variational inequalities on random sets”. In: *Numerical Functional Analysis and Optimization* 27.5-6 (2006), pp. 619–636.

[107] J. Gwinner and F. Raciti. “Random equilibrium problems on networks”. In: *Mathematical and Computer Modelling* 43.7-8 (2006), pp. 880–891.

[108] J. Gwinner and F. Raciti. “Some equilibrium problems under uncertainty and random variational inequalities”. In: *Annals of Operations research* 200.1 (2012), pp. 299–319.

[109] M. Hajjem, H. Bouziri, E.-G. Talbi, and K. Mellouli. “Intelligent Indoor Evacuation Guidance System Based on Ant Colony Algorithm”. In: *IEEE/ACS 14th International Conference on Computer Systems and Applications (AICCSA)*. Oct. 2017, pp. 1035–1042. DOI: 10.1109/AICCSA.2017.47.

[110] Y. Han and H. Liu. “Modified social force model based on information transmission toward crowd evacuation simulation”. In: *Physica A: Statistical Mechanics and its Applications* 469 (2017), pp. 499–509. DOI: 10.1016/j.physa.2016.11.014.

[111] Y. Han, H. Liu, and P. Moore. “Extended route choice model based on available evacuation route set and its application in crowd evacuation simulation”. In: *Simulation Modelling Practice and Theory* 75 (2017), pp. 1–16. DOI: 10.1016/j.simpat.2017.03.010.

[112] P. T. Harker. “Generalized Nash games and quasi-variational inequalities”. In: *European journal of Operational research* 54.1 (1991), pp. 81–94.

[113] C. W. Hongzhi Wang, Y. Z. Yifeng Guo, and M. Zhu. “Emergency Escape Route Planning for the Louvre Summary”. In: *Academic Journal of Computing & Information Science* 2 (2019), pp. 78–84. DOI: https://doi.org/10.25236/AJCIS.010041.

[114] J. Hu et al. “Simulation of queuing time in crowd evacuation by discrete time loss queuing method”. In: *International Journal of Modern Physics C* 30.08 (2019), p. 1950057. DOI: 10.1142/S0129183119500578.

[115] S.-H. Huang, Y.-H. Huang, C. A. Blazquez, and G. Paredes-Belmar. “Application of the Ant Colony Optimization in the Resolution of the Bridge Inspection Routing Problem”. In: *Appl. Soft Comput.* 65.C (Apr. 2018), pp. 443–461. ISSN: 1568-4946. DOI: 10.1016/j.asoc.2018.01.034.

[116] Z.-M. Huang et al. “Ant Colony Evacuation Planner: An Ant Colony System With Incremental Flow Assignment for Multipath Crowd Evacuation”.

In: *IEEE Transactions on Cybernetics* 51.11 (2021), pp. 5559–5572. DOI: 10.1109/TCYB.2020.3013271.

[117] G. Idone and A. Maugeri. "Generalized constraints qualification conditions and infinite dimensional duality". In: *Taiwanese Journal of Mathematics* 13.6A (2009), pp. 1711–1722.

[118] K. Ijaz, S. Sohail, and S. Hashish. "A Survey of Latest Approaches for Crowd Simulation and Modeling Using Hybrid Techniques". In: *Proceedings of the 2015 17th UKSIM-AMSS International Conference on Modelling and Simulation*. UKSIM '15. IEEE Computer Society, 2015, pp. 111–116. DOI: 10.5555/2867552.2868182.

[119] B. Jadamba and F. Raciti. "Variational inequality approach to stochastic Nash equilibrium problems with an application to Cournot oligopoly". In: *Journal of Optimization Theory and Applications* 165.3 (2015), pp. 1050–1070.

[120] J. Jahn. *Introduction to the theory of nonlinear optimization*. Springer Nature, 2020.

[121] Y.-H. Jia, Y. Mei, and M. Zhang. "A Bilevel Ant Colony Optimization Algorithm for Capacitated Electric Vehicle Routing Problem". In: *IEEE Transactions on Cybernetics* (2021), pp. 1–14. DOI: 10.1109/TCYB.2021.3069942.

[122] J. Jiang, Y. Shi, X. Wang, and X. Chen. "Regularized two-stage stochastic variational inequalities for Cournot-Nash equilibrium under uncertainty". In: *arXiv preprint:1907.07317* (2019).

[123] R. Jovanovic, M. Tuba, and S. Voß. "An efficient ant colony optimization algorithm for the blocks relocation problem". In: *European Journal of Operational Research* 274.1 (2019), pp. 78–90. DOI: 10.1016/j.ejor.2018.09.038.

[124] B. W. Kernighan and S. Lin. "An efficient heuristic procedure for partitioning graphs". In: *The Bell System Technical Journal* 49.2 (Feb. 1970), pp. 291–307. DOI: 10.1002/j.1538-7305.1970.tb01770.x.

[125] N. Khamis et al. "Optimized exit door locations for a safer emergency evacuation using crowd evacuation model and artificial bee colony optimization". In: *Chaos, Solitons, Fractals* 131 (2020), p. 109505. DOI: 10.1016/j.chaos.2019.109505.

[126] D. Kinderlehrer and G. Stampacchia. *An introduction to variational inequalities and their applications*. SIAM, 2000.

[127] A. Király and J. Abonyi. "Redesign of the supply of mobile mechanics based on a novel genetic optimization algorithm using Google Maps API". In: *Engineering Applications of Artificial Intelligence* 38 (2015), pp. 122–130.

[128] G. Korpelevich. "Extragradient method for finding saddle points and other problems". In: *Matekon* 13.4 (1977), pp. 35–49.

[129] I. S. Kotsireas, A. Nagurney, and P. M. Pardalos, eds. *Dynamics of Disasters–Key Concepts, Models, Algorithms, and Insights: Kalamata, Greece, June–July 2015*. Vol. 185. Springer Proceedings in Mathematics & Statistics. Cham: Springer, 2016. DOI: 10.1007/978-3-319-43709-5.

[130] V. Krebs. *A network of books about recent US politics sold by the online bookseller Amazon.com*. http://www.orgnet.com. 2008.

[131] A. A. Kulkarni and U. V. Shanbhag. "On the variational equilibrium as a refinement of the generalized Nash equilibrium". In: *Automatica* 48.1 (2012), pp. 45–55.

[132] S. Kullback. *Information Theory and Statistics*. Wiley, 1959.

[133] L. Lampariello and S. Sagratella. "A bridge between bilevel programs and Nash games". In: *Journal of Optimization Theory and Applications* 174.2 (2017), pp. 613–635.

[134] A. Lancichinetti and S. Fortunato. "Benchmarks for testing community detection algorithms on directed and weighted graphs with overlapping communities". In: *Physical Review E* 80 (1 July 2009), p. 016118. DOI: 10.1103/PhysRevE.80.016118.

[135] A. Lancichinetti, S. Fortunato, and F. Radicchi. "Benchmark Graphs for Testing Community Detection Algorithms". In: *Physical Review E* 78 (1 July 2008), p. 046110. DOI: 10.1103/PhysRevE.78.046110.

[136] D.-S. Lee et al. "The implications of human metabolic network topology for disease comorbidity". In: *Proceedings of the National Academy of Sciences* 105.29 (2008), pp. 9880–9885. DOI: 10.1073/pnas.0802208105.

[137] A. Legrain, H. Bouarab, and N. Lahrichi. "The nurse scheduling problem in real-life". In: *Journal of Medical Systems* 39.160 (2015).

[138] M. Li and C. Zhang. "Two-stage stochastic variational inequality arising from stochastic programming". In: *Journal of Optimization Theory and Applications* 186.1 (2020), pp. 324–343.

[139] Y. Li et al. “A review of cellular automata models for crowd evacuation”. In: *Physica A: Statistical Mechanics and its Applications* 526 (2019), p. 120752. DOI: 10.1016/j.physa.2019.03.117.

[140] Y. H. Lim, J. M. Charette, and S. J. Baserga. “Assembling a protein-protein interaction map of the SSU processome from existing datasets”. In: *PLOS ONE* 6.3 (2011), e17701. DOI: 10.1371/journal.pone.0017701.

[141] H. Liu, B. Xu, D. Lu, and G. Zhang. “A path planning approach for crowd evacuation in buildings based on improved artificial bee colony algorithm”. In: *Applied Soft Computing* 68 (2018), pp. 360–376. DOI: 10.1016/j.asoc.2018.04.015.

[142] J. P. Luna. “Decomposition and approximation methods for variational inequalities, with applications to deterministic and stochastic energy markets”. PhD thesis. Instituto nacional de matemática pura e aplicada, Rio De Janeiro, Brazil, 2013.

[143] D. Lusseau et al. “The bottlenose dolphin community of Doubtful Sound features a large proportion of long-lasting associations”. In: *Behavioral Ecology and Sociobiology* 54 (2003), pp. 396–405. DOI: 10.1007/s00265-003-0651-y.

[144] M. W. Macy and A. Flache. “Learning dynamics in social dilemmas”. In: *Proceedings of the National Academy of Sciences* 99.suppl 3 (2002), pp. 7229–7236. DOI: 10.1073/pnas.092080099.

[145] D. Marbach et al. “Wisdom of crowds for robust gene network inference”. In: *Nature Methods* 9.8 (2012), pp. 796–804. DOI: 10.1038/nmeth.2016.

[146] R. Martí, M. Laguna, and F. Glover. “Principles of scatter search”. In: *European Journal of Operational Research* 169.2 (2006), pp. 359–372. DOI: 10.1016/j.ejor.2004.08.004.

[147] G. Mastroeni, M. Pappalardo, and F. Raciti. “Generalized Nash equilibrium problems and variational inequalities in Lebesgue spaces”. In: (2020).

[148] A. Maugeri and F. Raciti. “On existence theorems for monotone and non-monotone variational inequalities”. In: *J. Convex Anal* 16.3-4 (2009), pp. 899–911.

[149] A. Maugeri and F. Raciti. “Remarks on infinite dimensional duality”. In: *Journal of Global Optimization* 46.4 (2010), pp. 581–588.

[150] R. Milo et al. “Network Motifs: Simple Building Blocks of Complex Networks”. In: *Science* 298.5594 (2002), pp. 824–827. DOI: 10.1126/science.298.5594.824.

[151] A. Mohd Ibrahim, I. Venkat, and P. De Wilde. “The Impact of Potential Crowd Behaviours on Emergency Evacuation: An Evolutionary Game-Theoretic Approach”. In: *Journal of Artificial Societies and Social Simulation* 22.1 (2019). DOI: 10.18564/jasss.3837.

[152] A. Mullard. “Protein–protein interaction inhibitors get into the groove”. In: *Nature Reviews Drug Discovery* 11 (2012), pp. 173–175. DOI: 10.1038/nrd3680.

[153] K. Nabetani, P. Tseng, and M. Fukushima. “Parametrized variational inequality approaches to generalized Nash equilibrium problems with shared constraints”. In: *Computational Optimization and Applications* 48.3 (2011), pp. 423–452.

[154] L. M. Naeni, R. Berretta, and P. Moscato. “MA-Net: A Reliable Memetic Algorithm for Community Detection by Modularity Optimization”. In: *Proceedings of the 18th Asia Pacific Symposium on Intelligent and Evolutionary Systems, Volume 1*. Ed. by H. Handa, H. Ishibuchi, Y.-S. Ong, and K. C. Tan. Cham: Springer International Publishing, 2015, pp. 311–323. DOI: 10.1007/978-3-319-13359-1_25.

[155] A. Nagurney. *Network economics: A variational inequality approach*. Vol. 10. Springer Science & Business Media, 1998.

[156] A. Nagurney, J. Cruz, and J. Dong. “Global supply chain networks and risk management: a multi-agent framework”. In: *Multiagent based Supply Chain Management*. Springer, 2006, pp. 103–134.

[157] A. Nagurney, J. Cruz, J. Dong, and D. Zhang. “Supply chain networks, electronic commerce, and supply side and demand side risk”. In: *European journal of operational research* 164.1 (2005), pp. 120–142.

[158] A. Nagurney, J. Dong, and D. Zhang. “A supply chain network equilibrium model”. In: *Transportation Research Part E: Logistics and Transportation Review* 38.5 (2002), pp. 281–303.

[159] A. Nagurney and D. Li. *Competing on supply chain quality*. Springer, 2016.

[160] A. Nagurney, D. Li, S. Saberi, and T. Wolf. “A dynamic network economic model of a service-oriented Internet with price and quality competition”. In: *Network Models in Economics and Finance*. Springer, 2014, pp. 239–264.

[161] A. Nagurney, J. Loo, J. Dong, and D. Zhang. “Supply chain networks and electronic commerce: A theoretical perspective”. In: *Netnomics* 4.2 (2002), pp. 187–220.

[162] A. Nagurney and F. Toyasaki. “Reverse supply chain management and electronic waste recycling: a multitiered network equilibrium framework for e-cycling”. In: *Transportation Research Part E: Logistics and Transportation Review* 41.1 (2005), pp. 1–28.

[163] A. Nagurney and F. Toyasaki. “Supply chain supernetworks and environmental criteria”. In: *Transportation Research Part D: Transport and Environment* 8.3 (2003), pp. 185–213.

[164] A. Nagurney and D. Zhang. *Projected dynamical systems and variational inequalities with applications*. Vol. 2. Springer Science & Business Media, 1995.

[165] J. Nash. “Non-cooperative games”. In: *Annals of mathematics* (1951), pp. 286–295.

[166] J. F. Nash et al. “Equilibrium points in n-person games”. In: *Proceedings of the national academy of sciences* 36.1 (1950), pp. 48–49.

[167] Y. Nesterov and L. Scrimali. “Solving strongly monotone variational and quasi-variational inequalities”. In: *Core Discussion Paper 2006/107* (2006).

[168] M. E. J. Newman. “Fast algorithm for detecting community structure in networks”. In: *Physical Review E* 69 (6 June 2004), p. 066133. DOI: 10.1103/PhysRevE.69.066133.

[169] M. E. J. Newman. “Finding community structure in networks using the eigenvectors of matrices”. In: *Physical Review E* 74 (3 Sept. 2006), p. 036104. DOI: 10.1103/PhysRevE.74.036104.

[170] M. E. J. Newman and M. Girvan. “Finding and evaluating community structure in networks”. In: *Physical Review E* 69 (2 Feb. 2004), p. 026113. DOI: 10.1103/PhysRevE.69.026113.

[171] T. O’Shea-Wheller, A. Sendova-Franks, and N. Franks. “Differentiated Anti-Predation Responses in a Superorganism”. In: *PLoS ONE* 10.11 (2015), e0141012. DOI: 10.1371/journal.pone.0141012.

[172] G. Oggioni, Y. Smeers, E. Allevi, and S. Schaible. “A generalized Nash equilibrium model of market coupling in the European power system”. In: *Networks and Spatial Economics* 12.4 (2012), pp. 503–560.

[173] S. Ogulata, M. Koyuncu, and K. Esra. “Personnel and patient scheduling in the high demanded hospital services: a case study in the physiotherapy service”. In: *Journal of medical systems* 32.3 (2008), pp. 221–228.

[174] S. N. Ogulata and R. Erol. “A hierarchical multiple criteria mathematical programming approach for scheduling general surgery operations in large hospitals”. In: *Journal of Medical Systems* 27.3 (2003), pp. 259–270.

[175] X. Pan, C. S. Han, K. Dauber, and K. H. Law. “A multi-agent based framework for the simulation of human and social behaviors during emergency evacuations”. In: *AI & SOCIETY* 22.2 (Nov. 2007), pp. 113–132. DOI: 10.1007/s00146-007-0126-1.

[176] J.-S. Pang and M. Fukushima. “Quasi-variational inequalities, generalized Nash equilibria, and multi-leader-follower games”. In: *Computational Management Science* 2.1 (2005), pp. 21–56.

[177] M. Passacantando. “Stability of equilibrium points of projected dynamical systems”. In: *Optimization and Control with Applications*. Springer, 2005, pp. 407–421.

[178] M. Pavone, G. Narzisi, and G. Nicosia. “Clonal selection: an immunological algorithm for global optimization over continuous spaces”. In: *Journal of Global Optimization* 53 (4 2012), pp. 769–808. DOI: 10.1007/s10898-011-9736-8.

[179] H. Peng, C. Ying, S. Tan, B. Hu, and Z. Sun. “An Improved Feature Selection Algorithm Based on Ant Colony Optimization”. In: *IEEE Access* 6 (2018), pp. 69203–69209. DOI: 10.1109/ACCESS.2018.2879583.

[180] Y. Peng, S.-W. Li, and Z.-Z. Hu. “A self-learning dynamic path planning method for evacuation in large public buildings based on neural networks”. In: *Neurocomputing* 365 (2019), pp. 71–85. DOI: 10.1016/j.neucom.2019.06.099.

[181] Y. Ping, Y. Chao, Z. Li, and L. Cuiming. “Based on Game Theory and Ant Colony Algorithm’s Research on Group Robot Cooperative System Control”. In: *2010 International Conference on Electrical and Control Engineering*. IEEE. 2010, pp. 532–535. DOI: 10.1109/iCECE.2010.137.

[182] C. Pintea et al. “A Fuzzy Approach of Sensitivity for Multiple Colonies on Ant Colony Optimization”. In: *Soft Computing Applications, Advances*

in Intelligent Systems and Computing. Vol. 634. 2018, pp. 87–95. DOI: 10.1007/978-3-319-62524-9_8.

[183] J.-C. Rain et al. "The protein-–protein interaction map of Helicobacter pylori". In: *Nature* 409.6817 (2001), pp. 211–215. DOI: 10.1038/35051615.

[184] T. Rambha, L. K. Nozick, R. Davidson, W. Yi, and K. Yang. "A stochastic optimization model for staged hospital evacuation during hurricanes". In: *Transportation research part E: logistics and transportation review* 151 (2021), p. 102321.

[185] E. Rashedi, H. Nezamabadi-pour, and S. Saryazdi. "GSA: A Gravitational Search Algorithm". In: *Information Sciences* 179.13 (2009), pp. 2232–2248. DOI: 10.1016/j.ins.2009.03.004.

[186] T. Ravasi et al. "An Atlas of Combinatorial Transcriptional Regulation in Mouse and Man". In: *Cell* 140.5 (2010), pp. 744–752. DOI: 10.1016/j.cell.2010.01.044.

[187] G. Reddy and S. Phanikumar. "Multi Objective Task Scheduling Using Modified Ant Colony Optimization in Cloud Computing". In: *International Journal of Intelligent Engineering and Systems* 11 (June 2018), pp. 242–250. DOI: 10.22266/ijies2018.0630.26.

[188] R. T. Rockafellar. *Convex analysis*. Vol. 18. Princeton university press, 1970.

[189] R. T. Rockafellar and J. Sun. "Solving Lagrangian variational inequalities with applications to stochastic programming". In: *Mathematical Programming* 181.2 (2020), pp. 435–451.

[190] R. T. Rockafellar and J. Sun. “Solving monotone stochastic variational inequalities and complementarity problems by progressive hedging”. In: *Mathematical Programming* 174.1 (2019), pp. 453–471.

[191] R. T. Rockafellar and R. J.-B. Wets. “Scenarios and policy aggregation in optimization under uncertainty”. In: *Mathematics of operations research* 16.1 (1991), pp. 119–147.

[192] R. T. Rockafellar and R. J. Wets. “Stochastic variational inequalities: single-stage to multistage”. In: *Mathematical Programming* 165.1 (2017), pp. 331–360.

[193] R. Rockafellar and R. J.-B. Wets. *Variational Analysis*. Heidelberg, Berlin, New York: Springer Verlag, 1998.

[194] J. B. Rosen. “Existence and uniqueness of equilibrium points for concave n-person games”. In: *Econometrica: Journal of the Econometric Society* (1965), pp. 520–534.

[195] R. Ross et al. “Reduction in obesity and related comorbid conditions after diet-induced weight loss or exercise-induced weight loss in men: a randomized, controlled trial”. In: *Annals of Internal Medicine* 133.2 (2000), pp. 92–103. DOI: 10.7326/0003-4819-133-2-200007180-00008.

[196] S. Sagratella. “Algorithms for generalized potential games with mixed-integer variables”. In: *Computational Optimization and Applications* 68.3 (2017), pp. 689–717.

[197] M. Salarpour and A. Nagurney. “A multicountry, multicommodity stochastic game theory network model of competition for medical supplies in-

spired by the Covid-19 pandemic". In: *International Journal of Production Economics* 236 (2021), p. 108074.

[198] J. Schellenberger, J. O. Park, T. M. Conrad, and B. Ø. Palsson. "BiGG: a Biochemical Genetic and Genomic knowledgebase of large scale metabolic reconstructions". In: *BMC Bioinformatics* 11.1 (2010), p. 213. DOI: 10.1186/1471-2105-11-213.

[199] H. Seraji, R. Tavakkoli-Moghaddam, and R. Soltani. "A two-stage mathematical model for evacuation planning and relief logistics in a response phase". In: *Journal of Industrial and Systems Engineering* 12.1 (2019), pp. 129–146.

[200] Z. Shahhoseini and M. Sarvi. "Traffic Flow of Merging Pedestrian Crowds: How Architectural Design Affects Collective Movement Efficiency". In: *Transportation Research Record* 2672.20 (2018), pp. 121–132. DOI: 10.1177/0361198118796714.

[201] Y. Shao, J. Bard, X. Qi, and A. Jarrah. "The traveling therapist scheduling problem". In: *IE Transactions* 47.7 (2014), pp. 683–706.

[202] A. Shapiro, D. Dentcheva, and A. Ruszczynski. *Lectures on stochastic programming: modeling and theory*. SIAM, 2021.

[203] B. Shen, X. Xu, and Q. Yuan. "Selling secondhand products through an online platform with blockchain". In: *Transportation Research Part E: Logistics and Transportation Review* 142.C (2020). DOI: 10.1016/j.tre.2020.102066. URL: https://ideas.repec.org/a/eee/transe/v142y2020ics1366554520307171.html.

[204] S. S. Shen-Orr, R. Milo, S. Mangan, and U. Alon. “Network motifs in the transcriptional regulation network of Escherichia coli”. In: *Nature Genetics* 31 (1 May 2002), pp. 64–68. DOI: 10.1038/ng881.

[205] X. Shi, Z. Ye, N. Shiwakoti, D. Tang, and J. Lin. “Examining effect of architectural adjustment on pedestrian crowd flow at bottleneck”. In: *Physica A: Statistical Mechanics and its Applications* 522 (2019), pp. 350–364. DOI: 10.1016/j.physa.2019.01.086.

[206] N. Shiwakoti, X. Shi, and Z. Ye. “A review on the performance of an obstacle near an exit on pedestrian crowd evacuation”. In: *Safety Science* 113 (2019), pp. 54–67. DOI: 10.1016/j.ssci.2018.11.016.

[207] N. Siyam, O. Alqaryouti, and S. Abdallah. “Research Issues in Agent-Based Simulation for Pedestrians Evacuation”. In: *IEEE Access* 8 (2020), pp. 134435–134455. DOI: 10.1109/ACCESS.2019.2956880.

[208] A. G. Spampinato, R. A. Scollo, S. Cavallaro, M. Pavone, and V. Cutello. “An Immunological Algorithm for Graph Modularity Optimization”. In: *Advances in Computational Intelligence Systems*. Ed. by Z. Ju, L. Yang, C. Yang, A. Gegov, and D. Zhou. Vol. 1043. Cham: Springer International Publishing, 2020, pp. 235–247. DOI: 10.1007/978-3-030-29933-0_20.

[209] J. Steiner. *Maze Maker*. 2004. URL: http://ccl.northwestern.edu/netlogo/models/community/maze-maker-2004.

[210] R. Storn and K. Price. “Differential Evolution – A Simple and Efficient Heuristic for global Optimization over Continuous Spaces”. In: *Journal of Global Optimization* 11.4 (1997), pp. 341–359. DOI: 10.1023/A:1008202821328.

[211] R. Storn and K. Price. *Differential Evolution: a Simple and Efficient Adaptive Scheme for Global Optimization over Continuous Spaces*. Tech. rep. TR-95–012. International Computer Science Institute, Mar. 1995.

[212] S. R. Sundaresan, I. R. Fischhoff, J. Dushoff, and D. I. Rubenstein. "Network metrics reveal differences in social organization between two fission–fusion species, Grevy's zebra and onager". In: *Oecologia* 151 (2007), pp. 140–149. DOI: 10.1007/s00442-006-0553-6.

[213] E.-G. Talbi. *Metaheuristics: from Design to Implementation*. Wiley Publishing, 2009.

[214] B. Tang et al. "Hierarchical modularity in ERα transcriptional network is associated with distinct functions and implicates clinical outcomes". In: *Scientific Reports* 2 (2012), p. 875. DOI: 10.1038/srep00875.

[215] I. W. Taylor et al. "Dynamic modularity in protein interaction networks predicts breast cancer outcome". In: *Nature Biotechnology* 27.2 (2009), pp. 199–204. DOI: 10.1038/nbt.1522.

[216] C. Valouxis and E. Housos. "Hybrid optimization techniques for the workshift and rest assignment of nursing personnel". In: *Artificial intelligence in Medicine* 20 (2000), pp. 155–175.

[217] J. Van den Bergh, B. Jeroen, D. Bruecker Philippe, D. Erik, and D. Boeck Liesje. "Personnel scheduling: A literature review". In: *European Journal of Operational Research* 226 (2013), pp. 367–385.

[218] C. Von Mering et al. "Comparative assessment of large-scale data sets of protein–protein interactions". In: *Nature* 417.6887 (2002), pp. 399–403. DOI: 10.1038/nature750.

[219] S. Wang, H. Liu, K. Gao, and J. Zhang. “A Multi-Species Artificial Bee Colony Algorithm and Its Application for Crowd Simulation”. In: *IEEE Access* 7 (2019), pp. 2549–2558. DOI: 10.1109/ACCESS.2018.2886629.

[220] W. Wang et al. “Closed-loop supply chain network equilibrium model with retailer-collection under legislation”. In: *Journal of Industrial & Management Optimization* 15.1 (2019), pp. 199–219.

[221] D. Warner. “Scheduling nursing personnel according to nursing preference: a mathematical programming approach”. In: *Oper. Res.* 44 (1976), pp. 842–856.

[222] U. Wilensky. *NetLogo*. Center for Connected Learning and Computer-Based Modeling, Northwestern University, Evanston, IL. 1999. URL: http://ccl.northwestern.edu/netlogo/.

[223] D. M. Wilkinson and B. A. Huberman. “A method for finding communities of related genes”. In: *Proceedings of the National Academy of Sciences* 101.suppl 1 (2004), pp. 5241–5248. DOI: 10.1073/pnas.0307740100.

[224] H. Wolfe and J. Young. “Staffing The Nursing Unit, Part I: Controlled Variable Staffing”. In: *Nursing Research* 14.3 (1965), pp. 236–243.

[225] T. Wong, M. Xu, and K. Chin. “A two-stage heuristic approach for nurse scheduling problem: A case study in an emergency department”. In: *Computers & Operations Research* 51 (2014), pp. 99–110.

[226] I. Xenarios et al. “DIP: the Database of Interacting Proteins”. In: *Nucleic Acids Research* 28.1 (Jan. 2000), pp. 289–291. DOI: 10.1093/nar/28.1.289.

[227] X.-S. Yang. "A New Metaheuristic Bat-Inspired Algorithm". In: *Nature Inspired Cooperative Strategies for Optimization (NICSO 2010)*. Ed. by J. R. González, D. A. Pelta, C. Cruz, G. Terrazas, and N. Krasnogor. Berlin, Heidelberg: Springer, 2010, pp. 65–74. DOI: 10.1007/978-3-642-12538-6_6.

[228] D. Yanrui, Z. Zhen, W. Wenchao, and C. Yujie. "Identifying the Communities in the Metabolic Network Using'Component'Definition and Girvan-Newman Algorithm". In: *2015 14th International Symposium on Distributed Computing and Applications for Business Engineering and Science (DCABES)*. IEEE. 2015, pp. 42–45. DOI: 10.1109/DCABES.2015.18.

[229] H. Yu et al. "High-Quality Binary Protein Interaction Map of the Yeast Interactome Network". In: *Science* 322.5898 (2008), pp. 104–110. DOI: 10.1126/science.1158684.

[230] F. Yücel and E. Sürer. "Implementation of a generic framework on crowd simulation: a new environment to model crowd behavior and design video games". In: *Mugla Journal of Science and Technology* 6 (2020), pp. 69–78. DOI: 10.22531/muglajsci.706841.

[231] W. W. Zachary. "An Information Flow Model for Conflict and Fission in Small Groups". In: *Journal of Anthropological Research* 33.4 (1977), pp. 452–473. DOI: 10.1086/jar.33.4.3629752.

[232] N. Zarrinpanjeh et al. "Optimum path determination to facilitate fire station rescue missions using ant colony optimization algorithms (case study: city of Karaj)". In: *ISPRS - International Archives of the Photogrammetry, Remote Sensing and Spatial Information Sciences* XLIII-B3-2020 (Aug.

2020), pp. 1285–1291. DOI: 10.5194/isprs-archives-XLIII-B3-2020-1285-2020.

[233] D. Zhang, X. You, S. Liu, and H. Pan. "Dynamic Multi-Role Adaptive Collaborative Ant Colony Optimization for Robot Path Planning". In: *IEEE Access* 8 (2020), pp. 129958–129974. DOI: 10.1109/ACCESS.2020.3009399.

[234] G. Zhang, H. Sun, J. Hu, and G. Dai. "The Closed-Loop Supply Chain Network Equilibrium with Products Lifetime and Carbon Emission Constraints in Multiperiod Planning Horizon". In: *Discrete Dynamics in Nature and Society* 2014 (June 2014), pp. 1–16. DOI: 10.1155/2014/784637. URL: https://ideas.repec.org/a/hin/jnddns/784637.html.

[235] L. Zhang, M. Liu, X. Wu, and S. M. AbouRizk. "Simulation-based route planning for pedestrian evacuation in metro stations: A case study". In: *Automation in Construction* 71 (2016), pp. 430–442. DOI: 10.1016/j.autcon.2016.08.031.

[236] X. Zhang et al. "An integrated ant colony optimization algorithm to solve job allocating and tool scheduling problem". In: *Proceedings of the Institution of Mechanical Engineers, Part B: Journal of Engineering Manufacture* 232 (Mar. 2016). DOI: 10.1177/0954405416636038.

[237] Y. Zhang, P. Gao, and J. S. Yuan. "Plant protein-protein interaction network and interactome". In: *Current Genomics* 11.1 (2010), pp. 40–46. DOI: 10.2174/138920210790218016.

[238] X. Zheng and Y. Cheng. "Modeling cooperative and competitive behaviors in emergency evacuation: A game-theoretical approach". In: *Computers*

& Mathematics with Applications 62.12 (2011), pp. 4627–4634. DOI: 10.1016/j.camwa.2011.10.048.

[239] X. Zheng, T. Zhong, and M. Liu. "Modeling crowd evacuation of a building based on seven methodological approaches". In: *Building and Environment* 44.3 (2009), pp. 437–445. DOI: 10.1016/j.buildenv.2008.04.002.

[240] J. Zhu et al. "Integrating large-scale functional genomic data to dissect the complexity of yeast regulatory networks". In: *Nature Genetics* 40.7 (2008), pp. 854–861. DOI: 10.1038/ng.167.

[241] X. Zong, J. Yi, C. Wang, Z. Ye, and N. Xiong. "An Artificial Fish Swarm Scheme Based on Heterogeneous Pheromone for Emergency Evacuation in Social Networks". In: *Electronics* 11.4 (2022). DOI: 10.3390/electronics11040649.